

**SPATIAL-MEMORY CONTROL OF  
DEFENSIVE ACTIONS**

**Ruben Duque do Vale**

St. John's College

University of Cambridge

This thesis is submitted for the degree of *Doctor of Philosophy*

January 2020



## **Declaration**

All the work described in this thesis was carried out in the Laboratory of Molecular Biology – University of Cambridge, and the Sainsbury Wellcome Centre - UCL, under the supervision of Professor Tiago Branco.

This thesis is the result of my own work and includes nothing which is the outcome of work done in collaboration except as declared in the Preface and specified in the text. It is not substantially the same as any that I have submitted, or, is being concurrently submitted for a degree or diploma or other qualification at the University of Cambridge or any other University or similar institution. I further state that no substantial part of my thesis has already been submitted, or, is being concurrently submitted for any such degree, diploma or other qualification at the University of Cambridge or any other University or similar institution. It does not exceed 60,000 words, excluding figures, tables and bibliography, as specified by the Degree Committee for the Faculty of Biology.



**Thesis title:** Spatial-memory control of defensive actions

**Author:** Ruben Duque do Vale

## Summary

Adapting anti-predatory defensive strategies to the properties of the environment is critical for survival. Here, I investigated the dependence of mouse instinctive defensive behaviours on memory of the spatial environment, and the neural mechanisms responsible for accurate escape towards refuge.

First, using behavioural assays, I show that the choice and execution of defensive behaviours rely on rapidly acquired memory and are promptly updated following acute changes in the environment. In the presence of a known refuge mice escape directly to it, even if this requires approaching the source of threat. Escape is initiated by a memory-guided, accurate head-rotation movement towards the location of the refuge, indicating knowledge of the spatial goal prior to flight start.

Second, I demonstrate that the superior colliculus (SC) is essential to accurately orient to shelter during escape, in agreement with its known role in both sensory- and memory-guided head orientation. To identify which upstream areas provide information about refuge location to the SC, I retrogradely traced the SC afferents and performed loss-of-function experiments in candidate areas, which showed that the retrosplenial cortex (RSC) plays a critical role in escape accuracy. Furthermore, channelrhodopsin-2-assisted connectivity studies showed a functional connection between RSC and SC, and chemogenetic inactivation of this projection impaired accurate orientation to refuge during escape.

To understand how the RSC and SC control orientation to shelter during escape, I performed simultaneous single-unit recordings from the RSC and SC with Neuropixels probes. Both RSC and SC were found to encode the angular offset between the mouse's heading and the shelter, at the single-neuron and population levels. Chemogenetic inactivation of SC-projecting RSC neurons disrupts encoding of head-shelter offset in both regions, but it does not compromise the SC motor function during a sensory-orientation task.

In summary, I show that escape is a flexible behaviour and its accuracy critically depends on a monosynaptic projection from the RSC to SC. In addition, I show RSC-dependent egocentric encoding of goal direction at SC, an area critical for orientation during escape, providing a possible mechanism for controlling ethologically relevant goal-directed navigation.



This dissertation is dedicated to *Vitor Brotas* who taught me to learn, to look, to see, to think  
and to do.



## **Statement of contributions**

Due to the interdisciplinarity nature of this project, some of the data presented in this dissertation was acquired with the help of colleagues in the Branco Lab. Under the supervision of Professor Tiago Branco, I designed all the experiments and I collected and analysed all the data presented in this thesis, except for the following datasets, on which I actively collaborated with other researchers in the lab:

### Chapter 5

Histological processing and imaging: Panagiota Iordanidou.

Channelrhodopsin-assisted connectivity mapping experiments: Yu Lin Tan, Oriol Pavon and Dr. Vanessa Stempel.

### Chapter 6

Neuropixel implantation, electrophysiology recordings and data analysis: Dr. Dario Campagner.

Histological processing and imaging: Panagiota Iordanidou and Dr. Dario Campagner.

Orientation assay: Dr. Dario Campagner.

## Acknowledgments

I was very lucky to have a PhD mentor who really listens. Each of my ideas, the good and the least good, were taken into consideration, and I was always given the feedback needed to improve my project and to make me the best scientist I could be. I would like to thank *Tiago Branco* for the scientific supervision and mentoring during the past five years, and for being a role model for the rest of my career.

When I started my PhD, I did not know how to run any of the experiments presented here. I owe my colleagues from the *Branco Lab*, who taught me so much and actively contributed with positive criticism and suggestions to this project. I would like to thank present and past members of the Branco lab, especially to *Dario Campagner*, *Dominic Evans*, *Panagiota Iordanidou*, *Oriol Pavon*, *Yu Lin Tan* and *Vanessa Stempel*, for their invaluable direct contribution to the work presented here. I particularly thank my good friends *Dario* and *Dominic*, for teaching me so much and investing so much of their time and energy to help me countless times. I aim to be as good a scientist and colleague as they are.

I would also like to thank the following people:

*Gregory Jefferis* for continued support during my PhD.

*Mate Lengyel*, *Christoph Schmidt-Hieber*, *John O'Keefe*, *Peter Dayan*, *Tom Mrsic-Flogel*, *Troy Margrie*, *Scott Sternson*, *Isaac Bianco*, *Athena Akrami*, *Neil Burgess*, *Carlos Brody*, *Chris Harvey*, *Andre Marques Smith*, *Sepideh Keshavarzi*, *Adam Tozer*, *Balazs Ujfalussy*, *Matthew Phillips* and *Yaara Lefler* for discussions and feedback.

All members of the *Laboratory of Molecular Biology (LMB)* and *Sainsbury Wellcome Centre (SWC) animal units* for helping me caring for the wellbeing of the mice employed in this project.

The *workshops of the LMB* (particularly *Joshua Firman* and *Steve Scotcher*) and *SWC* (particularly *Robb Barrett*) for building various behavioural arenas and various items for my set-ups.

*Kostas Betsios*, who programmed the software used to acquire behavioural data and implemented various upgrades to accommodate my experimental designs.

*Rasmus S. Petersen* for sharing code for the tuning entanglement decoupling analysis.

*Panagiota Iordanidou, Molly Strom* and *Tulin Okbinoglu* for generating and providing viruses used in this work.

*Rob Campbell* for assistance with serial-section imaging.

*Federico Claudi* for help in setting up DeepLabCut.

*Nick Steinmetz* for help in setting up Neuropixels recordings.

*The LMB and SWC scientific communities* for all the discussions and for providing such inspiring environments to learn and to grow as a young scientist. I thank the *Boehringer Ingelheim Fonds* for welcoming me into their exciting PhD Fellowship group and for generous funding. I also thank *St. John's College* for support during my PhD.

Finally, a special thank you to family and friends, especially *Eduardo do Vale* and *São do Vale* for all their involvement, excitement and support, *Suvi do Vale* and *Meri do Vale* for making me and my life so much better in so many ways, and *João Nuno Silva* for being the best of friends.

# Table of Contents

<b>1. INTRODUCTION .....</b>	<b>1</b>
1.1. Cognitive contribution to instinctive behaviours .....	2
1.2. Instinctive anti-predator defensive behaviours and their flexibility .....	3
1.2.1. Selection of defensive actions .....	4
1.2.2. Initiation of defensive actions.....	6
1.2.3. Execution of defensive actions - the flexibility of escape .....	9
1.3. Mammalian neural circuits controlling anti-predatory defensive actions.....	14
1.3.1. Amygdala and associated circuits' contribution to anti-predator defence.....	14
1.3.2. Hypothalamic anti-predator defensive circuits.....	15
1.3.3. Role of the superior colliculus in anti-predator defensive behaviours .....	16
1.3.4. Role of the inferior colliculus in anti-predator defensive behaviours .....	18
1.3.5. Role of the periaqueductal gray in anti-predator defensive behaviours .....	18
1.4. Defensive behaviours in humans .....	20
1.5. Strategies to navigate the environment .....	21
1.5.1. Random and systematic navigation strategies .....	22
1.5.2. Taxon navigation .....	23
1.5.3. Praxic navigation .....	24
1.5.4. Path integration.....	24
1.5.5. Route navigation.....	25
1.5.6. Locale (or place response) navigation .....	26
1.5.7. Combining multiple navigation strategies into a single behavioural output .....	26
1.6. Cells and circuits for spatial memory and navigation: knowing one's location in space .....	27
1.6.1. Hippocampal place cells .....	27
1.6.2. The head direction system .....	28
1.6.3. Medial entorhinal cortex: grid, boundary, speed and object-vector cells.....	30
1.6.4. Cells mapping egocentric location in space.....	32
1.7. Goal directed orientation and navigation .....	33
1.7.1. Contribution of the retrosplenial cortex for spatial memory and navigation.....	33
1.7.2. Mechanisms for goal directed navigation.....	35
1.7.3. Mechanisms of head-orienting movements .....	37
<b>2. AIMS .....</b>	<b>41</b>
<b>3. METHODS.....</b>	<b>43</b>
3.1. Animals .....	44
3.2. Escape behaviour assay.....	44
3.2.1. Experimental set-up.....	45
3.2.2. General procedure.....	47
3.2.3. Sensory stimuli .....	48
3.2.4. Analysis .....	48
3.3. Exploration behaviour assay and chronic extracellular recordings .....	50
3.3.1. Set-up.....	50
3.3.2. Procedure .....	51
3.3.3. Data acquisition and processing .....	51
3.3.4. Single cell tuning analysis .....	52
3.3.5. Tuning Entanglement Decoupling (TunED) analysis.....	54
3.3.6. Population decoding analysis .....	57

3.3.7. Recordings paired with chemogenetic loss of function analysis .....	58
3.4. Orientation behaviour assay.....	60
3.5. General surgical procedures.....	61
3.6. Retrograde circuit tracing .....	62
3.7. Loss-of-function protocols.....	63
3.7.1. Chemogenetic loss-of-function experiments .....	63
3.7.2. Muscimol-driven loss of function.....	66
3.8. General data analysis .....	67
<b>4. RESULTS: Rapid learning controls anti-predator escape</b>	
<b>behaviour.....</b>	<b>69</b>
4.1. A behavioural setup to study navigation during anti-predatorial defensive behaviours .....	70
4.2. Escape behaviour is a goal-directed behaviour characterized by navigation towards refuge .....	71
4.3. Environmental features determine the choice of defensive action .....	76
4.4. Memory of shelter location guides defensive flight .....	79
4.5. Memory of shelter location is formed and updated rapidly .....	84
4.6. Discussion.....	86
<b>5. RESULTS: A projection from retrosplenial cortex to superior</b>	
<b>colliculus is critical for orienting during escape .....</b>	<b>93</b>
5.1. Loss of function of the superior colliculus decreases orientation accuracy during escape.....	94
5.2. Retrosplenial cortex projects monosynaptically to the superior colliculus and is necessary for accurate orientation during escape .....	97
5.3. Monosynaptic projection from retrosplenial cortex to superior colliculus is critical for orientation during escape .....	102
5.4. Discussion.....	110
<b>6. RESULTS: Retrosplenial cortex encodes angular distance to</b>	
<b>shelter and feeds this information to the superior colliculus.....</b>	<b>115</b>
6.1. Neurons in retrosplenial cortex and superior colliculus encode the angular distance to shelter .....	116
6.2. Loss of function of superior colliculus-projecting retrosplenial neurons disrupts head-shelter offset encoding in both areas .....	123
6.3. Loss of function of colliculus-projecting retrosplenial neurons does not impair motor control of orientation movements by the superior colliculus .....	125
6.4. Discussion.....	129
<b>7. GENERAL DISCUSSION .....</b>	<b>135</b>
7.1. Significance of findings .....	137
7.2. Strengths of the study .....	139
7.3. Limitations of the study.....	140
7.4. Experimental outlook.....	141
7.5. Concluding remarks.....	144
<b>8. REFERENCES .....</b>	<b>145</b>

## Illustrations

Figure 1: Ydenberg and Dill’s economical model of flight initiation distance .....	8
Figure 2: Blanchards’ concept defensive distance .....	9
Figure 3: Schematic representation of behavioural apparatus.....	46
Figure 4: Measurement of head direction and head-shelter offset .....	53
Figure 5: Examples of TunED analysis identifying a head-shelter offset cell and a head-direction cell.....	56
Figure 6: Schematic representation of data partition for training and testing linear discriminant analysis classifier prediction accuracy after inactivation of retrosplenial neurons projecting to superior colliculus .....	59
Figure 7: Escape behaviour is a goal-directed action to reach safety.....	72
Figure 8: Aversive auditory stimulus does not cause escape when mouse is already in shelter.....	73
Figure 9: Escape is accurate and linear, relying on initial head orientation to shelter.....	75
Figure 10: Updates of defensive strategy in the presence or absence of a reachable shelter .....	78
Figure 11: Memory of shelter location guides defensive flight.....	80
Figure 12: Mice escape accurately to the shelter in the dark.....	81
Figure 13: Flight termination is signalled by having reached the stored target location and does not require reaching safety .....	83
Figure 14: A single, short visit to the shelter is sufficient to encode the memory of shelter presence and location .....	85
Figure 15: Mice rapidly update the memory of shelter location upon its abrupt displacement.....	86
Figure 16: Superior colliculus loss of function impairs orientation accuracy during escape .....	96
Figure 17: Example of high-error escape following superior colliculus loss of function.....	97
Figure 18: Retrograde tracing from VGluT2 <sup>+</sup> superior colliculus neurons.....	99
Figure 19: Retrograde tracing from VGAT <sup>+</sup> superior colliculus neurons .....	100
Figure 20: DREADD-mediated loss of function of retrosplenial cortex impairs orientation to shelter during escape .....	102

Figure 21: Inactivation of superior colliculus-projecting retrosplenial neurons impairs orientation to shelter during escape to the same extent as global retrosplenial inactivation .....	104
Figure 22: Inactivation of the projection from retrosplenial cortex to superior colliculus impairs orientation during escape .....	106
Figure 23: Example of high-error escape following loss of function of the projection from retrosplenial cortex to superior colliculus .....	107
Figure 24: Inactivation of the projection from superior colliculus projecting retrosplenial neurons to anterior cingulate cortex does not impair orientation during escape .....	109
Figure 25: Muscimol-mediated retrosplenial loss of function strongly impairs orientation during escape.....	110
Figure 26: An exploration assay paired with single unit recordings .....	117
Figure 27: Example of head-direction cell and head-shelter offset cell in retrosplenial cortex .....	119
Figure 28: Tuning of head-shelter offset cells in retrosplenial cortex and superior colliculus tile the egocentric head-shelter offset space .....	120
Figure 29: Retrosplenial cortex and superior colliculus accurately encode head-shelter offset and head direction at a population level .....	122
Figure 30: Inactivation of retrosplenial neurons projecting to superior colliculus decreases coding accuracy of head-shelter-offset and head direction from both areas.....	124
Figure 31: Superior colliculus predicts near future head-rotation movements and inactivation of retrosplenial neurons projecting to the superior colliculus does not impair coding of this variable .....	126
Figure 32: Inactivation of retrosplenial neurons projecting to superior colliculus does not impair orientation to sensory stimulus while impairing orientation to memorised shelter position during escape .....	128
Table 1: Coordinates for viral injections for chemogenetic procedures.....	65
Table 2: Coordinates for canula implantation for chemogenetic procedures.....	66

## Abbreviations

**μL:** microliter

**AAV:** adeno-associated virus

**ACC:** anterior cingulate cortex

**AHN:** anterior hypothalamic nucleus

**AMA:** anterior motor areas

**AP:** antero-posterior

**ChR2:** channelrhodopsin-2

**CI:** confidence interval

**cm:** centimetre

**CNO:** clozapine-N-oxide

**dB:** decibel

**DLC:** DeepLabCut

**dIPAG:** dorso-lateral periaqueductal gray

**dPAG:** dorsal periaqueductal gray

**DREADD:** designer receptor exclusively activated by designer drugs

**DV:** dorso-ventral

**EBC:** egocentric boundary cell

**EYFP:** enhanced yellow fluorescent protein

**FEF:** frontal eye fields

**FID:** flight initiation distance

**fMRI:** functional magnetic resonance imaging

**fps:** frames per second

**GFP:** green fluorescent protein

**h:** hour

**IC:** inferior colliculus

**kHz:** kilohertz

**LDA:** linear discriminant analysis

**LEC:** lateral entorhinal cortex

**LED:** light-emitting diode

**LP:** lateral posterior nucleus of the thalamus

**M2:** secondary motor cortex

**MEC:** medial entorhinal cortex

**min:** minute

**ML:** medio-lateral

**mL:** millilitre

**mm:** millimetre

**ms:** millisecond

**mSC:** medial superior colliculus

**nm:** nanometre

**PAG:** periaqueductal gray

**PBGN:** parabigeminal nucleus

**PPC:** posterior parietal cortex

**RFP:** red fluorescent protein

**ROC:** receiver operator characteristic

**RSC:** retrosplenial cortex

**s:** seconds

**SC:** superior colliculus

**SD:** standard deviation

**SEM:** standard error of the mean

**TunED:** Tuning entanglement decoupling

**vIPAG:** ventro-lateral periaqueductal gray

**VMH:** ventromedial hypothalamic nucleus

**VMHdm:** dorso-medial division of the ventromedial hypothalamic nucleus



## **1. INTRODUCTION**

*The general aim of the present work is to understand how memory of the immediate spatial environment controls defensive actions. In this introductory chapter I will review the two topics that constitute the foundation of this question: i) instinctive defensive behaviours and their flexibility as a function of cognitive aspects; ii) spatial memory and goal directed navigation. I will summarize the current understanding of each of these topics from both behavioural and mechanistic perspectives individually, focusing primarily in rodent literature since my work was performed on mice.*

## **1.1. Cognitive contribution to instinctive behaviours**

Instinctive behaviours are a group of actions that can be driven by internal or external triggers, independently of learning, nevertheless their selection, initiation, execution and termination can be changed by experience (Evans et al., 2019, Tinbergen, 1951). These behaviours are essential for all animal species, both promoting the survival of the behaving animal as well as the generation and fitness maintenance of its offspring. Examples of instinctive behaviours that are critical for the survival of the behaving animal include feeding and anti-predator defensive behaviours, whereas sexual and maternal behaviour are fundamental for the preservation of the genetic pool of the behaving animal through its descendants (Tinbergen, 1951).

It is important to highlight that instinctive actions are not necessarily independent of memory and experience. In fact, the opposition between instinctive and learned behaviours has been criticized for over sixty years (Lehrman, 1953, Jensen, 1961). Instinctive behaviours should not be regarded as the dichotomic contrary of learned behaviours, but rather as behaviours which at least partially rely on non-learned algorithms. Even anti-predator defensive behaviours, which can be triggered without prior learning (Bolles, 1970) and must be employed rapidly and effectively to avoid critical loss of fitness, are very flexibly modulated by the animal's memory as well as its current internal state (Evans et al., 2019).

We routinely observe examples of how experience and learned knowledge can modulate instinctive behaviours. Birds instinctively flee from rapidly approaching objects (Schiff, 1965), yet urban-based birds allow for closer human approach before engaging in a flight than their rural and wild counterparts (Lowry et al., 2013). Animals can identify at least some food as such without specific prior experience and engage in consummatory

behaviour; yet the experienced palate and consumption context will influence the decision to consume such food in the future (Chen et al., 2015, Birch, 1999).

Animals innately execute instinctive behaviours proficiently due to evolutionary pressure, although learning can optimize these behaviours (Mery and Burns, 2010). This makes instinctive behaviours a great tool to study aspects of cognition; on the one hand the behaviour does not fully rely on training, which accelerates and simplifies the study, and on the other hand the contribution of learning and memory can be dissected by the experimenter, through the comparative study of naïve animals and individuals with different levels of experience in the various dimensions of the behavioural assay. Additionally, instinctive behaviours are ethologically significant, and their study reflects computations the brain evolved to do.

## **1.2. Instinctive anti-predator defensive behaviours and their flexibility**

Evolution selects animals that are able to avoid predation and survive long enough to pass on their genetic information through reproduction (Vermeij, 1982, Cooper and Blumstein, 2015). Anti-predatory defensive behaviours are observed across animals of different complexity, from invertebrates (Herberholz and Marquart, 2012, Card, 2012) to primates (van Schaik and van Noordwijk, 1989, Wright, 1998), and each species has a repertoire of defensive behaviours, which can include very distinct actions such as increased vigilance, freezing or escape (Caro, 2005). The choice of defensive action and its execution depends on various internal factors like hunger (Schadegg and Herberholz, 2017, Filosa et al., 2016) and memory of previous predatory attacks (Bateman and Fleming, 2014, Pereyra et al., 2000) and external factors like presence of food or water in the environment (Liden et al., 2010, Burnett et al., 2016) and distance to the predator and to refuge (Ydenberg and Dill, 1986, Dill and Houtman, 1989).

In a recent review (Evans et al., 2019) our group deconstructed one form of defensive behaviour, the escape behaviour, into the sequence of occurrences that compose it. A similar framework can be generalized to the study of the whole family of defensive behaviours, which are characterized by the following sequence of events:

- i) Threat detection
- ii) Selection of defensive action<sup>1</sup>
- iii) Defensive response initiation
- iv) Defensive response execution
- v) Defensive response termination
- vi) Updating of priors for future threat encounters

Understanding that defensive behaviours involve multivariable decisions controlled not only by sensory input but also by memory has been key for the design of the present study. I will next summarize the evidence that supports the view that defensive behaviours are flexible and controlled by dynamic internal and external factors. I will focus particularly on the influence of environmental features and memory thereof on the selection, initiation and execution of defensive actions.

### **1.2.1. Selection of defensive actions**

Before initiating a defensive action, prey must decide which defensive strategy from their arsenal to employ, and in various species this choice depends on several internal and external variables.

The hunger state of the prey is a good example of an internal factor that can dictate the choice of defensive action. Crayfish preferentially freeze when hungry and escape when fed, since escaping will terminate foraging behaviours that may lead to finding food resources (Schadegg and Herberholz, 2017). A related but external modulator of the choice of defensive action in crayfish is the availability of food resources in the environment; crayfish were shown to be biased to freeze instead of fleeing when the concentration of food odour in the environment was higher, since escaping might dictate the loss of available resources (Liden et al., 2010).

---

<sup>1</sup> Even though the selection of defensive action must be made prior to initiating it, this does not mean that the choice is only computed after threat detection. In fact, as I will describe below, various factors affect this selection process and many of them can be computed before the encounter with the predator. Nevertheless, since the characteristics of the predatory encounter typically are a strong determinant of defensive action selection, I listed this step after threat detection.

Both examples above represent variables that are immediately accessible to the animal: its hunger state and the olfactory input that signals the presence of food in the environment. This shows that the environment can control the choice of defensive actions but does not demonstrate it does so in a memory-based manner.

Availability of refuge in the environment is known to influence the choice of defensive actions. Diverse animals including lizards (Hennig et al., 1976), crabs (O'Brien and Dunlap, 1975) and rats (De Oca et al., 2007, Blanchard et al., 1986) preferentially engage in freezing responses when a refuge is not present or reachable, whereas defensive actions are biased towards escape when a refuge is available. Despite being a great foundation to study the role of spatial features in the choice of defensive behaviours, these studies have not explored a few important aspects for the present work, namely: i) to what level is the knowledge about the environment features memory-based vs. sensory-based; ii) how flexible is the choice of defensive action as a function of the environment; iii) how the metrics of escape execution vary as a function of the environment; iv) how flexible the selection of defensive action is in response to ethologically relevant threatening stimuli.

In a laboratory context, mice were shown to either run to a previously visited shelter or to freeze when presented with an overhead looming stimulus (Yilmaz and Meister, 2013). Nevertheless, the authors did not dissect the causes of this behavioural dichotomy. Another study used a similar paradigm and reported mice escape to the looming stimulus when a shelter is available in the environment; when no shelter is present, mice either freeze immediately or run to a corner of behavioural arena and freeze there (Wei et al., 2015).

Aversive sound stimuli have also been used in a laboratory context to study defensive behaviours, as 17-22 kHz sweeps<sup>2</sup> were shown to elicit freezing and escape defensive behaviours in mice (Mongeau et al., 2003). This study also explored the influence of the environment in the choice of defensive actions reporting that when this ultrasound stimulus was presented in the home-cage of a mouse flight behaviour was preferred, whereas when it was presented in an unfamiliar cage, mice more often engaged in freezing.

Environmental features are only one of various factors that bias the choice of defensive actions. In addition to the already mentioned hunger state, other factors known to

---

<sup>2</sup> Interestingly rats vocalized within the range of frequencies when confronted with predatory threat themselves (Blanchard et al., 1991) suggesting this could be a cross-species response to threat.

influence this decision include the ongoing behaviour of the animal, particularly its locomotion speed at the time of threat detection (Zacarias et al., 2018, Eilam et al., 1999) and the pattern of predator motion and approach (De Franceschi et al., 2016, Bhattacharyya et al., 2017).

It is important to highlight that the choice of defensive action is being treated in a relatively simple way focusing on the initial defensive behaviour exhibited by the animal, but it has been shown that during the same prey-predator encounter a prey can use multiple defensive strategies. For instance if an animal freezes and yet this does not prevent detection or a predator attack, the prey may engage in escape or even attack the predator, particularly when capture is imminent (De Franceschi et al., 2016, Blanchard et al., 1981, Lingle and Pellis, 2002, Edut and Eilam, 2003).

Another important example of the relation between memory of space and defensive behaviours is the case of place aversion. This defensive behaviour is characterized by the avoidance of an area of the environment where risk of predation is higher which is usually accompanied by risk assessment behaviour when exploring the vicinity of that area (Endres and Fendt, 2007, Blanchard et al., 2001). In fact the risk of predation and consequent place avoidance are critical factors in shaping foraging behaviour, social behaviour and even morphology of prey animals (Kotler et al., 1994, Abramsky et al., 1996). The memory of past predatory threat associated to a specific area of the environment has been shown to be enough to elicit spontaneous escapes in the absence of sensory evidence upon entering such area (Evans et al., 2018).

### **1.2.2. Initiation of defensive actions**

In the controlled environment of the laboratory animals typically respond to a similar stimulus in a similar manner. For example, responses to a visual looming stimulus have been widely studied and animals tend to respond when the stimulus reaches a size that determines a critical visual angle for the prey (Dunn et al., 2016, Yamamoto et al., 2003, Fotowat and Gabbiani, 2007, Gabbiani et al., 1999). However, in a more naturalistic setting more variables will determine the initiation of a defensive action.

Engaging in a defensive action has a given cost resulting from the energy spent to perform the defensive action plus the loss of resources associated with the interruption of other ongoing behaviours. On the other hand the cost of not engaging in a defensive action is

potential loss of fitness resulting from the predatorial confrontation, which ultimately can dictate the death of the prey (Ydenberg and Dill, 1986, Cooper and Blumstein, 2015).

The decision to initiate a defensive behaviour relies on the computed trade-off between the costs of engaging or not in a defensive action. Thus, it is not certain a prey will engage in a costly defensive behaviour such as an escape, when it detects a predator (Ydenberg and Dill, 1986). Ydenberg and Dill focused on this trade-off in their economic model of escape and highlighted the dynamism of the costs associated with this decision with a classic and clear example, the flight initiation distance (FID). The FID is the distance between the prey and predator at which the former initiates an escape, which can be seen as the distance at which the cost of not escaping becomes greater than the cost of doing so. Both costs are dynamical and depend on various internal and external factors, creating a range of optimal escape distances, dependent on context (Figure 1).

This economical model of FID relates to the concept of defensive distance, proposed by the Blanchards (Blanchard and Blanchard, 1989, Blanchard and Blanchard, 1990) and further explored by McNaughton and Corr (McNaughton and Corr, 2004). Defensive distance relates to the physical distance between the prey and the predator but is an internal construct of the perceived immediacy of threat. Braver individuals match a larger defensive distance to a given real distance to the predator, meaning they will have a shorter FID. In addition, the same individual may represent defensive distances dynamically depending on some of the aforementioned internal and external variables. The concept of defensive distance extends other models by not only considering a FID but rather different threat immediacy distances which will trigger different defensive actions (Figure 2).

The concepts of FID and defensive distance highlight the flexibility to initiate and to select and initiate a defensive action, respectively. A good example of such flexibility is that some animals have a higher FID when further away from their goal refuge (Dill and Houtman, 1989, Hemmi, 2005). The increased distance to safety inflates the cost of non-fleeing (remaining) for a similar prey-predator distance in the Ydenberg and Dill's model and would represent a shift from the red to the blue curve in my adaptation of the Blanchard defensive distance model.

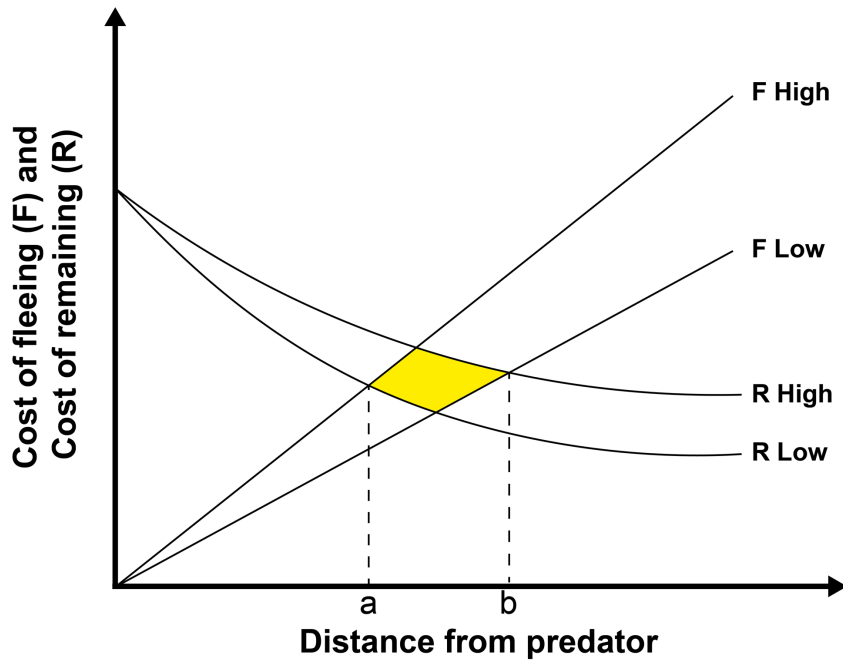


**Figure 1: Ydenberg and Dill's economical model of flight initiation distance**

The cost of remaining (R) is proportional to risk of capture which is maximum when the distance between the prey and predator equals zero. The cost of fleeing (F) increases linearly with distance as it correlates with the attack onset time and it represents, for instance the loss of foraging opportunity; if the animal escapes too soon, when the predator is far it will lose greater foraging opportunity. Both these variables are adjusted dynamically as a function of internal and external factors and thus create a range of possible optimal flight initiation distances, marked here by the intersection of the range of possible R and F slopes (yellow area) and which define a minimum (a) and maximum (b) optimal flight initiation distance. Adapted from Ydenberg and Dill, 1986.

Ongoing behaviour of the animal is also known to modulate the latency and even the probability of engaging in a defensive behaviour. Foraging behaviour decreases responses to innately aversive visual stimuli (Krause and Godin, 1996) and feeding behaviour increases latency to escape (Cooper, 2000). Such examples are particularly interesting as they illustrate the competition between defensive behaviours and mutually exclusive behaviours also driven by instinct.

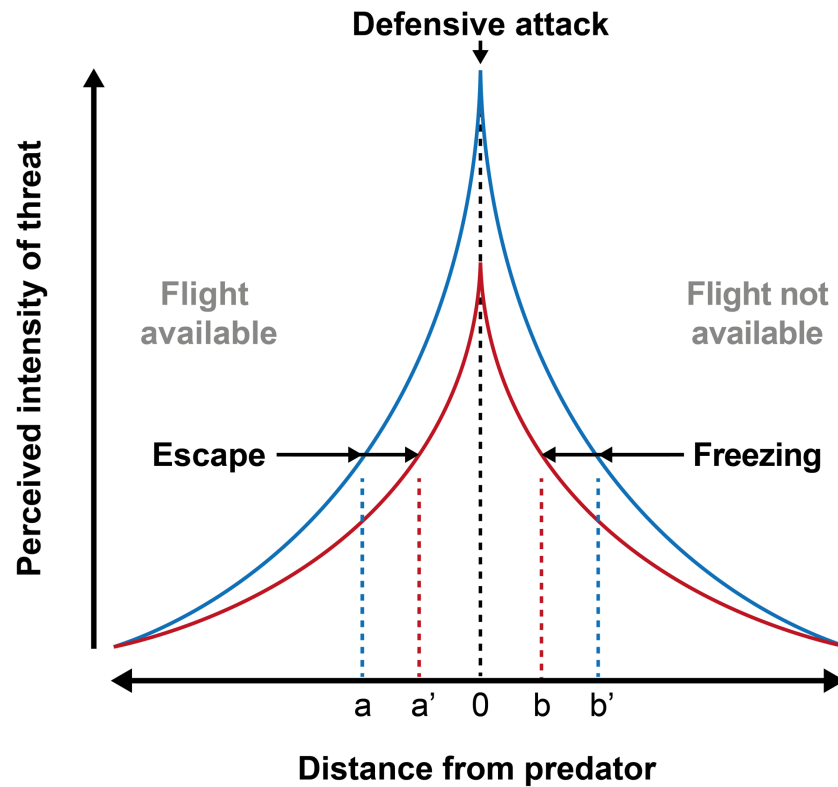


**Figure 2: Blanchard's concept defensive distance**

Blue and red lines can represent either different individuals with distinct representation of threat immediacy to a similar predator distance, or the same individual in two different contexts that modulate its defensive distance. When flight is possible animals will escape at a given defensive distance that will correspond to different actual distances depending on the perceived level of threat ( $a$  and  $a'$ ); whereas when flight is not possible animals will engage in freezing also at different distances ( $b$  and  $b'$ ). If the predator approaches further, animals will often engage in defensive attack. Adapted from Blanchard and Blanchard, 1990.

### 1.2.3. Execution of defensive actions - the flexibility of escape

Following the selection and initiation of a defensive action, its execution is modulated by various factors. In this section I will focus on the execution of escape as this defence strategy is particularly flexible, as a function of various variables including environment features (Evans et al., 2019). The ultimate goal of escape is to avoid predation which can be achieved either by moving away from the source of danger or by reaching safety. I will describe each of these escape strategies and summarize the evidence of their flexibility.

Escapes characterized by movement away from threat are usually thought to be more simplistic as they do not require knowledge about the spatial location of refuge or routes to get to it. A widely studied example of escape away from threat is the C-start escape observed in fish and amphibians. The C-start is characterized by a first stage in which the animal bends its body in a 'C' shape, heading away from the threat, and a second stage in which there is a flip of the tail on the opposite direction straightening the animal directly away from the threat source. After the C-start the animal swims in the opposite direction of the approaching predator (Eaton et al., 1977, Kimmel et al., 1974, Eaton et al., 1988). Nevertheless, even this apparently simple behaviour is known to be modulated by environmental features. Frogs have shown to modulate the directionality of their escape from visual approaching stimuli in respect to obstacles in the environment (Ingle, 1990). This adjustment of the directionality of escape is done for both visible obstacles or shortly after its displacement (up to 60 seconds), even if the frog is passively displaced. This suggests that the frog memorizes the location of the obstacle in an allocentric spatial framework, and that it computes its own current and future position weighing in the threat direction and environmental features.

Fish and amphibian are known to be able to employ two distinct circuits which mediate slightly different escapes from threat. Both strategies are characterized by an initial C-start turn, subtending different angular speeds but achieving the same rotation amplitude. These alternatives represent a trade-off between manoeuvrability, reliability and latency to respond, and the choice between them is a result of the perceived immediacy of threat (Bhattacharyya et al., 2017). While responses mediated by the Mauthner-system<sup>3</sup> can display latencies below 10ms, non-Mauthner responses are more flexible and thus unpredictable in terms of navigation, despite being slower. Although Mauthner-system mediated escapes suffer more pronounced habituation, these short latency responses have an all-or-nothing profile, in the sense that when they are executed they do not suffer from a decrease of amplitude upon successive stimulation (Burgess and Granato, 2007, Bhattacharyya et al., 2017).

---

<sup>3</sup> The Mauthner-system is composed of reticulospinal cells, which include the Mauthner cells and it is present in fish and amphibians. It is a sensory-motor transformation unit, activated by presentation of different modalities of sensory stimuli to the ipsilateral hemi-body and which triggers the contraction of contralateral muscles resulting in a contralateral C-start response. This system has been widely studied and its properties are well summarized in (Korn and Faber, 2005)

Another pair of neurons that has been widely studied in the context of control of escape away from threat is the giant fibre of the fly which can be seen as homologous to the Mauthner cell. These descending command interneurons receive sensory input and project to motor neurons that control the muscles responsible for the jump that is characteristic of fast escape responses in flies (Card and Dickinson, 2008a, Von Reyn et al., 2014, Bacon and Strausfeld, 1986). Similarly to fish, flies have a dichotomic escape response to looming stimuli, which is characterized by similar manoeuvrability, stability and speed trade-offs and which relies on parallel neural circuitry. (Card and Dickinson, 2008a, Von Reyn et al., 2014).

The parallel circuits involved in mediating different escape profiles in fish, amphibians and insects shows that even the same categorical defensive action, an escape, can be very different. Particularly, longer latency responses observed in these animals are remarkably flexible; for instance, flies perform flexible postural adjustments in the 200 ms that precede take-off, which optimize stability and directionality of escape away from threat (Card and Dickinson, 2008b). Interestingly, parallel circuits for escape are not limited to less complex species. In fact, even humans are thought to rely on different pathways when responding to danger, depending on its immediacy (Qi et al., 2018). As for mice, the model used in the present study, it is unclear whether categorically distinct modes of escape exist. However it is known that mice flexibly adjust the vigour of their escape as a function of threat salience (Evans et al., 2018).

Escaping directly away from threat may not always be an optimal strategy, especially if the predator is faster than the prey. Some animals incorporate an element of unpredictability into their escape away from the predator. Cockroaches, for instance, chose one of a few stereotyped angles between 90 to 180° in relation to the predator, in an apparently random manner (Domenici et al., 2008), making it difficult for the predator to predict the future path of the prey. In addition, during escape various animals engage in change of directionality to decrease the probability of ballistic capture; for instance, some rodents engage in escapes characterized by gait transitions, varying direction and speed (Moore et al., 2017, Edut and Eilam, 2004).

When confronted with predation threat some animals escape towards refuge, if one is available. Crabs, for example, flee away from threat in the absence of a refuge (Oliva et al., 2007), but towards a refuge when possible (Zeil and Layne, 2002). Burrow-directed escape relies on a memorized and currently updated vector, which results from the

integration of the motor output of the animal during an outing<sup>4</sup>. This is supported by a number of experiments described in the aforementioned work: i) crabs execute the same motor response to reach shelter they would otherwise, after being displaced by the experimenter, therefore missing the shelter; ii) tests in which the burrow was covered resulted in crabs stopping at approximately the correct place and searching for the burrow there; iii) demonstration that crabs do not rely on seeing the burrow to direct their escape and can orient equally well if a barrier is positioned between their position and the location of the burrow; iv) demonstration that crabs map distance as function of motor output rather than other alternatives such as optic flow; v) evidence that a dummy burrow positioned more than 10cm away from the home burrow does not mislead the escape action in crabs; on the other hand small displacement of the burrow location shifts the directionality of escape towards the new location, suggesting that when the crab is closer to the remembered goal location and can see the goal, then and only then, it will use this visual information to guide escape (Zeil, 1998, Zeil and Layne, 2002, Layne et al., 2003b, Layne et al., 2003a).

Gerbils were shown to escape effectively towards a refuge when confronted with an aerial predator, even if the refuge is not accessible to vision, showing that rodents can use spatial memory to guide navigation during escape (Ellard and Goodale, 1988, Ellard and Eller, 2009). When a barrier was placed in the environment, making trajectories more complex, gerbils initiated an escape response in the wrong direction in half of the trials which were followed by corrective turns, the majority of which at points in space where the refuge was not visible yet. When there were multiple alternative paths to reach the refuge, gerbils tended to use the shortest available route (Ellard and Eller, 2009). In the absence of a refuge, gerbils either ran directly away from threat or directly towards it to undercut the predator. (Ellard and Goodale, 1988). Other studies have described refuge-directed anti-predator escapes from different animals including various species of rodents (Yilmaz and Meister, 2013, Clarke et al., 1993, Dill and Houtman, 1989), larger mammals (Stankowich and Coss, 2006, Blank, 2018), some species of lizards (Zani et al., 2009), and of some species of birds (Lima, 1993). Further details about escape trajectories are extensively discussed in Domenici et al., 2011a, Domenici et al., 2011b.

Another example of the behavioural complexity and flexibility of defence is the response to conspecific and other prey threat calls. Monkeys have been shown to emit alarm calls that code aerial or terrestrial threat, triggering distinct and appropriate responses in

---

<sup>4</sup> This strategy of tracking and navigating space is known as path integration and it is further described in the 'strategies to navigate the environment' section of the introduction of this work.

conspecifics (Seyfarth and Cheney, 1980). In addition, monkeys respond appropriately to specific calls for terrestrial or aerial threat emitted by other species, for example starlings' alarm calls (Seyfarth and Cheney, 1990). Birds (Collias, 1987) and meerkats (Manser et al., 2001), have also been shown to employ different alarm calls for ground and aerial predation threat. Flexible responses to the different stimuli were observed in meerkats (Manser et al., 2001) and birds who emit different calls for aerial and terrestrial predators are known to respond very differently to such threats (Binazzi et al., 2011), although vocalization-elicited defence has not been systematically studied.

Complex escape scenarios in which multiple refuges are available or conspecifics are present in the environment have also been studied and again show the flexibility of defensive actions. For example, gerbils were shown to escape preferentially to the closest of previously visited refuges at the time of threat presentation, when multiple refuges are available (Ellard, 1993). In addition, conspecifics' responses were shown to modulate responsiveness to weaker threatening stimuli and also influence the selection of goal when multiple refuges are available (Ellard and Byers, 2005). The presence of conspecifics is also known to modulate execution of escape: for example fish schools exhibit a straighter and more uniform navigation profile than those of isolated individuals, presumably to avoid collisions between prey (Domenici and Batty, 1997, Pitcher and Wyche, 1983).

The complexity of the environment not only demands more complex navigation trajectories but it is also associated with higher incidence of accidents, such as slips, falls and crashes (Wynn et al., 2015). Even though speed is critical for the success of an escape (Husak, 2006, Walker et al., 2005), animals were shown to decrease their running speed in complex environments in the context of escape (Higham et al., 2001). Accordingly, optimal compromise between speed and manoeuvrability has been shown to increase the probability of successful escape in relation to a maximum-speed escape (Wynn et al., 2015).

### **1.3. Mammalian neural circuits controlling anti-predatory defensive actions**

During the 20<sup>th</sup> century major contributions were made to the understanding of instinctive behaviours, by Lorenz, Von Frisch, Tinbergen amongst others. More recently, developments in population-specific neural activity manipulation and recording have allowed progress in the understanding of the neural implementation of various instinctive behaviours. In this section I will summarize the current understanding of key circuits involved in defensive actions, focusing on the contributions of different brain areas and their organization into behaviourally-relevant pathways. The circuits controlling anti-predatory and non-predatory defence have been comprehensively discussed in (Silva et al., 2016a).

#### **1.3.1. Amygdala and associated circuits' contribution to anti-predator defence**

The amygdala has been extensively studied in the context of fear conditioning, but it is also known to be involved in anti-predator defensive behaviours. It receives information about aversive olfactory cues, from diverse olfactory centres (Pérez-Gómez et al., 2015), and it is essential to control olfactory-driven defensive actions in mice. Lesions of the medial amygdala decrease responses to olfactory cues of predatory threat (Li et al., 2004), and both this area as well as the lateral amygdala and the basomedial amygdala are engaged in the presence of a predator (Martinez et al., 2011). The medial amygdala is thought to be a relay of olfactory threat information whereas the lateral and basomedial divisions are thought to convey information about non-olfactory threat cues; these areas project to hypothalamus which in turn recruits the periaqueductal gray (PAG) to control defensive responses (Gross and Canteras, 2012).

Optogenetic inhibition of the projection from the olfactory bulb to the cortical amygdala results in reduced response to innately aversive olfactory cues, and defensive responses elicited by aversive olfactory cues can be recapitulated with optogenetic activation of cortical amygdala neurons (Root et al., 2014). On the other hand, the activity of serotonin-2A receptor expressing cells in the central amygdala was shown to be decreased in freezing responses to innately aversive odours. Chemogenetic inactivation of this cell population upregulates freezing responses to olfactory aversive stimuli and their stimulation downregulates these freezing responses (Isosaka et al., 2015).

In addition, inactivation studies of two areas associated with the amygdala, the bed nucleus of the stria terminalis and the lateral septum, demonstrated that both are necessary for freezing behaviour in response to innately aversive olfactory cues (Endres and Fendt, 2008, Fendt et al., 2003).

### **1.3.2. Hypothalamic anti-predator defensive circuits**

The contribution of hypothalamic circuitry in defensive behaviours has been known for some decades, nevertheless, the hypothalamus was thought to be a relay between the amygdala and downstream areas that directly elicit defensive actions. More recently, various studies have shown a more central and active role of the hypothalamus for defence.

Optogenetic stimulation of a specific neural population<sup>5</sup> of the dorsomedial division of the ventromedial hypothalamic nucleus (VMHdm), in mice, was shown to elicit either freezing or escape behaviour, depending on the optogenetic stimulation intensity (Kunwar et al., 2015). Interestingly, this and other studies showed that inactivation of this population of neurons in the VMHdm impairs defensive responses to living predators but not to overhead looming stimuli (Silva et al., 2013, Kunwar et al., 2015).

The VMHdm is also important for learning the valence of contexts associated with predation risk. Reversible inactivation of the VMHdm not only compromises defensive actions upon exposure to predators, but also impairs the place-aversion response that naturally ensues (Silva et al., 2016b).

Hypothalamic circuits are known to be particularly important for defensive responses to olfactory stimuli which converge onto the VMH (Pérez-Gómez et al., 2015). In contrast, it has been pointed out in a recent review (Silva et al., 2016a) that various pathways which are known to control defensive responses to visual and auditory stimuli bypass the hypothalamic system.

The hypothalamic nucleus VMHdm has been suggested to play a role in orchestrating escape versus freezing responses. While it send collaterals to both the dorsolateral PAG (dIPAG) and the anterior hypothalamic nucleus (AHN), the former was shown to mediate

---

<sup>5</sup> Neurons expressing the gene Nuclear receptor subfamily 5, group a, also known as Steroidogenic factor 1.

freezing responses and the latter escapes (Wang et al., 2015). The VMH projects monosynaptically to the PAG (Canteras et al., 1994), and optogenetic stimulation of its terminals over the dPAG induces freezing but not running. In contrast, stimulating VMH terminals at the AHN can trigger freezing, escape and jumping responses (Wang et al., 2015).

Interestingly, Wang and colleagues report that when the animals were in their homecage, lower intensity ChR2 activation of VMHdm neurons elicited pure freezing responses, whereas at higher intensity and frequency it elicited freezing responses followed by running and jumping. Contrarily, if mice were placed in an arena which contained a refuge which they had the chance to explore, similar optogenetic activation of VMHdm neurons elicited escape towards the shelter. Once the animals reached the refuge they would stay inside despite continuous light stimulation. Finally, in the same arena if a shelter was not present animals froze or ran to a corner of the arena. In addition to providing further insight about the role of the hypothalamus in defensive behaviours, taken these data constitute great evidence for the flexibility of defensive behaviours as a function of the animal's immediate space (Wang et al., 2015).

### **1.3.3. Role of the superior colliculus in anti-predator defensive behaviours**

In addition to being essential for coordinating orientation movements, the superior colliculus (SC) is pivotal in initiating defensive actions and this dual role has been widely studied for some decades (Comoli et al., 2012, Dean et al., 1989).

Recordings from the SC demonstrated that it contains neurons that respond to looming and ultrasound stimuli (Shang et al., 2015, Zhao et al., 2014, Evans et al., 2018). Work from our group demonstrated that a feedforward monosynaptic connection between excitatory cells in the medial SC (mSC) and dorsal PAG (dPAG) is necessary for escape behaviour. The mSC glutamatergic neurons code saliency of threat and their activity is predictive of escape; the network activity of the mSC, which relies on its recurrent excitation and short-term synaptic facilitation, amplifies and sustains signals of threat and eventually engages the dPAG to drive escape (Evans et al., 2018).

A circuit from the SC to the lateral posterior nucleus of the thalamus (LP) and from here to the amygdala has been proposed as being important for engaging in defensive behaviours in the context of visual threats (Wei et al., 2015). This study also showed that optogenetic silencing of intermediate layer of the SC decreases the probability of freezing

to overhead looming stimuli. In addition, Chr2-driven activation of CaMKII neurons in the intermediate layer of the medial SC (but not the lateral SC) was enough to elicit freezing responses. The same study reported that muscimol inactivation of the basolateral amygdala impaired defensive behaviours visually or optogenetically-triggered at the SC. The authors, however, do not show the behavioural effect of inactivation of the LP, although they demonstrate that inactivating the two other nodes of their proposed pathway impairs freezing responses. Work from our lab showed that inactivation of the LP does not impair escape behaviour, suggesting that the projection from the SC to LP may be dedicated to control freezing responses (Evans et al., 2018).

Another recent study (Shang et al., 2015) proposed that divergent pathways from the SC to the LP and the parabrachial nucleus (PBN) competed to control freezing and escape responses, respectively. Although the authors reported that optogenetic stimulation of the SC terminals at the PBN elicits escapes, they did not test whether this was due to the effect of antidromic activation of the SC neurons, while work from our group showed that inactivation of the PBN did not impair escape (Evans et al., 2018).

In addition to eliciting freezing or escape (Bittencourt et al., 2005, Evans et al., 2018), stimulation of the SC has long been known to elicit orienting movements. Dean and colleagues demonstrated that chemical or electric stimulation of distinct areas of the SC elicit either contralateral stereotyped movements or actions that the authors described as “resembling defensive behaviours”, namely running (with a directionality that could not be predicted by the site of stimulation) and freezing. Contralateral stereotyped movements were elicited more often in the lateral portion of the mid and deep layers of the rostral SC, whereas defensive behaviours were more common when stimulating the rostro-medial portion of the SC as well as the deeper layers of the caudal portion of the SC (Dean et al., 1988, Sahibzada et al., 1986).

Electrical stimulation of the SC also results in modulation of respiratory- and heart-rate as well as blood pressure (Keay et al., 1988), and the authors of this study hypothesise these effects are preparatory for engaging in physically demanding defensive actions. This highlights the overarching function of the SC in orchestrating defensive behaviours which go much beyond a mere acceleration towards a shelter.

#### **1.3.4. Role of the inferior colliculus in anti-predator defensive behaviours**

The inferior colliculus (IC) has been suggested to be involved in defensive behaviours by the means of stimulation and inactivation studies. Stimulation of the IC triggers defensive actions, including freezing and escape, whereas loss of function of this area increases latency and decreases probability to respond in fear-conditioning paradigms (Brandao et al., 1993). The role of the IC mediating defensive responses to innately aversive stimuli, namely sound stimuli, has only recently been investigated (Xiong et al., 2015). The authors employed a broadband noise (1 – 64 kHz) sound stimulus which, in a two chamber arena, was shown to elicit escapes, but not freezing. Muscimol inactivation of the inferior colliculus (IC) reduced the probability of flight drastically. In addition, the authors show that a projection from the auditory cortex to the inferior colliculus drives flight responses and inhibition of this projection reduces sound-elicited flights. Optogenetic stimulation of a projection from IC to PAG elicits flight responses.

#### **1.3.5. Role of the periaqueductal gray in anti-predator defensive behaviours**

The PAG is regarded as a downstream area for various pathways that control behaviour, including amygdala-hypothalamus axis and midbrain circuits.

The PAG is divided into different areas with the dorsal columns receiving from the medial hypothalamic system (Motta et al., 2009, Canteras et al., 1994), SC and IC (Evans et al., 2018, Xiong et al., 2015). The ventral PAG receives a projection from the central amygdala and this circuit is known to mediate conditioned freezing responses to aversive stimuli (Johansen et al., 2010).

Inactivation of the PAG decreases defensive behaviours from predatory threat (Sukikara et al., 2010, Silva et al., 2013), and our group showed that inactivating the dPAG impairs escape to overhead looming stimuli (Evans et al., 2018). Additionally, inactivation of the projection from the mSC to dPAG abolishes escape to looming stimuli as well as the optogenetic elicited escapes by stimulation of glutamatergic SC neurons (Evans et al., 2018), corroborating the aforementioned observation. On the contrary, optogenetic stimulation of the dorsal PAG elicits escape responses in mice (Evans et al., 2018, Deng et al., 2016). Additionally, it has been long known that responses elicited by stimulation of the amygdala or hypothalamus are abolished in the context of PAG lesions (Hunsperger, 1963, De Molina and Hunsperger, 1962), illustrating the role of the PAG as

a convergence point of various nodes of the defensive circuit and an essential hub for triggering defensive behaviours.

Recordings from single units in dorsal PAG showed neurons whose firing-rate increased during flight (flight cells) and neurons whose firing-rate increased as the distance from the predator decreased, while the animal was actively assessing the environment (assessment cells; Deng et al., 2016). Assessment cells' activity shuts off upon initiation of escape and flight cells' activity increases immediately before flight onset, reaching firing-rate peak significantly before maximum escape speed was attained. Remarkably, flight cell's instantaneous firing-rate does not correlate with instantaneous velocity, but rather with maximum flight speed on a given trial. Another study (Masferrer et al., 2018) reported the same two types of cells in dPAG and a third type which decreased firing rate as the prey approached the predator, meaning they are negatively correlated with assessment cells. The authors stress that since dPAG's flight cells' activity peaks significantly before peak speed is attained, the PAG is a motor pattern initiator rather than a motor execution-control area.

Reversible inactivation of the dPAG was shown to decrease defensive behaviours in the presence of a predator, but defence was restored upon subsequent re-exposition to the environment in the absence of predatory cues. This latter observation contrasts with what is seen following VMHdm inactivation and suggests that, despite being essential to engage in an escape, the PAG is not essential to form a memory of the context of predatory encounters (Silva et al., 2016b). A projection from the prefrontal cortex to the lateral and ventro-lateral portions of the PAG has been shown to be essential for discriminating previously threatening contexts from neutral ones (Rozeske et al., 2018).

The downstream projections of the PAG that are responsible for escape are not yet known, although it has been hypothesized (Ferreira-Pinto et al., 2018, Bandler and Shipley, 1994) that the cuneiform nucleus and/or lateral paragigantocellular nucleus' neurons are strong candidates as both receive monosynaptic input from PAG and are known to control high speed locomotion.

An inhibitory projection from the central amygdala to GABAergic neurons in the ventro-lateral PAG (vIPAG) has been shown to produce disinhibition of excitatory cells in the vIPAG, which in turn activates premotor areas, namely the magnocellular nucleus of the medulla, eliciting freezing (Tovote et al., 2016). The same study shows that an excitatory projection from the dIPAG to vIPAG GABAergic neurons inhibits freezing and is elicits flight responses. This suggests that the vIPAG is important in gating the freezing/flight

dichotomy based on upstream input from the amygdala and dPAG. Additionally, the authors showed that ChR2 stimulation of glutamatergic cells in vIPAG elicits freezing, whereas optogenetic inhibition of these neurons inhibited freezing responses in both fear-conditioning context and in the presence of a dummy predator. Taken together, these data demonstrate that GABAergic neurons in vIPAG play a key role in defence and that through its inputs they control the choice of defensive action.

Similarly to the SC, which is known to be involved in approach and avoidance behaviours (Dean et al., 1989), there is overlap of defensive and predatory functions at the level of the PAG. Specifically, an excitatory projection from the lateral hypothalamus to the PAG was shown to drive escape whereas an inhibitory projection with same origin and destination was shown to drive predation (Li et al., 2018).

#### **1.4. Defensive behaviours in humans**

While we can study the responses of humans to threat, it is important to not transpose back to animals the human experience of threatening situations. Humans can experience fear or terror, but we cannot know how animals experience a situation of danger such as predatory threat. LeDoux's work has focused on the importance of distinguishing the cognitive circuits that control the experienced fear from threat and the defensive circuits that elicit behavioural and physiological responses to threat, highlighting this is essential to make progress in the study of pathology and pharmacological approaches of fear and anxiety disorders (LeDoux and Pine, 2016, LeDoux, 2014). As pointed out by LeDoux and Daw, it is important to understand the human circuitry responsible for responses to threat since pathologies characterized by impaired threat processing are frequent, and although humans are not typically affected by predatory threat, many of the circuits that are employed by other mammals for defence are the same that mediate human responses to social threats (LeDoux and Daw, 2018).

There are few studies investigating anti-predator responses in humans and most are based on virtual reality assays. When confronted with a virtual predator, humans have a shift of activity (assessed by fMRI) from the ventromedial prefrontal cortex (vmPFC), hippocampus, amygdala and hypothalamus to the PAG, as the threat approaches the subject (Mobbs et al., 2007, Mobbs et al., 2009). Increased activity in the PAG was also correlated with increased subjective degree of dread in the subjects.

Electrical stimulation of different brain areas known to be important for rodent defence elicit high anxiety responses in humans: VMH stimulation induce panic attacks and a sensation of imminent death (Wilent et al., 2010) whereas PAG stimulation was reported to trigger the sensation of being chased (Amano et al., 1982).

Humans, unsurprisingly, present flexibility of defensive behaviours. A recent comparative study in rats and humans investigated the neural substrates responsible for engaging in escape or freezing (Terburg et al., 2018). The authors showed that the basolateral amygdala is essential in both species to bias defensive behaviours away from freezing and towards escape in situations of escapable threat. This work is a rare example of the study of functional conservation of defensive circuits across humans and other species, and it shows that at least some of the circuit elements that control these behaviours not only are the same but have similar functions in humans and non-human animals.

Investigating defensive behaviours could help further our knowledge of the physiopathology of anxiety disorders such as post-traumatic stress disorder or panic disorder, in humans. In addition, the study of defensive behaviours can be a powerful tool to investigate sensory and cognitive processing, motor control and decision-making in various species, including humans, due to the robustness, reliability and flexibility of these behaviours. This short section illustrates the overlap of circuits mediating defensive behaviours in humans and rodents. The homology of neural circuits between species makes animal studies of defensive circuits a potential asset for targeted pharmacological treatment of some stress and anxiety disorders. In addition it may help optimizing the targeted use of cranial electrotherapy stimulation, which is used nowadays for the treatment of a few psychiatric diseases including refractory anxiety disorders (Kirsch and Nichols, 2013).

## **1.5. Strategies to navigate the environment**

*This work focuses on how memory of space modulates defensive actions in animals and thus it is important to summarize the current understanding of how animals navigate the world. This section is focused on the behavioural perspective of navigation whereas the next section describes the neural circuits that underlie spatial memory and navigation.*

One of the main functions of the brain is to control movement, allowing animals to search various types of resources in the environment, such as food or sexual partners, or to avoid predation (Poulter et al., 2018).

Field studies have shown that various animals, including different species of insects (Menzel et al., 2005, Huber and Knaden, 2015), birds (Wallraff and Wallraff, 2005, Chernetsov et al., 2008, Thorup et al., 2007), fish (Quinn et al., 1999) and mammals (Tsoar et al., 2011, Horton et al., 2011) are capable of accurately navigate across very long distances. Accurate navigation requires the use of cues which can be sensory acquired or internally generated. Various sensory cues are used by different animals to guide goal-directed navigation in an allocentric framework, including direct sunlight and polarized skylight (Wehner and Müller, 2006), celestial cues (Emlen, 1970) the magnetic field of earth (Putman et al., 2014, Holland et al., 2006), sound cues (Tolimieri et al., 2000) or olfactory cues (Papi et al., 1971, Benvenuti and Wallraff, 1985). In addition, internally-generated, self-motion cues (also known as idiothetic cues) are used to orient navigation in various species, including humans (Mittelstaedt and Mittelstaedt, 1980, Mittelstaedt and Glasauer, 1991, Müller and Wehner, 1988, Mittelstaedt and Mittelstaedt, 1982). Importantly, different modalities of cues can be used together to guide navigation (Able and Able, 1990, Frost and Mouritsen, 2006).

In addition to using different cues, animals can use distinct strategies to navigate. David Redish beautifully reviewed the different strategies that animals can use to navigate the environment, namely: random, taxon and praxic (known collectively as response strategies), route, locale and path integration navigation strategies (Redish, 1999). Next, I will succinctly characterize each of these strategies. It is critical to understand the different strategies animals can use to navigate in order to dissect them in a controlled manner in the lab. Additionally, since different strategies rely on different neural circuits this can help directing the investigation of neural mechanisms responsible for specific spatial memory guided behaviours.

### **1.5.1. Random and systematic navigation strategies**

When animals cannot locate goals, they have got to rely random or systematic strategies to search the environment. The random component of navigation has been studied in the

context of foraging as a means of maximizing the covered area of exploration while minimizing the length of a foraging bout (Bovet, 1983).

For example, the crustacean *H. reaumurii*, successfully finds its refuge, after being displaced, by employing an effective search pattern that can be described as quasi-Brownian. Although this strategy relies on random orientation movements it also demands that the animal is capable of returning to the starting point of exploration to engage on further anchored, random exploration. Such strategy is an effective systematic way of exploring an unknown environment when the goal location cannot be detected or inferred by cues (Hoffmann, 1983). Although examples like this tend to be categorized as random they should be called systematic search strategies as they actually rely on the animal keeping track of its previous position using either internal or external cues, while it uses none of this information to infer goal position (Bartumeus and Catalan, 2009, Baum, 1987).

### **1.5.2. Taxon navigation**

Animals can navigate towards a sensory-assessible cue that directly signalizes goal. The key characteristic of taxon navigation is that it depends on a single cue which may be part of the goal itself or be adjacent to it, and the animal navigates directly towards it. Computationally this is a simple strategy involving a stimulus-response association, however it has limited flexibility (Redish, 1999, O'keefe and Nadel, 1978).

By means of lesions studies in the context of tasks that demanded taxon navigation, this strategy was shown to rely on: i) the superior colliculus which, as discussed above, not only is important for avoidance but also for approach navigation, such as the taxon strategy (Dean and Redgrave, 1984); ii) the caudate nucleus (Packard and McGaugh, 1992) and iii) substantia nigra pars compacta (Da Cunha et al., 2003). On the contrary, the hippocampus is not necessary for this strategy as shown by mice being able to navigate to a goal if it is either visible or cued, in the context of hippocampal memory system lesions (McDonald and White, 1994, Da Cunha et al., 2003, Packard and McGaugh, 1992).

### 1.5.3. Praxic navigation

This strategy relies on the animal executing a fixed motor program. A prime example of this strategy is illustrated in the work from Eichenbaum and colleagues, who demonstrated that even after hippocampal lesions animals could solve the Morris water maze<sup>6</sup> if their starting location was always the same and the hidden goal position was stable (Eichenbaum et al., 1990). Additionally, much older studies had already shown that rodents can navigate complex environments, even when they were critically sensory deprived, relying on stereotyped motor programs (Honzik, 1936, Watson, 1907).

Lesion studies suggest that the caudate nucleus is essential for praxic navigation (Packard and McGaugh, 1996), which is supported by recordings demonstrating a critical role of the striatum in stimulus-response habit learning (Jog et al., 1999). It is unclear whether the posterior parietal cortex is essential for navigation with some studies suggesting it is (Save and Moghaddam, 1996) while others propose the contrary (Kesner et al., 1989, Redish, 1999).

David Redish highlighted the fact that often taxon and praxic strategies are employed in a combined manner (Redish, 1999). He referred to work testing navigation in the Morris water maze in the context of hippocampal lesions, in which rats are only able to navigate to a goal if it is cued locally, but instead of navigating directly towards it they circle the tank in a specific, patterned manner that leads them to the cue (Eichenbaum et al., 1990, Morris et al., 1982).

### 1.5.4. Path integration

Path integration is a navigation strategy characterized by the ongoing integration of the traversed trajectory based on internal cues, which can be used to guide navigation back to the starting point of the trajectory. This strategy does not imply that the animal retraces

---

<sup>6</sup> The Morris Water maze (Morris, 1981) is a widely used navigation task, developed by Richard Morris with the aim of testing spatial navigation in rodents. A platform is submerged in a cylindrical tank filled with water which is made opaque, and the animal tries to find this platform using distal visual cues positioned by the experimenter. After the animals learns the task, swimming to the platform from different start points, a test trial is conducted in which the platform is removed from the water maze. The metrics of learning and retrieving memory of the location of the platform typically tested are the time to reach the correct quadrant and the fraction of time the animal spends in that quadrant.

its past steps back to the starting point, but rather it computes a straight vector towards goal which can be used to navigate straight towards it (Mittelstaedt and Mittelstaedt, 1980, Etienne and Jeffery, 2004). Animals as simple as ants (Müller and Wehner, 1988) and as complex as mammals (Etienne and Jeffery, 2004, Etienne et al., 1996) have been shown to be able to rely on this strategy for accurate navigation.

This strategy relies on tracking angular and linear distance to the starting point of the path. In vertebrates, the semi-circular canals respond to angular but not linear acceleration and are essential for tracking the angular component that supports path integration, while otolithic signals provide information about linear distances; such information can be complemented by proprioceptive signals of locomotion, efferent copies of locomotor signals and sensory signals such as optic flow (Mittelstaedt and Mittelstaedt, 1982, Etienne et al., 1996). These external signals can be critical for the success of navigation as path integration accumulate errors, particularly for larger distances, for which a similar angular error will generate a larger final offset to goal. Therefore, this strategy is often used in combination with visual cues to help minimize such error (Etienne et al., 1996).

As mentioned above vestibular information is essential for path integration which has been corroborated by lesions studies (Wallace et al., 2002, Stackman and Herbert, 2002). The retrosplenial cortex (RSC) has also been suggested to be important for this navigation strategy (Cooper and Mizumori, 1999, Cooper and Mizumori, 2001, Sherrill et al., 2013, Elduayen and Save, 2014, Chrastil et al., 2015), as have the medial entorhinal cortex (Fuhs and Touretzky, 2006, McNaughton et al., 2006) and the head-direction network (McNaughton et al., 1991). There is no consensus on the role of the hippocampus in path integration, since some studies suggest it is not necessary for this strategy (Alyan and McNaughton, 1999, Shrager et al., 2008) while others claim it is essential (Maaswinkel et al., 1999, Whishaw and Maaswinkel, 1998, Golob and Taube, 1999).

#### **1.5.5. Route navigation**

This strategy involves sequences of navigation trajectories that lead an animal from a sub-goal to the next and eventually to the ultimate goal location, while relying on taxon and praxic strategies. Although this strategy is characterized by relatively simple computations, it takes a long time to train as the sequence of positions and associated goal or sub-goal vectors must be learned. (Redish, 1999).

The circuits that coordinate taxon and praxic navigation are also responsible for controlling route navigation. In addition, it has been suggested that the hippocampus may play a role in orchestrating the transitions between sequential sub-goals (Redish, 1999, Jordan, 2019, Goodroe et al., 2018) although further investigation is needed to understand how the chaining and transitioning of spatial sub-goals is actually implemented.

#### **1.5.6. Locale (or place response) navigation**

Work from Tolman (Tolman, 1948) showed animals can use untraversed shortcuts after having explored an environment, suggesting a navigation strategy that relies on a, so called, cognitive map. Unlike taxon navigation, locale navigation relies on the integration of various cues, which together contribute for this neural based map (Redish, 1999). This cognitive map was proposed to be a product of the hippocampus by seminal work from John O'Keefe (O'keefe and Nadel, 1978).

The standard Morris water maze experiment in which a rat navigates from a varying starting point towards a non-sensory detectable goal location based on the integration of visual cues constitutes a prime example of locale navigation and was shown to critically depend on the hippocampus (Morris et al., 1982, Morris, 1981).

The cognitive map relies on various cell types distributed across different circuits, including place cells, head direction cells, grid cells and border cells, amongst others, which are the focus of the next section of this introductory chapter.

#### **1.5.7. Combining multiple navigation strategies into a single behavioural output**

Although multiple navigation strategies have been described, they are not mutually exclusive and often an animal will have access to the necessary cues to employ more than one strategy. For instance, if an animal is positioned at the platform of the cued version of Morris water maze it can navigate back to it by either a path integration, taxon or locale strategy as well as by any combination of the three.

By artificially making cues contradictory in the environment, experimenters can test which navigation strategy is hierarchically dominating a given task, which naturally does not mean such strategy is the only one employed to navigate in the original task, when the cues are unaltered.

An elegant study from Packard and McGaugh demonstrated that the preferred strategy to navigate a simple environment can change with experience. After 8 days of training in a simple navigation task, rats' choice was dominated by a locale strategy, whereas when they were trained longer, the praxic strategy took over the control of navigation in the task. In this study the authors also demonstrated different neural substrates associated with the different dominant strategies: locale strategy was dependent on the hippocampus whereas the praxic strategy relied on the caudate nucleus. Disruption of the caudate nucleus lead to a maintenance of dominance of locale navigation even after the longer training period (Packard and McGaugh, 1996).

Animals concurrently use combinations of navigations strategies in natural navigation to optimize accuracy (Sutherland and Dyck, 1984, Maaswinkel and Whishaw, 1999, Chavarriaga et al., 2005, Kalia et al., 2013). However, by employing manipulations of sensory cues and their acquisition by animals, it has been demonstrated that the different strategies and cues used to guide navigation are used in a hierarchical fashion (Maaswinkel and Whishaw, 1999, Packard and McGaugh, 1996).

## **1.6. Cells and circuits for spatial memory and navigation: knowing one's location in space**

Navigation and spatial memory rely on various cell types distributed across different brain areas. The circuits that compute current and future locations in space, as well as environmental features, such as boundaries or goals, have been extensively studied in the past 50 years. Here I present a brief summary of the neural circuits that support navigation in mammals.

### **1.6.1. Hippocampal place cells**

Place cells were first described by John O'Keefe in the rat's hippocampus (O'Keefe and Dostrovsky, 1971), and have since been described in various species including mice (McHugh et al., 1996), bats (Ulanovsky and Moss, 2007) and humans (Ekstrom et al., 2003). These cells fire when an animal is in a given region of the environment, which is called the place field of the cell. Place fields are not topographically arranged in the

hippocampus, meaning that neighbouring cells only have adjacent place fields by chance. The entire environment is mapped by the place cell population and the same cell fires in multiple environments, not maintaining a place field relation with other cells' across environments (O'Keefe, 1976, O'Keefe and Conway, 1978, Wilson and McNaughton, 1993). These cells are regarded as the fundamental neural basis of the cognitive map described by Tolman (O'Keefe and Nadel, 1978).

The properties of place cells have been widely studied and reviewed (Redish, 1999, Best et al., 2001, Moser et al., 2008). Some of these characteristics are particularly important for the questions studied here, namely: i) place fields are anchored to the environment, which means that when distal cues are moved, place fields move accordingly (Muller and Kubie, 1987); ii) their place fields are stable if cues are removed from the environment and in the dark (O'Keefe and Speakman, 1987, Quirk et al., 1990); iii) place fields depend on head direction in unidimensional arenas but not in open fields, where the heading of the mouse does not affect firing rate (McNaughton et al., 1983).

While the hippocampus is fundamental for locale navigation, animals can still navigate successfully after hippocampal lesions using other navigation strategies (McDonald and White, 1994, Devan et al., 1996). In addition, the hippocampus is known to be a fundamental hub of learning and memory beyond spatial memory (Eichenbaum et al., 1999) and place cells are now known to not exclusively map spatial dimensions (Aronov et al., 2017).

Finally, although place cells have been initially found and extensively studied in the hippocampus, cells with similar properties can also be found in the subiculum (Sharp and Green, 1994) and medial entorhinal cortex (Quirk et al., 1992), although these present broader place fields.

### **1.6.2. The head direction system**

The head direction system represents allocentric orientation of the head of an animal irrespective from its location in the environment. Cells that encode the animal's head direction have been initially found in the postsubiculum (Taube et al., 1990b, Taube et al., 1990a) and since they have been identified in vary other areas including the dorsal tegmental nucleus (Sharp et al., 2001), lateral mammillary nucleus (Stackman and Taube, 1998), anterior thalamic nucleus (Taube, 1995), lateral dorsal thalamic nucleus (Mizumori and Williams, 1993), striatum (Wiener, 1993), RSC (Chen et al., 1994, Cho

and Sharp, 2001) and entorhinal cortex (Sargolini et al., 2006). In humans, fMRI studies showed head-direction signals in the RSC, entorhinal cortex and thalamus (Baumann and Mattingley, 2010, Marchette et al., 2014, Jacobs et al., 2010, Shine et al., 2016).

Lesions of different areas containing head direction cells result in distinct phenotypes that include impairment in working-memory-based navigation tasks and taxon, locale and path integration navigation strategies, highlighting the fundamental role of the head direction system in navigation (Vann and Aggleton, 2002, Vann and Aggleton, 2003, Vann and Aggleton, 2005, Clark et al., 2013, Frohardt et al., 2006).

The general proprieties of head direction cells and of their network system have been reviewed in detail by Jeffrey Taube (Taube, 2007). Here I present a brief summary of the fundamental characteristics of head direction cells:

The head-direction-cells' tuning is controlled by sensory cues, namely visual and olfactory, but not auditory (Goodridge et al., 1998, Taube et al., 1990b, Jacob et al., 2017). Anchoring the system to sensory cues prevents drifting of the tuning of the head direction cells, although these can also be updated by idiothetic cues (Yoder et al., 2011, Knierim et al., 1998). When visual cues are made in conflict with idiothetic cues, the former typically dominate the tuning of head direction cells although incompletely, with both inputs weighing in (Zugaro et al., 2000, Goodridge and Taube, 1995, Blair and Sharp, 1996).

Despite not being lost in the dark, head-direction mapping accumulates error in such condition. Notably, this drift is equal in all head direction cells, as the preferred angular distance between cells is constant (Bicanski and Burgess, 2016, Goodridge et al., 1998, Taube et al., 1990b, Yoganarasimha et al., 2006). Head direction cells reorient to visual cues as rapidly as 80ms after having drifted in the dark (Zugaro et al., 2003). As a consequence of being anchored to cues in the environment, rotation of such cues proportionally rotate the tuning of head direction cells, as also seen in place cells (Taube et al., 1990b, Taube, 1995).

Head direction cells in different areas have distinct anticipatory time intervals<sup>7</sup>, ranging from 25 ms in the anterior nucleus of the thalamus and retrosplenial cortex to 75 ms in the lateral mammillary nucleus. The details of anticipatory coding in the head direction

---

<sup>7</sup> The anticipatory time interval of head direction cells is the time interval the cell's coding activity anticipates the future head direction of the animal.

system have been reviewed (Taube, 2007) and subject of modelling work (Zirkelbach et al., 2019).

The coding of cells classified as head direction is not limited to such variable. In some areas, such as the anterior thalamic nucleus (Taube, 1995) and the RSC (Cho and Sharp, 2001), head direction cells also encode angular head velocity. In addition, place-dependent head direction cells were found in the RSC (Cho and Sharp, 2001), and presubicular and parasubicular cortices of the rat (Cacucci et al., 2004). The authors of the latter study propose that these ‘theta-modulated place-by-direction cells’ mediate the integration of head direction information into the theta-modulated network. Interestingly, these cells do not remap across environments, maintaining a preferred absolute firing direction.

### **1.6.3. Medial entorhinal cortex: grid, boundary, speed and object-vector cells**

The medial entorhinal cortex (MEC) has been widely studied in the context of spatial memory, after May-Britt and Edvard Moser’s group described the existence of grid cells in mice (Hafting et al., 2005, Fyhn et al., 2004). Since then various other cell types that are important to map location in space have been described in the MEC: head direction cells (Sargolini et al., 2006), border cells (Solstad et al., 2008), speed cells (Kropff et al., 2015) and object-vector cells (Høydal et al., 2019). Although they have been widely studied in rodents, grid cells have also been reported in human studies (Doeller et al., 2010, Jacobs et al., 2013).

Grid cells are exclusive to the MEC, the pre- and parasubiculum. These respond to the location the animal occupies in the environment, presenting periodic hexagonally arranged firing fields, meaning that the same cell will fire at multiple discrete and regularly spaced locations in the environment (for a review see (Rowland et al., 2016, Moser et al., 2014)). Neighbouring grid cell’s fields are not necessarily adjacent, meaning they are not topographically arranged, although the scale of the grids is topographically arranged along the dorsoventral axis of the MEC (Hafting et al., 2005, Brun et al., 2008).

Unlike place cells, the firing fields relations between cells are preserved across environments in grid cells (Fyhn et al., 2007). The stable and periodical structure of the grid fields has made the grid cells be regarded as the metric system for space mapping (Moser et al., 2008). Similarly to place cells (Gothard et al., 1996), grid cells’ fields are maintained in the dark and the network activity can be updated by idiothetic cues during

path integration (Hafting et al., 2005). Also like place cells and head direction cells, grid cells anchor their activity to external reference cues, and if these are rotated, grid cell fields rotate similarly (Hafting et al., 2005).

Speed cells are a dedicated population of cells found in the MEC, that encode the running speed of the animal in a context invariant manner (Kropff et al., 2015). Together with grid cells, speed cells are good candidates to mediate path integration as together they provide absolute measurements of space and movement along it (Moser et al., 2014). Evidence of the involvement of the MEC in path integration is not consensual with rodent studies showing this area is necessary for path integrating (Parron and Save, 2004, Van Cauter et al., 2012) and human studies making the opposite point (Shrager et al., 2008). Interestingly, a similar dichotomy between the performance of rats and humans following hippocampal lesions has been reported, which the authors suggest may be attributed to humans being able to navigate based on a, hippocampal independent, working-memory framework (Kim et al., 2013).

Border cells have also been found in the MEC and adjacent parasubiculum by the Moser Lab. These cells signal geometric boundaries of the local environment by firing when the animal occupies a given position in relation to an edge of such environment. For example, a border cell will fire when an animal is south of any given number of borders in an environment. The authors hypothesize these cells are essential for anchoring both grid and place fields to the geometric reference frame of the environment (Solstad et al., 2008).

Finally, object-vector cells were recently described by the Moser lab in the MEC. These cells fire when the animal position defines a given vector in relation to an object in the environment, independently of the object absolute position or identity and of the animal moving direction (Høydal et al., 2019).

Taken together the presence of various types of spatial mapping cells in the MEC make this region well equipped to contribute with various metrics essential for navigation. The MEC's central role for spatial memory is illustrated by the fact that its lesion decreases the number of active place cells in the hippocampus and a decrease in spatial precision and stability of the remaining cells. Rats with lesions of the MEC were shown to be critically impaired in the Morris water maze task but not as much as rats with simultaneous lesions of MEC and hippocampus (Hales et al., 2014).

#### 1.6.4. Cells mapping egocentric location in space

Recent papers reported the existence of ‘egocentric boundary vector cells’ (EBCs) in the RSC (Alexander et al., 2019), lateral entorhinal cortex (LEC) (Wang et al., 2018) and dorsomedial striatum (Hinman et al., 2019). These cells map the position of the animal in relation to the boundaries of the environment, but unlike boundary cells, which fire when the animal is located adjacent to the border, EBCs fire when the boundaries are located at a given orientation and distance relative to the animal, in egocentric coordinates.

The RSC is reciprocally connected with egocentric and allocentric networks, making it a great candidate for performing allocentric-egocentric representation transformations. In fact, it had previously been suggested that the translation between allocentric representation and egocentric space happens in the posterior parietal cortex (PPC) and RSC (Byrne et al., 2007, Bicanski and Burgess, 2018, Wilber et al., 2014), and it is plausible that EBCs play an important role in such transformation. In addition, RSC and PPC, together with the postrhinal cortex (LaChance et al., 2019) and LEC (Wang et al., 2018) have been suggested to contribute to creating an allocentric representation from the egocentric-by-nature sensory information that the animal acquires.

Another recent study (Laurens et al., 2019), in which the authors recorded from multiple areas known to be involved in navigation, equally showed cells in the RSC and in the hippocampus, that encode the egocentric position of the arena’s boundary. The authors report that approximately half of the neurons recorded in RSC showed tuning to egocentric boundaries and of these approximately 50% were significantly tuned to HD, suggesting a role for the RSC in combining different dimensions of spatial mapping.

Although cells encoding egocentric vector distance between an animal and the centre of an arena have been found in the postrhinal cortex (LaChance et al., 2019), it is unclear how they behave in complex and nonsymmetric environments, which would be critical to understanding their computation. Nevertheless, this study adds up to the building evidence of egocentric vector coding in the cortex.

In addition to EBCs, egocentric vector representation of objects and goals have been found in the LEC. The activity of these cells in the LEC together with the various metrics of space mapped by different cell types in the MEC have been suggested to drive the allocentric representation of space in the hippocampus (Wang et al., 2018). The relation between egocentric goal bearing cells in the LEC and goal-vector cells described in the

hippocampus (Sarel et al., 2017) is still unknown as are their contribution towards goal-directed navigation.

## **1.7. Goal directed orientation and navigation**

In the last section I summarized the contributions of various brain regions and cells to map the ongoing position of an animal in space. While place and grid cells map space in an allocentric framework, animals operate in egocentric motor space and a transformation between allocentric and egocentric reference frames should be necessary for goal directed navigation. As mentioned above, the RSC is thought to be involved in this transformation (Bicanski and Burgess, 2018, Burgess et al., 2001, Byrne et al., 2007) and if that is the case, this area would also be a good candidate for informing premotor or motor areas about the ongoing egocentric offset in relation to the allocentric position of a goal in the environment.

In this section I will summarize i) the contribution of the RSC for spatial memory and goal directed navigation, ii) the current views on how animals implement goal-directed navigation and finally, iii) the mechanisms for a specific type of goal-directed movement relevant to this work, the head-orienting movement.

### **1.7.1. Contribution of the retrosplenial cortex for spatial memory and navigation**

The RSC receives afferents from the subiculum (Witter et al., 1990), the major output of the hippocampus (Swanson and Cowan, 1977), and other hippocampal and parahippocampal subregions (Sugar et al., 2011, Miyashita and Rockland, 2007); areas known to have head direction cells, namely: the postsubiculum (van Groen and Wyss, 1990), the anterior thalamic nuclei (Vogt, 1985, van Groen and Wyss, 1992) and the lateral dorsal nucleus of the thalamus (Robertson et al., 1980, van Groen and Wyss, 1992); and from the visual cortex (van Groen and Wyss, 1992). Importantly for this work, the efferent projections of the RSC include the mid layers of the SC, the PAG and ventral pontine nucleus (van Groen and Wyss, 1992, Künzle, 1995, Oh et al., 2014). In addition, the RSC projects to other cortical areas involved in motion and navigation such as the secondary motor cortex and the PPC (Yamawaki et al., 2016).

In rats, 6-8% of the cells in the RSC have head-direction tuning (Chen et al., 1994, Cho and Sharp, 2001). Like head-direction cells in other areas, RSC head direction signal correlates better with future heading, having a 25 (Cho and Sharp, 2001) to 50 ms (Lozano et al., 2017) look-ahead. 19% of head direction cells in the dysgranular part of the RSC were shown to be modulated by movement, especially angular motion (Chen et al., 1994). The authors suggest that this characteristic may be important to integrate egocentric motor coordinates and allocentric head direction. Additionally, 'direction-dependent place cells' have been found in the RSC; these cells showed higher activity when the animal displayed given combinations of location, head-direction and (in some of the cells) ongoing linear and angular speeds (Cho and Sharp, 2001). One of the hypotheses that the authors raise for the function of such cells is that they may anticipate arrival at a future location.

A subset of head-direction-tuned RSC neurons was found to be dissociable from the categorical head direction cells (Jacob et al., 2017). These were named bidirectional cells, and their firing-tuning exhibits bidirectionality in symmetric environments, demonstrating they are dominated by sensory cues rather than by an absolute head direction signal. The authors of the study hypothesise that these cells may mediate the integration between visual inputs and the global head direction system, and this interface may be responsible for determining cue stability in relation to the head orientation and be suitable for anchoring the head direction system.

The RSC was shown to encode position along route-centred space, and both position-dependent and -independent right or left turns along a zigzagging corridor (Alexander and Nitz, 2015). In addition, in a study involving navigation to a cued, rewarded arm of a T-maze, some RSC neurons were shown to encode the rewarded arm, while others exhibited conjunctive coding of current position and future arm choice (Vedder et al., 2016). Nevertheless, the discrete choice imposed by constrained mazes makes it difficult to extrapolate these findings to an open environment with non-stereotypical goal locations.

Allocentric head direction signal has also been reported in human RSC, through fMRI studies (Shine et al., 2016). The human RSC has been shown to be critical to establish ongoing orientation relative to elements from the external world, by representing the locations and heading direction anchored to local topographic features (Marchette et al., 2014). It has also been shown that the RSC encodes the location of permanent objects in an environment, which may be key to its allocentric anchoring function (Auger and

Maguire, 2013, Auger et al., 2012). fMRI data from human navigation in virtual-reality show that both the posterior hippocampus and the RSC track distance to goal in memory based but not in external cue guided navigation. While the hippocampus does so in familiar and recently learned environments, the RSC only tracks goal distance in familiar environments (Patai et al., 2019). The RSC was shown to be involved in goal-directed path integration in humans (Sherrill et al., 2013). Interestingly the same study showed recruitment of the hippocampus, particularly once the periphery of the goal location was reached.

Lesions of the RSC in humans lead to different spatial memory deficits than those following hippocampal lesions. Humans with retrosplenial lesions are able to identify familiar places but fail at orienting from one of such places to another, a disorder known as topographic disorientation (Takahashi et al., 1997, Osawa et al., 2008, Ino et al., 2007). Lesions of the RSC in rats were shown to impair allocentric navigation tasks such as the Morris water maze task (Vann and Aggleton, 2002, Harker and Whishaw, 2002, Sutherland et al., 1988), taxon and praxic navigation tasks (Cain et al., 2006), and path integration based tasks (Whishaw et al., 2001, Cooper and Mizumori, 1999, Cooper and Mizumori, 2001).

The organisation of the head direction system follows a hierarchical structure (Cho and Sharp, 2001) and lesion of the RSC was shown to disrupt the stability of heading representation in the anterodorsal thalamus, even in the presence of salient visual cues (Clark et al., 2010). The authors of the study showed that the lesion weakens landmark but not idiothetic control over head direction cells in the anterodorsal thalamus, suggesting that the RSC is essential to process landmark features and map head direction onto them.

By recording the activity of neurons in hippocampal CA1 and CA3 while conducting the retrosplenial lesions, Cooper and Mizumori reported temporary shifts in place fields following temporary inactivation of the retrosplenial cortex even in illuminated environments (Cooper and Mizumori, 2001).

### **1.7.2. Mechanisms for goal directed navigation**

Much more is known about the neural mechanisms that map ongoing position of the animal in the environment than how such information is used to guide navigation. The

body of work on allocentric-egocentric transformations leads to interesting hypothesis but a general mechanism for goal directed navigation still does not exist.

There are different theories concerning how animals navigate to goals. One theory, supported by experimental data (Pfeiffer and Foster, 2013, Johnson and Redish, 2007), is that place cell activity's sequences encode future paths to learned goals; such sequences recorded in rats were shown to predict immediate future navigation even for paths that had not been travelled before in a known environment. Furthermore, it has been proposed by modelling that animals may probe look-ahead trajectories until simulation a place cell sequence that leads it to a goal located place cell (Erdem and Hasselmo, 2012, Erdem and Hasselmo, 2014).

Both place cell (Hok et al., 2007, Hollup et al., 2001, Dupret et al., 2010) and grid cell (Boccaro et al., 2019) maps have been shown to reorganize in the presence of a goal in the environment, with goal locations being more densely mapped by both cell types. In addition the firing rate of many CA1 and entorhinal cortex cells is modulated by the past or future position (Frank et al., 2000). Despite this, it is not known if and how sequential activation of hippocampal cells control future navigation or are a readout of another area doing so. Recent work favoured the second option, by proposing that a pathway from prefrontal cortex to CA1 via the nucleus reuniens conveys the representation of future path to the hippocampus (Ito et al., 2015). The same study showed that inactivation of the nucleus reuniens in the thalamus significantly decreased the trajectory dependency in CA1 firing.

Another way goal directed navigation could be implemented is by tracking a vector towards goal. This is the conceptual model of path integration, and although many areas have been shown to be involved in this navigation strategy, we still do not have a mechanistic understanding of this computation. As mentioned above, egocentric goal-vector cells have been found in the LEC of rats (Wang et al., 2018) and in hippocampal CA1 of bats (Sarel et al., 2017) and could potentially support a vector-based navigation system.

Although both theories present cell whose activity can predict the immediate future path of an animal it is still unknown if and how either of these signals is used to guide behaviour.

### 1.7.3. Mechanisms of head-orienting movements

To get to a goal, animals need to orient to it. In this section I summarize the neural mechanisms that control head-orienting movements.

Although most orientation research focuses on eye orientation movements (particularly saccades), to a great extent, eye and head orientation movements rely on similar circuits (Freedman et al., 1996, Walton et al., 2007, Scudder et al., 2002), and particularly for larger movements, these two movements are combined in a coordinated manner (Freedman and Sparks, 1997, Guitton et al., 1984, Freedman, 2008).

Saccadic and head-orienting movements have been widely studied in the context of orientation towards a visual target, and their execution depends on representation of the goal in retinal, head or body and motor coordinates. The computed retinal error<sup>8</sup> is in turn used to compute a motor error<sup>9</sup> which determines the amplitude and direction of the orientation movement (Sparks, 1989). These computations are dynamic and also occur during the movement itself (Becker and Fuchs, 1969, Hallett and Lightstone, 1976). However, orientation movements can be performed also in the dark and towards memorized locations, despite typically having slightly slower dynamics (Becker and Fuchs, 1969).

Both retinal error and motor error representations have been found in the SC in monkeys (Mays and Sparks, 1980). The superficial layer of the SC maps visual stimuli in retinotopic space and the intermediate layer computes saccades in motor space (Mays and Sparks, 1980). Activity in the intermediate layer of the SC does not depend on visual stimulation and can be for example driven by auditory cues (Jay and Sparks, 1987) or by afferents from the frontal eye fields (FEF) possibly controlling memory guided voluntary saccades (Gaymard et al., 1998a, Sommer and Wurtz, 2000).

Stimulation of a given region of the SC elicits a contralateral, egocentrically reproducible saccade (Robinson, 1972), or a coordinated gaze and head orienting movement if the animal is not head-fixed (Freedman et al., 1996). The amplitude of saccades elicited by SC stimulation is independent from the initial eye position, hence not goal directed, demonstrating that SC cells do not encode motor space allocentrically but rather controls saccades in an egocentric reference frame. The amplitude of the saccade elicited depends on the position along the anterior-posterior axis of the SC where the stimulus is triggered:

---

<sup>8</sup> offset between target and the fovea.

<sup>9</sup> offset between target and the position of the head.

small saccades are elicited anteriorly and larger saccades posteriorly (Robinson, 1972). Recordings from the SC in head-free monkeys show that neurons encode the total amplitude of head and eye movement rather than the amplitude of the movement of the eye-over-head (Freedman and Sparks, 1997). In addition, recordings from cat SC showed that it encodes the egocentric angular distance to the final position rather than a saccade or sequence of saccades to get there (Bergeron et al., 2003, Mohler and Wurtz, 1976), suggesting the SC is not a purely motor control area but rather acts to ensure the appropriate movements are made to reach the target direction.

Monkey's deep SC neurons, discharge prior to saccades of fixed amplitudes, even in the absence of new visual stimuli, as this is also observed in darkness (Schiller and Stryker, 1972, Wurtz and Goldberg, 1971). SC control of saccades has been proposed to be implemented via the medial pontine reticular formation (Keller, 1979, Sparks and Mays, 1980), where it directly projects to (Grantyn and Grantyn, 1982), and which in turn projects to oculomotor neurons (Scheibel and Scheibel, 1958). The amplitude of the saccade is determined by spatial distribution of collicular activity rather than being encoded in the pattern of spike activity of single cells (Sparks and Mays, 1980), in contrast with the linear correlation between pontine reticular spike burst duration and the amplitude of the saccades (Luschei and Fuchs, 1972, Keller, 1974, Cohen, 1972). Head rotation movements are thought to be controlled by tectoreticulospinal neurons which firing rate is proportional to the speed of rotation and the burst duration determines the amplitude of rotation (Grantyn et al., 1993, Scudder et al., 2002). Finally, it has been shown that stimulation of the paramedian pontine reticular formation can elicit both eye or conjugated eye and head orientation movements, suggesting it controls both ocular motor neurons as well as cervical motor neurons (Gandhi et al., 2008).

In rodents, SC stimulation elicits head rotation movements, which depend on the location of stimulation along the anteroposterior SC axis and also on the number of trains in the stimulation protocol (King et al., 1991). Previous primate studies had shown that prolonged stimulation of the SC elicits a sequence of saccades similar in direction and amplitude (Schiller and Stryker, 1972). A study involving lesions and recordings from the SC in freely moving rats showed that this circuit is essential for the execution of orientation-dependent locomotion (Felsen and Mainen, 2008). Accordingly, another study reported that lesions of rat's lateral division of the SC with muscimol induces ipsilateral rotation movements and impairs contralateral head orienting movements (Wang and Redgrave, 1997). A recent study performed in mice demonstrates that neurons in the SC encode future head rotations in egocentric space and, as observed in other

species, the firing rate of neurons correlates to speed of rotation but not amplitude of movement (Wilson et al., 2018).

Apart from the SC functioning as a sensory-motor transformation area that guides saccades to sensory stimuli, it receives various cortical and subcortical inputs. Projections from the FEF and ACC to the SC (Comoli et al., 2012, Savage et al., 2017) are thought to be important for memory driven orienting movements.

Stimulation of the FEF also elicits contralateral saccades with an amplitude that depends on stimulation location (Robinson and Fuchs, 1969). Similarly to the SC the FEF has a topographic arrangement representing the target of saccades in retinotopic coordinates; smaller saccades are elicited ventro-laterally and larger saccades dorso-medially (Bruce et al., 1985). The FEF projects to the deep layers of the SC (Kuypers and Lawrence, 1967), and yet stimulation of the FEF triggers saccades with shorter latencies (15 ms) than SC stimulation (20 ms), suggesting that eye movements elicited from the FEF can bypass the SC to control directly the pontine nuclei (Robinson, 1972, Robinson and Fuchs, 1969). Lesions of the FEF produce only mild reduction of the gain of contralateral visually-guided saccades, but make memory-guided saccades highly inaccurate, suggesting the FEF is essential to control memory-guided saccades towards targets in space via the superior colliculus and brainstem premotor areas (Pierrot-Deseilligny et al., 1995).

Neurons in the ACC have been shown to encode the direction of the previous saccade and its associated reward in a variable-reward task, making this region a potentially critical hub for forming associations between actions and outcomes (Hayden and Platt, 2010). The posterior cingulate has also been shown to encode saccade reward in monkeys (McCoy et al., 2003). Finally, studies in human patients with lesions of the posterior portion of the right ACC have shown increased latency and decreased gain of memory-guided saccades (Gaymard et al., 1998b).



## **2. AIMS**

Defensive behaviours are a powerful entry-door to study cognitive functions such as spatial memory and goal-directed navigation (Evans et al., 2019). Previous studies demonstrated that the choice of defensive action is flexible as a function of environmental features. Specifically, it has been shown in various species that escape is favoured in the presence of a refuge, while freezing is preferred when no refuge is available (Hennig et al., 1976, Blanchard et al., 1986, Wei et al., 2015, De Oca et al., 2007, O'Brien and Dunlap, 1975). Nevertheless, not much more is known about the space-dependent flexibility of defensive behaviour, namely what are the temporal dynamics of learning and updating of knowledge about the environment features that dictate the flexibility of choice of defensive actions. Flexibility of execution of defensive actions, particularly escape, has also not been explored. It has been shown before (Yilmaz and Meister, 2013, Clarke et al., 1993, Dill and Houtman, 1989, Ellard and Eller, 2009, Ellard and Goodale, 1988) that mice escape to refuges, although navigation profile and strategy during escape have not been described.

This work aims to investigate how mice adapt the choice and execution of anti-predatory defensive actions to the environment they occupy, and the neural basis of how the representation of the environment controls defensive actions. To do so, I have employed a top-down approach, aiming to first dissect the behavioural component, namely understanding the dynamic proprieties of choice of defensive action and the navigational features of escape towards a refuge. Since I consider escape can be a powerful tool in the study of goal-directed navigation I aim to detail this behaviour and propose a framework to study navigation and spatial memory based on escape behaviour. After having described the behaviour my goal is to identify neural substrates controlling navigation in escape and understand the mechanism through which goal location is mapped and how it is used to guide goal-directed behaviour.

### **3. METHODS**

### 3.1. Animals

Male C57BL/6J wild-type mice, between 6 - 24 weeks-old, were used for all behavioural experiments. All wild-type animals were acquired from Charles Rivers and were housed in a holding-room for at least one week before the beginning of experimental procedures. Mice were single-housed immediately after surgery or at least 72 h before behavioural experiments when no surgical procedure was performed. Except for probe recording experiments, all behavioural assays were conducted during the light phase of the light cycle.

Mice used for whole-cell patch-clamp recordings were VGluT2::EYFP (resulting from in-house cross of VGluT2-ires-Cre with R26-stop-EYFP, both from Jackson Laboratory (stocks #016963 and #006148, respectively)), or VGAT::EYFP (resulting from in-house cross of VGAT-Cre with R26-stop-EYFP, both from Jackson Laboratory (stocks #016962 and #006148, respectively)), and were sacrificed at 5 – 8 weeks old. Mice used for rabies tracing were VGluT2-ires-Cre or VGAT-Cre (Jackson Laboratory, stock #016963 and #016962, respectively) and were sacrificed at 9 – 20 weeks old. All genetically modified animals were bred in the Sainsbury Wellcome Centre. Genotyping performed by Transnetyx using real-time PCR, on an ear notch acquired at 2 weeks old.

All animals were housed with *ad libitum* access to food and water on a 12 h light cycle; home-cages of all mice contained a shelter, which was different from the shelter used in the behavioural assays. All animal procedures were performed under the UK animals act of 1986 (PPLs: 70/7652 and PFE9BCE39).

### 3.2. Escape behaviour assay

*Here I describe the general experimental set-up, procedure and data analysis for the escape behaviour assays used in results chapters 4 and 5. When different experiments were performed or simple modifications were done to test specific hypotheses, such modifications are described in the results text. More significant modifications in the set-up, procedure or data analysis methods are detailed below.*

### 3.2.1. Experimental set-up

Unless otherwise specified in the results, for all experiments shown in chapter 4 ('Results: rapid learning controls anti-predator escape behaviour') the behavioural arena was a modified Barnes maze (Barnes, 1979) consisting of a 92 cm diameter, white acrylic circular platform with 20 equidistant, circular holes, located radially, 5 cm from the edge of the platform. 19 of these holes were closed with black plastic plugs (1 cm deep), while the remaining one led to a black, underground Perspex shelter (dimensions: 15 x 5.8 x 4.7 cm), which the mouse could freely and easily enter and exit. The platform was elevated 45 cm from the floor to prevent mice from climbing down as no walls were present in the arena. The central area of the arena was a 22 cm diameter fixed platform, and the periphery (70 cm diameter) was mounted on a motorized frame which allowed remotely-controlled rotation over 360° in both directions. The platform was surrounded by explicit visual cues consisting of 2D printed symbols with a variety of shapes, colours and patterns, with dimensions ranging from 100 to 310 cm<sup>2</sup>, that were attached to the inside of the arena cabinet unless otherwise noted. An olfactory cue consisting of a small portion of the animal's own home-cage bedding was placed inside the shelter. The behavioural apparatus was enclosed inside a sound-deadening and light-proof cabinet, to prevent external cues from affecting the experiment. For the arena rotation experiment, the platform was surrounded with an opaque black cylinder with 112 cm diameter and 55 cm height, that prevented visualization of non-explicit cues inside the behavioural cabinet; in addition, the explicit visual cues were attached to the behavioural platform to allow coherent rotation with the shelter (Figure 3A and B).

For the experiments shown in chapter 5 ('Results: a projection from retrosplenial cortex to superior colliculus is critical for orientation during escape') a similar set-up was used with the difference that the arena was a single 92 cm diameter platform, with no holes, and the shelter was an over-ground red translucent Perspex box. The shelter was positioned facing the centre of the arena; its dimensions were 20 x 10 x 10 cm and it had a 5 cm wide entrance that faced the centre of the arena.

Experiments were recorded at 30-50 frames per-second with a near-infrared camera, with a long-pass filter (>700 nm); 6 infrared lights (Abus TV6700) were distributed in the environment. When conducting experiments in light conditions, I used a projector (InFocus IN3126 or BenQ MW843UST) pointed at a translucent screen (Xerox 100 micron drafting film) centred 64 cm above the arena to illuminate the environment.

Experiments presented in chapter 4 were conducted with a background luminance of 6.7 lux, whereas experiments presented in chapters 5 and 6 were conducted with a luminance of 2.7 lux, after observing such decrease in luminance significantly increased exploration of the arena; experiments performed in the dark had a background luminance below 0.04 lux. Additionally, the projector was used to project overhead aversive visual stimuli. An ultrasound speaker (Pettersson L60) was also placed centrally above the arena and was used to deliver aversive auditory stimuli. The computer used to elicit auditory stimulus was connected to the speaker via a soundcard (Xonar D2) and an amplifier (QTX PRO240). I used custom-designed software (LabVIEW-based, developed by Kostas Betsios) to track the position of the mouse online and to deliver the different modalities of aversive stimuli (Figure 3B).

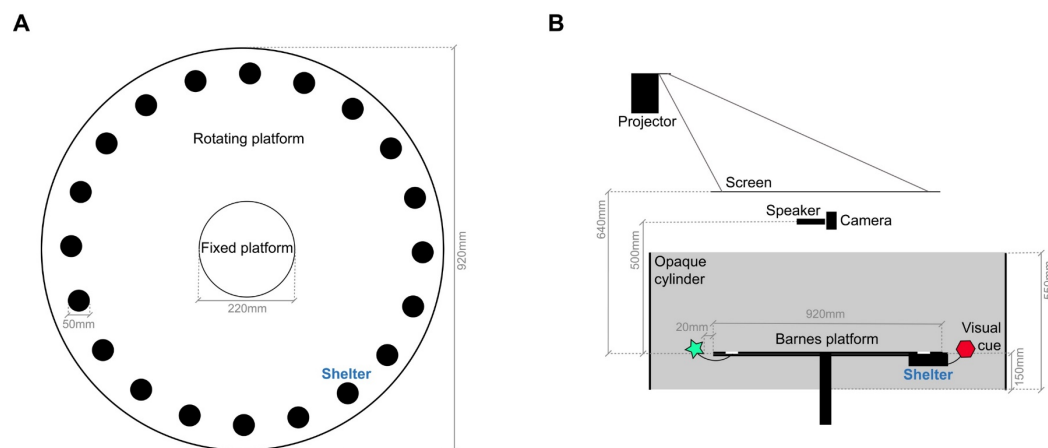


**Figure 3: Schematic representation of behavioural apparatus**

A is a top-view and B a side-view schematic of the main components of the behavioural set-up. While the centre of the platform is fixed the external part can be rotated. In all experiments excluding the arena rotation assay the visual cues were attached to the arena cabinet, whereas in the rotation experiment these were attached to the rotating platform (as depicted in B), allowing coherent rotation of the arena, the visual cues and the shelter. The dark circles in top view (A) are the holes that potentially can lead to the shelter and are all visually identical (an example shelter location is indicated). The entire arena is enclosed in a light-proof, sound-dampening cabinet. Adapted from Vale et al., 2018.

### 3.2.2. General procedure

Mice were single housed at least 72 h before the behavioural assay<sup>10</sup> and were brought into the testing room at least 10 minutes before the start of the experiment. Before each experiment the behavioural platform and shelter were meticulously cleaned with 70% ethanol, rinsed with water and dried. The position of the shelter for each experiment was determined randomly before the experiment, and some bedding from the animal's home-cage was placed inside the shelter. This olfactory cue was used to ensure consistency throughout the experiment, as one has no control over mice's biological waste which is often deposited in the shelter throughout the experiment and can serve as an olfactory cue.

The mouse was then gently placed in the centre of the behavioural platform and video acquisition was initiated. A 7 min habituation period was given, during which the mouse had to fully enter the shelter at least once, which in my experience always happened. Under no circumstance was the mouse passively displaced or removed from the shelter. After these 7 min and when the animal voluntarily came outside of the shelter, sensory stimuli were manually triggered. Multiple stimuli of a single sensory modality were delivered in a session, with at least 90 s interstimulus interval. In addition, the mouse had to visit the shelter, at least once, between the delivery of consecutive stimuli.

For the experiments shown in chapter 5 ('Results: a projection from retrosplenial cortex to superior colliculus is critical for orientation during escape') only auditory stimuli were presented. The first half of the experiment was conducted with lights on, and after delivering 7 auditory stimuli or 45 minutes (whichever first), the lights were turned off and the mouse was given 5 minutes to explore the environment, before further stimuli were presented.

Experiments were stopped at the end of 90 minutes or if the mouse stopped exploring the environment, remaining inside the shelter.

---

<sup>10</sup> Mice were single-housed for two reasons: 1) we find that baseline exploratory behaviour of single-housed mice is more comparable across animals than across group-housed mice; 2) following surgical procedures, such as intracerebral injections or implantations, mice were single-housed for health and safety reasons; in order to maintain similar housing conditions across mice, wild-type naïve mice were also single-housed.

### 3.2.3. Sensory stimuli

Visual stimuli were backprojected on to a screen positioned above the behavioural arena and consisted of an expanding dark circle (Webster contrast = -0.98) on a gray background (luminance = 6.7 lux). Unless otherwise specified, the expanding spot was centred above the online-tracked position of the mouse, subtending a visual angle of  $2.6^\circ$  at onset and expanding linearly at  $224^\circ/\text{s}$  over 200 ms to  $47.4^\circ$ , at which it remained for 250 ms.

For sound-elicited escape assays presented in chapter 4 ('Results: rapid learning controls anti-predator escape behaviour') I used a train of three frequency modulated upsweeps from 17 to 20 kHz over 3 s, lasting in total 9 s. For sound-elicited escape assays presented in chapter 5 ('Results: a projection from retrosplenial cortex to superior colliculus is critical for orientation during escape') I presented a single frequency modulated upsweep from 17 to 20 kHz lasting 2 s. Sound pressure level was measured in the centre of the arena floor and varied between 73 and 81 dB. The sound stimuli were always elicited from a speaker centred 50 cm above the arena floor.

### 3.2.4. Analysis

Onset of escape from threatening stimuli was determined by visual inspection of the video recordings and considered as either the onset of a head-rotation movement or an acceleration (whichever first) after the mouse visibly detected the stimulus<sup>11</sup>. Latency to escape refers to the time interval between stimulus presentation and the onset of escape.

Escape termination was defined as a deceleration to less than 9 cm/s (mean baseline speed during exploration) above one of the holes or arrival at shelter<sup>12</sup>. Accuracy of escape was measured in relation to the position at which escape was terminated, as the number of holes by which the target was missed. Since there are 10 holes in  $180^\circ$ , each hole-increment determines an error of 18 degrees or 10%; therefore, the percentual accuracy of escape was computed as:

---

<sup>11</sup> Mice reliably startle in response to the sound stimuli used, and either startle or suddenly interrupt locomotion upon presentation of the expanding visual stimulus

<sup>12</sup> Arrival at shelter was defined when the animal had the torso and all four limbs inside the ramp that leads to the underground shelter, or when it had more than half of the body inside the over-ground shelter.

$$\text{Accuracy of escape (\%)} = 100 \% - (\text{number of holes to shelter} \times 10\%)$$

Escape error is used in chapter 5, instead of accuracy of escape. Because the focus was on orientation to shelter, I measured the (egocentric) angular offset between the mouse's heading and the direction of the shelter, after the mouse performs a head-rotation or accelerates after detecting the auditory stimulus (This metric is illustrated in results, Figure 16C).

Probability of flight was quantified as the percentage of trials in which the mouse accelerated above two standard deviations of the mean baseline speed (measured 3 seconds before stimulation) during the length of the stimulus.

Probability of freezing was quantified as the percentage of trials in which the mouse remained immobile for at least 500 ms following presentation of the sensory stimulus, as previously described (De Franceschi et al., 2016).

Linearity of escape was measured only for escapes with 100% accuracy and was expressed as the ratio between path length during escape and the distance to shelter upon onset of escape. Foraging linearity was calculated by testing the linearity of the exploration bout that preceded the presentation of each stimulus, from the moment the mouse left the shelter. It was computed as the ratio between displacement during this period and the distance between the shelter and the position the mouse occupied upon stimulus presentation.

Head-shelter offset angle was measured manually using a custom-designed Python-based graphic interface. Angles were measured between 0 and 180° where 0° means the mouse heading is perfectly aligned to the centre of the shelter entrance, irrespective of its position in the arena.

Time to shelter was quantified as the time from presentation of the aversive stimulus until the mouse entered the shelter.

In the assay where the shelter was displaced without rotating the arena (Figure 15) flights were considered as targeting the old or new shelter location if they had an accuracy of 80-100% towards one of the respective targets.

Of the 36 animals to which visual stimuli were presented, 2 were excluded from the study for not responding to these stimuli. No animal was unresponsive to the auditory stimuli. Trials in which mice were rearing or leaning down the arena upon stimulus presentation were excluded from the data analysis (< 1%). The arena rotation experiment presented in chapter 4 relies on rotating the shelter and sensory cues in the environment but not the mouse; trials in which the mouse left the fixed platform during rotation and was therefore displaced passively, were excluded from data analysis (54 %). For the analysis of results presented in chapter 5, trials in which the animal did not visibly respond to the sensory stimulus by accelerating or by engaging in an orienting movement were excluded (< 3%).

### **3.3. Exploration behaviour assay and chronic extracellular recordings**

#### **3.3.1. Set-up**

*The setup used for this experiment was similar to the one used in the standard escape assay. Below I list the differences in the set-up.*

Extracellular recordings from freely moving animals were performed in a 92 cm diameter white platform without walls, elevated 45 cm from the ground, and containing an over-ground shelter (20 x 10 x 10 cm; 10 cm wide entrance) positioned by the edge and facing the centre of the platform. Two explicit visual cues were positioned in the environment: an LED, always positioned on the ‘West wall’ of the behavioural cabinet, and an A2 white sheet, always positioned in the ‘South wall’ of the cabinet, both distal to the platform. A rotary joint (adapted from Doric AHRJ-OE\_PT\_AH\_12\_HDMI) was used to prevent the cables from twisting, which would generate tension and might bias the animals’ head movements.

### 3.3.2. Procedure

4 male adult C57BL/6J wild-type mice were single-housed after probe implantation in a reversed 12 h light cycle and tested during the dark phase. The minimum interval between consecutive experiments was 72 h.

Each session included 3 epochs: in the first one the mouse was placed in the circular arena for 30 minutes without the shelter; in the second the shelter was introduced on the ‘East side’ of the arena (named shelter position 1); in the third epoch the shelter was moved by the experimenter to the ‘North side’ of the arena (named shelter position 2) (as shown in results: Figure 26C). The mouse was allowed to explore the arena freely for at least 30 minutes for each epoch.

All experiments were performed in the presence of visible lights (luminance of 2.7 lux).

### 3.3.3. Data acquisition and processing

Recordings were performed with Neuropixels probes (384 recording sites, phase 3A, option 1; Jun et al., 2017b) implanted chronically through the retrosplenial cortex (RSC) and superior colliculus (SC) of the right hemisphere. Extracellular potentials were acquired using the software SpikeGLX (<https://github.com/billkarsh/SpikeGLX>, Janelia Research Campus) and were amplified (500 x), high-pass filtered (300 Hz) and sampled at 30 kHz. Custom-designed LABView-based software (Mantis software, [mantis64.com](http://mantis64.com)) was used to acquire the video of the experiment at 40 fps.

All implanted probes were coated with DiI (Invitrogen) before the surgery, and upon termination of the experimental protocol, brains were perfused and either sectioned with a cryostat (Leica 3050 S) and imaged with an epifluorescence microscope (Zeiss Axio Imager 2) or imaged by serial micro-optical sectioning 2-photon tomography (Zheng et al., 2013, Ragan et al., 2012, Li et al., 2010), to confirm the location of probe implantation and to determine which recording sites of the probe were located in RSC and in SC. Probe location was assigned according to the Allen Mouse Brain Reference Atlas (© 2015 Allen Institute for Brain Science. Allen Brain Atlas API. Available from: [brain-map.org/api/index.html](http://brain-map.org/api/index.html)).

Data analysis was performed in MATLAB. Spike sorting was done using Janelia Rocket Cluster 3.0 (Jun et al., 2017a) or Kilosort 2.0 (Pachitariu et al., 2016) and manually

refined. Only units that had an absolute refractory period of at least 1 ms were included in subsequent analysis.

Behavioural variables were extracted from video recordings using DeepLabCut (DLC), a method for markerless pose estimation based on transfer learning with deep neural networks (Mathis et al., 2018). I used this method to track the position of the centre of mass of the mouse and the ears. The DLC algorithm was trained with 1000 frames from one of the recording sessions (for which the mouse's centre of mass and ears were manually tagged) for 1 million training iterations. I performed quality checks to the DLC output by inspecting 100 randomly chosen frames per orientation<sup>13</sup>, per quadrant with overlaid DLC tags; this allowed me to settle for a training-set of 1000 manually tagged frames. In addition, frames in which the mouse's speed exceeded 2 m/s were considered to be tracking errors and excluded, as mice do not reach such speed in my set-up. I also excluded from further analysis all timepoints the mouse was either inside the shelter or leaning down from the behavioural platform.

Head direction and head-shelter offset were calculated using DLC tracked ear-positions<sup>14</sup>: Head direction was defined as the angle between the direction perpendicular to a line segment that joins both ears and a horizontal axis intercepting the midpoint of the same line segment. Head-shelter offset was defined as the angle between the same direction as above and a line segment connecting the centre point between the ears and the shelter entrance (Figure 4).

#### **3.3.4. Single cell tuning analysis**

I used the Rayleigh vector length (Batschelet, 1981) in head direction and head-shelter offset spaces, as previously described in head-direction tuning testing in rodents (Taube et al., 1990a, Boccara et al., 2010, Wills et al., 2010), to quantify the tuning of each cell to each of these variables. A neuron was considered to be significantly tuned to a variable when the length of its Rayleigh vector exceeded the 95<sup>th</sup> percentile of the distribution of Rayleigh vectors lengths computed for 1000 shuffled datasets, generated by shifting recorded spike trains from all cells coherently by a uniform amount chosen randomly

---

<sup>13</sup> The head-direction space was divided into 8, 45°-wide bins, and inspected 100 frames per bin.

<sup>14</sup> The algorithm reliably tagged left and right ears correctly.

between 1 and 100 s. To ensure the tuning estimation was not biased by potential behavioural biases, I binned the variable space into 16 bins and sampled them equally.

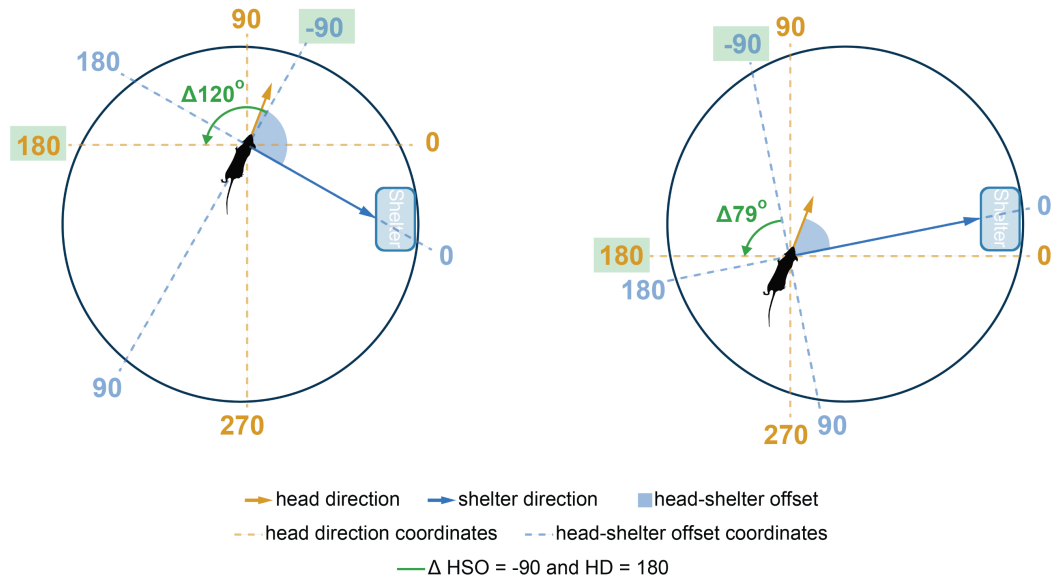


**Figure 4: Measurement of head direction and head-shelter offset**

Schematic representation showing how head direction (yellow arrow, angle measured in relation to horizontal axis) and head-shelter-offset (blue shaded area, measured between heading direction and shelter direction (blue arrow)) with the mouse in two different locations of the maze. The coordinate axes are shown for both spaces (yellow: head-direction space; blue: head-shelter offset space, both for current mouse's position). The green arrow highlights the angular distance between two arbitrarily chosen reference points in the different coordinate spaces, showing they are not anchored to each other; in the first scenario the angular distance between head-shelter offset -90 and head-direction 180° is 120°, whereas in the second panel it is 79°.

Single units from RSC or SC were classified as head direction cells if all the following criteria were met: i) for each epoch (including the no shelter epoch) the neuron had to display a significant head direction Rayleigh vector (larger than the 95<sup>th</sup> percentile computed after data shuffling); ii) for each epoch the neuron tuning to head direction had to be decoupled from tuning to head-shelter offset (using the Tuning Entanglement Decoupling (TunED) method, see below); iii) head-direction tuning had to be stable across all epochs (above chance ROC decoding (Gu et al., 2010, Nikbakht et al., 2018) along the direction in which Rayleigh vector pointed during the first epoch of the experiment, in the subsequent periods).

Single units from RSC or SC were classified as head-shelter offset cells if all the following criteria were met: i) for each epoch<sup>15</sup> the neuron has to display a significant head-shelter offset Rayleigh vector (larger than the 95<sup>th</sup> percentile computed after data shuffling); ii) for each epoch the neuron tuning to head-shelter offset must be decoupled from tuning to head direction (using TunED method, see below); iii) head-shelter offset tuning has to be stable across all epochs (above chance ROC decoding along the direction in which Rayleigh vector points during the shelter position 1 epoch, in shelter position 2 epoch); iv) head-shelter offset tuning must rotate with the shelter, which was considered the case when after rotation the tuning to shelter position 2 could not be significantly explained by the tuning to shelter position 1 (this was done by applying the TunED method to test if tuning to shelter position 2 was merely driven by tuning to shelter position 1).

### 3.3.5. Tuning Entanglement Decoupling (TunED) analysis

The TunED analysis was developed by Dr. Rasmus S. Petersen (unpublished) and determines if a cell that is statistically tuned to two variables which are correlated is in fact driven by the tuning to one of the variables ( $v_1$ , ‘driver’) while the tuning to the other variable ( $v_2$ , ‘passenger’) is an artefact of the correlation between these variables.

Because head direction and head-shelter offset are correlated in my set-up, a cell could have statistically significant tuning to both variables having in account just the test of the Rayleigh vector lengths against the shuffled distribution for both variables. As mentioned above, only cells which tuning to either head direction or head-shelter offset could be decoupled from artefact tuning to the other variable were considered to be head direction or head-shelter offset cells<sup>16</sup>, and I used the TunED analysis to determine this for each cell with significant Rayleigh vector length for both variables.

The method takes a list of spike-counts  $r$  along with simultaneously measured stimulus variables  $v_1$  (driver) and  $v_2$  (passenger). Let

$$P(r = i | v)$$

---

<sup>15</sup> The first epoch in which there was no shelter was not considered for the analysis of head-shelter offset tuning.

<sup>16</sup> I.e. If for a cell significantly tuned to both head-direction and head-shelter offset we could not show that one of these tunings was an artefact arising from the correlation between them this cell was not categorized as either an head direction cell or a head-shelter offset cell.

be the probability that the neuron's spike count  $r$  takes a given value, given a discrete value for the variable  $v$ , the tuning curve of the neuron to stimulus variable  $v$  is then the conditional mean spike count

$$\mu(v) = \sum_i i P(r = i|v)$$

To determine whether a neuron is only tuned to the driver variable  $v_1$  or indeed significantly tuned to both  $v_1$  and  $v_2$ , the method formulates the null hypothesis that the neuron's activity is purely driven by the  $v_1$ . In this case it can be shown that the tuning curve to  $v_2 - \mu(v_2)$  can be expressed as:

$$\mu_{NH}(v_2) = \int dv_1 \mu(v_1)P(v_1|v_2)$$

Where the suffix NH denotes this is not the actual tuning curve to  $v_2$  but instead it is derived by the above null hypothesis.

Data used in the TunED analysis was bootstrapped 1000 times, generating 1000 tuning curves for real tuning to each variables (Figure 5, left panels, dark red and dark blue tuning curves) as well as 1000 tuning curves for apparent tuning for the same variable using the null-hypothesis equation above (Figure 5, left panels, light red and light blue tuning curves). For each variable, the Euclidean distance between the real and apparent tuning was calculated for each bootstrap iteration (Figure 5, right panels, red and blue distributions). The Euclidean distance between the distributions of head-shelter offset and head-direction differences between real and apparent tuning was computed (Figure 5, right panel, grey distribution). If the generated distribution was not significantly different from 0 (CI < 95%), tuning could not be decoupled, and the cell was not considered an head-shelter offset or head-direction cell. However, if this distribution was different and larger than zero the cell was considered a head-shelter offset cell, otherwise, if it was smaller than zero, the cell was categorized as a head-direction cell (see equations in Figure 5A, right panel).

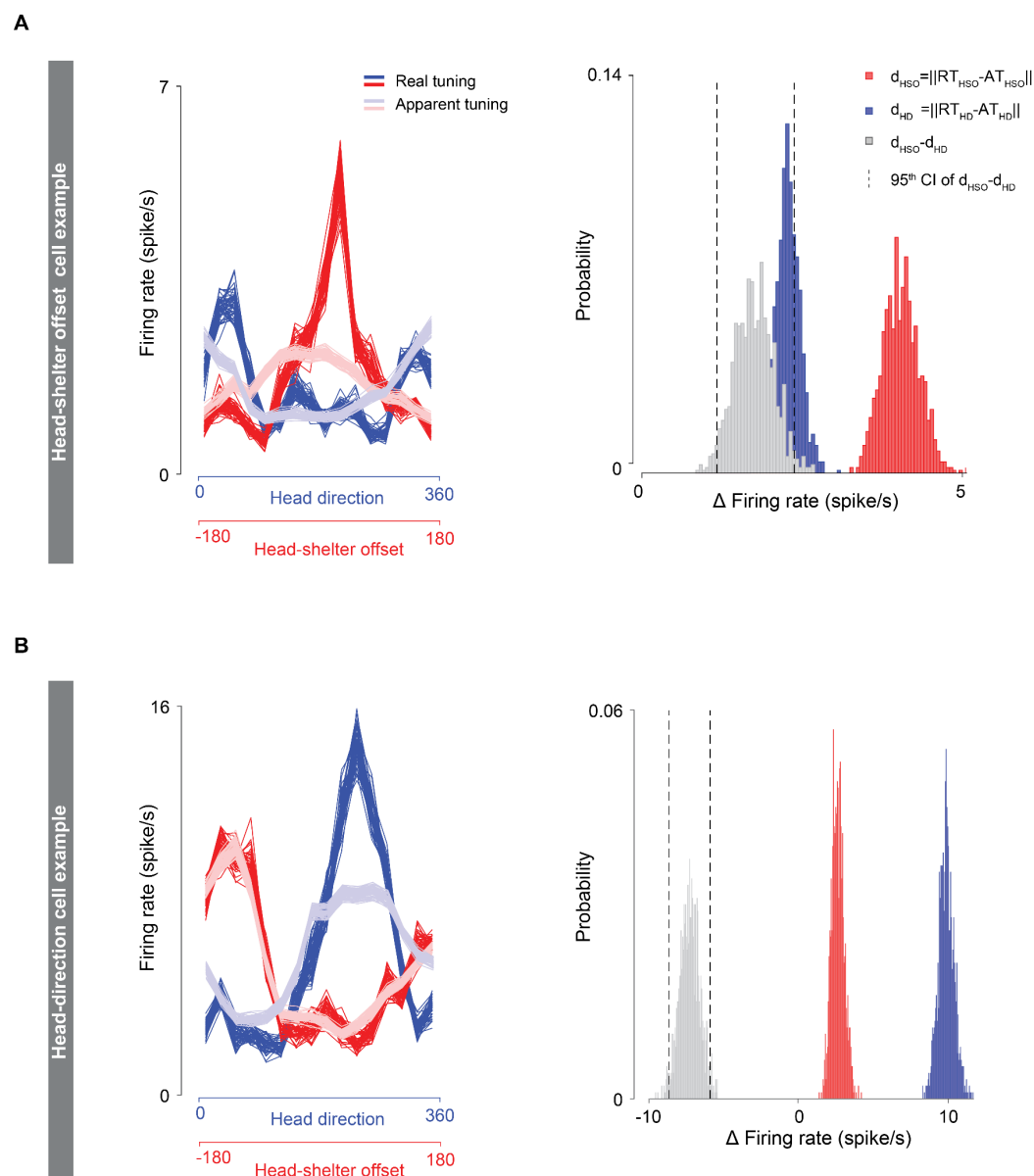


**Figure 5: Examples of TunED analysis identifying a head-shelter offset cell and a head-direction cell**

A and B shows example cells which Rayleigh vectors lengths for both head-shelter offset and head-direction were statistically significant. TunED analysis revealed that tuning of cell A to head-direction was an artefact of tuning to head-shelter offset (left panel: tuning to head-direction is explained by tuning to head-shelter offset, but not otherwise, as seen in drop in firing rate between light and dark red); the difference of differences between real and apparent tuning to head-shelter offset and head-direction cell was positive and significantly different from zero, which shows in reality this cell is only tuned to head-shelter offset (right panel and legend). Opposite case shown in B, depicting a head-direction cell with artefact tuning to head-shelter offset. Data was bootstrapped 1000 times but only 50 iterations are shown in left panels of A and B.

### 3.3.6. Population decoding analysis

I studied population encoding of three behavioural variables: head-direction, head-shelter offset and near future (100 ms<sup>17</sup>) change in head direction<sup>18</sup>. To test how well neurons in the RSC and SC encode these variables as a population, I trained and tested multiclass linear discriminant analysis (LDA) classifiers (Balakrishnama and Ganapathiraju, 1998, Rao, 1948, Nikbakht et al., 2018, Ghogh and Crowley, 2019, Nicolelis et al., 1998, Reyes-Puerta et al., 2015) to predict the behaviour variables given the neural activity of all neurons recorded from each brain area.

For head-direction and head-shelter offset variables, angles were clustered into 16 bins of 22.5° each (360°/16). For change in head direction only shifts between -27° and +27° were taken into the training and cross-validation data subsets, as larger shifts were very poorly sampled in the data; this 52° shift span was clustered into 9 bins of 6° each. Moving average smoothing (100 ms) was applied to all data for this analysis.

For each recording and for each behavioural variable it was ensured that each of the bins was equally populated<sup>19</sup>. Data was pooled across experiments ensuring each experiment contributed with the same number of samples for each bin<sup>20</sup>. I divided each epoch<sup>21</sup> into 6 bins of equal duration and for each epoch I used bins 1, 3 and 5 to train the classifier, whereas bins 2, 4 and 6 were used to test prediction accuracy of the model. The LDA algorithm computes the optimal solution to divide the n dimensional space, where n is the number of neurons recorded, into 9 or 16 classes – the number of angle bins I defined here. This allows to build a confusion matrix that shows the probability of predicting a given behavioural bin (given the neural data) as a function of the real behavioural bin the mouse occupied for the variable in study. Prediction accuracy was computed as the probability of the classifier predicting the correct bin for the studied variable, for the whole cross-validation data subset.

---

<sup>17</sup> A 100 ms interval was chosen based on previously reported kinematic profiles of orientation movement in relation to SC firing (Shen and Paré, 2014, Wilson et al., 2018).

<sup>18</sup>  $\Delta$  head direction (100 ms) = head direction 100 ms in the future – current head direction.

<sup>19</sup> By randomly taking x timepoints from the recording to each bin, where x is the number of timepoints for the bin that was less sampled during the experiment.

<sup>20</sup> By randomly taking x samples from each recording, where x is the number of samples of the recording with less samples after downsampling as described above.

<sup>21</sup> No shelter, shelter position 1, shelter position 2. For head-shelter offset LDA, the ‘no shelter period’ was not taken into consideration.

To test the prediction accuracy given by chance, I shuffled the IDs of bin labels 100 times, and calculated the average prediction accuracy for the shuffled datasets by training and testing LDA classifiers as detailed above. Bins from the real data confusion matrix that were predicted with a larger probability than the highest probability for the same bin across all 100 shuffled tests were considered to be predicted above chance.

### 3.3.7. Recordings paired with chemogenetic loss of function analysis

Probes were implanted into animals expressing hm4D(Gi) in SC-projecting RSC neurons (see below for viral infection strategy). I assessed the effect of inactivating these neurons (by intraperitoneally injecting the hm4D(Gi) agonist CNO) and controlled the effect of inactivation by injecting saline intraperitoneally in the same mice, for all analyses described below. The effect of inactivation was assessed separately in RSC and SC neurons.

I computed the change in firing rate index ( $\Delta FR_{\text{index}}$ ) for each neuron in RSC and SC following administration of CNO and saline as:

$$\Delta FR_{\text{index}} = (FR_{\text{after injection}} - FR_{\text{before injection}}) / (FR_{\text{after injection}} + FR_{\text{before injection}})$$

And the distribution of change in firing rate index for all cells following CNO was compared against saline to test if chemogenetic inactivation of RSC neurons significantly decreased firing rate in RSC and/or SC.

At a single neuron level, I tested if there was a change in the percentage of neurons classified as head direction or head-shelter offset neurons following treatment with CNO vs saline, for each area as follows:

$$\% \Delta \text{ tuned neurons} = (\%NP_{\text{CNO}} - \%NP_{\text{Sal}}) / \%NP_{\text{Sal}}$$

Where NP is neurons preserved (i.e. still classified as head direction or head-shelter offset cells).

At a population level I calculated the change in prediction accuracy of LDA classifiers following injection of CNO or saline in relation to the prediction accuracy calculated for the cross-validation data subset as described previously. I trained the classifier on half of the data from the period before injection (data subsets shown in blue in Figure 6) and tested prediction accuracy before injection (data subsets shown in yellow in Figure 6) and after injection (data subsets shown in green in Figure 6). This was repeated 10 times for each variable and brain region, by randomly choosing the samples of data for each bin when down-sampling to lowest occupancy bins, as described above. To test lower performance in prediction accuracy after chemogenetic inactivation I tested the statistical significance of the drop of prediction accuracy after CNO vs the drop in prediction accuracy after saline (both in relation to baseline prediction accuracy, calculated from data subsets prior to injection (shown in yellow in Figure 6), with a 1- tailed paired t-test.

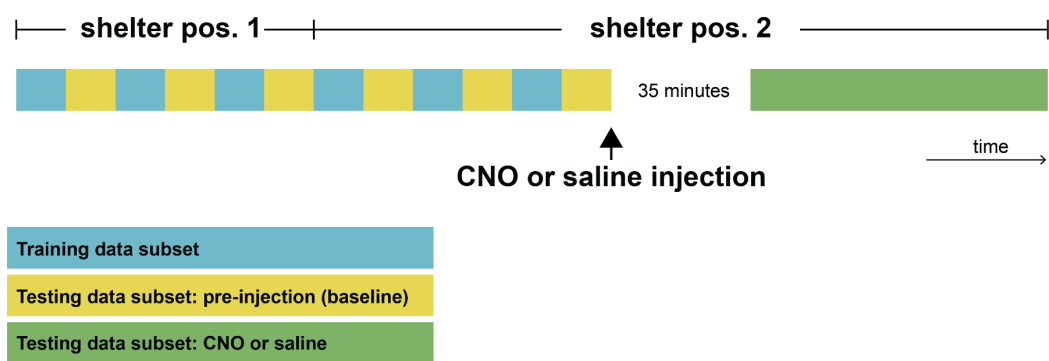


**Figure 6: Schematic representation of data partition for training and testing linear discriminant analysis classifier prediction accuracy after inactivation of retrosplenial neurons projecting to superior colliculus**

Shelter was moved from position 1 to position 2 after at least 30 minutes. Each of the two epochs considered before injection was divided into 3 alternate training and test data subsets. The baseline decoding accuracy was calculated with this cross-validation data subset. The effect of CNO and saline injection was computed by using the period after injection (the first 35 min after injection were discarded) as the cross-validation dataset. The change in prediction accuracy between baseline and following injection was calculated.

### 3.4. Orientation behaviour assay

Orientation experiments were performed in a set-up similar to the escape behaviour assay presented in chapter 5 (results: a projection from retrosplenial cortex to superior colliculus is critical for orientation during escape). It consisted of a 92 cm diameter round white platform, elevated 45 cm from the floor. Two speakers were positioned in opposite sides of the arena, 180° degrees apart in relation to the centre of the platform, and 10 cm away from the edges. The speakers faced the centre of the arena and were positioned at the same height as the floor of the arena. All experiments were performed in the dark and no shelter was present in the arena.

The stimulus used to elicit orientation towards the source of sound was a 300 ms long tone at 2.5 kHz, with a sound pressure of 75 – 80 dB at the centre of the arena.

The procedure of the experiment consisted in gently placing a mouse in the centre of the arena and allowing it to explore for 7 minutes. Subsequently, 7 stimuli were presented at least 90 s apart, by a speaker randomly determined on a trial by trial basis.

Orientation error was measured in degrees in relation to the tone emitting speaker the same way escape error was measured in relation to the shelter entrance. This analysis was performed by measuring the angular offset between the mouse's heading and the direction of the correct speaker in relation to the mouse, after the orientation movement. Trials in which the mouse was rearing upon stimulus presentation were excluded (< 5%). I aimed to present stimuli when mice subtended an offset smaller than 120°<sup>22</sup> towards the speaker, and trials in which this was not verified *a posteriori* were excluded.

---

<sup>22</sup> I chose this cut-off based on work showing that coding of sound location in azimuthal plane is drastically less accurate above this range (Sterbing et al., 2002, King et al., 1988, Slee and Young, 2013) and preliminary experiments done in the lab that showed a marked drop in performance above 120° offset.

### 3.5. General surgical procedures

All experimental procedures were conducted in a designated surgical suite and the experimenter used sterile gown and gloves.

Animals were anaesthetised with an intraperitoneal injection of ketamine and xylazine (95 mg/kg and 15.2 mg/kg, respectively). Analgesia (carprofen, 5 mg/kg) was administered subcutaneously before surgery. The scalp was shaved, and a chlorhexidine-based solution was used to disinfect it before the incision was made. The animal was placed in a heat pad and a temperature sensor was placed under the animal abdomen; the heat pad was regulated to maintain the animal temperature at 37.0°C. The animal was secured in a stereotaxic apparatus (Kopf Instruments, models 1900 and 963) and a mixture of O<sub>2</sub> (1 – 1.5 L/m) and isoflurane (between 0.5 and 1.5%) were administered through a mask. Depth of anaesthesia was assessed by breathing depth and frequency and response to foot pinching and was used to determine the concentration of isoflurane necessary for anaesthesia maintenance. Eye gel (Lubrital) was applied to prevent dehydration of the cornea.

The experimenter performed a sagittal incision of the scalp extending beyond bregma and lambda, to expose the skull. The skull was levelled AP by adjusting the position the mouse in the stereotaxic apparatus so that the distance between bregma and lambda in the dorso-ventral axis (z axis) was smaller than 0.05 mm. The epicranial aponeurosis was scraped, and one or more craniotomies were made in the region(s) of interest using a 0.5 or a 0.7 burr and a dental drill.

Viral constructs were delivered using pulled glass pipettes (10 µl Wiretrol II pulled with a Sutter P-97). Prior to the surgery, glass pipettes were half-filled with mineral oil and topped up with the viral construct, using an hydraulic micromanipulator coupled to an injection system (Narishige, MO-10). For the injection, the pipette was inserted into the brain without prior durement and lowered to the goal depth. Virus was injected slowly (~ 50 nL/min) and the pipette was retracted from the brain 5 min after each injection. When two injection sites were aligned along the dorso-ventral axis, the deepest injection was performed first and the pipette was withdrawn to the upper injection site 2 min after the first injection.

Guide cannulas were lowered into the target location with a holder connected to the micromanipulator system and implanted using light-cured dental cement (3M RelyX Unicem 2). For probe implantation a layer of Vaseline was used to cover the probe shank

before applying cement to fix the implant and a ground pin (World Precision Instruments, 0.031'' gold-plated pin) was implanted in the contralateral olfactory bulb.

Mice were sutured using absorbable sutures (Vicryl Rapide 6-0) and atipamezole was administered subcutaneously (0.05 mg/kg) if the time elapsed since anaesthesia was below 90 minutes. Animals were placed in a clean homecage after surgery and remained in a heated recovery chamber until fully recovered, when they were transferred back to the standard animal holding room.

### 3.6. Retrograde circuit tracing

Monosynaptic rabies tracing (Wickersham et al., 2007) from VGluT2<sup>+</sup> or VGAT<sup>+</sup> SC cells<sup>23</sup> was set-up with two surgeries. In the first procedure a mix of AAV1-Flex-N2cG-nucGFP<sup>24</sup> and AAV1-EF1a-Flex-GT-GFP<sup>25</sup> (1:2) was injected in the left hemisphere SC (AP: lambda -0.40; ML: -1.00; DV: -1.75, adjusted for a 10° angle of injection with the pipette going from medial at penetration to lateral at target site; injection volume = 20 - 25 nL). SAD-B19<sup>AG</sup>-mCherry rabies virus was injected 5 days after the first procedure (same target location, but injection performed without angling the injection system; injection volume = 0.24 – 0.30 nL). Animals were perfused 9 – 10 days after the second procedure.

With the exception of one brain that was sectioned using a cryostat (Leica 3050 S) and imaged with an epifluorescence microscope (Zeiss Axio Imager 2), all brains were imaged by serial micro-optical sectioning 2-photon tomography (Zheng et al., 2013, Ragan et al., 2012, Li et al., 2010), imaging red and green channels of automatically sectioned 40 µm coronal sections. Images were inspected visually, and projection of interest were identified in reference to the Allen Mouse Brain Atlas (© 2015 Allen Institute for Brain Science. Allen Brain Atlas API. Available from: [brain-map.org/api/index.html](http://brain-map.org/api/index.html)).

---

<sup>23</sup> Using VGluT2-ires-Cre or VGAT-Cre transgenic animals, respectively.

<sup>24</sup> Coding for the glycoprotein which is deleted in the rabies virus subsequently injected.

<sup>25</sup> Coding for the TVA receptor necessary for the rabies virus (EnvA-pseudotyped) to infect target cells.

### 3.7. Loss-of-function protocols

#### 3.7.1. Chemogenetic loss-of-function experiments

All animals used in chemogenetic loss-of-function experiments were male C57BL/6J wild-type mice. For non projection-specific inactivation I used an AAV coding for non-flexed inhibitory DREADD hM4D(Gi) (AAV8-hSyn-hM4D(Gi)-mCherry) (Armbruster et al., 2007), which was injected into target locations (see Table 1 for coordinates; for each brain region listed in the table all injection sites were targeted, unless stated otherwise; injection volume = 100 – 120 nL per site, unless stated otherwise). To inactivate SC-projecting RSC neurons I injected a retro-AAV (Tervo et al., 2016) coding for Cre (rAAV2-retro-CMV-bGlo-iCre-GFP) in the SC and, in the same procedure, I injected an AAV coding for flexed hM4D(Gi) (AAV2-hSyn-DIO-hM4D(Gi)-mCherry) in the RSC.

Following viral injections I waited at least 4 weeks before conducting experiments. On the experiment day I injected either CNO (1 mg dissolved in 1 ml 0.9% saline on the day of the experiment and injected at a final concentration of 10 mg/kg; Hellobio CNO freebase) or saline intraperitoneally, during brief isoflurane anaesthesia (2 – 4% in oxygen, 1 L/min; no longer than 2 min under anaesthesia). The animals were immediately placed in their homecage and I waited 35 minutes before starting the behavioural experiment. I waited at least 72 h before repeating the experiment with saline or CNO (whichever was not administered in the first session).

A subset of mice whose SC-projecting RSC neurons were targeted with hM4D(Gi) had cannulas implanted either in the SC or in the anterior cingulate cortex (ACC) for specific inactivation of the respective projection<sup>26</sup> (Stachniak et al., 2014). Guide cannulas (Plastics One guide cannulas, C23G-1.0/SPC or C23G-2.0/SPC) were implanted into the target location (Table 2) at least 4 weeks after viral injection, and at least 96 h before behavioural experiments. Dummy cannulas (Plastics One, C235DC) were cut to fit the guide cannula and position inside it immediately after surgery, to prevent obstruction of the guide cannula lumen. On the day of the procedure the animal was anaesthetised with isoflurane (1 – 2.5% in oxygen, 1 L/min) for cerebral microinfusion of CNO or saline.

---

<sup>26</sup> I observed that at least a subset of SC-projecting RSC neurons also project to the ACC (see results, Figure 24A).

CNO was diluted in buffered saline containing (in mM): 150 NaCl, 10 D-glucose, 10 HEPES, 2.5 KCl, 1 MgCl<sub>2</sub> and to a final concentration of 10 μM. Injection of CNO or vehicle was performed via internal cannulas (C2351/Spc protruding 0.5 mm below guide cannulas) sealed with Kwik-Sil to the guide cannulas. I injected 0.8 – 1.2 μL of CNO solution or saline per hemisphere using a microinjection unit (Hamilton, 10μl Model 1701 syringe; in Kopf Instruments Model 5000) connected to the internal cannula through tubing (Plastics One FEP tubing, CMA3409501) and a plastic disposable adaptors (Plastics One, CMA3409500). After infusion the tubing was cut near the internal cannula and sealed with Kwik-Sil, leaving the internal cannulas inside the guide cannulas, in the brain. I waited 35 minutes after infusion to initiate the behavioural experiment. After the end of the experiment the internal cannulas were replaced with dummy cannulas and I waited at least 5 days to infuse the mouse's brain region of interest with saline or CNO (whichever was not administered in the first session).

For Neuropixels recording experiments paired with chemogenetic loss of function, the intraperitoneal injection of CNO or saline was done during the behavioural experiment. The mouse was not removed from the arena and when possible was not anaesthetised for the injection. Although the recording was never interrupted, the 35 minutes following the injection were excluded from further analysis.

Brains from loss-of-function experiments were imaged to confirm injection sites. I used a cryostat (Leica 3050 S) to produce 50 μm thick coronal sections of the regions of interest and imaged them with an epifluorescence microscope (Zeiss Axio Imager 2), after staining against GFP and RFP and mounting them in SlowFade Gold (containing DAPI). Brains with significant contamination of non-intended brain regions or which had no infection of the targeted area were excluded from the study.

**Table 1: Coordinates for viral injections for chemogenetic procedures**

All values are in mm in relation to lambda unless specified. Injection volumes were 100 – 120 nL per injection side unless otherwise specified.

AP: antero-posterior; ML: medio-lateral; DV: dorso-ventral; SC: superior colliculus; RSC: retrosplenial cortex; M2: secondary motor cortex; ACC: anterior cingulate cortex; PPC: posterior parietal cortex

	<b>Viral injection coordinates</b>			<b>Notes</b>
	<b>AP</b>	<b>ML</b>	<b>DV</b>	
<b>SC</b>	- 0.40	+/- 1.10	- 1.90	
	- 0.40	+/- 1.00	- 1.50	
	+ 0.40	1.00	- 2.50 and - 2.00	Only targeted for injection of non-flex hM4D(Gi) coding virus for loss of function of the SC
	0	+/- 1.00	- 2.00	
<b>RSC</b>	+ 0.40	+/- 0.65	- 1.00 and - 0.70	
	+ 1.10	+/- 0.40	- 1.20 and - 0.90	
<b>M2</b>	Bregma +1.10	+/- 0.70	- 1.40	Only one of these two sites were targeted in each mouse. 180 nL per injection site
	Bregma + 1.41	+/- 0.85	-1.60 and - 1.10	
	Bregma + 1.93	+/- 1.10	-1.65 and - 1.10	
	Bregma +2.52	+/- 1.80	- 2.00 and - 1.50	
	Bregma +2.52	+/- 1.00	- 1.75 and - 1.25	
<b>ACC</b>	Bregma + 1.10	+/- 0.25	- 1.80	180 nL per injection site
<b>PPC</b>	+ 1.88	+/- 1.25	- 0.70	
	+ 1.88	+/- 1.75	- 0.90	

**Table 2: Coordinates for cannula implantation for chemogenetic procedures**

All values are in mm in relation to lambda unless specified.

AP: antero-posterior; ML: medio-lateral; DV: dorso-ventral; SC: superior colliculus; ACC: anterior cingulate cortex;

	<b>Cannula implantation coordinates</b>			<b>Notes</b>
	<b>AP</b>	<b>ML</b>	<b>DV</b>	
<b>SC</b>	- 0.30	+/- 1.00	- 1.20 (internal extends to - 1.70)	Dual cannula with 2.0 mm spacing
<b>ACC</b>	Bregma + 1.10	+/- 0.60	- 1.10 (internal extends to -1.60)	Dual cannula with 1.2 mm spacing

### 3.7.2. Muscimol-driven loss of function

All animals used in muscimol driven loss-of-function experiments (Majchrzak and Di Scala, 2000) were male C57BL/6J wild-type mice. One cannula (Plastics One, C31GS-4/Spc) was implanted in each hemisphere's RSC (AP: + 0.40; ML: +/- 0.60; DV: - 0.80, all in mm in relation to Lambda) and a dummy cannula (Plastics One, C315DCS-4/SPC) was secured inside it to prevent obstruction of the lumen.

I waited at least 96 h before conducting any behavioural experiments. All animals were submitted to a pre-test at least 48 h before infusion of muscimol as they had to be perfused immediately after the experiment following muscimol infusion in order to confirm the muscimol spread. The experiment was similar to the escape behavioural assay presented in chapter 4; after a 7 minute adaptation period I presented an aversive auditory stimulus to the mouse (a train of three frequency modulated upsweeps from 17 to 20 kHz over 3 s, lasting in total 9 s), and assessed the escape behaviour. I also tried to elicit escapes with the aversive looming stimulus but mice consistently stopped exploring after escaping from this stimulus, thus I was not able to collect enough data to assess responses from the visual stimulus.

At least 48 h after doing the aforementioned behavioural pre-test I infused 1.0 – 1.2  $\mu$ L Muscimol-BODIPY-TMR-X (0.5mg/ml) (ThermoFisher) per hemisphere, using the same infusion protocol as described above for intracerebral CNO infusions. After infusion with muscimol mice were immediately sacrificed, the brains were removed and sectioned coronally with a vibrotome (Campden Instruments Ci 7000 smz-2). Sections were mounted with SlowFade Gold (containing DAPI) and imaged with an epifluorescence microscope (Zeiss Axio Imager 2). Mice with no visible injection in the RSC were excluded, no mouse had to be excluded due to contamination of non-targeted areas.

Controls were done with infusion of saline in a different cohort of mice, which were similarly sacrificed after the experiment and the positioning of the implanted cannulas was confirmed by microscopy.

### **3.8. General data analysis**

Data analysis was performed with Python 2.7 and Prism. Datasets were tested for normality with the Shapiro–Wilk test, and a parametric test was used if the data were normally distributed, otherwise I used a non-parametric test, as detailed in the results text next to each comparison. Statistical comparisons were performed in SciPy Stats or Prism, and statistical significance was considered when  $p < 0.05$ . Additionally, figures indicate the value of statistical test performed with asterisks (\*  $p < 0.05$ ; \*\*  $p < 0.01$ ; \*\*\*  $p < 0.001$ ; \*\*\*\*  $p < 0.0001$ ). Numbers of mice and trials are indicated in the text, referent to each experiment.



#### **4. RESULTS:**

### **Rapid learning controls anti-predator escape behaviour**

*The results reported in this chapter have been published as “Vale, R., Evans, D. A., & Branco, T. (2017). Rapid spatial learning controls instinctive defensive behavior in mice. Current Biology, 27(9), 1342-1349” and parts of it are transcribed or adapted from the published manuscript.*

#### **4.1. A behavioural setup to study navigation during anti-predatorial defensive behaviours**

In this chapter I will describe the results of a battery of behavioural experiments that aim to characterize the dependency of defensive actions on spatial features such as the presence of a shelter in the environment and its location, as well as the flexibility of these behaviours as a function of abrupt changes in environmental features. Particular emphasis is given to the study of escape behaviour, and the behavioural setup has been designed specifically to characterize how mice escape from innately aversive sensory cues.

The experimental setup and behavioural procedures are detailed in the methods chapter. In summary, the setup consists of a 92 cm diameter circular arena which has 20 equally spaced holes in its periphery, 5 cm away from the edge. Unless otherwise specified, 19 of these holes are covered from below, having a depth of 1 cm (pseudo-holes), while one leads to an underground shelter. Aversive visual stimuli can be presented above any position of the arena in respect to the mouse which is tracked in real-time through custom-built software. Aversive auditory stimuli are delivered by a speaker positioned above the centre of the arena. These two different stimuli have distinct advantages: while the visual stimulus can be delivered above any position of the arena, which proved essential to determine the goal of escape, the auditory stimulus can be used in the dark.

The general procedure consists of an initial 7 min habituation period in which the mouse visits the shelter at least once. Importantly, the mouse is never moved passively in any experiment, meaning the mouse enters and leaves the shelter at its own will as many or as few times as it decides. After this habituation period visual and/or auditory aversive stimuli (Mongeau et al., 2003, Yilmaz and Meister, 2013) are presented and the behavioural responses are video-recorded.

## **4.2. Escape behaviour is a goal-directed behaviour characterized by navigation towards refuge**

In the introduction of this work I described different strategies of escape, which can be grouped into escapes away from threat and escapes towards a refuge. The computations involved in these two strategies are very different, as an escape purely away from threat requires solely integration of sensory information about the source of threat, whereas an escape towards a refuge requires knowledge of the presence of a shelter and its location, and the computation of a trajectory towards it.

In order to test which strategy mice preferentially engage in, I designed an experiment that dissociates trajectories towards the shelter from trajectories away from threat. A naïve mouse was placed in the Barnes arena and after a short exploration period (7 min) during which mice always spontaneously entered the arena's underground shelter, I presented aversive visual stimuli centred between the animal's position and the shelter (on-path stimuli). If mice directed their escape away from threat, they would also move away from the shelter. However, I observed the contrary. Similar, to what is observed following directly overhead visual stimuli (on-top stimuli), on-path stimuli triggered escape towards the shelter (Figure 7A, B), with short reaction times ( $202 \pm 16\text{ms}$ ,  $N = 51$  responses, from 26 animals), independently of the initial location of the mouse (Figure 7C). I found no difference in escape trajectories depending on the visual stimulus being centred above the mouse or in between its position and the refuge, with mice running towards the aversive stimuli to reach the shelter, in the latter condition (Figure 7A, B, see also Figure 9A and B).

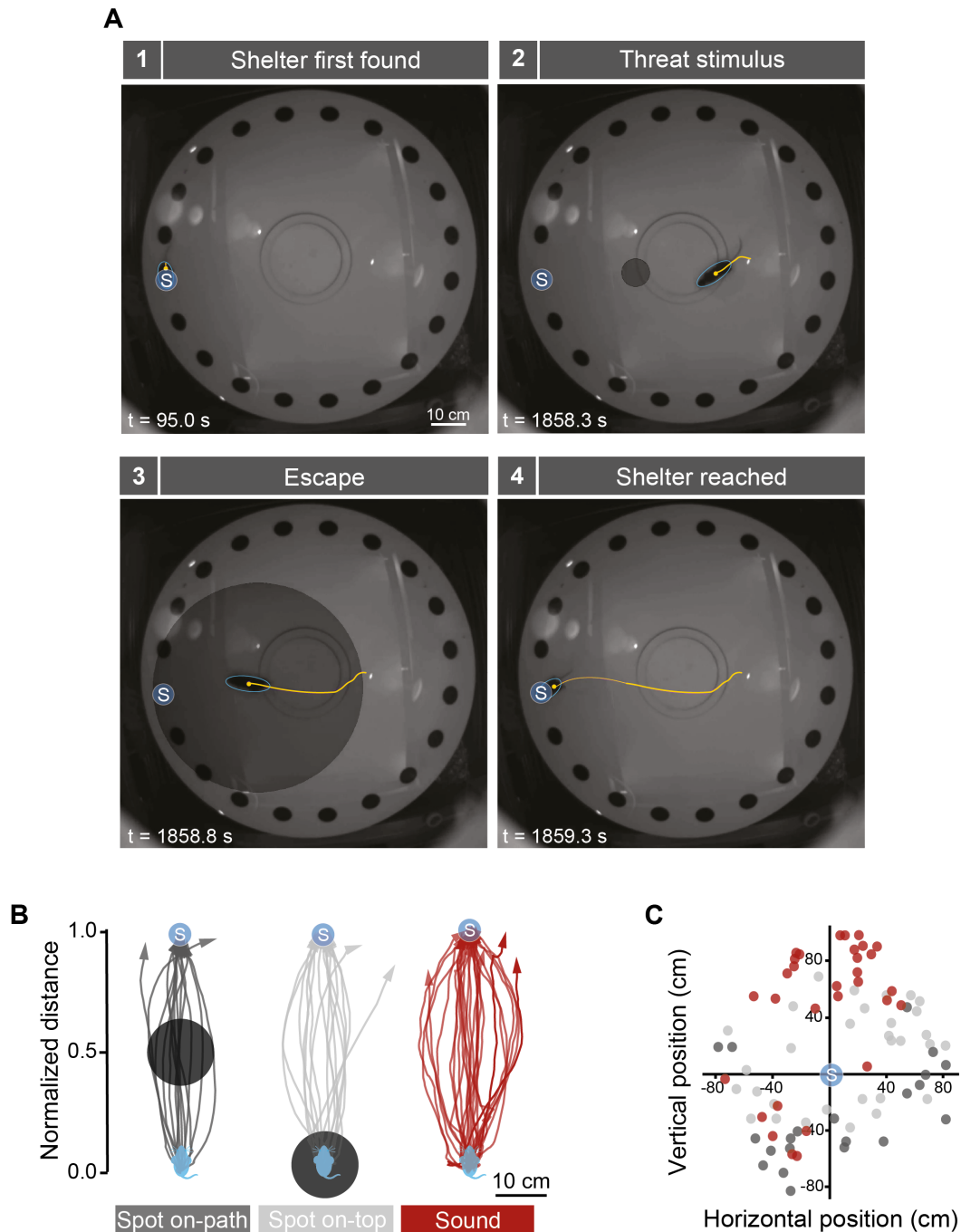


### Figure 7: Escape behaviour is a goal-directed action to reach safety

(A) Video frames from one trial showing escape to a previously explored shelter after presentation of an expanding spot projected from above, between the mouse and the shelter location (on-path). Yellow lines indicate the mouse's trajectory during the preceding 2 s.

(B) Example trajectories from several mice, recorded between stimulus onset and the end of flight, showing that flight path and target are independent of stimulus position or quality (number of animals = 10 on-path, 16 on-top, and 15 sound).

(C) Initial position of mice in all trials plotted in relation to shelter location.

For all figures, the blue circle represents the shelter location.

These data suggest that the goal of escape behaviour in mice is to reach safety. To further test this hypothesis, I reasoned that presentation of threat while the animal is in the shelter should not cause escape behaviour. Indeed, auditory stimuli delivered both in the Barnes Maze and in a modified version with an above-ground shelter<sup>27</sup> did not trigger escape when the mouse was inside the shelter, despite the sound pressure level inside the shelter being within 2 dB of the sound pressured measured above the platform where robust escapes were triggered (escape probability = 100% outside versus 6% inside shelter, N = 76 responses from 11 animals; Figure 8). This result supports the previous one, showing that escape is an action which goal is to reach safety, rather than a simple stimulus-reaction, since the ongoing perception of safety can veto escape from innately aversive threats.

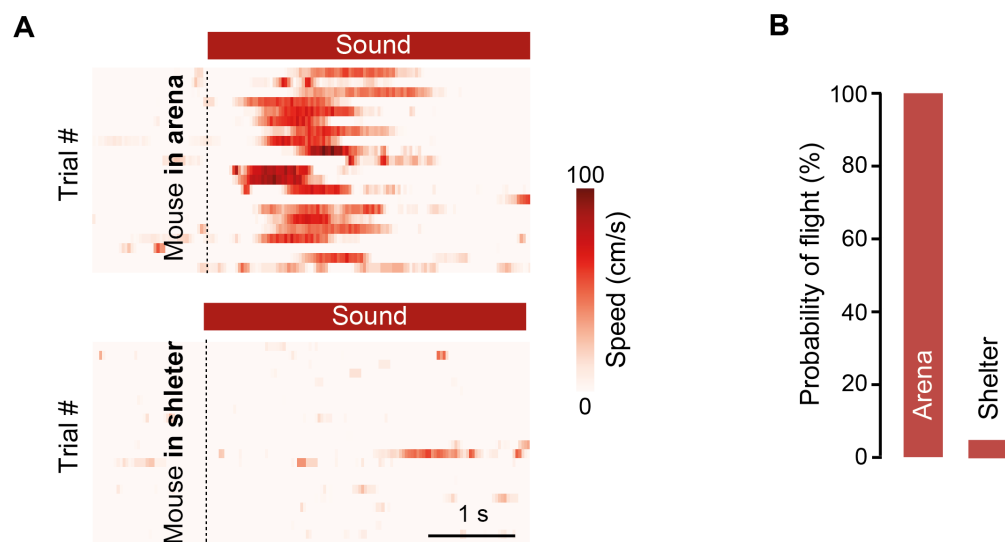


**Figure 8: Aversive auditory stimulus does not cause escape when mouse is already in shelter**

(A) Raster plots showing speed profile of several mice during the first seconds following sound stimulus presentation while exploring the arena (top panel) or when the same mice were inside an over-ground shelter (bottom panel).

(B) The probability of flight is dramatically reduced when animals are already inside a shelter.

<sup>27</sup> The over-ground shelter was 20 x 10 x 10 cm with a 5 cm wide entrance that was positioned facing the centre of the arena, and it was made of red translucent Perspex allowing visualization of the mouse inside the shelter

Accuracy of escape was measured as the proximity between the arena's hole at which the mice terminated escape and the hole leading to the shelter; if the mouse ran to the correct hole, accuracy of escape was 100% and since there are 20 holes in the arena disposed circularly, each hole away from the shelter represents a 10% drop in accuracy. Similar accuracy to reach the shelter was observed when the visual aversive stimulus was presented on-top and on-path (mean accuracy: on-top,  $97\% \pm 1\%$ , on-path  $89\% \pm 5\%$ ,  $p=0.32$ , t test between on-top and on-path, Figure 9A). I observed that escape was quasi-linearly directed towards the shelter and also not different in response to the two stimuli locations (mean linearity ratio: on-top  $109\% \pm 2\%$ , on-path  $106\% \pm 1\%$ ,  $p = 0.27$ , t-test between on-top and on-path, Figure 9B), interestingly this straight navigation is significantly different from foraging navigation bouts (mean linearity:  $209\% \pm 30\%$ ,  $p<0.0001$ , t-test between flights and foraging).

In order to achieve very straight escape paths, animals must orient towards goal before initiating the approach. I observed that the first body movement leading to escape was head rotation toward the shelter location. This orientation behaviour was independent of the initial offset angle in relation to the shelter and it was reduced to less than  $10^\circ$  before the mouse covered the first 10% of the distance to shelter, and thus preceded the onset of full flight (Figure 9C, D, E). Interestingly, I observed that mice rotated to the side which is closer to the shelter in egocentric angular space in 91.5% of the trials (Figure 9D), suggesting the mouse computes the flight target before the start of the head rotation movement.

The evidence thus far shows that the goal of escape is to reach safety and that to do so mice employ flexible actions as a function of spatial features, namely the location of refuge in space. Mice exhibit accurate and linear escapes after orienting towards the shelter, irrespective of their position upon escape initiation, therefore flexibly employing the necessary motor sequence to reach the shelter.

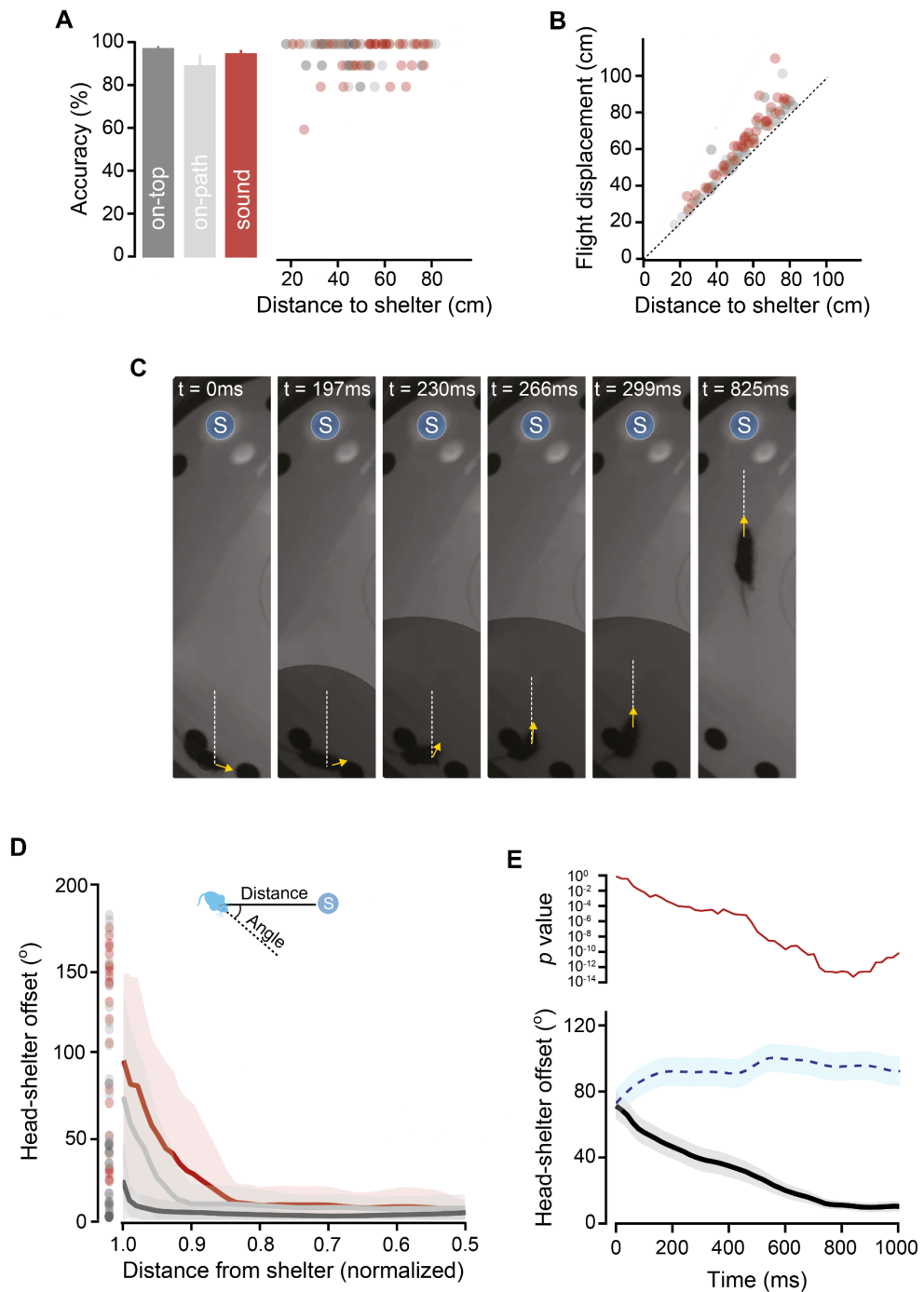


### Figure 9: Escape is accurate and linear, relying on initial head orientation to shelter

(A) Accuracy of escape. Bars show average accuracy and circles are single-trial accuracy data points as function of distance to shelter, showing no correlation between distance and accuracy.

(B) Circles represent, for single trials, the total displacement during escape for 100% accurate flights, plotted against linear distance to the shelter.

(C) Video frames from one trial during initiation of escape from an expanding spot on-top, highlighting the initial head rotation preceding the initiation of running. The yellow line indicates head direction, and the dashed white line represents the shelter direction, making the angle between these two lines the head-shelter angular offset.

(D) Head-shelter offset (angles measured between the yellow and white lines illustrated in (C)) for 100% accurate flights, showing that the head is pointing toward the position of the shelter early in the coverage of distance to the shelter. Circles indicate the initial head-shelter offset angles for different trials, computed against the side that the mouse subsequently rotated to. Lines indicate average head rotation profile, and the shaded areas indicate the SD (N = 59 trials from 38 animals).

(E) Bottom: evolution over time of head angles upon threat presentation (solid line, same data shown in (D), pooled for all three different stimuli) and head angles over the same duration of time in the absence of stimulation (obtained from shuffling stimulation times across mice) (dashed line). Top: p-value for the comparison between the two angle distributions for each time point, obtained with Kolmogorov-Smirnov tests. The two distributions are significantly different after 100 ms. Shaded areas are SEM.

### 4.3. Environmental features determine the choice of defensive action

Previous studies showed that various species engage in escape when a refuge is present in the environment whereas freezing is preferred when a shelter is not present or reachable (Hennig et al., 1976, Blanchard et al., 1986, Wei et al., 2015, De Oca et al., 2007, O'Brien and Dunlap, 1975). Nevertheless, the temporal dynamics that mediate such flexibility in action selection have not been probed. Here I designed an experiment to test whether mice can rapidly switch defensive strategies following abrupt changes in the environment, namely upon placing or removing a shelter within reach of the mouse.

I placed a naïve mouse on the Barnes arena after closing the entrance to the underground shelter<sup>28</sup>, and after 7 min of exploration I presented a visual stimulus on-top of the mouse and observed that this triggered freezing responses (freezing probability = 71.4%, mean freezing time  $629.9 \pm 100.0$  ms; flight probability = 10.7%, for a 550 ms visual stimulus; N = 28 trials from 7 mice; Figure 10A). To test if the duration of freezing depended on the visual stimulus duration I presented a longer expanding spot (5 s duration), which resulted in longer freezing responses, sometimes lasting as long as 50 s (freezing probability = 95.2%, mean freezing time =  $7.9 \pm 2.7$  s; flight probability = 4.8%; N = 22 trials from 7 mice; Figure 10B). Subsequently, and still during the same behavioural session, I opened the underground shelter entrance without removing the mouse from the arena, and allowed the mouse to explore the arena for 5 minutes. If the mouse did not

---

<sup>28</sup> Making it equal to all other holes; no olfactory cue was present under the hole

enter the shelter in these 5 minutes this exploration time was prolonged in 5 minutes blocks until the mouse visited the shelter at least once. Subsequently I presented the same visual stimulus to the mouse and observed that the defensive strategy changed to escape (flight probability = 88.9% and 90.0% for 550 ms and 5 s visual stimuli, respectively; N = 27 trials from 7 mice and N = 20 trials from 7 mice for 550 ms and 5 s visual stimuli, respectively; Figure 10A, B).

In order to test if the opposite change of defensive action is also rapidly made by mice, I had to modify the behavioural setup, since we found that mice often jump down from the arena when access to the previously visited shelter was blocked. Therefore, a cylindrical arena surrounded by walls and containing an over-ground shelter<sup>29</sup> was used for this experiment. I presented slow expanding visual spots which triggered escapes to the shelter (flight probability = 90.5%; N = 21 trials from 7 mice; Figure 10C). Subsequently, I removed the shelter from the arena and allowed the mouse to explore for 5 minutes after which I presented the same visual stimulus, which now elicited freezing responses (flight probability = 9.5%; N = 21 trials from 7 mice; Figure 10C). After this, I reintroduced the shelter and allowed for an additional exploration period as described above for the experiment in the standard arena. Delivering the same visual stimuli again caused mice to escape to the shelter (flight probability = 81.0%; N = 21 trials from 7 mice; Figure 10C).

These data show that instinctive defensive escape is conditional on the knowledge of an existing reachable shelter in the environment and that in the absence of a memory of shelter presence, mice switch their defensive strategy to freezing.

---

<sup>29</sup> The over-ground shelter was 20 x 10 x 10 cm with a 5 cm wide entrance that was positioned facing the centre of the arena, and it was made of red translucent Perspex.

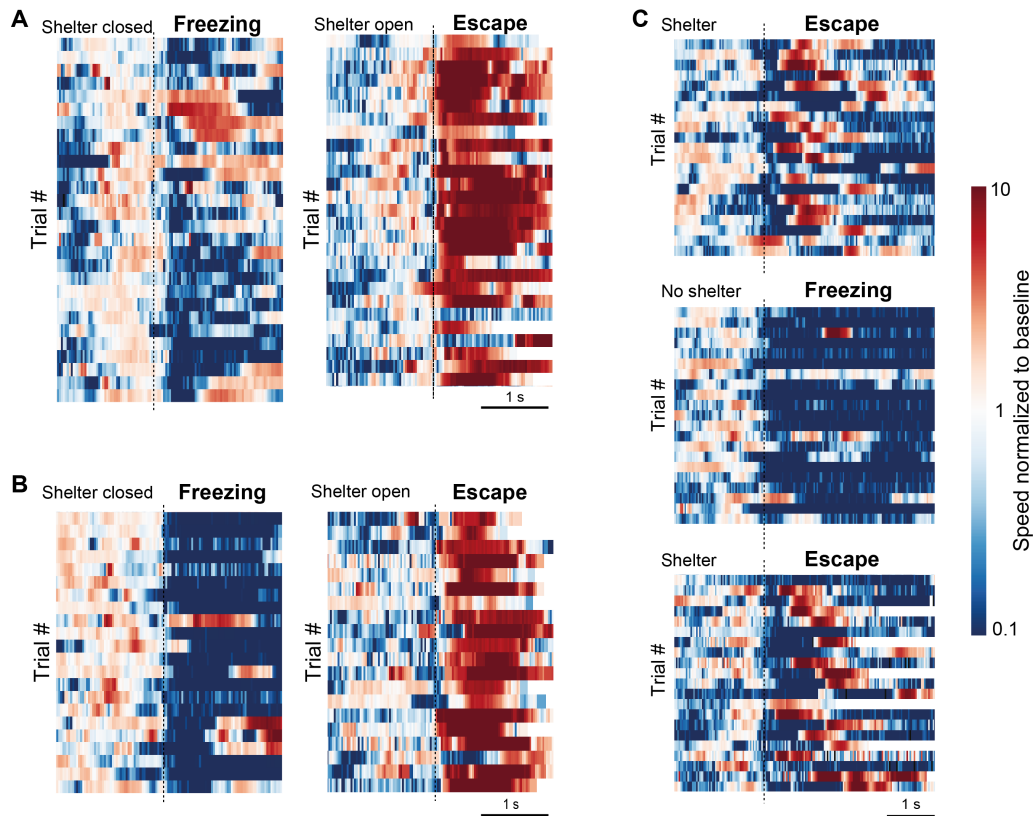


**Figure 10: Updates of defensive strategy in the presence or absence of a reachable shelter**

(A) Raster plots showing speed profiles upon threat stimulation before (left panel) and after the shelter has been opened (right panel), for fast expanding visual stimuli in the Barnes Maze. Trials have been aligned by reaction time (dashed line).

(B) Raster plots showing speed profiles upon threat stimulation before (left panel) and after the shelter has been opened (right panel), for slowly expanding visual stimuli in the Barnes Maze. Trials have been aligned by reaction time (dashed line).

(C) Raster plots for speed profiles with slowly expanding visual stimuli in a cylinder arena showing that the defensive strategy can be rapidly updated from freezing to escape or vice-versa depending on the presence or absence of a reachable shelter. Dashed lines indicate onset of stimulation.

Colour-bar applies to all panels.

#### 4.4. Memory of shelter location guides defensive flight

I investigated the navigation strategies that mice use to accurately navigate to the shelter during escape. Specifically, I tested whether spatial landmarks in the local surroundings of the shelter are used immediately before and during escape to guide navigation. To do so I designed a variant version of the Barnes maze in which the central part of the arena was fixed and the periphery could be automatically rotated using an engine, together with the shelter and a set of olfactory and visual cues, which have been shown to guide navigation in mice (Pompl et al., 1999).

Baseline responses (3 per animal) were first elicited with sound stimuli similarly to the standard escape assay. I then waited for the mouse to leave the shelter and spontaneously go to the central fixed platform<sup>30</sup>, at which point I used a remotely controlled motor to rotate the peripheral ring of the arena, the visual cues and the shelter as a block by a random angle (range = 36°- 90°, mean = 56°; corresponding to two to five holes, mean = 3.1 holes), and the sound stimulus was delivered again (Figure 11A)<sup>31</sup>. All mice tested invariably ran toward the previous shelter location, rather than to the new one, with accuracy, trajectory, linearity, reaction times and head orientation profile that were not different from those of pre-rotation escapes (Figure 11B-D). Notably, I observed that mice stayed in the vicinity of the pre-rotation location for  $4.6 \pm 0.2$  s, which is 2.5 times longer than the time mice spent in the wrong location during missed flights in control conditions ( $p < 0.001$ , t-test for time in wrong location between control and post-rotation; Figure 11E) further indicating goal-directedness toward this location.

These data suggest that landmarks proximal to the shelter are not required for the computation of shelter location upon escape. This is further supported by data from sound threat presentation in complete darkness, which evokes perfectly accurate escape responses, both when the animal explores the arena in darkness or in the presence of light (Figure 12A, B).

---

<sup>30</sup> A small Petri dish with some bedding from the animal's own home-cage was placed in the centre platform to attract the animal there and for it to stay longer at this location.

<sup>31</sup> Animals that left the central fixed platform during rotation and/or before the sound stimulus were excluded from further analysis.

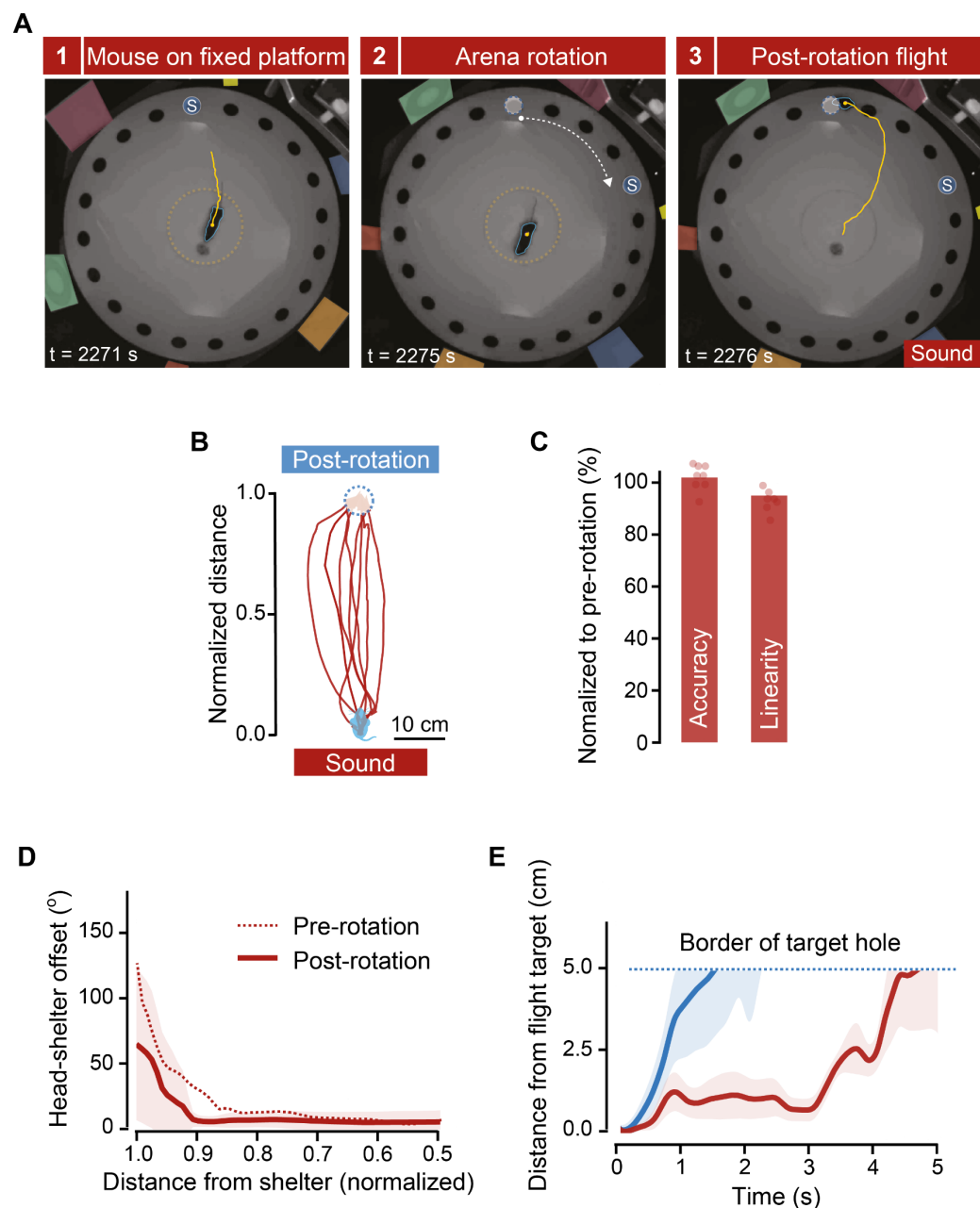


**Figure 11: Memory of shelter location guides defensive flight**

(A) Video frames from one trial showing escape from aversive sound immediately after the outside of the arena had been rotated, together with the shelter and local cues (panels on the outside, color-coded for clarity). The dashed yellow line marks the border of the fixed platform, the full yellow line shows the trajectory of the mouse in the 1 s previous to the frame, and the dashed blue circle shows shelter location before rotation.

(B) Trajectories from different mice after arena rotation, showing escape toward the previous shelter location (dashed blue circle).

(C) Escape behaviour is not significantly changed by arena rotation (accuracy =  $102\% \pm 1\%$ , linearity =  $96\% \pm 2\%$  of control). Reaction time is also not affected ( $93\% \pm 14\%$ ).  $p > 0.10$  for all comparisons, paired t-test between pre- and post-rotation;  $N = 8$  animals.

(D) Head rotation profile during escape initiation is not affected by arena rotation ( $p = 0.39$ , paired t-test between pre- and post-rotation for distance from shelter at  $10^\circ$  head-shelter offset angle). Post-rotation angles are measured in relation to the shelter position before rotation. Shaded area indicates the SD.

(E) Plot showing when the mouse leaves the initial target hole area after the flight. Red indicates flights after rotation, and blue indicates flights in control conditions where the shelter target was missed. The shaded area indicates the SEM.

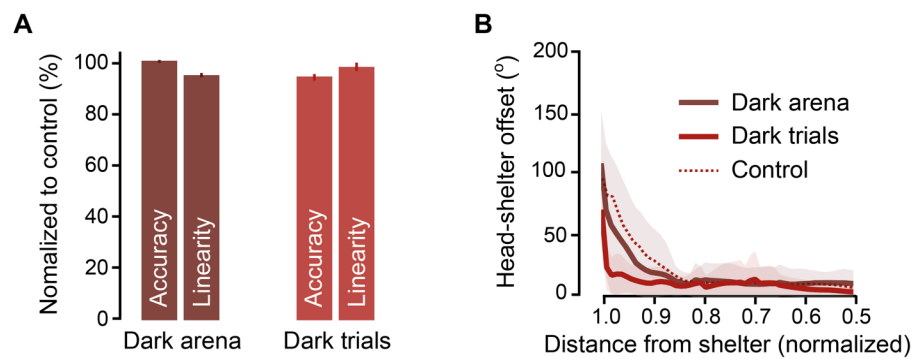


**Figure 12: Mice escape accurately to the shelter in the dark**

Escape in the absence of light was tested in two different conditions: i) ‘dark arena’, where the arena was dark for the whole duration of the experiment, and ii) ‘dark trials’, where the lights were turned off 1 s before presentation of each sound stimulus.

(A) Accuracy and linearity are not significantly different when compared to escape responses to sound with lights on (t-test against control,  $p > 0.3$  for all comparisons,  $N = 18$  trials from 6 animals for both conditions). Error bars are the SEM.

(B) Head-rotation profile is similar between the two dark conditions and control, with animals correctly orienting to the shelter location before the onset of flight. Shaded area indicates the SD.

After demonstrating that navigation to shelter during escape relies on spatial memory rather than taxon navigation, I tested whether termination of escape is controlled by the safety conferred by arriving inside the shelter. I used a circular arena with the same dimensions as the Barnes maze but without the peripheral pseudo-holes or shelter. Instead a shelter<sup>32</sup> was positioned above ground in the centre of the arena, as such positioning permits both under- or overshooting, and allows us testing where the mouse interrupts escape upon abrupt removal of the shelter.

I observed that mice reliably escape to the shelter in the centre of the arena, when exposed to aversive auditory stimuli. Upon removing the shelter immediately before a sound stimulus mice still navigated in the correct direction and stopped in the centre of the arena (Figure 13A-C). Not only did mice stop escape at the centre of the arena but also they persisted in such location, which is normally aversive to mice (Figure 13D), sometimes up to 15 s (mean =  $2.5 \pm 1.1$  s).

These data show that mice escape towards a memorized shelter location and that reaching safety is not required to terminate flight.

---

<sup>32</sup> This shelter was circular (10 cm diameter) with entrances from different sides, and it was made of red translucent Perspex

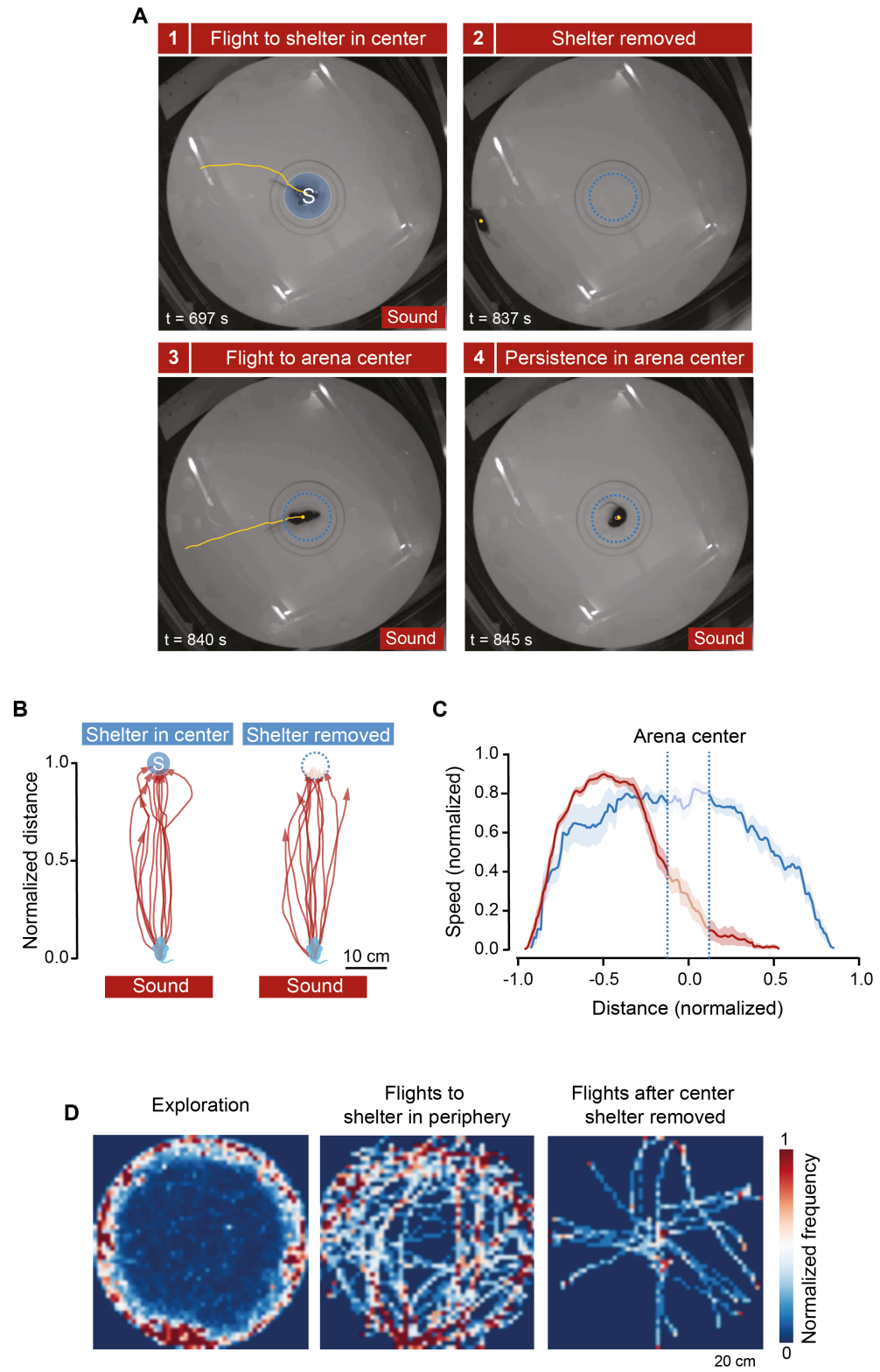


**Figure 13: Flight termination is signalled by having reached the stored target location and does not require reaching safety**

(A) Video frames from one trial showing sound-evoked flight to a shelter in the centre of the arena and persistence of escape to the arena centre after the shelter has been removed.

(B) Escape trajectories for different mice before (left panel) and after (right panel) shelter removal.

(C) Speed profile for escape responses in standard escape assay which trajectory crosses the centre of the arena (blue; from the same dataset shown in Figure 7), and after the shelter has been removed from the arena centre (red). Distance between the mouse and the centre of the arena was normalized between -1 and 0 and the distance between the centre of the arena and the edge between 0 and 1.

(D) 2D histograms for the position of all mice during exploration (left), flights in standard escape assay (centre) and flights after the centre shelter was removed (right). Unless mice have experienced a shelter in the arena centre, they actively avoid the arena centre during exploration (probability of stopping in centre is  $<0.005$ ) and during escape runs to the periphery (11/87 flights pass through the centre and for these, the probability of stopping in the centre is 0.09).

#### **4.5. Memory of shelter location is formed and updated rapidly**

I showed that mice escape accurately to an underground shelter without any previous training, after exploring the Barnes maze for 7 minutes. I next questioned whether mice learn the presence and location of refuge during shorter exposures to the shelter. This was tested by skipping the fixed 7 min habituation period and exposing animals to threat immediately after they visited the shelter for the first time. Even though animals were inside the shelter as little as 18 s (range = 18 to 270 s, N = 12 animals, Figure 14A), this was enough to support shelter-directed escape responses that were indistinguishable from those of the control condition (Figure 14B;  $p = 0.79$  for accuracy and  $p = 0.78$  for linearity, t-test against control escapes after 7 min exploration period). This result demonstrates that memory of presence and location of a shelter in the environment can be formed very rapidly. Notably, I observed a significant negative correlation between the total time spent in shelter and the reaction time (Pearson's  $r = -0.46$ ;  $p = .007$ ), suggesting that computation of the escape trajectory may depend on the strength of the shelter location memory (Figure 14C).

Next, I investigated how shelter place memory copes with changes in the environment, namely changes in the location of the shelter. I designed an experiment in which after eliciting baseline escapes to sound stimuli (3 per assay), the location of the shelter was changed to the opposite hole ( $180^\circ$  away to the initial location, in reference to the centre of the arena). After animals spontaneously visited the new shelter location (mean time = 33.1 s, range = 4 - 82 s), sound stimuli were presented. I found that animals escaped to the new shelter location in less than two trials (mean =  $1.8 \pm 0.3$  trials), with four out of

nine mice escaping to the new location on the first trial. Notably, some animals still escaped to the old location after having successfully fled to the new one on a previous trial; nevertheless, after four trials (mean value; over a period of  $10.5 \pm 6.8$  min), all animals escaped repeatedly to the new location (Figure 15A, B).

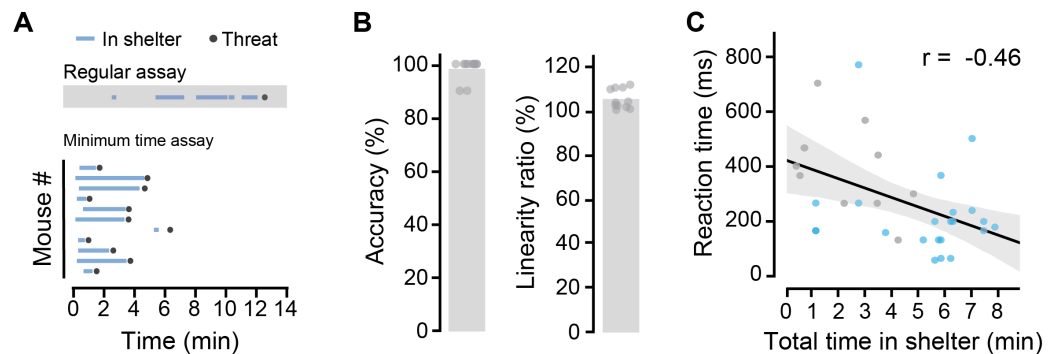


**Figure 14: A single, short visit to the shelter is sufficient to encode the memory of shelter presence and location**

(A) Raster plot showing periods of time inside the shelter from the onset of arena exploration (blue lines) and threat stimulus presentation (black dots). An example raster from a regular assay for comparison (as shown in Figure 7) with multiple entries in the shelter during the 7 min exploration phase is shown at the top.

(B) Average (bars) and data points (circles) for accuracy and linearity of escape after a single visit to shelter, normalised to escapes after 7-minute exploration.

(C) Time to initiate escape is negatively correlated with the total amount of time spent in the shelter before stimulation. Grey circles are data from the single visit assay, and blue circles are data from the standard assay. The black line is a regression line fit to all data points, and the shaded area is 95% confidence interval for the regression.

I observed that escapes to the old location were immediately followed by secondary flights to the new location (including four out of five first trial escapes that were primarily directed at the old shelter location; Figure 15A), suggesting that despite reaching the wrong target, mice already held the memory of the new shelter location. This shows that the new shelter location can be stored in a single trial and that safety devaluation of the

old location supports a permanent update of the escape target after a small number of trials.

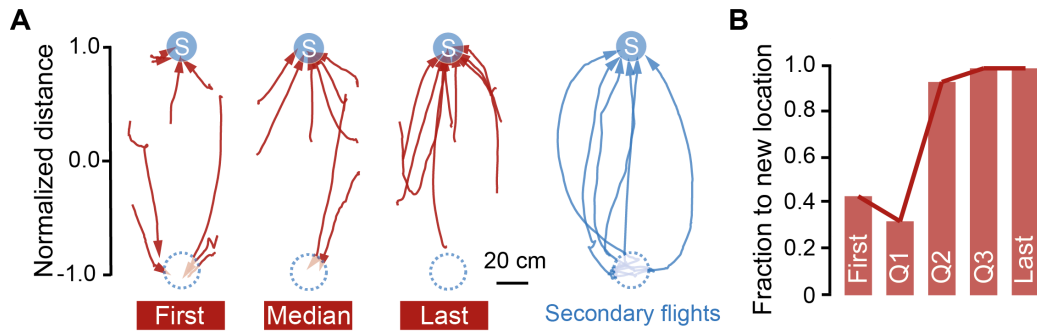


**Figure 15: Mice rapidly update the memory of shelter location upon its abrupt displacement**

(A) Escape trajectories after the original shelter has been closed (dashed blue circle) and a new one opened in a different position (blue circle marked with “S”) for the first and last trials (red left and right, respectively) and the median trial (red, centre). Trajectories in blue (right) are for secondary flights, which immediately follow escapes to the original location.

(B) Evolution of escape behaviour after shelter location has been moved, as in (B), showing the fraction of flights across all mice that reach the new shelter location, for the first, three quartiles (Q1–Q3), and last trials.

## 4.6. Discussion

In this chapter I have described novel behavioural assays designed for studying how the spatial environment and memory thereof control navigation during escape. I have shown that the goal of escape is to reach shelter rather than increasing distance to threat, and to do so mice navigate accurately and linearly after orienting towards the goal. Mice do not use cues near the shelter to guide orientation to shelter during escape, rather relying on memory of shelter location. This memory is formed rapidly, and mice quickly adapt their defensive strategies following changes in features of the environment.

### **Set-up and experimental design**

The design and optimization of the behavioural set-up were critical for the findings presented here and were the result of a series of tests and improvements of the assays. I decided to use the Barnes maze (Barnes, 1979) as a starting point since it is a widely studied navigation paradigm and not as intrinsically anxiogenic as other common assays like the Morris Water Maze (Harrison et al., 2009) which I thought could pervert the study defensive actions which are also associated with anxiety (Amaral et al., 2010, Tovote et al., 2015).

Unwanted visual and auditory cues were isolated by placing the behavioural set-up inside a custom-built light-proof, sound-deadening cabinet, and in some experiments, I placed a 112 cm diameter cylinder around the behavioural platform to block visual cues inside the cabinet. In addition, the behavioural platform and shelter were meticulously cleaned between experiments to minimize olfactory cues. Specifically, for the rotation experiment, I designed the central fixed platform as small as possible, so that the area rotated by the engine was large and included most of the animal waste which could be used as a cue to navigate to shelter. By having a good control over the cues in the environment it was possible to show mice don't use cues proximal to the shelter to navigate towards it, and that visual, auditory and olfactory cues are not primarily used to orient to goal in the task.

Both visual and olfactory aversive stimuli were used because each had advantages for variations of the standard escape assay: visual stimuli can be easily centred above any position of the arena, including above the online-tracked position of the mouse; while auditory stimuli can be used in the dark and in our experience mice show less habituation to this stimulus modality. These different stimuli were critical for demonstrating that the goal of escape is to reach safety and that mice can do so robustly even in the absence of light. In addition, using different stimuli improves the robustness of my findings as they were consistent across stimulation modalities.

Two features of the protocol set my assay apart from the majority of navigation tasks: animals were never trained in any of the tasks, and they were never displaced passively between trials. Concerning the first, it is common in various widely-used navigation tasks that rodents are trained for various sessions across different days (Morris, 1984, Olton and Samuelson, 1976, Barnes, 1979). Here I demonstrate that mice can learn the location of the shelter in less than 30 seconds. Importantly, one does not need to train the animal in the task itself as the drive to escape does not need to be learned since it is innate;

therefore, I am purely testing learning of a spatial location but not of the rules of the task. However, in most experiments described here, mice had 7 min to explore the environment, during which they engaged in spontaneous homings, which can be viewed as a form of training for the assays. Concerning the second distinctive feature of the protocol, by not moving animals passively I did not prevent them from using idiothetic cues to path integrate during exploration (Stackman et al., 2003, Etienne et al., 1986). Although the rotation assay does not demonstrate that mice escape by primarily using a path integration strategy, it suggests that might be the case (see discussion below) and thus it was critical that mice were never displaced passively.

The biggest limitation of the escape assay was the number of trials I could elicit per experiment, as often mice stayed inside the underground shelter for extremely long periods, and as mentioned above I opted to never remove them passively. To address this problem, the experiments shown in the next chapter have been done using an over-ground shelter from which mice tend to exit more often (which is essential to test mice during neural activity manipulations and recordings). After preliminary experiments I opted to not have walls in the platform since despite decreasing anxiety and increasing spontaneous exploration (Pellow et al., 1985, Treit and Fundytus, 1988), these distorted navigation during escape, as in our experience mice gravitate towards walls during escape.

### **Escape is a quasi-linear acceleration to shelter, following orientation towards it**

I showed that the goal of escape is reaching shelter using high contrast visual stimulus that elicits very robust and fast escapes (Evans et al., 2018). This demonstrates that even when faced with strong evidence of eminent threat mice do not primarily direct escape away from threat.

The results I presented in this chapter show that this behaviour is composed of two modules: an initial orientation to shelter, followed by a run towards it. This strategy allows escapes to be quasi-linear at the cost of increasing the time it takes to leave the location the mouse occupies upon threat detection, because the head-rotation takes some time and mice only start running after its completion.

My observation that the initial movement orients the mouse towards the shelter differs from the findings from Ellard and Eller (Ellard and Eller, 2009) who studied escape trajectories from gerbils. The authors report that the majority of animals initially moved

away from the shelter followed by a corrective movement, whereas I observe a rotation that immediately decreases the head-shelter offset of the mouse. This difference may be species specific or related to the difference in visual stimulus used.

Remarkably mice rotate to the side that bears a smaller angular distance to shelter in 91.5% of the trials, and in the remaining trials mice rotated less than 200°. This shows that rotation through the 'far side' only occurs in situations in which the angular distance to shelter through both sides is approximately the same. More importantly, this result shows that the goal of the rotation movement is memorized rather than relying on cues near the shelter to interrupt a random-sided rotation. Both the experiments conducted in the dark and the rotation assay support the finding that mice do not rely on cues proximal to the shelter to guide orientation and navigation towards it during escape.

Since mice orient to old shelter location following rotation of the shelter together with all visual and olfactory cues in the environment, it is very much likely they rely on idiothetic cues to escape to shelter, using path integration. Although, in my standard assay I do not observe the typical error accumulation as a function of displacement that characterizes path integration (Etienne and Jeffery, 2004), this could be due integration of sensory information during exploration to offset the error; alternatively error accumulation might not be clearly observed due to the relatively small size of the arena and the short exploration bouts mice engage in my assay. It is important to clarify the goal of the rotation assay was to test whether mice rely on place memory or simply navigate towards a memorized cue near the shelter by employing for example olfactory gradient ascent towards olfactory cues in the shelter (Gire et al., 2016) or navigation towards the salient LED cue near the shelter, similarly to the cued version of the Morris water maze (Vorhees and Williams, 2006). My rotation experiment result shows that mice rely on place memory to orient and navigate to shelter and that this is not primarily computed in relation to visual or olfactory cues. Therefore, and since the set-up is also sound-deadening, I hypothesise mice rely on idiothetic cues to escape. In order to explicitly test this a few different experimental strategies could be sought. One example is to remove and disorient the mouse in which case path integration would be compromised, as referred above. However, this procedure would have two problems: mice often do not respond to aversive stimulus immediately upon being placed in the behavioural arena, and this experiment would only be interpretable if mice solely rely on idiothetic cues to escape to shelter. A more elegant test would be to rotate the mouse below the vestibular detection threshold (Guedry, 1974), which would offset the path integrator from the real location of the shelter determining a predictable error in orientation if mice primarily orient by path integration.

### **Mice learn rapidly presence and location of shelter**

One of the most fascinating findings of the results presented above is that mice very accurately escape to shelter after visiting it only once. This differs from performance in other navigations assays. By the end of the first training day (consisting of four trials) in the traditional Barnes maze assay, mice make on average more than 10 errors before entering the shelter, and even after four days of training mice make on average 5 errors<sup>33</sup> (O’Leary et al., 2011, Patil et al., 2009). The strategy to reach shelter is also distinct from the quasi-linear strategy I observed, with mice in the standard Barnes assay navigating on average approximately 8 meters on average before entering the shelter even after four days of training, whereas only 10% trials being characterized by a direct search strategy (Patil et al., 2009).

Although the error metrics are different from our measured escape error, the average number of errors in my standard assay measured in the classic Barnes assay metrics would be less than 1. Some studies report the distance between first visited Barnes pseudo-hole and the correct one (similar to my escape accuracy metrics) to be near chance (50 - 65%) by the end of the first training day (Pitts, 2018, O’Leary and Brown, 2009), whereas I observe a 97% escape accuracy to overhead aversive visual stimuli in naïve mice. This higher accuracy may be due to differences in the experimental protocol such as the passive displacement of mice between trials in the traditional Barnes assay, and the presentation of predatory-mimicking stimuli in my assay which may increase the reward-value of the shelter and thus manipulate motivation.

As mentioned above, the fact that mice do not need to learn the rules of the task but just the location of the shelter may be also critical for this performance difference. The simplicity and robustness of my assay makes it a powerful tool in the study of spatial memory. While assays like the traditional Barnes maze or the Morris water maze have been extensively applied and are invaluable, they usually rely on relatively long training periods, which last more than 15 days for the former and more than five for the latter (Seeger et al., 2004, Bach et al., 1995, Vorhees and Williams, 2006). My assay triggers very accurate escapes which can be the baseline for the study of effects of manipulations and disease-models on spatial memory. However, I do not propose that my assay should replace either the traditional Barnes assay or the Morris water maze which are designed

---

<sup>33</sup> This is the number of total errors, i.e. pseudo-holes visited until the mouse actually enters the shelter. The average of primary errors (number of pseudo-holes the mouse traverses before visiting the correct one even if it does not enter it) reported by Patil and colleagues is 6 on first day and 2 on fourth day.

to address specific questions about spatial learning, spatial memory and navigation (Vorhees and Williams, 2006) but rather be considered as an alternative, when suitable and advantageous.

### **Flexibility of defensive behaviours**

Various assays presented in this chapter illustrate how flexible defensive actions are, specifically as a function of features of the spatial environment. Previous work had showed animals including mice favour freezing in the absence of a shelter, while escape is preferred when refuge is reachable (Hennig et al., 1976, Blanchard et al., 1986, Wei et al., 2015, De Oca et al., 2007, O'Brien and Dunlap, 1975). My work demonstrated that this change of defensive strategy happens rapidly following changes in the environment and that the change in preference between freezing or flight is rapidly implemented in either direction. In addition, I demonstrate this in a very controlled manner by presenting the same stimulus within the same session (a few minutes apart) to the same animal.

The execution of escape is also highly flexible. Not only is escape characterized by a flexible sequence of movements adjusted to bring the animal to shelter, but changes in the environment also promptly modify the execution of escape. When the shelter entrance was closed, and another was opened in the opposite side of the arena (which is equivalent to rotating the shelter but none of the cues in the environment), I observed that mice rapidly updated the goal of escape to the new shelter position. Two remarks are particularly interesting about the results of this experiment: first, although almost half of the mice ran to the new location after having visited it only once, some of these animals still escape to the old location of the shelter in subsequent trials. Second, following escapes to the old shelter location mice robustly ran to the new location of the shelter. Taken together these observations indicate that mice store the two locations of the shelter (current and past) and that the choice to run to one or another derives from some valuation process of each shelter. While the new shelter location has been visited more recently the old shelter location not only has been visited more times but also it has rewarded the mouse with safety upon escaping from baseline trials. The reason why mice return to the old shelter location is unclear. Possibilities include the mechanism of goal-location encoding being noisy, or mice interpreting the shelter entrance being opened or closed as a probabilistic event.

I have conducted anecdotal experiments in which two shelters are always present in the Barnes Maze and found that mice do not appear to have a preferred shelter. Instead upon presentation of aversive auditory stimuli, mice escape to one of the shelters, seemingly not based on linear or angular distance, last shelter visited, or total time spent in each shelter. The question of how mice negotiate different refuges is a very interesting one as it involves assessing the ongoing value of refuges to compute an escape towards one of them.

Although we do not know how mice compute the value of a shelter, we know that at least they take into account their current situation in the environment to decide on engaging a defensive action. When an aversive sound stimulus was presented inside of the shelter mice did not engage in an acceleration, suggesting they either know they are in a safe place or in the safest place in the arena. To dissect these two options one could design an experiment in which two identical shelters are available, and test if mice run to the other shelter upon presentation of an aversive stimulus inside the shelter mice currently occupy (which would favour the hypothesis that mice evaluate the ongoing relative safety in relation to the options available). In my simpler experiment I show mice do not escape when they are inside the shelter, but it was not possible to assess if they engage in freezing as mice tend to naturally stay immobile inside the shelter and after the stimulus, they continued to do so<sup>34</sup>.

In comparison to my assay, flexibility of navigation to a new goal location in the Morris water maze has slower dynamics, with mice taking on average 4 days (4 sessions per day) to spend above-chance time on the correct quadrant of the maze (Vorhees and Williams, 2006). Similarly, reversal training in the traditional Barnes assay is associated with low accuracy and large number of errors during the first days of training (O'Leary and Brown, 2009).

---

<sup>34</sup> Freezing is an active response in which the muscles of the whole body contract and the animal stays immobile except for respiratory movements. While it is easy to observe sudden immobility during exploration of the Barnes maze as it was very unusual, mice usually are immobile inside the shelter. Although the shelter for this experiment was over-ground and see-through, I could not confirm the mouse freezes or simply does not respond to the sound stimulus.

## **5. RESULTS:**

**A projection from retrosplenial cortex to superior colliculus is critical for orienting during escape**

In the previous results chapter, I showed that an accurate memory-guided head-orienting movement towards the refuge direction precedes acceleration in escape. In this chapter, I probe the neural circuits involved in this orientation behaviour, by using a projection-specific chemogenetic inactivation strategy.

## **5.1. Loss of function of the superior colliculus decreases orientation accuracy during escape**

The superior colliculus (SC) is known to play a critical role in orientation movements of the eyes (Robinson, 1972, Sparks, 1986, Lee et al., 1988, Dorris et al., 1997, Dash et al., 2015, McPeck and Keller, 2004) and head (King et al., 1991, Freedman et al., 1996, Freedman and Sparks, 1997, Walton et al., 2007, Wilson et al., 2018, Masullo et al., 2019). Thus, I hypothesised inactivation of the SC would impair orientation in escape. To test this hypothesis, I injected an AAV virus coding for the inhibitory DREADD hM4D(Gi) (Armbruster et al., 2007) in the SC, bilaterally (Figure 16A). After waiting for four weeks for expression I injected randomly saline or the DREADD agonist CNO intraperitoneally, 35 minutes before testing the animals in a behavioural assay.

In this assay mice were placed in a circular arena with 92 cm diameter, containing an over-ground shelter (20 x 10 x 10 cm) located randomly at the edge of the arena, with the entrance (5 cm wide) facing the centre of the arena. After seven minutes of exploration during which mice visit the shelter at least once, innately aversive ultrasound stimuli were presented (2 s long, upswing from 17 to 20 kHz, 80-82 dB at arena floor level), with at least 90 s interstimulus interval. After seven stimuli or 40 minutes (whichever first) the lights in the arena were turned off, and after a five minutes adaptation period the same stimuli were presented in the dark. The experiment was terminated once seven stimuli were delivered in light and in dark, or after 90 min, whichever first. Mice were retested after at least 72 h in the same task, following injection of saline or CNO (whichever was not administered on the first test).

Loss of function of the SC did not obviously impair linear and angular movements during exploration. Mice reliably accelerated in response to the threatening auditory stimulus when treated with CNO (CNO treated animals: mean peak speed 3 s before sound = 34.65 cm/s; mean peak speed 3 s after sound = 63.84 cm/s;  $p < 0.0001$ , two-tailed, paired t-test;  $N = 31$  responses from 3 animals. Saline treated animals: mean peak speed 3 s before sound = 22.03 cm/s; mean peak speed 3 s after sound = 64.92 cm/s;  $p < 0.0001$ , two-tailed, paired t-test;  $N = 31$  responses from 3 animals; Figure 16B), and peak speed in

escape was not different for saline and CNO treated animals ( $p = 0.801$ , two-tailed unpaired t-test). However, escapes were initiated with a larger angular offset between the mouse's heading and the shelter direction (we call this metric 'escape error', and measure it in degrees, in an egocentric reference frame. An escape error of  $0^\circ$  means the mouse perfectly oriented to the shelter entrance whereas an escape error of  $180^\circ$  means the mouse oriented completely opposite to the shelter before accelerating (Figure 16C)).

Escape error was similar in light and in dark for each of the injections (saline light vs. dark,  $p = 0.705$  ( $N = 31$  escapes from 3 animals); CNO light vs. dark,  $p = 0.555$  ( $N = 31$  escapes from 3 animals); two-tailed Mann-Whitney test) and the light and dark trials were pooled. I observed that loss of function of the SC increased the median escape error (saline =  $12.0^\circ$  ( $N = 31$  escapes from 3 animals); CNO =  $23.0^\circ$  ( $N = 31$  escapes from 3 animals);  $p = 0.025$ , two-tailed Mann-Whitney test, Figure 16D) and that the number of high-error escapes<sup>35</sup> increased (saline = 9.7%, CNO = 29.0%, Figure 17).

The increase in escape error following SC loss of function resulted in a significant increase in the time it took the mouse to reach shelter following the presentation of the stimulus (median saline = 1533 ms ( $N = 31$  escapes from 3 animals); median CNO = 2133 ms ( $N = 31$  escapes from 3 animals);  $p = 0.0004$ ; two-tailed Mann-Whitney test; Figure 16E), which was not explained by a difference in angular offset at time of stimulus presentation, latency to initiate escape, average rotation speed or peak speed of escape (for all values of two-tailed Mann-Whitney test between saline and CNO,  $p > 0.10$ ).

---

<sup>35</sup> Defined as the mouse not escaping to the correct egocentric quadrant, i.e. an escape error larger than  $45^\circ$

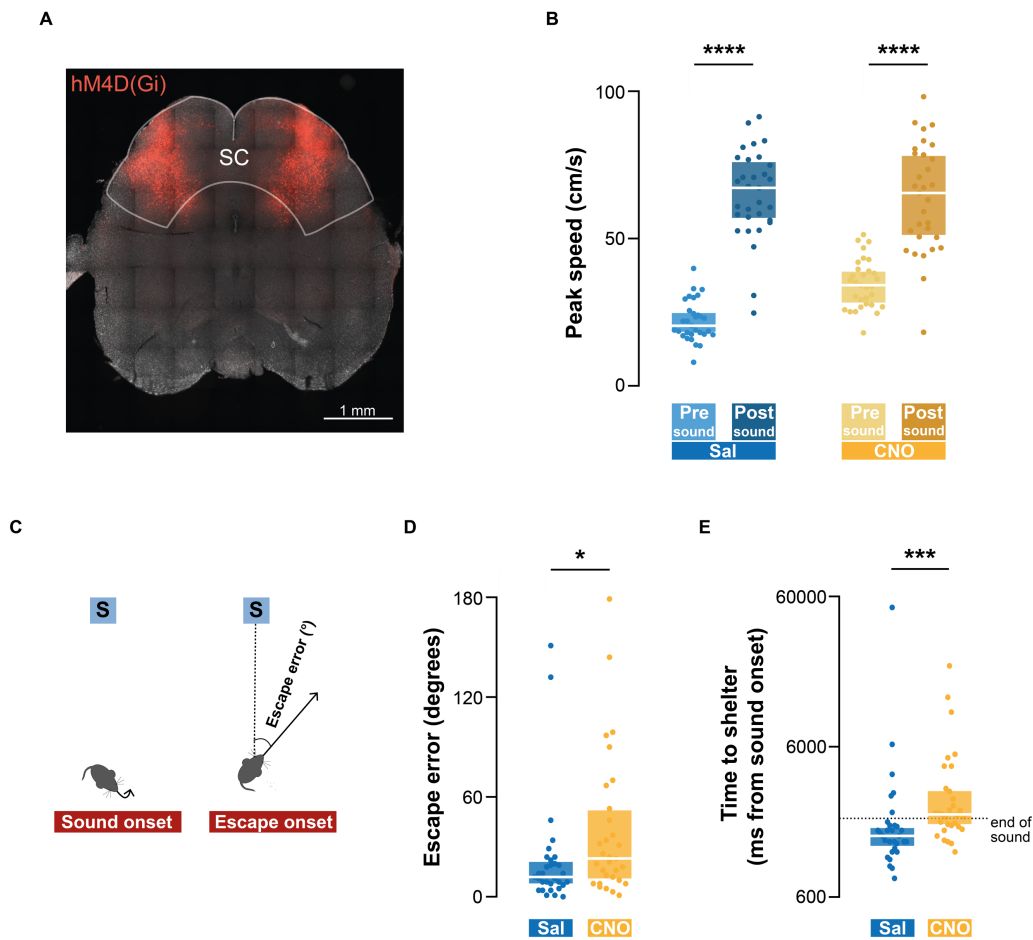


**Figure 16: Superior colliculus loss of function impairs orientation accuracy during escape**

(A) Representative image showing injection spread of AAV8-hSyn-hM4D(Gi)-mCherry in the superior colliculus (SC).

(B) Both control (saline-treated) and loss of function (CNO-treated) groups engaged in acceleration in response to sound stimulus, as seen by the increase in peak speed in the 3 s after stimulus for both conditions ( $p < 0.0001$  for pre vs post sound in both conditions).

(C) Representation of the escape error metric characterized by the angular distance between the mouse's heading and the shelter upon initiation of sound elicited escape.

(D) Loss of function of the SC (following administration of CNO) significantly increases escape error.

(E) Loss of function of the SC (following administration of CNO) significantly increases the time of arrival to shelter in escape. Y-scale is logarithmic to better show the result.

For B, D and E, white line marks the median and the box the interquartile range. Each point is an individual trial.

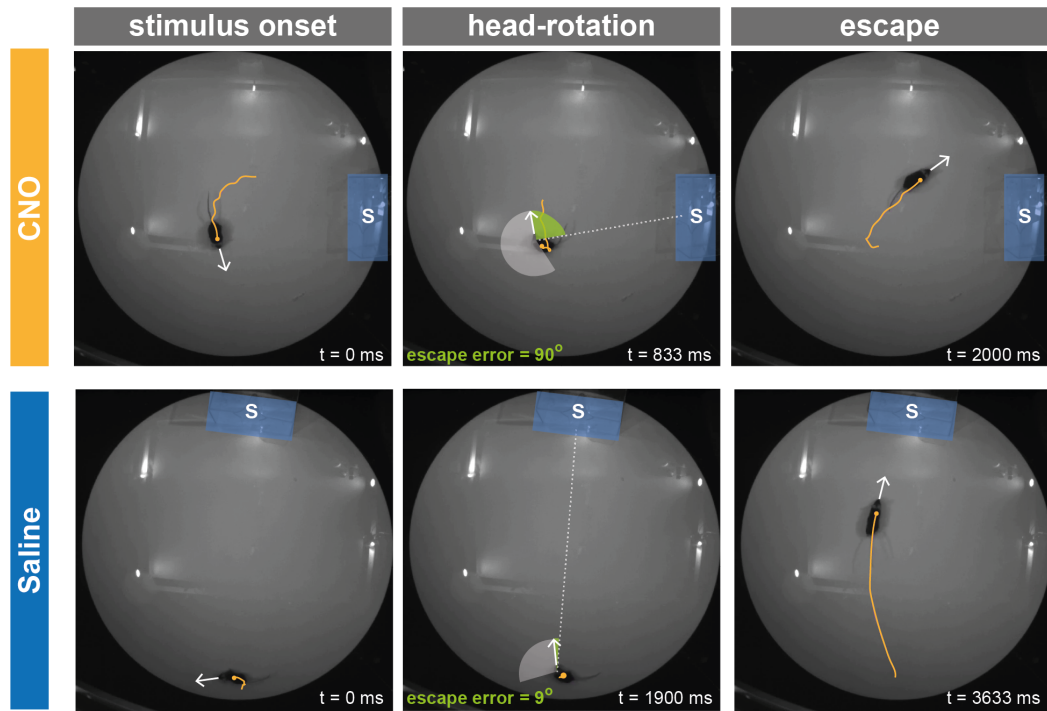


**Figure 17: Example of high-error escape following superior colliculus loss of function**

The top panels show an example escape with high escape error, following CNO administration to a mouse. Note the mouse rotates to the angular far side to the shelter. Bottom panels show an accurate escape from the same mouse following saline administration, 72h after the loss of function test. Time (t) is measured from the presentation of the aversive sound stimulus. White arrows show ongoing heading of the mouse; yellow lines show mouse's trajectory in the previous second. White dotted lines correspond to a 0° escape error. Green angle shows the escape error, measured between the animal current heading and the perfect escape direction. White angle shows the orientation-movement of the mouse following presentation of aversive sound. The blue rectangle with an 'S' highlights the position of the shelter.

## **5.2. Retrosplenial cortex projects monosynaptically to the superior colliculus and is necessary for accurate orientation during escape**

While the SC is essential for orientation movements, it has been shown that some cortical areas are also critical for orientation, particularly in situations more complex than simple orientation towards a salient sensory cue. Cortical regions that have been implied in

orientation include the posterior parietal cortex (PPC), anterior motor areas (AMA; including frontal eye fields, secondary motor cortex and prefrontal cortex) and retrosplenial cortex (RSC). Cortical contributions to orientation are diverse: PPC (Paré and Wurtz, 1997, Heide et al., 1995, Pierrot-Deseilligny et al., 1995, Paré and Wurtz, 2001) and AMA (Schiller et al., 1980, Schlag-Rey et al., 1992, Pierrot-Deseilligny et al., 1995, Paus et al., 1993, Murakami et al., 2014, Erlich et al., 2011) are critical for the control of orientation particularly to memorized goals, while RSC is essential to establish an allocentric reference frame of orientation and anchor the local environment representation to it (Julian et al., 2018, Jacob et al., 2017, Iaria et al., 2007, Lin et al., 2015).

I hypothesised that the SC may be controlled by an upstream cortical area that either computes the head-shelter angular offset or at least provides allocentric information to the SC which could then itself perform such computation. To test whether any cortical area projecting to the SC is essential for orienting during escape, I started by tracing back from the SC to identify candidate afferents. I performed monosynaptic retrograde rabies tracing from VGluT2<sup>+</sup> (Figure 18A) and from VGAT<sup>+</sup> (Figure 19A) neurons in SC and found direct, ipsilateral projections from PPC, RSC and AMA to both subpopulations of collicular neurons (Figure 18B and Figure 19B). Projections from PPC (Fries, 1984, Collins et al., 2005, Oh et al., 2014), RSC (van Groen and Wyss, 1992, Künzle, 1995, Oh et al., 2014, Comoli et al., 2012, García Del Caño et al., 2000) and AMA (Fries, 1984, Huerta et al., 1986, Stanton et al., 1988, Collins et al., 2005, Oh et al., 2014) have previously been reported.

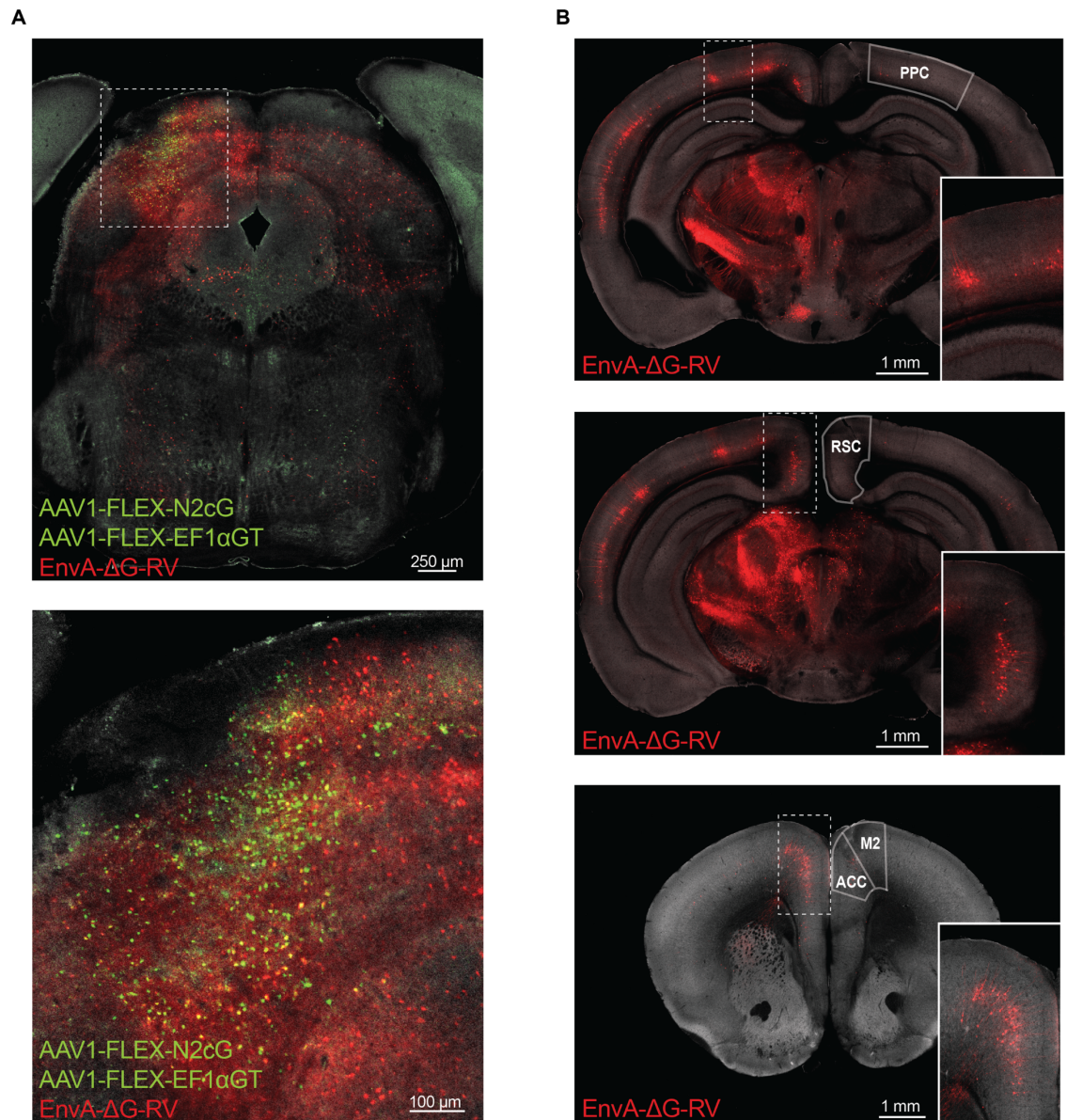


**Figure 18: Retrograde tracing from VGlut2<sup>+</sup> superior colliculus neurons**

(A) Pseudo-starter cells infected by helper AAV viruses (green) and glycoprotein-deleted rabies virus (red) are shown in yellow. Top figure shows topography of injection and bottom a higher magnification of the area marked with the dotted white box above.

(B) Illustration of monosynaptic cortical projections to VGlut2<sup>+</sup> neurons in SC. Top: projection from posterior parietal cortex (PPC); middle: projection from retrosplenial cortex (RSC); bottom: projection from anterior motor areas (AMA), namely secondary motor cortex (M2) and anterior cingulate cortex (ACC).

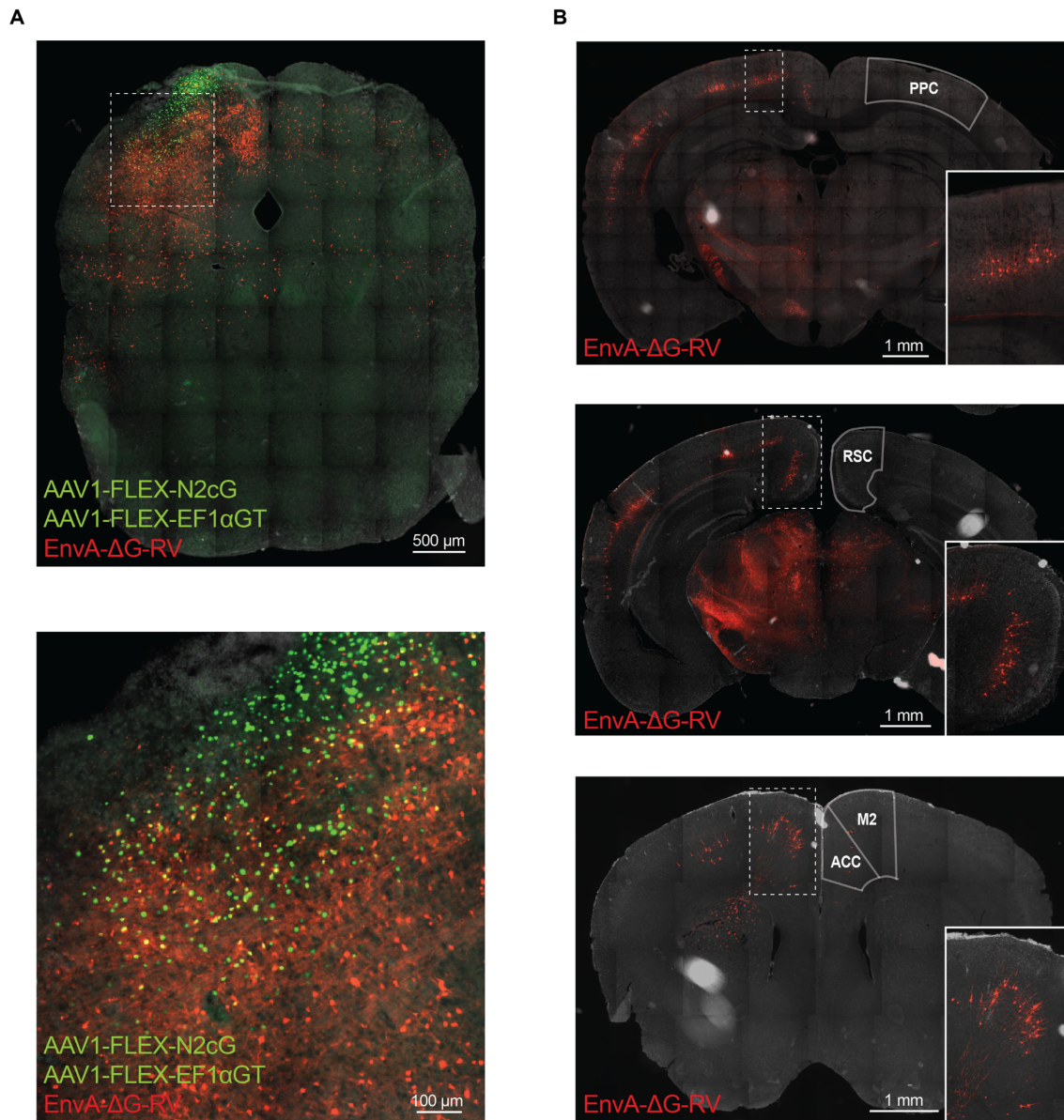


**Figure 19: Retrograde tracing from VGAT<sup>+</sup> superior colliculus neurons**

(A) Pseudo-starter cells infected by helper AAV viruses (green) and glycoprotein-deleted rabies virus (red) are shown in yellow. Top figure shows topography of injection and bottom a higher magnification of the area marked with the dotted white box above.

(B) Illustration of monosynaptic cortical projections to VGAT<sup>+</sup> neurons in SC. Top: projection from posterior parietal cortex (PPC); middle: projection from retrosplenial cortex (RSC); bottom: projection from anterior motor areas (AMA), namely secondary motor cortex (M2) and anterior cingulate cortex (ACC).

To test if any of these SC-projecting cortical areas (RSC, PPC or AMA) are essential for accurate orienting during escape, I performed loss-of-function experiments using a similar strategy to the one described above for the SC<sup>36</sup> (Figure 20A).

Of the probed areas, only the RSC was shown to be critical for the accuracy of orientation in escape. DDREAD-mediated loss of function of RSC but not of AMA or PPC increased the escape error (RSC: control median = 9.0° (N = 24 responses from 4 mice); CNO median = 28.0° (N = 51 responses from 4 mice);  $p = 0.0062$ , two-tailed Mann-Whitney test. PPC: saline median = 13.5° (N = 22 responses from 3 animals); CNO median = 10.0° (N = 31 responses from 3 animals),  $p = 0.545$ , two-tailed Mann-Whitney test. AMA: saline median = 27.5° (N = 28 responses from 3 animals), CNO = 9.0° (N = 31 responses from 4 animals),  $p = 0.097$ , two-tailed Mann-Whitney test). For all areas there was no statistical significance between escape error in light and dark for control or CNO injections ( $p > 0.10$ , two-tailed Mann-Whitney test, for light vs dark for all three cortical areas), and responses in light and dark were pooled.

---

<sup>36</sup> The inactivation experiments of the anterior motor areas (Cingulate and Secondary Motor Cortices) were conducted in a different set-up from the remainder experiments in this chapter, using an underground shelter, similarly to the previous results chapter. Although the same test was done for saline and CNO injections, these results should not be directly compared to the loss-of-function experiments targeting the other cortical areas.

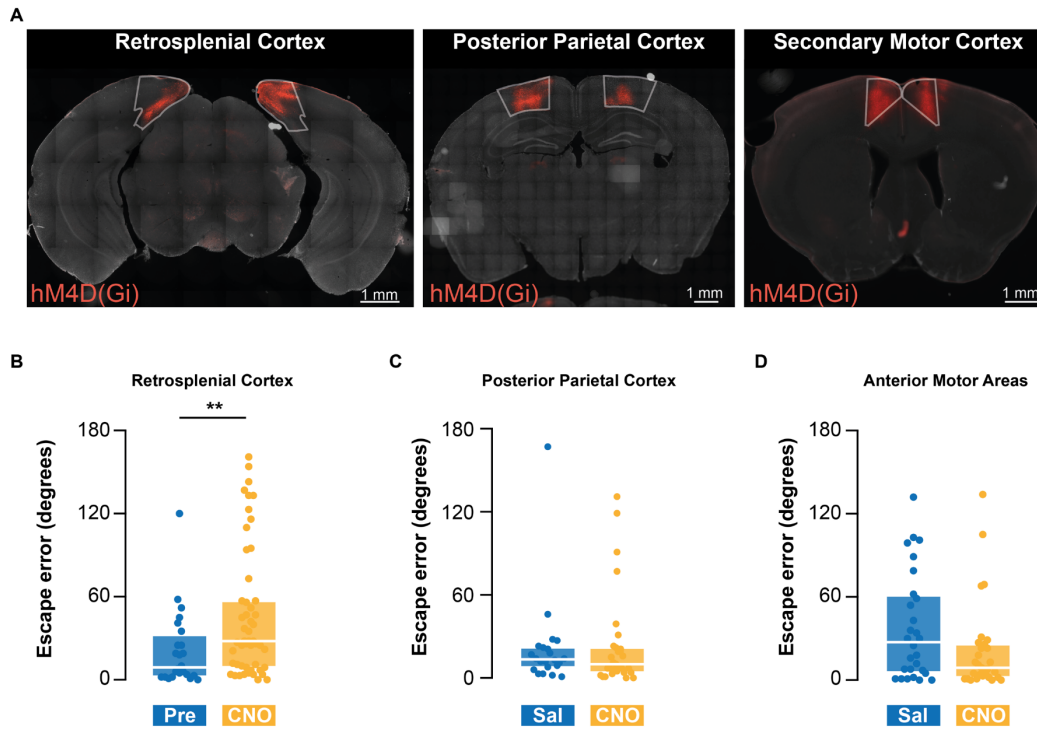


**Figure 20: DREADD-mediated loss of function of retrosplenial cortex impairs orientation to shelter during escape**

(A) Representative image showing injection spread of AAV8-hSyn-hM4D(Gi)-mCherry in the retrosplenial cortex (RSC), posterior parietal cortex (PPC) and Secondary motor cortex (M2), left, centre and right panels, respectively.

(B) DDREAD-mediated loss of function of the RSC significantly increases escape error (in comparison to post-surgery pre-test).

(C) DDREAD-mediated loss of function of PPC does not change escape error ( $p = 0.545$ ).

(D) DDREAD-mediated loss of function of AMA (secondary motor or anterior cingulate cortices) does not change escape error ( $p = 0.097$ ).

For B, C and D, white line marks the median and the box the interquartile range. Each point is an individual trial.

### 5.3. Monosynaptic projection from retrosplenial cortex to superior colliculus is critical for orientation during escape

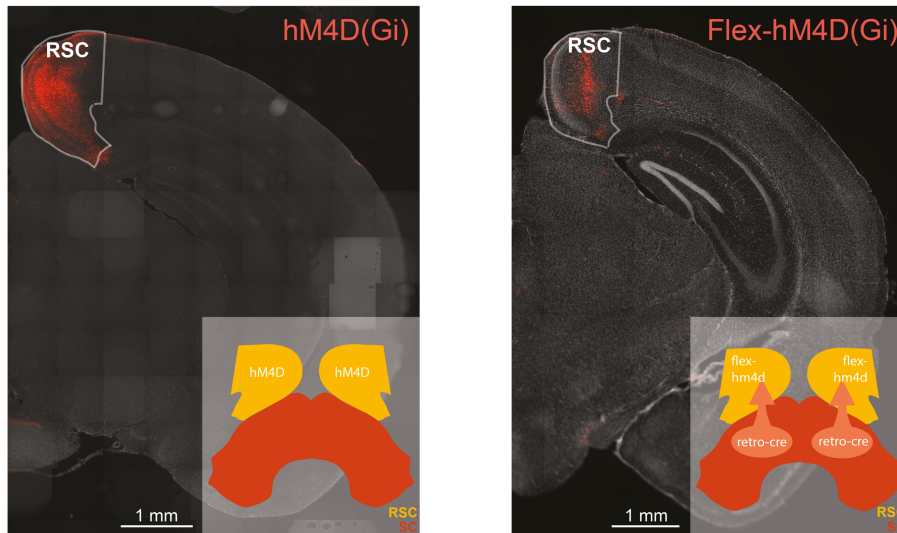
Having observed a decrease in orientation accuracy following either SC or RSC loss of function, I next aimed to confirm that the projection from RSC to SC is functional by performing channelrhodopsin-2-assisted connectivity mapping (Petreanu et al., 2007). I

injected a non-flexed-ChR2-coding AAV (AAV1-CAG-ChR2(H134R)-mCherry-WPRE) in the RSC in VGluT2::EYFP and VGAT::EYFP mice, and sacrificed the animals after 9-14 days. Histology was performed *post hoc* to confirm that the injection was restricted to the RSC. Colleagues in the lab performed whole-cell patch-clamp recordings from EYFP-expressing cells in the SC., and showed that 40.6% of VGluT2<sup>+</sup> neurons (N = 69 cells from 4 mice) and 46.6% of VGAT<sup>+</sup> neurons (N = 73 cells from 3 mice) received monosynaptic input from RSC. Notably, optogenetic stimulation of RSC inputs was sufficient to trigger action potentials in SC VGAT<sup>+</sup> but not SC VGluT2<sup>+</sup> cells.

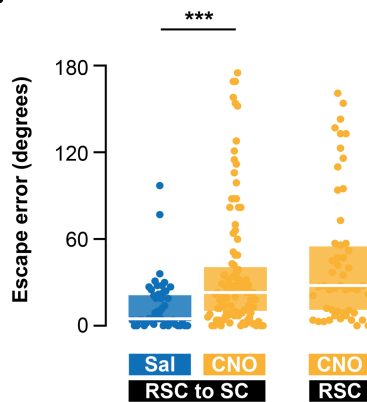
To test the necessity of SC-projecting RSC neurons for orienting during escape, I specifically targeted this subpopulation by injecting a retro-AAV coding for Cre (pAAV-CMV-bGlo-iCre-GFP) into the SC. At this stage only neurons projecting to SC will have Cre; subsequently I injected a flexed-hM4D(Gi)-coding AAV (AAV2-hSyn-DIO-hM4D(Gi)-mCherry) into the RSC, which resulted in only SC-projecting RSC neurons expressing the DREADD.

Despite targeting a smaller fraction of RSC neurons (Figure 21A left vs. right panels), the phenotype obtained by this inactivation strategy was not different to the unspecific loss of function of the RSC (escape error,  $p = 0.155$  ; time to shelter,  $p = 0.171$ , two-tailed Mann-Whitney test). I observed an increase in escape error in mice treated with CNO (saline median =  $5.0^\circ$  (N = 46 trials from 6 animals); CNO median =  $23.0^\circ$  (N = 104 trials from 11 animals),  $p = 0.0001$ , two-tailed Mann-Whitney test, Figure 21B). The frequency of high-error escapes following inactivation of SC-projecting RSC neurons was 24.0% (vs. 4.3% following administration of saline). Time to shelter also significantly increased following inactivation of SC-projecting RSC neurons (CNO median = 2166 ms (N = 104 trials from 11 animals); saline median = 1266 ms (N = 46 trials from 6 animals);  $p < 0.0001$ , two-tailed Mann-Whitney test, Figure 21C), and it this metric was also not different from the global RSC inactivation ( $p = 0.171$ , two-tailed Mann-Whitney test).

A



B



C

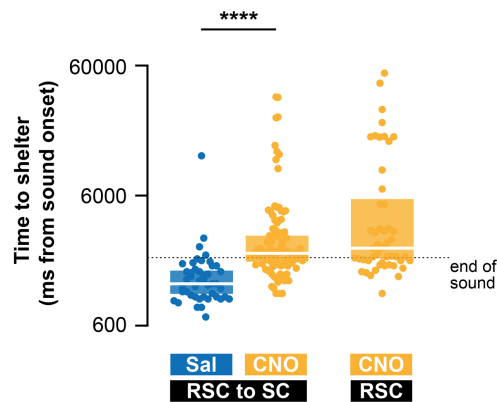


**Figure 21: Inactivation of superior colliculus-projecting retrosplenial neurons impairs orientation to shelter during escape to the same extent as global retrosplenial inactivation**

(A) Representative image of injection spread of AAV8 coding for non-flexed hM4D(Gi) (left) and AAV2 coding for flexed hM4D(Gi), following injection of retro-AAV coding for Cre into the SC (right). The projection-specific infection is limited to layer V of RSC and the number of cells expressing hm4D-mCherry is obviously smaller than in the non-specific inactivation. Schematics in bottom right of each panel illustrate the respective loss of function strategy.

(B) Loss of function of SC-projecting RSC neurons leads to a significant increase in escape error, which is not different from the non-specific loss of function of RSC ( $p = 0.155$ )

(C) Loss of function of SC-projecting RSC neurons leads to a significant increase in time to shelter, which is not different from the non-specific loss of function of RSC. Y-scale is logarithmic to better show the result ( $p = 0.171$ )

For B, and C, white line marks the median and the box the interquartile range. Each point is an individual trial.

While the previous result shows that SC-projecting RSC neurons are critical for correctly orienting to shelter during escape, it does not prove that this projection itself is essential, as, alternatively, a parallel projection from the same SC-projecting RSC neurons to a different target might be controlling the behaviour. To address this, I performed projection-specific loss of function by combining the viral strategy that leads to specific targeting of SC-projecting RSC neurons with implantation of cannulae over the SC. This allows local delivery of CNO onto the RSC-SC terminals of the neurons expressing hm4D(Gi), and thus selective inactivation of this projection (Stachniak et al., 2014, Evans et al., 2018) (Figure 22A and B).

I found that inactivation of the projection from RSC to SC impairs orientation during escape shown by an increase in escape error (saline median =  $15.0^\circ$  (N = 36 responses from 6 animals), CNO median =  $31.0^\circ$  (N = 53 responses from 6 animals);  $p = 0.001$ , two-tailed Mann-Whitney test; Figure 22D). Furthermore, following inactivation of this projection I observed an increase frequency of high-error escapes from 11.1% (saline control) to 41.5% (Figure 23). Light and dark trials have been pooled for this analysis results since there was a significant impairment of orientation in both conditions (light: saline vs CNO,  $p = 0.015$ . Dark: saline vs CNO,  $p = 0.018$ , two-tailed Mann-Whitney test, Figure 22C) and no significant difference in escape error in light and dark (saline: light vs dark,  $p = 0.187$ ; CNO: light vs dark,  $p = 0.142$ , two-tailed Mann-Whitney test).

Despite orienting incorrectly following threatening stimuli, mice still reliably escaped as shown by their robust stimulus-triggered acceleration (Figure 22E) (for both inactivation and control, mean peak speed 3 s before vs after stimulus,  $p < 0.0001$ , two-tailed paired t-test). There was no significant difference in peak speed after CNO infusion vs saline ( $p = 0.864$ , two-tailed unpaired t-test), or latency to initiate escape ( $p = 0.382$ , two-tailed unpaired t-test, saline vs CNO), yet there was a significant increase in the time of arrival to shelter following inactivation of the projection from RSC to SC (Figure 22F). Although there was a significant difference in angular offset to shelter upon stimulation, this was not significantly correlated to escape error (saline: Pearson  $r = 0.086$ ,  $p = 0.629$ , and CNO: Pearson  $r = 0.053$ ,  $p = 0.723$ , two-tailed Pearson correlation coefficients) or to time to shelter (saline: Pearson  $r = -0.049$ ,  $p = 0.787$  and CNO: Pearson  $r = -0.072$ ,  $p = 0.063$ , two-tailed Pearson correlation coefficients), meaning that this initial difference in angular offset to goal does not justify the increase in time to reach shelter following inactivation of the RSC-SC projection.

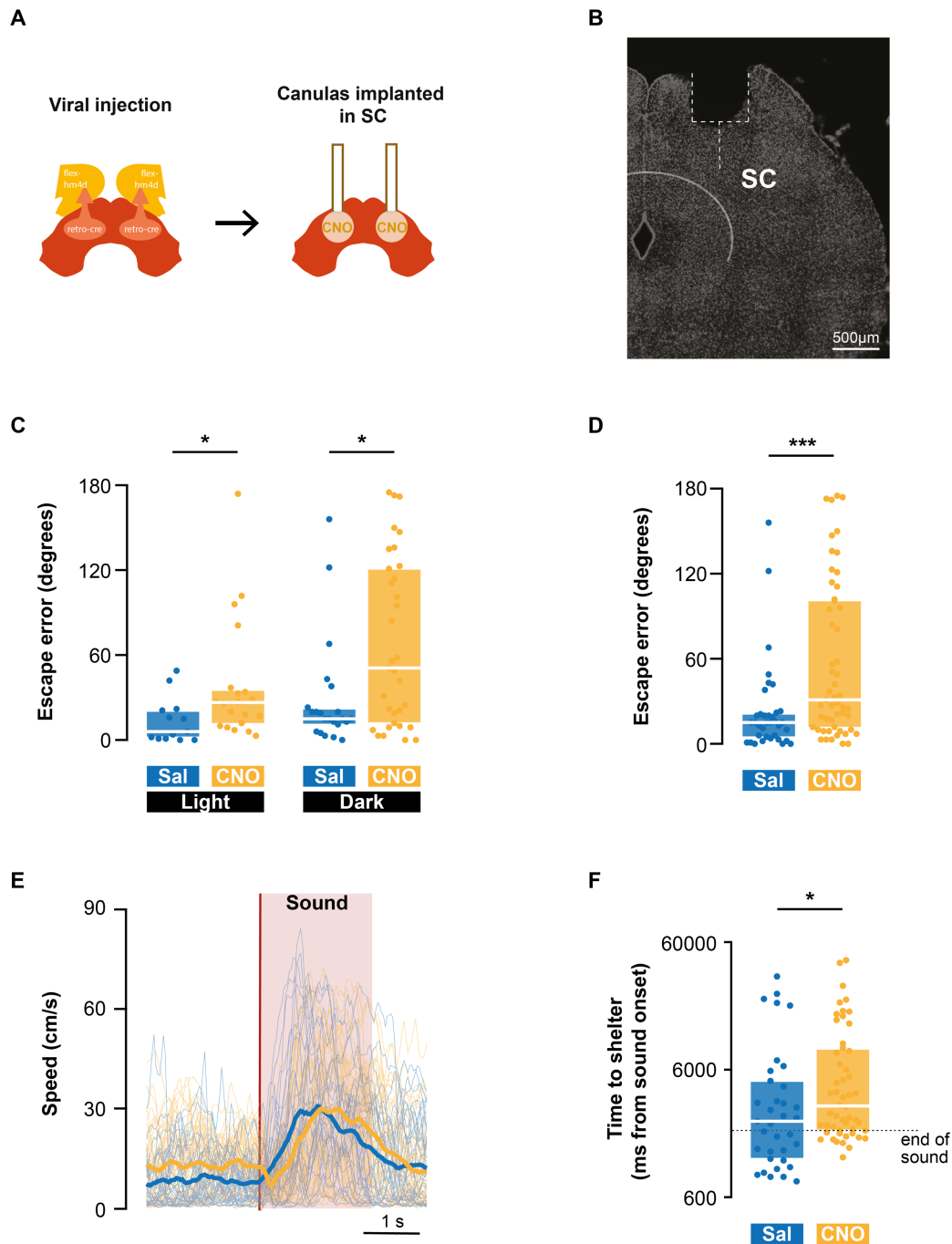


**Figure 22: Inactivation of the projection from retrosplenial cortex to superior colliculus impairs orientation during escape**

(A) Schematic of the projection-specific inactivation strategy, involving infecting superior colliculus (SC)-projecting retrosplenial (RSC) neurons and administering CNO directly to terminals of the cortical neurons in SC, via cannulas implanted into the latter.

(B) Representative image showing placement of guide cannula in SC. The lesion shows the location of the guide cannula which is implanted in the skull of the animal and through which an internal cannula is positioned in place, down to 0.5 mm below its opening (white dotted line).

(C) Inactivation of the projection significantly impairs orientation during escape in light ( $p = 0.015$ ) and dark ( $p = 0.018$ ).

(D) Data from C, pooled.

(E) Speed profiles between 2 s before and 3 s after sound stimulus, showing similar speed profiles in inactivation of the projection from RSC to SC and control (comparison of peak speed, CNO vs. saline  $p = 0.864$ ).

(F) Loss of function of the projection leads to a significant increase in time to shelter ( $p = 0.033$ ).

For C, D and F, white line marks the median and the box the interquartile range. Each point is an individual trial.

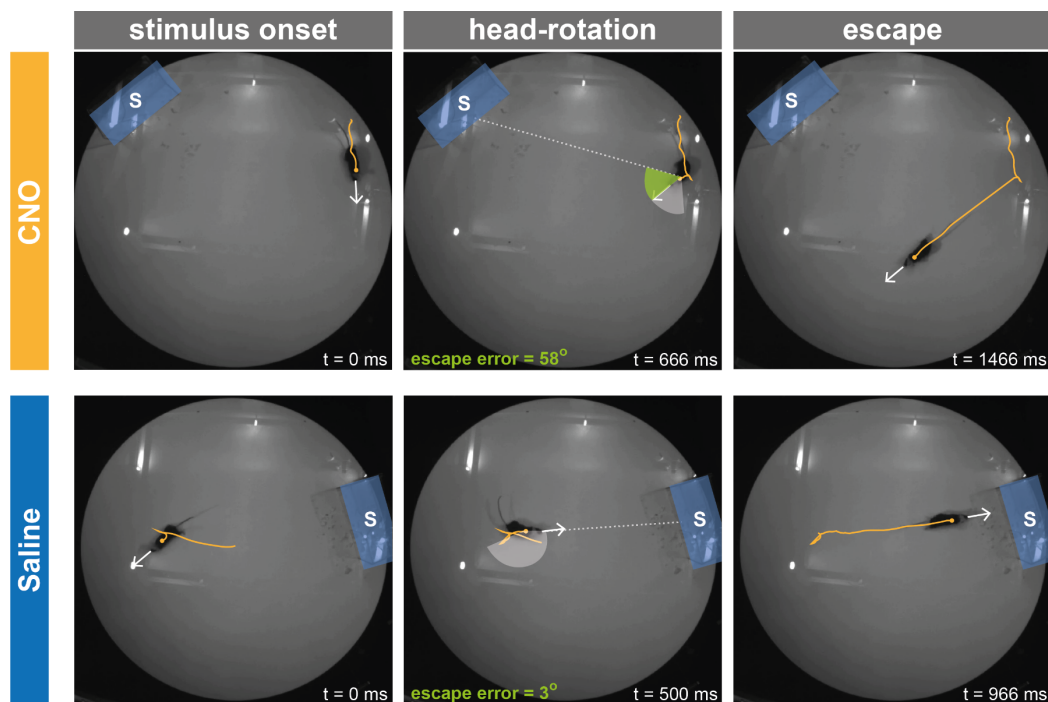


**Figure 23: Example of high-error escape following loss of function of the projection from retrosplenial cortex to superior colliculus**

The top panels show an example escape with high escape error, following CNO administration to a mouse. Bottom panels show an accurate escape from the same mouse following saline administration. Time (t) is measured from the presentation of the aversive sound stimulus. White arrows show ongoing heading of the mouse; yellow lines show mouse's trajectory in the previous second. White dotted line corresponds to a 0° escape error. Green angle shows the escape error, measured between the animal current heading and the perfect escape direction. White angle shows the orientation-movement of the mouse following presentation of aversive sound. The blue rectangle with an "S" highlights the position of the shelter.

To test whether the effect observed in the previous experiment was exclusively due to the inactivation of the targeted projection, I inactivated a collateral projection of SC-projecting RSC neurons. To identify collaterals from these neurons, an AAV coding for flexed mCherry (rAAV2-EF1a-DIO-hChR2(H134R)-mCherry) was injected in the RSC following injection of a retro-AAV coding for Cre to the SC. After performing immunohistochemistry, I observed that SC-projecting neurons in RSC also project to the anterior cingulate cortex (ACC) (Figure 24A). I then repeated the projection-specific chemogenetic approach detailed above, but implanting cannulas in the ACC to inhibit these terminals of SC-projecting RSC neurons (Figure 24B and C). Loss of function of this alternative projection did not change escape error (saline median = 18°, (N = 21 responses from 5 mice); CNO median = 18°, (N = 21 responses from 5 mice);  $p = 0.886$ , two-tailed Mann-Whitney test; Figure 24D) or time to shelter after presentation of sound (saline median = 4000 ms, (N = 21 responses from 5 mice); CNO median = 2400, (N = 21 responses from 5 mice);  $p = 0.137$ , two-tailed Mann-Whitney test; Figure 24E), when compared to control.

Despite observing a significant effect in escape error following inactivation of RSC, SC and the RSC-SC projection, the escape error in all these datasets was not random, but rather biased towards the shelter (for the RSC to SC projection: Chi-square test frequency distribution against random distribution, Chi-square = 129.3,  $p < 0.0001$ ). To test whether this was due to the DREADD-based inactivation strategy being only partially effective I inactivated the RSC with another tool, muscimol, a GABA<sub>A</sub> receptor agonist (Majchrzak and Di Scala, 2000). Local infusion of muscimol to RSC via preimplanted cannulae (Figure 25A) increased escape error (pre-test median = 3.5° (N = 22 responses from 6 animals), saline median = 8.0° (N = 25 responses from 3 animals), muscimol median = 65° (N = 21 responses from 6 animals), saline vs muscimol,  $p < 0.0001$ , two tailed Mann-Whitney test, Figure 25B). The escape angle was random with this inactivation method (Chi-square test frequency distribution against random distribution, Chi-square = 5.48,  $p = 14.0$ ). This suggests that the bias towards the shelter that accompanied the phenotype elicited by chemogenetic inactivation, was due to limitations of the inactivation method.

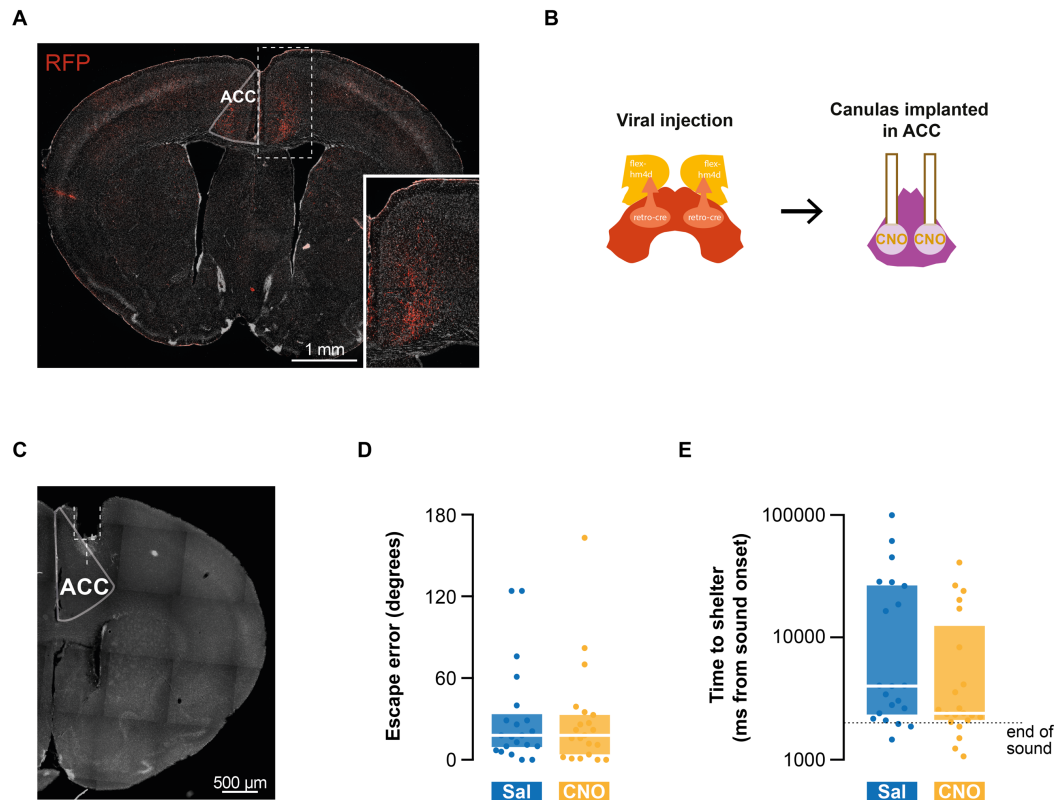


**Figure 24: Inactivation of the projection from superior colliculus projecting retrosplenial neurons to anterior cingulate cortex does not impair orientation during escape**

(A) Stained terminals at anterior cingulate cortex (ACC) of superior colliculus (SC)-projecting retrosplenial (RSC) neurons.

(B) Schematics of the experimental strategy to inactivate terminals at ACC of SC-projecting RSC neurons

(C) Representative image showing placement of guide cannula in ACC. The lesion shows the location of the guide cannula which is implanted in the skull of the animal and through which an internal cannula is positioned in place, down to 0.5 mm below its opening (white dotted line).

(D) No significant difference in escape error following inactivation of this projection vs control ( $p = 0.886$ ).

(E) No significant difference in time to shelter following presentation of threatening sound following inactivation of this projection vs control ( $p = 0.137$ ).



brain implants (for instance optic fibres for optogenetic-driven loss of function), making it easier to combine loss of function with neural activity recordings, as I did in chapter 6. Moreover, covering some of the areas studied here with optic fibres, necessary for an optogenetic approach, would be challenging due to their large volume and topography. Finally, hM4D(Gi) drives inactivation that lasts a few hours after which the effect is reversed, upon physiological clearance of CNO from the organism (Roth, 2016, Campbell and Marchant, 2018, Smith et al., 2016). This allows testing the same mouse in the behavioural assay after injecting CNO or saline, in a random order.

Despite having various technical advantages, chemogenetic inactivation of RSC had a weaker behavioural effect than muscimol-driven inactivation. I tested the effect of chemogenetic loss of function of different cortical areas projecting to SC and only observed a behavioural phenotype in orientation during escape after inactivation of RSC. However, we cannot be certain that other areas tested (PPC, M2 and ACC) do not contribute to the behaviour studied. It is possible that a different inactivation method paired with complete coverage of these areas would elicit a phenotype as well. The contribution of the loss of function results presented here is not to establish the full network that mediates orientation during escape, but to instead determine that the projection from the RSC to the SC is a critical circuit for controlling orientation to shelter during escape behaviour. The relative importance of this circuit node over others is highlighted by the fact that inactivation of other candidate areas with the same methods did not impair orientation to shelter during escape.

The PPC is involved in control of eye and head movements and is known to contribute to goal-directed navigation (Andersen and Buneo, 2002, Whitlock et al., 2008, Kurylo and Skavenski, 1991, Barash et al., 1991, Colby and Duhamel, 1996). Previous work has shown that inactivation or lesions of the PPC impairs memory-guided saccades (Chafee and Goldman-Rakic, 2000, Li et al., 1999), goal-directed reach movements (Hwang et al., 2012) and various navigation tasks (Harvey et al., 2012, Save and Poucet, 2000, Kolb et al., 1983). Similarly, AMA (secondary motor and anterior cingulate cortices) are known to control eye and head orientation movements (Barthas and Kwan, 2017, Bizzi and Schiller, 1970, Bruce and Goldberg, 1985) and integrate environment context information to guide navigation (Olson et al., 2019). In addition, inactivation studies of AMA have shown impairment of memory-guided saccades as well as visually-guided saccades (Schiller and Chou, 1998, Dias and Segraves, 1999) and of performance in various navigation and memory-guided orientation (de Bruin et al., 2001, Erlich et al., 2011).

Taking this evidence into account I decided to target the PPC and AMA in addition to the RSC which inactivation is known to produce spatial memory deficits (Mitchell et al., 2018, Vann et al., 2009).

Only loss of function of the RSC resulted in a decrease in accuracy in orienting to shelter during escape. Interestingly the RSC is known to be essential to integrate self-motion information and path integrate (Elduayen and Save, 2014, Cooper and Mizumori, 1999, Cooper and Mizumori, 2001). On the other hand, the role of PPC in idiothetic cue integration and path integration is not clear: while lesions of the PPC do not significantly impair head direction cells to maintain their tuning based on idiothetic cues (Calton et al., 2008) some studies suggests the PPC is necessary to path integrate (Parron and Save, 2004, Commins et al., 1999). Anterior motor areas have not been directly implied in path integration mechanisms. Since the results from chapter 4 support the hypothesis that mice primarily use path integration to navigate during escape, this may explain why I observe a strong phenotype upon RSC inactivation.

The frontal eye fields (FEF, part of secondary motor cortex), are known to control orientation movements partially in parallel with the SC, such that inactivation of one of the areas only leads to moderate phenotypes whereas lesion of both areas majorly disrupts eye and head orientation (Schiller, 1998). However the FEF is also known to exert direct control over SC to avoid conflicting downstream motor control (Schlag-Rey et al., 1992). Interestingly, I observed a trend of better performance in orientation to shelter following inactivation of anterior motor areas, although not statistically significant. This might be the result of removal competing FEF control-inputs to downstream effector centres that control orientation, or directly to the SC (Schlag-Rey et al., 1992, Segraves, 1992). The two alternatives could be tested by specific inactivation of the FEF projection to SC and to the pontine nuclei.

Loss of function of the SC resulted in an impairment in orientation to shelter during escape, as expected based on numerous previous studies showing that inactivation of the superior colliculus impairs orientation and navigation, as well as the choice of orientation target (Dean and Key, 1981, Lines and Milner, 1985, McPeck and Keller, 2004, Sprague and Meikle Jr, 1965, Felsen and Mainen, 2008). The phenotype I observed, despite significant, was small, which I hypothesize can be due to two reasons: first, I performed bilateral loss of function of the SC, which is known to result in weaker orientation impairments than unilateral inactivation (Lomber and Payne, 1996, Lomber et al., 2001),

possibly due to unilateral inactivation resulting in a sensory or motor imbalance between the inactivated and the functioning hemispheres. Second, I opted to not inactivate the medial portion of the SC, which is known to be involved in threat evidence integration and is critical for initiation of escape (Evans et al., 2018); however this area also contains neurons that control head-rotation movements (Wilson et al., 2018, Masullo et al., 2019) which could be responsible for the lack of a stronger phenotype in my experiments.

Finally, I targeted cortical areas that project to the SC and were strong candidates to be involved in orientation to shelter during escape. Other SC-projecting areas could have been investigated due to their role in orientated movement, particularly the basal ganglia (Hikosaka et al., 2000). In addition, areas that do not project directly to the SC, such as the hippocampal formation and the entorhinal cortex, are widely studied nodes in the spatial memory and navigation systems (Moser et al., 2015) but their contribution for orientation during escape is still unknown. Given recent work showing neurons tuned to angular offset to goals in hippocampus (Sarel et al., 2017) and lateral entorhinal cortex (Wang et al., 2018) it would be particularly interesting to probe the role of these brain areas in my behavioural assay.

### **Inactivation of the projection from RSC to SC shows that this circuit is essential to orienting to shelter during anti-predatory escape**

The existence of a RSC to SC projection has been previously documented (van Groen and Wyss, 1992, Künzle, 1995, Oh et al., 2014, Comoli et al., 2012, García Del Caño et al., 2000). Here I used rabies monosynaptic retrograde tracing from excitatory and inhibitory neurons in the SC to test if RSC input was segregated to a particular SC cell type, and observed that is not the case, since both cell types receive ipsilateral inputs from granular and dysgranular RSC. While I did not quantify the number of presynaptic cells from each postsynaptic population, no striking difference was observed. In the future, it would be valuable to further characterize this connection by quantifying anatomical convergence and divergence, and describing the topography of the projection. Projection to both glutamatergic and GABAergic SC neurons was shown to be functional by ChR2-assisted connectivity mapping by whole-cell patch-clamp recordings, indicating that both of these projections are capable of transmitting information from the RSC to the SC.

A caveat of typical chemogenetic strategies (where CNO is injected intraperitoneally) for circuit specific experiments is the lack of projection specificity due to collateral projections (Campbell and Marchant, 2018). I inactivated neurons in RSC that project to SC, by injecting a retro-AAV coding for Cre in the SC so that only cells projecting there could produce functional copies of hM4D(Gi) following injection of an AAV coding for flex-hM4D(Gi) into RSC. Inactivation of this subpopulation of cells impaired pre-escape orientation with similar magnitude to non-selective RSC inactivation, suggesting these neurons are the key units in RSC for this behaviour. However, this group of cells also sends collaterals to other brain areas, such as the ACC, as shown in Figure 24A. To deal with the potential caveat that the phenotype could be mediated by a collateral projection, and because the hM4D surface receptor is also expressed in axon terminals (Stachniak et al., 2014), I implanted cannulas over the SC to administer CNO locally and inactivate exclusively these RSC terminals (Zhu and Roth, 2014). Inactivation of the projection from RSC to SC elicited impairments similar to non-specific RSC loss of function. Finally, I controlled for the specificity of the local inactivation by locally delivering CNO to ACC terminals of the same RSC subpopulation, and no effect was observed.

I have shown that inactivation of the RSC-SC projection is not involved in threat detection and escape initiation, as mice still escape following inactivation of the projection, as shown by their stimulus-triggered acceleration. Yet, following inactivation, mice often escape towards an incorrect direction, dictating late or no arrival to shelter. This highlights the critical role of the RSC-SC projection in controlling the accuracy of escape to shelter, which is critical for survival.

## **6. RESULTS:**

**Retrosplenial cortex encodes angular distance to shelter and feeds this information to the superior colliculus**

## 6.1. Neurons in retrosplenial cortex and superior colliculus encode the angular distance to shelter

In the previous chapter I showed that the projection from retrosplenial cortex (RSC) to superior colliculus (SC) is essential for accurately orienting to shelter during escape. In the experiments described in this chapter I explored the mechanism for this memory-informed orientation movement. I used Neuropixels probes to record simultaneously from both areas (Figure 26A), and combined neural activity recordings with chemogenetic inactivation of SC-projecting RSC neurons (N = 4 mice, 27 recording sessions).

I designed a simple exploration assay to investigate how mice map the position of refuge in the environment: the mouse was positioned in a 92 cm diameter arena and following an adaptation period, an over-ground shelter (similar to the one used in the chemogenetic inactivation experiments) was placed on the periphery of the arena, and the mouse was allowed to explore freely for at least 30 min. Subsequently, the shelter was moved 90° anti-clockwise and the mouse was again given at least 30 min to explore the environment (Figure 26B). I did not deliver threatening sensory stimulus in this assay.

Since I was interested in understanding how mice map the position of the shelter and use this information to guide orientation towards it, I looked for a representation of the shelter location in egocentric space, which could directly be used to command the orientation movement towards the shelter. I defined ‘head-shelter offset’ as the angular offset between the ongoing heading of the animal and the perfect heading to the shelter at the position in space the mouse is currently occupying. Importantly, for the same allocentric head direction various head-shelter offsets are possible (Figure 26C).

I used DeepLabCut, a method for markerless pose estimation based on transfer learning with deep neural networks (Mathis et al., 2018), to track *a posteriori* the position of the centre of the body of the mouse and its ears, allowing to calculate head direction and head-shelter offset (Figure 26D, see methods for details).

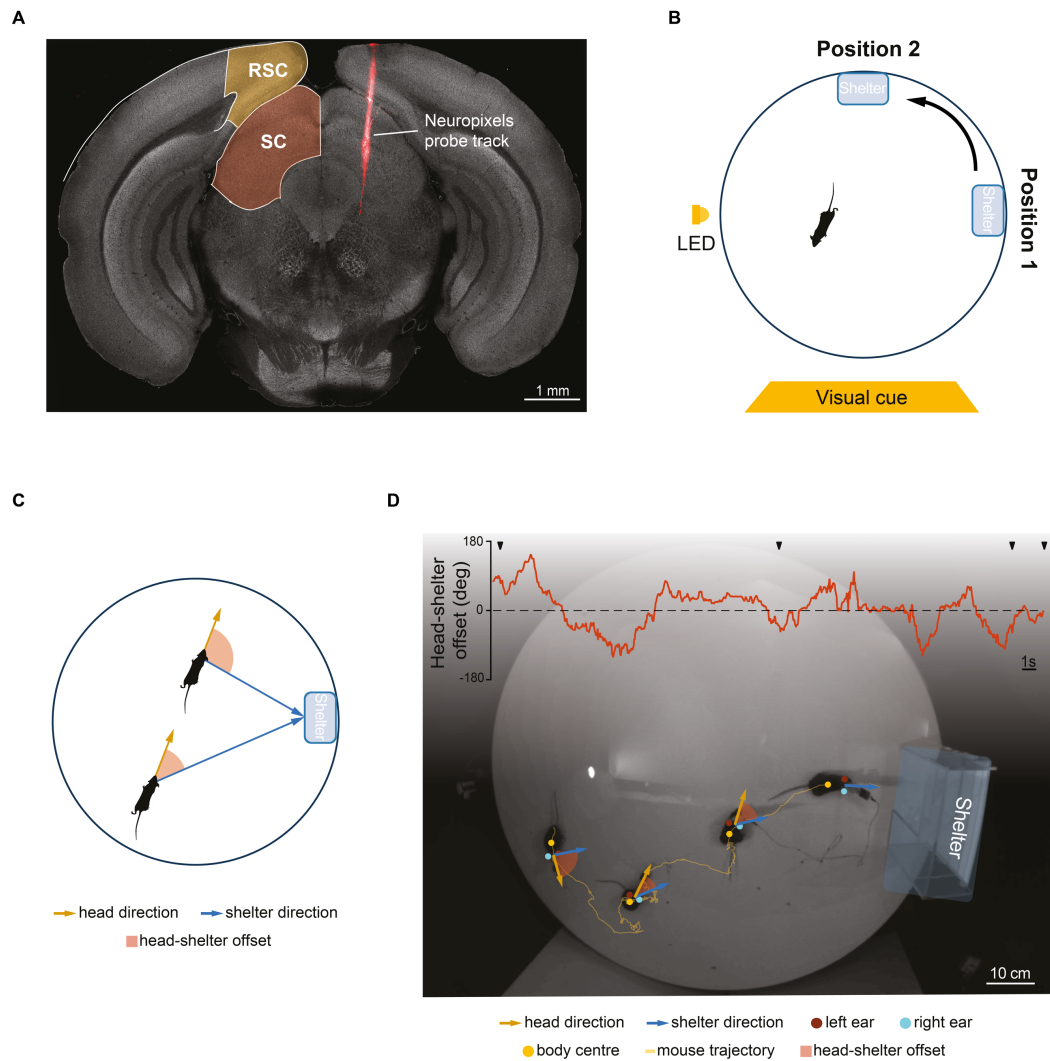


**Figure 26: An exploration assay paired with single unit recordings**

(A) Image showing a coronal section of the brain of a mouse tested in the exploration assay/recording. The neuropixels was bathed in DiI prior to implantation and its track is visible in the image, going through both the retrosplenial cortex (RSC) and superior colliculus (SC).

(B) Schematic top-view representation of the exploration assay, highlighting the rotation of the shelter, 90° anticlockwise, after 30 minutes of exploration with the shelter in position 1. An LED and a large white sheet, contrasting with the black background of the behavioural cabinet, were used as explicit cues and were not rotated with the shelter, similarly to inexplicit cues in the behavioural apparatus.

(C) Schematic top-view representation highlighting that the same head-direction angle can bear different head-shelter offset angles. The mouse on top, despite having the same heading as the mouse below, has a much larger shelter-offset angle, due to its position in the arena.

(D) Overlaid image of four top-view frames, showing the mouse in four different positions on the behavioural arena. Head-shelter offset is plotted in red and the four arrowheads indicate the four moments the mouse's position is shown. DeepLabCut was used to track body centre and ears, allowing the computation of head direction and head-shelter offset as highlighted in the figure.

Head direction cells have been extensively reported in the RSC (Chen et al., 1994, Cho and Sharp, 2001) and cells exhibiting significant firing rate modulation as a function of head direction have more recently been reported in SC (Wilson et al., 2018). However, cells encoding the angular distance to goal in egocentric space have not been previously described in either area. In our data, I observed cells significantly tuned to allocentric head direction and cells tuned to a specific angular offset to the shelter. I defined a series of criteria to classify a neuron as a head direction or head-shelter offset cell, as describe below (and detailed in methods chapter):

For a neuron to be classified as a head direction cell the following three criteria had to be met: 1) for each epoch the neuron had to display allocentric directional tuning above chance; 2) head-direction tuning had to be stable across all epochs; 3) for each epoch, tuning to head direction had to be decoupled from tuning to head-shelter offset by the TunED analysis<sup>37</sup>. An example of an RSC head direction cell is shown in Figure 27A.

For a neuron to be classified as a head-shelter offset cell it had to fulfil the following four criteria: 1) for each epoch the neuron must be significantly tuned to a given angular offset to shelter, irrespective of the position the mouse occupies in the arena; 2) head-shelter offset tuning has to be stable across all epochs (in respect to the ongoing position of the shelter); 3) head-shelter offset tuning must rotate with the shelter; 4) the tuning to head-shelter offset had to be decouplable from head-direction tuning by the TunED analysis. An example of an RSC head-shelter offset cell is shown in Figure 27B.

Following these criteria, I recorded 4.0 % shelter-offset cells in RSC and 8.5% in SC, while 4.0 % of RSC and 4.4% of SC neurons were classified as head direction cells (Figure 28A and C). I observed for both cell types in both brain regions that the directions of their Rayleigh vectors tile the respective space they map (Figure 28B and D).

---

<sup>37</sup> Since correlation between allocentric head direction and egocentric head-shelter offset arises from my experimental set-up, classification into either type of cell depended on the neuron tuning towards one of the variables being decoupled from the other variable. Decoupling of these two correlated variables was performed by means of tuning entanglement decoupling (TunED) analysis, a mathematical method developed by Dr. Rasmus S. Petersen (unpublished). This method tests how much of the tuning to each variable is explained by the tuning to the other variable, distinguishing whether a neuron is simply tuned to a driver variable or whether there is genuine tuning to both variables (see details in methods).

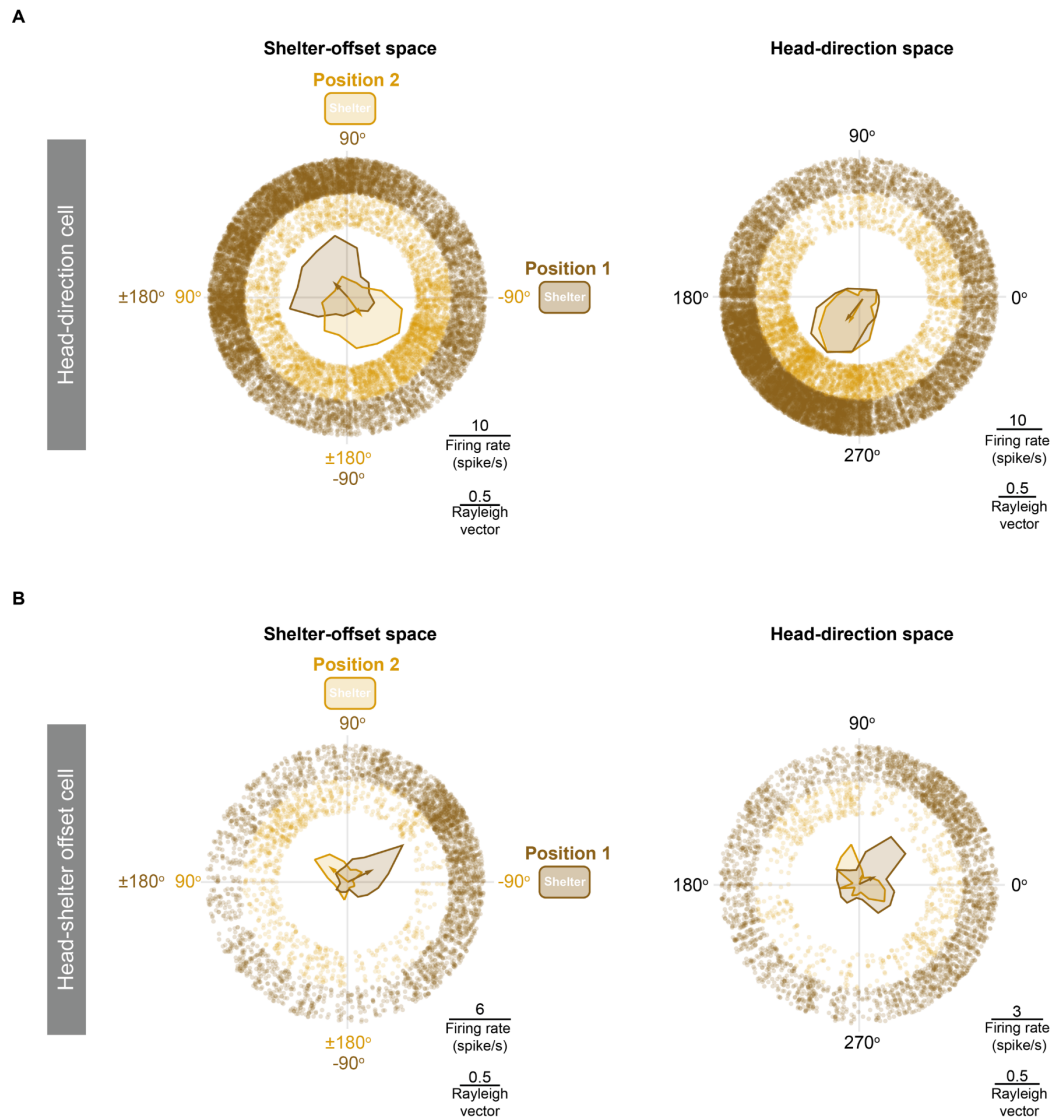


**Figure 27: Example of head-direction cell and head-shelter offset cell in retrosplenial cortex**

In both figures the left and right panel represent the same data (spiking profile of one neuron), plotted in different space coordinate references: on the left egocentric, head-shelter offset space and on the right the classic head-direction, allocentric space. Brown depicts spikes (each dot in the external circle represents a spike), tuning profile (represented by the outlined area in the centre of the circle) and Rayleigh vectors (shown as a vector in the centre of the circle), relative to shelter position 1, whereas yellow refers to data acquired after rotation of the shelter to position 2. In shelter-offset space (left panels) the axis are color-coded relative to the shelter position they refer to.

(A) Example head-direction cell in retrosplenial cortex (RSC). Tuning remains significant and stable upon rotation of shelter.

(B) Example head-shelter offset cell in RSC. The tuning of the cell remains significant and follows rotation of the shelter to position 2.

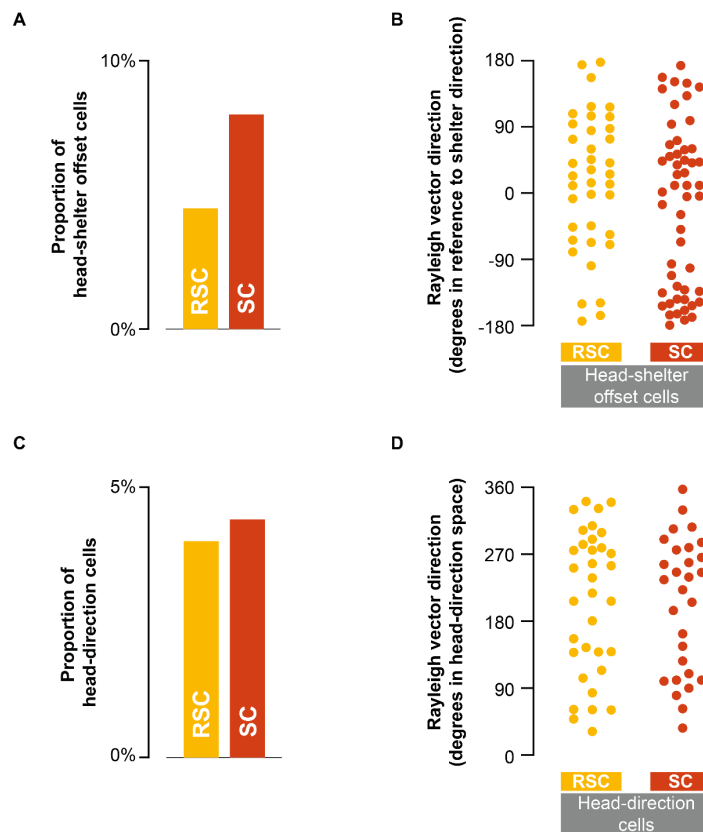


**Figure 28: Tuning of head-shelter offset cells in retrosplenial cortex and superior colliculus tile the egocentric head-shelter offset space**

(A) Proportion (%) of head-shelter offset cells in retrosplenial cortex (RSC) and superior colliculus (SC) out of 808 and 633 neurons recorded, respectively.

(B) Direction of Rayleigh vector for each of the identified head-shelter offset cells in RSC and SC (each dot represents one neuron). Direction measured in reference to the direction of the shelter position 1. As a population these cells tile the head-shelter offset space

(C) Proportion (%) of head direction cells in RSC and SC out of 808 and 633 neurons recorded, respectively.

(D) Direction of Rayleigh vector for each of the identified head direction cells in RSC and SC (each dot represents one neuron). As a population these neurons tile the head-direction space.

Next, I asked how well the population of neurons at these areas encode the head-shelter offset collectively.

I trained linear discriminant analysis (LDA) classifiers (one classifier using RSC neurons (N = 808 neurons from 4 mice) and another using SC neurons (N = 633 neurons from

same 4 mice) on a subset of the data, to predict the head-shelter offset given the firing rate of all neurons recorded in the region of interest, and cross-validated it. The decoder prediction accuracy for the animal's real head-shelter offset was 0.46 and 0.42 for the RSC and SC decoders, respectively, which was largely above chance (0.06 for either region; Figure 29A and B).

Similarly, LDA classifiers trained to predict head direction performed very much above chance in the cross-validation test, with prediction accuracies of 0.73 and 0.67 for neurons in RSC and SC respectively (chance was 0.06 for either region; Figure 29C and D).

Together these data show that neurons in RSC and SC map the offset to shelter during exploration, in a manner that directly encodes the angle that the animal must turn should it decide to orient to the shelter, irrespective of its position in the arena.

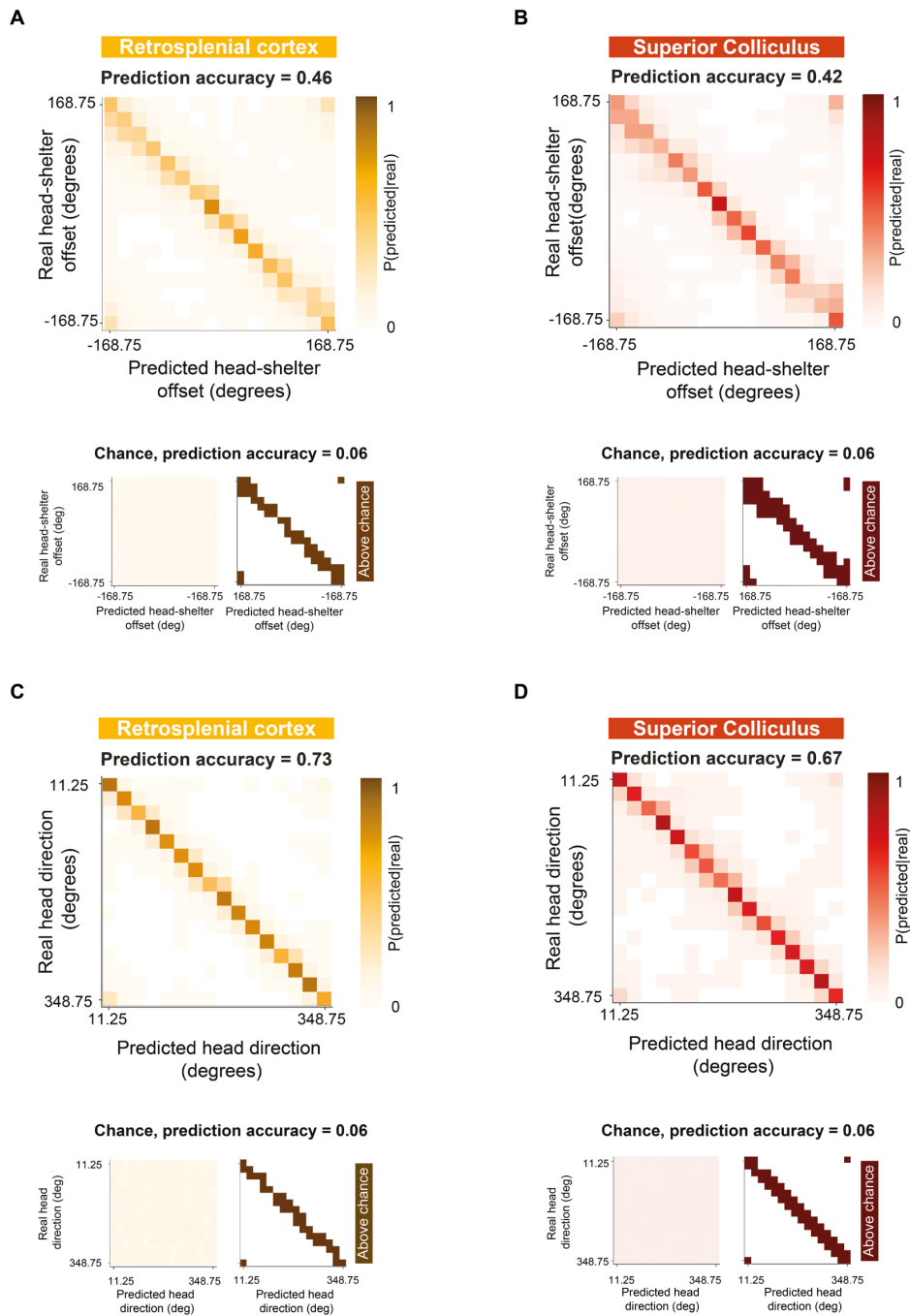


**Figure 29: Retrosplenial cortex and superior colliculus accurately encode head-shelter offset and head direction at a population level**

For all figures the top panel is the result of the cross-validation test in which the LDA classifier predicts the head-shelter offset angle to shelter (A and B) or head direction (C and D) given the firing rate of the recorded neurons in RSC (A and C) or SC (B and D); higher contrast colours mean the probability of a variable being classified into the respective bin was higher. The prediction accuracy was calculated as the probability of the model classifying correctly the real head-shelter offset or head direction, given the firing rate of the neurons in the region of interest.

For all figures, bottom left shows the performance of a classifier trained and tested with a shuffled dataset and bottom right shows the bins of the cross-validation test which were predicted above chance.

## 6.2. Loss of function of superior colliculus-projecting retrosplenial neurons disrupts head-shelter offset encoding in both areas

The head-shelter offset information is, in principle, all the animal needs to know to be able to execute accurate orienting to the shelter during escape. My experiments so far showed that inactivation of the projection from the RSC to the SC impairs this goal-directed behaviour, and that both brain areas contain cells that map head-shelter offset. In order to probe the effect of inactivating SC-projecting RSC neurons in the encoding of head-shelter offset, I paired chemogenetic inactivation with simultaneous recordings from RSC and SC (N = 2 animals, 7 sessions after CNO injection, 5 sessions after saline injection).

I injected a Cre-coding retro-AAV at the SC and an AAV coding for flexed hM4D(Gi) at the RSC, to achieve selective inactivation of SC-projecting RSC neurons. At least four weeks after, I implanted a Neuropixels probe into the ipsilateral RSC and SC (Figure 30A). Loss of function of SC-projecting RSC neurons, significantly decreased firing rate in RSC but not in SC, when compared with saline injection (RSC:  $p = 0.026$ ; SC:  $p = 0.369$ ; one-tailed Kolmogorov-Smirnov test; Figure 30B).

The results of the loss of function manipulation were analysed at single-neuron and population levels. Comparing animals treated with CNO and saline, I observed that the former showed a decrease in the percentage of cells classified as head-shelter offset cells and as head-direction cells in both the RSC (head-shelter offset cells: 33% decrease; head direction cells: 67% decrease) and SC (head-shelter offset cells: 60% decrease; head direction cells: 12% decrease) (Figure 30C and F).

At population level, I observed a significant decrease in performance of the LDA classifier following CNO-induced inactivation of SC-projecting RSC neurons, when compared against saline injection, for both head-shelter offset (average decrease in prediction accuracy after CNO in respect to saline: RSC =  $-69.17\% \pm 30.05\%$ ,  $p < 0.0001$ ; SC =  $-53.64\% \pm 37.23\%$ ,  $p < 0.0001$ ; 1-tailed paired t-test; (Figure 30D and E)), and head-direction (average decrease in prediction accuracy after CNO in respect to saline: RSC:  $-110.7\% \pm 19.5\%$ ,  $p < 0.0001$ ; SC:  $-28.16\% \pm 4.98\%$ ,  $p < 0.0001$ ; 1-tailed paired t-test (Figure 30G and H)). This shows that SC-projecting RSC neurons are critical for the encoding of head direction and head-shelter offset in the RSC, and that this input is essential for the SC to encode both variables.

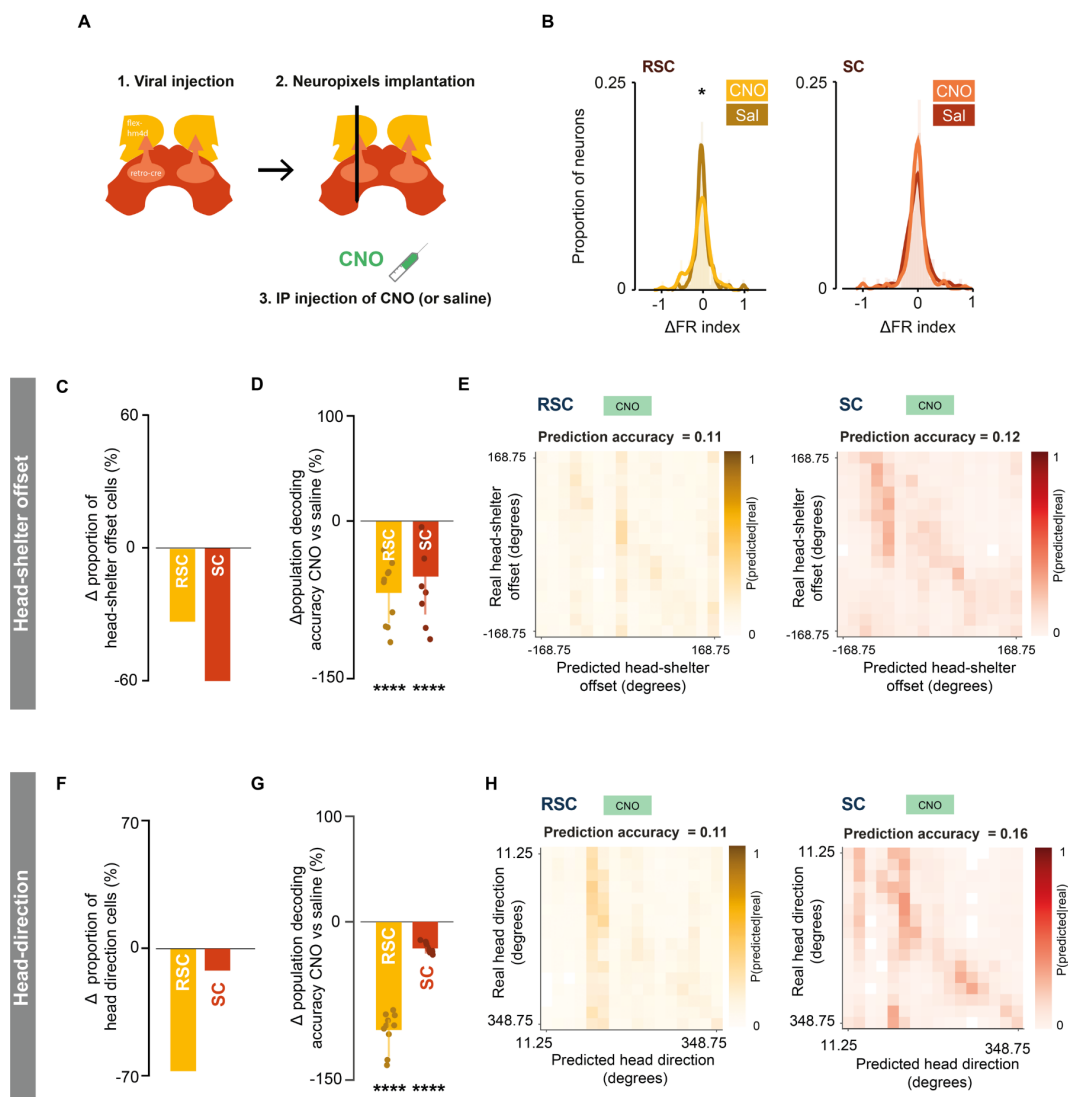


**Figure 30: Inactivation of retrosplenial neurons projecting to superior colliculus decreases coding accuracy of head-shelter-offset and head direction from both areas**

(A) Schematic illustration of the experimental procedure: after targeting SC-projecting RSC neurons with the inhibitory DREADD hM4D(Gi), a probe was implanted to simultaneously record from RSC and SC, and hM4D(Gi) was activated by injecting CNO i.p.. Saline was injected i.p. in control experiments.

(B) Inactivation of SC-projecting RSC neurons significantly decreased firing rate in RSC (left panel) but not in SC (right panel).

(C and F) Decrease in proportion of cells classified as head-shelter offset and head direction cells (respectively), computed in relation to saline control.

(D and G) Significant decrease in accuracy of population decoding of head-shelter offset and head direction cells (respectively), computed in relation to control. Ten classifiers were trained using different training and cross-validations subsets of the data, with similar lengths; each dot represents the comparison of a trained classifier against control (see methods for details).

(E and H) Cross-validation confusion-matrix of LDA classifiers for head-shelter offset and head direction cells (respectively) in RSC (yellow panels) and SC (red panels) following inactivation with hM4D(Gi). The central diagonal is not evident, showing poor performance of the decoder.

### **6.3. Loss of function of colliculus-projecting retrosplenial neurons does not impair motor control of orientation movements by the superior colliculus**

The SC is known to play a pivotal role in the control of head orientation movements (King et al., 1991, Freedman et al., 1996, Freedman and Sparks, 1997, Walton et al., 2007, Wilson et al., 2018, Masullo et al., 2019), and therefore the orientation phenotype I observe after inactivation of the projection from RSC to SC could be explained by a simple perturbation of the motor control function of SC. Alternatively, following the inactivation, the SC might still coherently control head-orientation movements, but implement an incorrect amplitude of rotation in relation to the position of the shelter, possibly due to a decrease in accuracy of mapping the position of the shelter as reported above (Figure 30C, D and E). To understand which of the hypotheses was responsible for orientation impairment following inactivation of the RSC-SC projection, I tested whether inactivation of SC-projecting RSC neurons impairs anticipatory coding of head rotation in the SC.

To achieve this, I measured how well the SC encoded head rotations in the near-future (100ms look-ahead, see methods for details), from an egocentric perspective (meaning a rotation of 30° is equal irrespective of the allocentric head direction going from 140 to 170° or from 20 and 50°). An LDA classifier trained to predict near-future head displacement given the firing rate of SC neurons performed above chance (classifier prediction accuracy = 0.34; chance = 0.11. Only angular displacements between -27 and 27° were considered due to low sampling at larger values). Inactivation of SC-projecting RSC neurons did not significantly decrease the classifier prediction accuracy, unlike what I observed for head direction and head-shelter offset classifiers (24.25% ± 21.56%;  $p = 1.0$ , 1-tailed paired t-test).

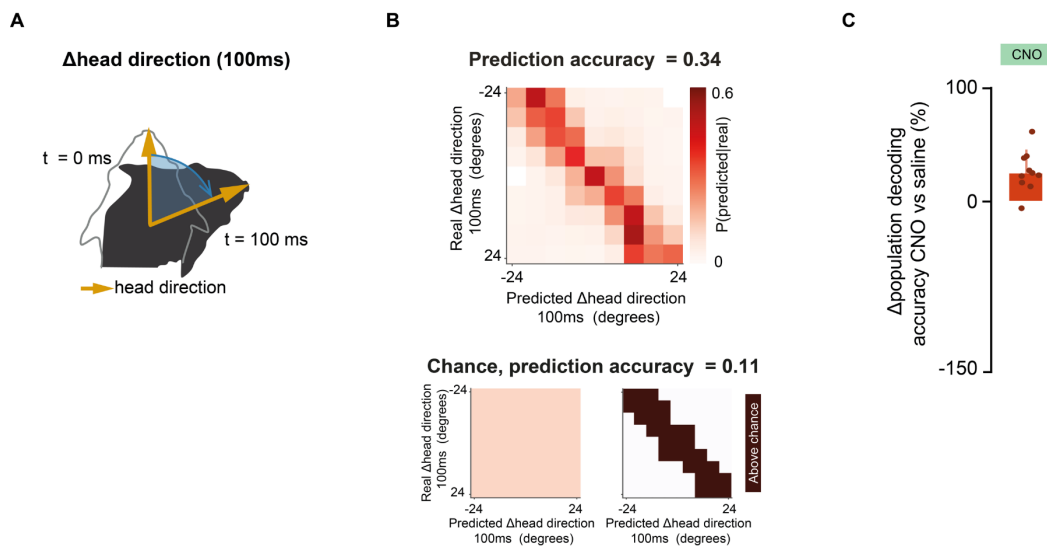


**Figure 31: Superior colliculus predicts near future head-rotation movements and inactivation of retrosplenial neurons projecting to the superior colliculus does not impair coding of this variable**

(A) Schematics showing the variable studied here. I measured the difference between current head direction and head direction 100 ms in the future, resulting in either positive values representing anti-clockwise movements, or negative values representing clockwise rotations.

(B) Result of the cross-validation of the LDA classifier for near-future head direction change, showing prediction accuracy above chance. The top panel shows the probability of the classifier categorizing the vector of SC firing rates into each bin given the real behavioural variable. Bottom left shows the cross-validation performance of a classifier trained and tested with a shuffled dataset, and bottom right shows the bins predicted above chance.

(C) Difference in population decoding accuracy between CNO and saline control shows that inactivation of SC-projecting RSC neurons does not decrease SC coding of future head-rotation movements.

These results suggest that the impairment in orienting during escape following inactivation of the projection from RSC to SC is not due to the SC no longer accurately controlling rotation movements. In order to test behaviourally if this loss of function does not disrupt orientation movements, I designed a simple sensory-guided orientation assay. This assay tests the SC ability to perform sensory-motor transformation by presenting a salient auditory cue, which typically triggers an orientation towards the sound source (Thompson and Masterton, 1978, Kelly et al., 1987, Beitel and Kaas, 1993). I used a circular platform with 92 cm diameter and experiments were all conducted in the dark. Two speakers were positioned in opposed sides of the arena, 10 cm away from the border.

The mouse was placed in the platform and after a 7 min habituation period I started delivering brief tones (300ms at 2.5 kHz) randomly from one of the speakers, with at least 90 s inter-stimulus interval (Figure 32A). Naïve mice performed this task reliably, orienting to the sound-emitting speaker immediately after the sound, with a median orientation error of 14.0° (measured in relation to the sound-emitting speaker for each trial) (Figure 32B).

Loss of function of the SC decreased performance in this assay (CNO median orientation error = 31.5° (N = 28 responses from 4 animals); saline median orientation error = 11.0° (N = 23 responses from same 4 animals, test);  $p = 0.046$ , two-tailed Mann-Whitney test), showing that the SC is necessary for optimal performance. In contrast, loss of function of SC-projecting RSC neurons did not impair performance (CNO median orientation error = 23.0° (N = 20 responses from 4 animals); saline median orientation error = 29.0° (N = 24 responses from same 4 animals);  $p = 0.579$ , two-tailed Mann-Whitney test), even though the same mice exhibited a phenotype in the escape assay (CNO median escape error = 18.5° (N = 32 responses from 4 animals); saline median orientation error = 5.0° (N = 37 responses from same 4 animals);  $p = 0.0015$ , two-tailed Mann-Whitney test).

These data are in accordance with the result from the LDA classifier following inactivation of SC-projecting RSC neurons, and support the hypothesis that this inactivation does not impair SC motor function. This suggests the orienting phenotype observed before acceleration during escape is due to impaired mapping of the shelter position rather than a motor incapacity to orient towards an accurately mapped goal.

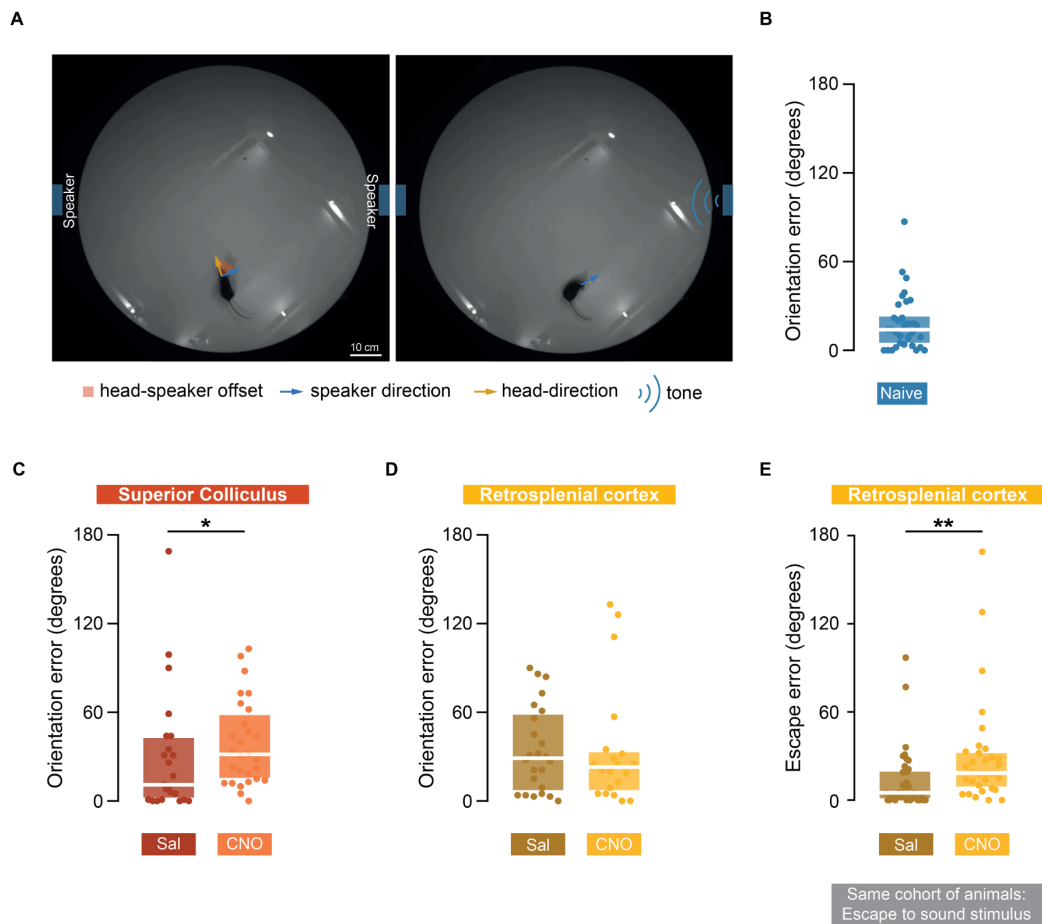


**Figure 32: Inactivation of retrosplenial neurons projecting to superior colliculus does not impair orientation to sensory stimulus while impairing orientation to memorised shelter position during escape**

(A) Top view of the behavioural arena. Highlighted in blue is the diametral opposite position of the two speakers. The speaker eliciting the tone was chosen randomly for each stimulus, and the orientation error to the speaker was measured as the head-speaker offset after orientation, in relation to the sound-eliciting speaker. The panel on the left shows the position and orientation of the mouse immediately before triggering the sound and the right panel shows the endpoint of the orientation movement of the mouse towards the correct speaker.

(B) Distribution of orientation angles in reference to correct speaker for naïve mice.

(C) Loss of function of the SC impairs orientation to sensory stimulus.

(D) Loss of function of SC-projecting RSC neurons does not impair orientation to sensory stimulus ( $p = 0.579$ ).

(E) The same cohort of animals as show in (D), show an impairment in orienting to shelter during escape.

For figures B to E each dot is one trial, the white line is the median and the coloured boxes represent the interquartile interval.

## 6.4. Discussion

In this chapter I showed that both RSC and SC encode the ongoing angular offset between the animal's heading and the shelter direction, which is the main information the animal needs to orient to shelter during escape. Both RSC and SC contain head-shelter offset cells (4.0 and 8.5%, respectively), which fire when the mouse's combination of head direction and position determine a given angular offset towards shelter direction. Cells with different offsets in both areas tile the entirety of angular space. Upon inactivation of SC-projecting RSC neurons there is a significant drop in the percentage of head-shelter offset cells found in RSC and SC, and there is a significant decrease in coding accuracy of head-shelter offset at a population level. Finally, I showed that this inactivation does not impair the SC canonical role in controlling head-rotation movements, suggesting that the RSC information arriving at SC informs the latter on the angular offset to shelter but is not a necessary input for SC's motor control function.

### Encoding of head-shelter offset in RSC and SC

Here, I performed recordings simultaneously from the RSC and SC while mice explored a simple platform with an over-ground shelter. I opted to focus on exploration for two reasons: first, because by focusing solely on escapes instead, there would not be enough sampling of the head angle space to study the encoding of head-shelter offset, as escapes are brief and the number of escapes one can trigger per experiment is limited. Second, because knowledge of the relative position of shelter should be constantly tracked to ensure the animal will be able to escape accurately upon threat detection, we should be able to observe its neural correlate during exploration. I aimed to find the neural correlate of the information needed to implement accurate orientation to the shelter: the ongoing head-shelter offset, which at any given time indicates how many degrees the animal should rotate by to be facing the shelter. This variable is egocentric by definition and, although it is partially correlated with head direction, the two coordinate spaces are not anchored to each other (as shown in methods, Figure 4).

I found neurons in both RSC and SC, which we named head-shelter offset cells, tuned to a specific head-shelter offset and which tuning follows the displacement from the shelter. Importantly, I showed that the tuning to head-shelter offset does not arise from a correlation artefact of tuning to head direction. This is the first time that cells with such propriety have been described in either RSC or SC. 'Goal cells' coding angular distance

to a memorized goal have been previously described in the bat hippocampus (Sarel et al., 2017). Although the majority of such goal cells lose their tuning upon displacement of the goal, and a significant proportion are more tuned to head direction than actually to angular offset to goal, some of these cells have general properties similar to our head-shelter offset cells. Even though some of the goal cells were shown to be tuned to angular-offset to goal even when the goal was not visible, the authors reported an overrepresentation of goal cells tuned to goal direction ( $0^\circ$  offset) only when the goal was visible. In this study, I did not observe a bias on head-shelter offset cells' preferred firing direction towards the shelter, although all my experiments were done in presence of light.

In rats, the activity of CA1 place cells has been shown to be modulated by head direction as well as by the angular offset in relation to a point within or outside of a behavioural arena (Jercog et al., 2019), although it has not been tested how such coding relates to explicit behavioural goal locations. On contrary, neurons in rat's lateral entorhinal cortex have been shown to map the position of goal in an egocentric framework, with neurons tuned to the egocentric offset to goal, and neurons that encode both angular offset and linear distance to goal (Wang et al., 2018), similarly to the findings of Sarel and colleagues (Sarel et al., 2017). Here I did not explore distance coding to shelter, as I focused on the orientation movement during escape.

In addition to head-shelter offset cells, I also recorded activity of head direction cells in the RSC and SC. 4% of neurons in RSC were classified as head-direction cells, a lower percentage than initially described in this cortical region (Chen et al., 1994), probably due the disentanglement with head-shelter offset tuning. In fact, a recent study that probed egocentric tuning of neurons in RSC to boundaries of the environment, also reported 4% of head-direction cells in this area (Laurens et al., 2019).

Importantly, I verified that the tuning of head direction cells and head-shelter offset cells as a population tiles the head direction and head-shelter offset spaces, respectively. Therefore, head-shelter offset cells encode the ongoing offset to shelter, which is precisely the information required to control an accurate rotation movement towards it. Classifiers were trained to predict head-shelter offset based on the firing rate of the full population of neurons in RSC or SC, which performed much above chance, demonstrating that both regions effectively encode this variable.

I did not look at the temporal dynamics of head-shelter offset re-tuning following displacement of the shelter. Sarel and colleagues have reported a 10 – 15 min decay in the tuning of cells that do not follow the displacement of the shelter and suggest this may

serve as a memory trace of the previous goal location. If the temporal dynamics for re-tuning would be similar in RSC and SC coding of head-shelter offset, this could explain why animals sometimes still escape to the old shelter location following shelter displacement even though they already have knowledge of the current shelter location (see Chapter 4, Figure 15, and the respective results section).

### **Loss of function of RSC disrupts head-shelter offset coding both in RSC and SC**

I simultaneously recorded from RSC and SC to assess the effect of chemogenetically inactivating SC-projecting RSC neurons in both areas. Although I only directly perturbed neurons in RSC, I observed a disruption of head-shelter offset and head-direction encoding in both areas. At a single neuron level, I observed a drop in the percentage of cells that qualified as either head-shelter offset or head-direction cells in comparison to control, in both RSC and SC. At a population level I registered a decrease in prediction accuracy of the classifiers trained to predict head-shelter offset or head direction, following CNO administration, in comparison to saline, also in both areas. Although the prediction accuracy of the classifiers does not drop to chance in either region for head-shelter offset, I hypothesise this is due to a incomplete infection of the RSC neuron population projecting to the SC. This could be tested by performing viral infections with different spreads and modelling the drop of accuracy of the classifiers as a function of number of infected cells.

My data suggest that SC-projecting RSC neurons are important nodes for the mapping of head-shelter offset, either by computing it or by receiving this information from another brain region. A remarkable feature of the RSC is that it receives inputs from various areas known to be involved in spatial memory navigation (Vann et al., 2009, Mitchell et al., 2018), which could potentially be involved in such computation upstream. In the future it would be interesting to study the afference profile of SC-projecting RSC neurons, which could be achieved through rabies retrograde tracing from the RSC following injection of a retro-AAV coding for Cre into the SC. Particularly, it would be valuable to know if these cells receive inputs from the anterodorsal and lateral-dorsal thalamic nuclei, which convey head-direction signal to the RSC (Taube, 2007), or from CA1 and subiculum (Mitchell et al., 2018), possibly conveying information from goal cells (Sarel et al., 2017).

Another important conclusion is that head-shelter offset signal in the SC arises from RSC, as inactivation of RSC disrupts coding of this variable downstream at the SC. However,

it should be noted that the inactivation performed here is specific for SC-projecting RSC neurons but not for the projection from RSC to SC; therefore, it is possible that the signal at the SC arises indirectly from RSC via an intermediary projection. Performing local infusion of CNO while recording would be technically very challenging, and I thus opted to not pursue it. Nevertheless, having in account the specificity of the projection from RSC to SC in controlling orientation during escape, it would not be surprising that the head-shelter offset signal would be directly conveyed from RSC to SC.

Another limitation of the recordings and inactivations performed here is that I did not test the effect of injecting CNO intraperitoneally in animals without DREADDs to control for the effect of CNO, which is metabolized to clozapine, an antipsychotic drug that acts on various endogenous receptors (Mahler and Aston-Jones, 2018, Manvich et al., 2018). However, we observed no behavioural effect following administration of CNO in animals that did not have hM4D(Gi) in either RSC or SC (see chapter 5, Figure 20 and Figure 24), showing that CNO on its own does not impair the memory of goal location.

### **Inactivation of SC-projecting RSC neurons does not disrupt SC encoding of near future head rotation**

The SC is a critical element in the control of head rotation movements (King et al., 1991, Freedman et al., 1996, Freedman and Sparks, 1997, Walton et al., 2007, Wilson et al., 2018, Masullo et al., 2019). The behavioural phenotype resulting from inactivation of the projection from RSC to SC could be the result of the SC no longer receiving an instructive input about head-shelter offset or the result of inactivating a projection which is permissive of SC's normal functioning in controlling head rotations in general<sup>38</sup>.

To understand if SC could still control head rotations coherently after inactivation its RSC afferent inputs, I started by testing the performance of a classifier in predicting near future angular head displacement following inactivation of the SC-projecting RSC neurons, in relation to control. No decrease in the performance of the classifier was observed following inactivation, as expected in the absence of disruption in SC motor function. Although this inactivation triggers a behavioural phenotype and disrupts coding of head-

---

<sup>38</sup> The distinction between instructive and permissive circuit elements has been described in a recent article (Wolff and Ölveczky, 2018).

shelter offset, it does not impair SC coding of near-future movement, which suggests that the observed phenotype is not due to motor control impairments.

To test behaviourally that SC could still control head-rotation movements, I designed an experiment in which orientation was sensory-guided, instead of relying on memory. If the RSC is conveying memory information about head-shelter offset to the SC but the input is not critical for SC motor function, this simple assay should show no phenotype after inactivation of the RSC. I observed that orienting accuracy to a salient auditory stimulus upon inactivation of the RSC-SC projection did not decrease, in agreement with the results from the classifier test. I validated the inactivation behaviourally by testing the same mice in the escape behaviour assay, and observed a significant increase in escape error, demonstrating that the same inactivation that impairs orientation to shelter during escape does not preclude correct motor control of orientation movements. In summary, these experiments show that the input from RSC to SC is not critical for motor control function of the SC, but it is essential for memory-guided orientation to shelter, suggesting that the RSC provides information about goal location to the SC.



## **7. GENERAL DISCUSSION**

While the drive to engage in anti-predatory defensive behaviours is instinctive, these behaviours are flexible and can be modulated by internal and external factors. The fundamental aim of this work was to study the control of environment features and memory thereof over instinctive defensive behaviours.

I developed behavioural assays to study the flexibility of defensive action selection and execution as a function of learned knowledge about the environment features, such as the presence or absence of refuge and its location in space. I showed that both choice and execution of defensive actions are rapidly adapted to the current state of the environment and that in the presence of a refuge mice rapidly learn its location and accurately escape towards it. In contrast, when refuge is not available mice engage in freezing responses. Importantly, I observed that before accelerating, mice reliably and accurately oriented to shelter and only after would initiate an acceleration towards it. Since mice escaped in a straight run, this memory-guided orientation action determines the accuracy of escape. I therefore focused on this specific component of escape navigation for the rest of my work, aiming to understand which brain areas are critical for the control of this orientation movement and how is the orientation goal memory represented in the brain.

I employed chemogenetic inactivation strategies to gain access to projection-specific neurons and showed that a monosynaptic projection from the retrosplenial cortex (RSC) to the superior colliculus (SC) is critical for controlling orientation to shelter during escape. Inactivation of this projection elicited a phenotype in which mice performed an incorrect rotation movement, which resulted in a subsequent acceleration not directed to the shelter.

Next, I used Neuropixels probes to record simultaneously from the SC and RSC and found that a subset of cells in both areas are tuned to a specific angular offset in relation to the shelter: head-shelter offset cells. I verified that the preferred offset for each neuron tiles the angular space, and that the population of neurons of both SC and RSC accurately encode head-shelter offset. In principle, ongoing head-shelter angular offset is all information animals need to accurately orient to shelter upon engaging in escape; to probe if encoding of this variable was impaired following phenotype-eliciting inactivation of SC-projecting RSC neurons, I paired chemogenetic loss of function with Neuropixels recordings. I observed a significant decrease in coding of head-shelter offset both at a single neuron and at a population levels in SC and RSC following this inactivation. Finally, I tested if the observed phenotype was due to a permissive or instructive role of the RSC projection over the SC, which is known to be critical to implement head-rotation movements. Recordings paired with RSC inactivation showed that SC's coding of near

future head rotation was not impaired. Additionally, I developed a simple SC-dependent sensory-driven orientation assay and observed no impairment in orientation following inactivation of SC-projecting RSC neurons. Taken together these data suggest the RSC has an instructive role over SC's implementation of head rotation, and that head-shelter offset coding in SC arises from its RSC inputs which are critical for accurately orienting to shelter during escape.

## **7.1. Significance of findings**

### **Development of a behavioural assay that reliably elicits accurate goal-directed navigation without prior training**

The study of defensive behaviours is valuable beyond itself as it provides a powerful tool to study various cognitive functions (Evans et al., 2019). The standard escape behaviour assay presented here is a valuable tool for the study of spatial memory and goal-directed navigation. In my assay, mice are not trained and rely on the instinctive drive to escape in order to engage in goal-directed navigation. I show that such navigation relies on rapidly acquired (less than 30 s) memory of presence and location of refuge. In addition, the optimized control over sensory cues achieved by isolating the mouse from unwanted cues and by having control over the position of explicit cues with the remotely-controlled rotation system, allows probing what sensory information is used to initiate, steer and terminate goal-directed navigation.

### **Mice learn the location of shelter in a new environment rapidly and adapt to changes in spatial features promptly**

My work demonstrates that mice learn the presence of a shelter and accurately escape to it after a single visit. Although comparison of performance with the classic Barnes maze assay (Barnes, 1979) is not straightforward, navigation to shelter in my experiment is more accurate than in the Barnes assay after the same number of trials. Such difference can be due to two critical differences in my protocol: first, before each trial the mouse is not placed in an opaque box in the centre of the arena (which can be regarded as a

disorientation method) and second, the mouse is not displaced passively, particularly immediately before the trial which would preclude path integration to goal.

My experiments demonstrate that mice rely on place memory to navigate to shelter and that this memory can be rapidly updated as reported by the fast dynamics of behavioural adaptation to changes in environmental features. Although it has been shown before that animals, including mice, change preference between freezing and escape in the absence or presence of shelter, respectively (Hennig et al., 1976, Blanchard et al., 1986, Wei et al., 2015, De Oca et al., 2007, O'Brien and Dunlap, 1975) the temporal dynamics of such adaptation had not been described. Here I showed that after exploring the environment for 5 min, following removal or placement of shelter, mice reliably change preference in favour of freezing or escape, respectively. Similarly, I showed that following shelter displacement, mice rapidly adjust navigation to be directed to the new shelter position.

Such flexibility of defensive actions further supports the cognitive control of instinctive behaviours (Evans et al., 2019), and demonstrate the strengths of using defensive behaviours assays to study spatial learning, spatial memory and navigation.

### **Mice rely on spatial memory to orient to shelter accurately during escape**

It had been previously demonstrated that gerbils escape to shelter even if it is behind a barrier that makes it not accessible to vision, although the navigation profile of such escapes was not detailed (Ellard and Eller, 2009). Here I showed that mice do not primarily rely on visualizing the shelter itself or on localizing a cue near it to guide the orientation movement. Instead, mice rely on a memory of place location, as shown by both their correct choice of optimal rotation side towards the shelter and accurate escape in the dark. Additionally, I rotated visual and olfactory cues coherently with the shelter and animals oriented to the old shelter location, showing they do not primarily use sensory cues to orient to shelter. This suggests that mice use path integration to navigate accurately to shelter in escape, relying on memory to map their relative position to shelter.

After two reports of cells that map angular offset to goal in egocentric space, found in the hippocampus (Sarel et al., 2017) and in the lateral entorhinal cortex (Wang et al., 2018), my work has identified a new class of cells that are tuned to a given angular offset to the shelter in both RSC and SC. Importantly, like the aforementioned studies, my work shows that the tuning of these cells follows displacements of the goal, therefore serving as a memory of the ongoing offset to goal. I also showed dependence on SC's head-shelter

offset signal on its RSC input by inactivating the latter and showing that coding of this variable in SC is significantly impaired.

Therefore, not only I show that escape to shelter is memory-guided but also, I describe a potential neural correlate of the information needed to guide orientation, in the brain areas shown to be essential for the behaviour. Supporting the hypothesis this information is used to guide orientation, inactivation of SC-projecting RSC neurons that disrupts coding of head-shelter offset also impairs correct orientation to shelter. Future work is needed to test if this hypothesis is true or not.

### **Projection from RSC to SC is critical for accurately orienting to shelter**

I showed that the functional monosynaptic projection from RSC to SC is essential for the accuracy of navigation to refuge. Inactivation of the projection leads to a significant increase in the time to reach the shelter following an aversive sensory stimulus, due to a decrease in accuracy of the orientation movement towards it. The severity of incorrect orientation phenotype is not smaller for projection-specific inactivation than for unselective inactivation of the RSC, suggesting this projection is the key element of RSC output to control orientation to shelter. In addition, I showed that the projection from RSC to SC is not critical for the implementation of orientation movements, suggesting that RSC's role is to inform the SC of the offset to shelter so that the latter can implement rotation towards it.

My work shows egocentric coding of the angular position of goal at RSC and SC, which is the information needed to implement goal-directed orientation. While we do not yet know if the computation of angular offset to goal is performed at the RSC or upstream, my work contributes to the understanding of the architecture and potential mechanisms of goal representation and goal-directed navigation.

## **7.2. Strengths of the study**

One of the most important strengths of this study was its top-down approach. I focused on first dissecting the behaviour, and subsequently I probed the role of candidate brain areas in controlling the behaviour. After determining that the projection from RSC to SC

was critically responsible for the behaviour, I performed probe recordings to study how these areas encoded the information needed to perform the assay.

I developed various behavioural assays to optimally answer the questions asked. I designed them partially based on previous widely-studied assays in order to have a baseline of performance that I could compare my relatively specific escape assay to. The assay was optimized to maximize the quality and number of trials I could obtain. This provided us with a relatively large number of escapes allowing the dissection of the various components of the behaviour from its initiation to termination.

To show that the specific projection from RSC to SC was critical for the behaviour studied, I combined projection-selective chemogenetic targeting with local delivery of CNO to the specific terminals of the infected neurons, achieving projection-specific inactivation, which I controlled for by inactivating other terminals of the same cells.

I implanted Neuropixels (Jun et al., 2017b), which are high-density 350+ recording sites probes to record from the two areas I was interested in simultaneously. These probes provided me with high quality data and large number of single units; in this study, more than 1200 neurons were recorded, allowing me to characterize the encoding of the behavioural variables of interest robustly. In addition, I paired recordings with projection-selective inactivation allowing me to first validate the inactivation electrophysiologically, and in addition, to study its effects in the coding of the behavioural variables of interest, both at a single neuron and at population levels simultaneously in RSC and SC.

### **7.3. Limitations of the study**

Although my results are robust for the animals tested, they were all conducted using male mice. While studies in neuroscience should ideally include both sexes (Prendergast et al., 2014), initial preliminary experiments in my set-up suggested that female mice stayed longer inside the shelter following escapes, which yield a lower number of escapes per animal. Therefore, I opted to conduct this study using only male mice.

Although the behavioural data strongly suggest that mice path integrate to navigate back to the shelter, I did not conduct any experiment in which I specifically perturbed this navigation strategy. Therefore, it cannot be claimed that this is the navigation strategy

used to navigate in escape, but simply that other strategies like taxon navigation are not primarily employed to navigate to shelter.

When probing different brain areas to assess their involvement in orientation to shelter I did not test some areas which are good candidates to participate in the control of the orientation behaviour, such as the basal ganglia. However, my goal was not to find all areas responsible for controlling the behaviour, but rather key nodes in the circuit that would allow us to study how the brain encodes the memory of goal location and uses this information to navigate towards it.

Finally, although I identified head-shelter offset cells and found that their signal is significantly impaired after inactivation that elicits a behavioural phenotype, I have not proven that the information provided by these cells is actually used to guide the navigation. In the future, the use of genetic tools might allow identification of specific markers for these cells, and thus the probing of their contribution to orientation during escape, for example by means of selective inactivation. In addition, further studies of behavioural features and their correlation with head-shelter offset coding could strengthen the hypothesis that these cells indeed control the behaviour.

## **7.4. Experimental outlook**

The results of this project, along with other recent studies focusing on control of goal-directed navigation and orientation, raise a number of questions that could be addressed by future work:

### **How do animals navigate to shelter in more realistic environments?**

Here I used a simple arena with no obstacles and a single refuge to study how animals accurately escape to shelter. However, paths in nature are often obstructed, and animals need to choose among various potential refuges. It would be interesting to determine how animals negotiate barriers in the environment that prevent a straight escape to shelter at behavioural level and how head-shelter offset cells map the position of goal in such case, namely if they encode offset to goal position or offset to future path around the barrier.

In addition, the presence or absence of a shelter is treated as a binary state of the environment, which is not a realistic model. Future studies should test whether mice still escape to refuge if it is very far away or if, at some point, mice switch their strategy to freezing and if such transition is based on actual distance to shelter or on time to reach it. Understanding how the choice between freezing and escape is computed may help understanding how the shelter position is memorized and how this memory is used to guide navigation to goal.

### **Does the RSC perform the computation of head-shelter offset?**

Various candidate inputs to the RSC could be probed to test whether they carry head-shelter offset information, namely the hippocampus (where cells coding angular offset to goal, have been described in bats (Sarel et al., 2017)), and thalamic nuclei conveying head-direction information to the RSC (Taube, 2007). Probing where this computation is performed will require combining manipulations of neural activity with recordings as various of these inputs are part of loops, by receive afferents from the RSC.

It would also be valuable to study the role of other canonical spatial-memory circuits like the medial entorhinal cortex in my behavioural assay, and test if they directly contribute to this goal-location mapping and goal-directed navigation as previously suggested (Bush et al., 2015).

Finally, although I focused on coding of egocentric angular distance to shelter, it would be critical to study if either RSC's or SC's head-shelter offset neurons, or others, encode the linear distance to shelter as previously described in goal cells in the hippocampus and lateral entorhinal cortex (Wang et al., 2018, Sarel et al., 2017).

### **Does the SC use head-shelter offset information to implement orientation to shelter?**

In this study I showed that head-shelter offset coding in SC relies on the RSC input, which targets both GABAergic and glutamatergic neurons in the SC. SC control of orientation movements has been widely studied in various species and it is organized topographically (Sparks, 1988). Future studies could address how different populations of neurons in SC use head-shelter offset information based on their cell type, topographical location in the SC motor map and SC layer they occupy.

The medial division of the SC (mSC) is known to be critical for integrating threat evidence and its projection to the dorsal periaqueductal gray (dPAG) is essential to initiate escape (Evans et al., 2018). It would be critical to understand how these two circuits (RSC→SC and mSC→dPAG) coordinate to control goal-directed escapes from threat. Mice continuously map their angular offset towards the shelter in the RSC and SC, nevertheless such information should be used selectively upon escape to guide orientation to shelter, while in other moments such information should not control navigation, otherwise mice would constantly be orienting towards the shelter. It is unknown how the orientation movement to shelter is triggered, but the study of this process could be critical for understanding the mechanism through which the brain selects the memory of a spatial location to become the next navigation target.

### **How stable and flexible is head-shelter offset coding?**

I behaviourally probed the temporal dynamics of adaptation to changes in the environment. Although I did not explore the temporal dynamics of this adaptation using neural recordings, I observed that head-shelter offset tuning follows the shelter position after it is displaced, and thus exhibits flexibility. It may be challenging to probe the temporal dynamics in the neural recordings following acute changes in goal position, if the memory trace of previous goal location decays in a few minutes, as shown in goal cells in the hippocampus (Sarel et al., 2017), and as is supported by my behavioural results showing fast adaptations to changes in the environment. If this was the case, the low sampling of data in this short period, during which animals spend a considerable proportion of time inside the shelter, would make the data acquisition and analysis extremely challenging.

It will also be interesting to study the long-term coding stability of these cells, which will require calcium imaging to track neurons. Particularly, comparing the stability of coding in both RSC and SC may provide an insight on the mechanism through which the circuit may use this information to implement goal-directed behaviour, especially after the topography of the projection has been further described.

**Is coding of head-goal offset in RSC and SC specific for shelter?**

In this work I only studied memory-guided orientation to shelter. In the future it will be critical to understand if the cells in RSC and SC specifically encode offset to shelter, or whether they can also encode other behaviourally-relevant goals and if inactivation of the projection from RSC to SC also impairs orientation to such goals. Stimulus-triggered orientation to a food source in an environment similar to my behavioural set-up would be a good starting point to address this question.

**7.5. Concluding remarks**

Although much is known about the neural mechanisms for tracking ongoing positions in space, our understanding of how animals map the position of goals and use it to guide oriented behaviour is largely unknown. This work presents a behavioural assay for studying ethologically relevant memory-guided goal-directed orientation. It provides evidence that the projection from RSC to SC is essential to orient to shelter during escape and shows that these areas contain the memory trace, encoded in motor space, necessary to guide orientation to goal.

## **8. REFERENCES**

- ABLE, K. P. & ABLE, M. A. 1990. Calibration of the magnetic compass of a migratory bird by celestial rotation. *Nature*, 347, 378.
- ABRAMSKY, Z., STRAUSS, E., SUBACH, A., RIECHMAN, A. & KOTLER, B. 1996. The effect of barn owls (*Tyto alba*) on the activity and microhabitat selection of *Gerbillus allenbyi* and *G. pyramidum*. *Oecologia*, 105, 313-319.
- ALEXANDER, A., CARSTENSEN, L., HINMAN, J., RAUDIES, F., CHAPMAN, G. W. & HASSELMO, M. 2019. Egocentric boundary vector tuning of the retrosplenial cortex. *bioRxiv*, 702712.
- ALEXANDER, A. S. & NITZ, D. A. 2015. Retrosplenial cortex maps the conjunction of internal and external spaces. *Nature neuroscience*, 18, 1143.
- ALYAN, S. & MCNAUGHTON, B. 1999. Hippocampectomized rats are capable of homing by path integration. *Behavioral neuroscience*, 113, 19.
- AMANO, K., TANIKAWA, T., KAWAMURA, H., ISEKI, H., NOTANI, M., KAWABATAKE, H., SHIWAKU, T., SUDA, T., DEMURA, H. & KITAMURA, K. 1982. Endorphins and pain relief. *Stereotactic and Functional Neurosurgery*, 45, 123-135.
- AMARAL, V. C. S., GOMES, K. S. & NUNES-DE-SOUZA, R. L. 2010. Increased corticosterone levels in mice subjected to the rat exposure test. *Hormones and Behavior*, 57, 128-133.
- ANDERSEN, R. A. & BUNEO, C. A. 2002. Intentional maps in posterior parietal cortex. *Annual review of neuroscience*, 25, 189-220.
- ARMBRUSTER, B. N., LI, X., PAUSCH, M. H., HERLITZE, S. & ROTH, B. L. 2007. Evolving the lock to fit the key to create a family of G protein-coupled receptors potently activated by an inert ligand. *Proceedings of the National Academy of Sciences*, 104, 5163-5168.
- ARONOV, D., NEVERS, R. & TANK, D. W. 2017. Mapping of a non-spatial dimension by the hippocampal-entorhinal circuit. *Nature*, 543, 719.
- AUGER, S. D. & MAGUIRE, E. A. 2013. Assessing the mechanism of response in the retrosplenial cortex of good and poor navigators. *Cortex*, 49, 2904-2913.
- AUGER, S. D., MULLALLY, S. L. & MAGUIRE, E. A. 2012. Retrosplenial cortex codes for permanent landmarks. *PloS one*, 7, e43620.
- BACH, M. E., HAWKINS, R. D., OSMAN, M., KANDEL, E. R. & MAYFORD, M. 1995. Impairment of spatial but not contextual memory in CaMKII mutant mice with a selective loss of hippocampal LTP in the range of the  $\theta$  frequency. *Cell*, 81, 905-915.
- BACON, J. P. & STRAUSFELD, N. J. 1986. The dipteran 'Giant fibre' pathway: neurons and signals. *Journal of comparative Physiology A*, 158, 529-548.
- BALAKRISHNAMA, S. & GANAPATHIRAJU, A. 1998. Linear discriminant analysis-a brief tutorial. *Institute for Signal and information Processing*, 18, 1-8.

- BANDLER, R. & SHIPLEY, M. T. 1994. Columnar organization in the midbrain periaqueductal gray: modules for emotional expression? *Trends in neurosciences*, 17, 379-389.
- BARASH, S., BRACEWELL, R. M., FOGASSI, L., GNADT, J. W. & ANDERSEN, R. A. 1991. Saccade-related activity in the lateral intraparietal area. II. Spatial properties. *Journal of neurophysiology*, 66, 1109-1124.
- BARNES, C. A. 1979. Memory deficits associated with senescence: a neurophysiological and behavioral study in the rat. *Journal of comparative and physiological psychology*, 93, 74.
- BARTHAS, F. & KWAN, A. C. 2017. Secondary motor cortex: where 'sensory' meets 'motor' in the rodent frontal cortex. *Trends in neurosciences*, 40, 181-193.
- BARTUMEUS, F. & CATALAN, J. 2009. Optimal search behavior and classic foraging theory. *Journal of Physics A: Mathematical and Theoretical*, 42, 434002.
- BATEMAN, P. W. & FLEMING, P. A. 2014. Switching to Plan B: changes in the escape tactics of two grasshopper species (Acrididae: Orthoptera) in response to repeated predatory approaches. *Behavioral ecology and sociobiology*, 68, 457-465.
- BATSCHULET, E. 1981. Circular statistics in biology. *ACADEMIC PRESS, 111 FIFTH AVE., NEW YORK, NY 10003, 1981, 388.*
- BAUM, W. M. 1987. Random and systematic foraging, experimental studies of depletion, and schedules of reinforcement. *Foraging behavior*. Springer.
- BAUMANN, O. & MATTINGLEY, J. B. 2010. Medial parietal cortex encodes perceived heading direction in humans. *Journal of Neuroscience*, 30, 12897-12901.
- BECKER, W. & FUCHS, A. 1969. Further properties of the human saccadic system: eye movements and correction saccades with and without visual fixation points. *Vision research*, 9, 1247-1258.
- BEITEL, R. E. & KAAS, J. 1993. Effects of bilateral and unilateral ablation of auditory cortex in cats on the unconditioned head orienting response to acoustic stimuli. *Journal of Neurophysiology*, 70, 351-369.
- BENVENUTI, S. & WALLRAFF, H. G. 1985. Pigeon navigation: site simulation by means of atmospheric odours. *Journal of Comparative Physiology A*, 156, 737-746.
- BERGERON, A., MATSUO, S. & GUITTON, D. 2003. Superior colliculus encodes distance to target, not saccade amplitude, in multi-step gaze shifts. *Nature neuroscience*, 6, 404.
- BEST, P. J., WHITE, A. M. & MINAI, A. 2001. Spatial processing in the brain: the activity of hippocampal place cells. *Annual review of neuroscience*, 24, 459-486.
- BHATTACHARYYA, K., MCLEAN, D. L. & MACIVER, M. A. 2017. Visual threat assessment and reticulospinal encoding of calibrated responses in larval zebrafish. *Current Biology*, 27, 2751-2762. e6.

- BICANSKI, A. & BURGESS, N. 2016. Environmental anchoring of head direction in a computational model of retrosplenial cortex. *Journal of Neuroscience*, 36, 11601-11618.
- BICANSKI, A. & BURGESS, N. 2018. A neural-level model of spatial memory and imagery. *ELife*, 7, e33752.
- BINAZZI, R., ZACCARONI, M., NESPOLI, A., MASSOLO, A. & DESSI-FULGHERI, F. 2011. Anti-predator behaviour of the red-legged partridge *Alectoris rufa* (Galliformes: Phasianidae) to simulated terrestrial and aerial predators. *Italian journal of zoology*, 78, 106-112.
- BIRCH, L. L. 1999. Development of food preferences. *Annual review of nutrition*, 19, 41-62.
- BITTENCOURT, A., NAKAMURA-PALACIOS, E., MAUAD, H., TUFIK, S. & SCHENBERG, L. 2005. Organization of electrically and chemically evoked defensive behaviors within the deeper collicular layers as compared to the periaqueductal gray matter of the rat. *Neuroscience*, 133, 873-892.
- BIZZI, E. & SCHILLER, P. H. 1970. Single unit activity in the frontal eye fields of unanesthetized monkeys during eye and head movement. *Experimental Brain Research*, 10, 151-158.
- BLAIR, H. T. & SHARP, P. E. 1996. Visual and vestibular influences on head-direction cells in the anterior thalamus of the rat. *Behavioral neuroscience*, 110, 643.
- BLANCHARD, D. C., WILLIAMS, G., LEE, E. & BLANCHARD, R. J. 1981. Taming of wild *Rattus norvegicus* by lesions of the mesencephalic central gray. *Physiological psychology*, 9, 157-163.
- BLANCHARD, R. J. & BLANCHARD, D. C. 1989. Attack and defense in rodents as ethoexperimental models for the study of emotion. *Progress in Neuro-Psychopharmacology and Biological Psychiatry*, 13, S3-S14.
- BLANCHARD, R. J. & BLANCHARD, D. C. 1990. An ethoexperimental analysis of defense, fear, and anxiety.
- BLANCHARD, R. J., BLANCHARD, D. C., AGULLANA, R. & WEISS, S. M. 1991. Twenty-two kHz alarm cries to presentation of a predator, by laboratory rats living in visible burrow systems. *Physiology & behavior*, 50, 967-972.
- BLANCHARD, R. J., FLANNELLY, K. J. & BLANCHARD, D. C. 1986. Defensive behaviors of laboratory and wild *Rattus norvegicus*. *Journal of Comparative Psychology*, 100, 101.
- BLANCHARD, R. J., YANG, M., LI, C.-I., GERVACIO, A. & BLANCHARD, D. C. 2001. Cue and context conditioning of defensive behaviors to cat odor stimuli. *Neuroscience & Biobehavioral Reviews*, 25, 587-595.
- BLANK, D. 2018. Escaping behavior in goitered gazelle. *Behavioural processes*, 147, 38-47.
- BOCCARA, C. N., NARDIN, M., STELLA, F., O'NEILL, J. & CSICSVARI, J. 2019. The entorhinal cognitive map is attracted to goals. *Science*, 363, 1443-1447.

- BOCCARA, C. N., SARGOLINI, F., THORESEN, V. H., SOLSTAD, T., WITTER, M. P., MOSER, E. I. & MOSER, M.-B. 2010. Grid cells in pre-and parasubiculum. *Nature neuroscience*, 13, 987.
- BOLLES, R. C. 1970. Species-specific defense reactions and avoidance learning. *Psychological review*, 77, 32.
- BOVET, P. 1983. Optimal randomness in foraging movement: a central place model. *Rhythms in biology and other fields of application*. Springer.
- BRANDAO, M., MELO, L. & CARDOSO, S. 1993. Mechanisms of defense in the inferior colliculus. *Behavioural brain research*, 58, 49-55.
- BRUCE, C. J. & GOLDBERG, M. E. 1985. Primate frontal eye fields. I. Single neurons discharging before saccades. *Journal of neurophysiology*, 53, 603-635.
- BRUCE, C. J., GOLDBERG, M. E., BUSHNELL, M. C. & STANTON, G. B. 1985. Primate frontal eye fields. II. Physiological and anatomical correlates of electrically evoked eye movements. *Journal of neurophysiology*, 54, 714-734.
- BRUN, V. H., SOLSTAD, T., KJELSTRUP, K. B., FYHN, M., WITTER, M. P., MOSER, E. I. & MOSER, M. B. 2008. Progressive increase in grid scale from dorsal to ventral medial entorhinal cortex. *Hippocampus*, 18, 1200-1212.
- BURGESS, H. A. & GRANATO, M. 2007. Sensorimotor gating in larval zebrafish. *Journal of Neuroscience*, 27, 4984-4994.
- BURGESS, N., BECKER, S., KING, J. A. & O'KEEFE, J. 2001. Memory for events and their spatial context: models and experiments. *Philosophical Transactions of the Royal Society of London. Series B: Biological Sciences*, 356, 1493-1503.
- BURNETT, C. J., LI, C., WEBBER, E., TSAOUSIDOU, E., XUE, S. Y., BRÜNING, J. C. & KRASHES, M. J. 2016. Hunger-driven motivational state competition. *Neuron*, 92, 187-201.
- BUSH, D., BARRY, C., MANSON, D. & BURGESS, N. 2015. Using grid cells for navigation. *Neuron*, 87, 507-520.
- BYRNE, P., BECKER, S. & BURGESS, N. 2007. Remembering the past and imagining the future: a neural model of spatial memory and imagery. *Psychological review*, 114, 340.
- CACUCCI, F., LEVER, C., WILLS, T. J., BURGESS, N. & O'KEEFE, J. 2004. Theta-modulated place-by-direction cells in the hippocampal formation in the rat. *Journal of Neuroscience*, 24, 8265-8277.
- CAIN, D. P., HUMPARTZOOMIAN, R. & BOON, F. 2006. Retrosplenial cortex lesions impair water maze strategies learning or spatial place learning depending on prior experience of the rat. *Behavioural brain research*, 170, 316-325.
- CALTON, J. L., TURNER, C. S., CYRENNE, D.-L. M., LEE, B. R. & TAUBE, J. S. 2008. Landmark control and updating of self-movement cues are largely maintained in head

- direction cells after lesions of the posterior parietal cortex. *Behavioral neuroscience*, 122, 827.
- CAMPBELL, E. J. & MARCHANT, N. J. 2018. The use of chemogenetics in behavioural neuroscience: receptor variants, targeting approaches and caveats. *British journal of pharmacology*, 175, 994-1003.
- CANTERAS, N., SIMERLY, R. & SWANSON, L. 1994. Organization of projections from the ventromedial nucleus of the hypothalamus: a Phaseolus vulgaris-leucoagglutinin study in the rat. *Journal of Comparative Neurology*, 348, 41-79.
- CARD, G. & DICKINSON, M. 2008a. Performance trade-offs in the flight initiation of *Drosophila*. *Journal of Experimental Biology*, 211, 341-353.
- CARD, G. & DICKINSON, M. H. 2008b. Visually mediated motor planning in the escape response of *Drosophila*. *Current Biology*, 18, 1300-1307.
- CARD, G. M. 2012. Escape behaviors in insects. *Current opinion in neurobiology*, 22, 180-186.
- CARO, T. 2005. *Antipredator defenses in birds and mammals*, University of Chicago Press.
- CHAFEE, M. V. & GOLDMAN-RAKIC, P. S. 2000. Inactivation of parietal and prefrontal cortex reveals interdependence of neural activity during memory-guided saccades. *Journal of neurophysiology*, 83, 1550-1566.
- CHAVARRIAGA, R., STRÖSSLIN, T., SHEYNIKHOVICH, D. & GERSTNER, W. 2005. A computational model of parallel navigation systems in rodents. *Neuroinformatics*, 3, 223-241.
- CHEN, L. L., LIN, L.-H., GREEN, E. J., BARNES, C. A. & MCNAUGHTON, B. L. 1994. Head-direction cells in the rat posterior cortex. *Experimental Brain Research*, 101, 8-23.
- CHEN, Y., LIN, Y.-C., KUO, T.-W. & KNIGHT, Z. A. 2015. Sensory detection of food rapidly modulates arcuate feeding circuits. *Cell*, 160, 829-841.
- CHERNETSOV, N., KISHKINEV, D. & MOURITSEN, H. 2008. A long-distance avian migrant compensates for longitudinal displacement during spring migration. *Current Biology*, 18, 188-190.
- CHO, J. & SHARP, P. E. 2001. Head direction, place, and movement correlates for cells in the rat retrosplenial cortex. *Behavioral neuroscience*, 115, 3.
- CHRASIL, E. R., SHERRILL, K. R., HASSELMO, M. E. & STERN, C. E. 2015. There and back again: hippocampus and retrosplenial cortex track homing distance during human path integration. *Journal of Neuroscience*, 35, 15442-15452.
- CLARK, B. J., BASSETT, J. P., WANG, S. S. & TAUBE, J. S. 2010. Impaired head direction cell representation in the anterodorsal thalamus after lesions of the retrosplenial cortex. *Journal of Neuroscience*, 30, 5289-5302.

- CLARK, B. J., RICE, J. P., AKERS, K. G., CANDELARIA-COOK, F. T., TAUBE, J. S. & HAMILTON, D. A. 2013. Lesions of the dorsal tegmental nuclei disrupt control of navigation by distal landmarks in cued, directional, and place variants of the Morris water task. *Behavioral Neuroscience*, 127, 566.
- CLARKE, M. F., DA SILVA, K. B., LAIR, H., POCKLINGTON, R., KRAMER, D. L. & MCLAUGHLIN, R. L. 1993. Site familiarity affects escape behaviour of the eastern chipmunk, *Tamias striatus*. *Oikos*, 533-537.
- COHEN, B. 1972. Unit activity in the pontine reticular formation associated with eye movements. *Brain Res*, 46, 403-410.
- COLBY, C. L. & DUHAMEL, J.-R. 1996. Spatial representations for action in parietal cortex. *Cognitive Brain Research*.
- COLLIAS, N. E. 1987. The vocal repertoire of the red junglefowl: a spectrographic classification and the code of communication. *The Condor*, 89, 510-524.
- COLLINS, C. E., LYON, D. C. & KAAS, J. H. 2005. Distribution across cortical areas of neurons projecting to the superior colliculus in new world monkeys. *The Anatomical Record Part A: Discoveries in Molecular, Cellular, and Evolutionary Biology: An Official Publication of the American Association of Anatomists*, 285, 619-627.
- COMMINS, S., GEMMELL, C., ANDERSON, M., GIGG, J. & O'MARA, S. M. 1999. Disorientation combined with bilateral parietal cortex lesions causes path integration deficits in the water maze. *Behavioural brain research*, 104, 197-200.
- COMOLI, E., DAS NEVES FAVARO, P., VAUTRELLE, N., LERICHE, M., OVERTON, P. G. & REDGRAVE, P. 2012. Segregated anatomical input to sub-regions of the rodent superior colliculus associated with approach and defense. *Frontiers in neuroanatomy*, 6, 9.
- COOPER, B. G. & MIZUMORI, S. J. 1999. Retrosplenial cortex inactivation selectively impairs navigation in darkness. *Neuroreport*, 10, 625-630.
- COOPER, B. G. & MIZUMORI, S. J. 2001. Temporary inactivation of the retrosplenial cortex causes a transient reorganization of spatial coding in the hippocampus. *Journal of Neuroscience*, 21, 3986-4001.
- COOPER, W. 2000. Tradeoffs between predation risk and feeding in a lizard, the broad-headed skink (*Eumeces laticeps*). *Behaviour*, 137, 1175-1189.
- COOPER, W. E. & BLUMSTEIN, D. T. 2015. *Escaping from predators: an integrative view of escape decisions*, Cambridge University Press.
- DA CUNHA, C., WIETZIKOSKI, S., WIETZIKOSKI, E. C., MIYOSHI, E., FERRO, M. M., ANSELMO-FRANCI, J. A. & CANTERAS, N. S. 2003. Evidence for the substantia nigra pars compacta as an essential component of a memory system independent of the hippocampal memory system. *Neurobiology of Learning and Memory*, 79, 236-242.

- DASH, S., YAN, X., WANG, H. & CRAWFORD, J. D. 2015. Continuous updating of visuospatial memory in superior colliculus during slow eye movements. *Current Biology*, 25, 267-274.
- DE BRUIN, J. P., MOITA, M. P., DE BRABANDER, H. M. & JOOSTEN, R. N. 2001. Place and response learning of rats in a Morris water maze: differential effects of fimbria fornix and medial prefrontal cortex lesions. *Neurobiology of learning and memory*, 75, 164-178.
- DE FRANCESCHI, G., VIVATTANASARN, T., SALEEM, A. B. & SOLOMON, S. G. 2016. Vision guides selection of freeze or flight defense strategies in mice. *Current Biology*, 26, 2150-2154.
- DE MOLINA, A. F. & HUNSPERGER, R. 1962. Organization of the subcortical system governing defence and flight reactions in the cat. *The Journal of physiology*, 160, 200-213.
- DE OCA, B. M., MINOR, T. R. & FANSELOW, M. S. 2007. Brief flight to a familiar enclosure in response to a conditional stimulus in rats. *The Journal of general psychology*, 134, 153-172.
- DEAN, P. & KEY, C. 1981. Spatial deficits on radial maze after large tectal lesions in rats: possible role of impaired scanning. *Behavioral and Neural Biology*, 32, 170-190.
- DEAN, P., MITCHELL, I. & REDGRAVE, P. 1988. Responses resembling defensive behaviour produced by microinjection of glutamate into superior colliculus of rats. *Neuroscience*, 24, 501-510.
- DEAN, P. & REDGRAVE, P. 1984. The superior colliculus and visual neglect in rat and hamster. I. Behavioural evidence. *Brain Research Reviews*, 8, 129-141.
- DEAN, P., REDGRAVE, P. & WESTBY, G. 1989. Event or emergency? Two response systems in the mammalian superior colliculus. *Trends in neurosciences*, 12, 137-147.
- DENG, H., XIAO, X. & WANG, Z. 2016. Periaqueductal gray neuronal activities underlie different aspects of defensive behaviors. *Journal of Neuroscience*, 36, 7580-7588.
- DEVAN, B. D., GOAD, E. H. & PETRI, H. L. 1996. Dissociation of hippocampal and striatal contributions to spatial navigation in the water maze. *Neurobiology of learning and memory*, 66, 305-323.
- DIAS, E. C. & SEGRAVES, M. A. 1999. Muscimol-induced inactivation of monkey frontal eye field: effects on visually and memory-guided saccades. *Journal of neurophysiology*, 81, 2191-2214.
- DILL, L. M. & HOUTMAN, R. 1989. The influence of distance to refuge on flight initiation distance in the gray squirrel (*Sciurus carolinensis*). *Canadian Journal of Zoology*, 67, 233-235.
- DOELLER, C. F., BARRY, C. & BURGESS, N. 2010. Evidence for grid cells in a human memory network. *Nature*, 463, 657.

- DOMENICI, P. & BATTY, R. 1997. Escape behaviour of solitary herring (*Clupea harengus*) and comparisons with schooling individuals. *Marine Biology*, 128, 29-38.
- DOMENICI, P., BLAGBURN, J. M. & BACON, J. P. 2011a. Animal escapology I: theoretical issues and emerging trends in escape trajectories. *Journal of Experimental Biology*, 214, 2463-2473.
- DOMENICI, P., BLAGBURN, J. M. & BACON, J. P. 2011b. Animal escapology II: escape trajectory case studies. *Journal of Experimental biology*, 214, 2474-2494.
- DOMENICI, P., BOOTH, D., BLAGBURN, J. M. & BACON, J. P. 2008. Cockroaches keep predators guessing by using preferred escape trajectories. *Current Biology*, 18, 1792-1796.
- DORRIS, M. C., PARE, M. & MUNOZ, D. P. 1997. Neuronal activity in monkey superior colliculus related to the initiation of saccadic eye movements. *Journal of Neuroscience*, 17, 8566-8579.
- DUNN, T. W., GEBHARDT, C., NAUMANN, E. A., RIEGLER, C., AHRENS, M. B., ENGERT, F. & DEL BENE, F. 2016. Neural circuits underlying visually evoked escapes in larval zebrafish. *Neuron*, 89, 613-628.
- DUPRET, D., O'NEILL, J., PLEYDELL-BOUVERIE, B. & CSICSVARI, J. 2010. The reorganization and reactivation of hippocampal maps predict spatial memory performance. *Nature neuroscience*, 13, 995.
- EATON, R. C., BOMBARDIERI, R. A. & MEYER, D. L. 1977. The Mauthner-initiated startle response in teleost fish. *Journal of Experimental Biology*, 66, 65-81.
- EATON, R. C., DIDOMENICO, R. & NISSANOV, J. 1988. Flexible body dynamics of the goldfish C-start: implications for reticulospinal command mechanisms. *Journal of Neuroscience*, 8, 2758-2768.
- EDUT, S. & EILAM, D. 2003. Rodents in open space adjust their behavioral response to the different risk levels during barn-owl attack. *BMC ecology*, 3, 10.
- EDUT, S. & EILAM, D. 2004. Protean behavior under barn-owl attack: voles alternate between freezing and fleeing and spiny mice flee in alternating patterns. *Behavioural brain research*, 155, 207-216.
- EICHENBAUM, H., DUDCHENKO, P., WOOD, E., SHAPIRO, M. & TANILA, H. 1999. The hippocampus, memory, and place cells: is it spatial memory or a memory space? *Neuron*, 23, 209-226.
- EICHENBAUM, H., STEWART, C. & MORRIS, R. 1990. Hippocampal representation in place learning. *Journal of Neuroscience*, 10, 3531-3542.
- EILAM, D., DAYAN, T., BEN-ELIYAHU, S., SCHULMAN, I., SHEFER, G. & HENDRIE, C. A. 1999. Differential behavioural and hormonal responses of voles and spiny mice to owl calls. *Animal Behaviour*, 58, 1085-1093.

- EKSTROM, A. D., KAHANA, M. J., CAPLAN, J. B., FIELDS, T. A., ISHAM, E. A., NEWMAN, E. L. & FRIED, I. 2003. Cellular networks underlying human spatial navigation. *Nature*, 425, 184.
- ELDUAYEN, C. & SAVE, E. 2014. The retrosplenial cortex is necessary for path integration in the dark. *Behavioural brain research*, 272, 303-307.
- ELLARD, C. & GOODALE, M. 1988. A functional analysis of the collicular output pathways: a dissociation of deficits following lesions of the dorsal tegmental decussation and the ipsilateral collicular efferent bundle in the Mongolian gerbil. *Experimental Brain Research*, 71, 307-319.
- ELLARD, C. G. 1993. Organization of escape movements from overhead threats in the Mongolian gerbil (*Meriones unguiculatus*). *Journal of Comparative Psychology*, 107, 242.
- ELLARD, C. G. & BYERS, R. D. 2005. The influence of the behaviour of conspecifics on responses to threat in the Mongolian gerbil, *Meriones unguiculatus*. *Animal Behaviour*, 70, 49-58.
- ELLARD, C. G. & ELLER, M. C. 2009. Spatial cognition in the gerbil: computing optimal escape routes from visual threats. *Animal cognition*, 12, 333-345.
- EMLEN, S. T. 1970. Celestial rotation: its importance in the development of migratory orientation. *Science*, 170, 1198-1201.
- ENDRES, T. & FENDT, M. 2007. Conditioned behavioral responses to a context paired with the predator odor trimethylthiazoline. *Behavioral neuroscience*, 121, 594.
- ENDRES, T. & FENDT, M. 2008. Inactivation of the lateral septum blocks fox odor-induced fear behavior. *Neuroreport*, 19, 667-670.
- ERDEM, U. M. & HASSELMO, M. 2012. A goal-directed spatial navigation model using forward trajectory planning based on grid cells. *European Journal of Neuroscience*, 35, 916-931.
- ERDEM, U. M. & HASSELMO, M. E. 2014. A biologically inspired hierarchical goal directed navigation model. *Journal of Physiology-Paris*, 108, 28-37.
- ERLICH, J. C., BIALEK, M. & BRODY, C. D. 2011. A cortical substrate for memory-guided orienting in the rat. *Neuron*, 72, 330-343.
- ETIENNE, A. S. & JEFFERY, K. J. 2004. Path integration in mammals. *Hippocampus*, 14, 180-192.
- ETIENNE, A. S., MAURER, R., SAUCY, F. & TERONI, E. 1986. Short-distance homing in the golden hamster after a passive outward journey. *Animal Behaviour*, 34, 696-715.
- ETIENNE, A. S., MAURER, R. & SÉGUINOT, V. 1996. Path integration in mammals and its interaction with visual landmarks. *Journal of experimental Biology*, 199, 201-209.

- EVANS, D. A., STEMPEL, A. V., VALE, R. & BRANCO, T. 2019. Cognitive Control of Escape Behaviour. *Trends in cognitive sciences*.
- EVANS, D. A., STEMPEL, A. V., VALE, R., RUEHLE, S., LEFLER, Y. & BRANCO, T. 2018. A synaptic threshold mechanism for computing escape decisions. *Nature*, 558, 590.
- FELSEN, G. & MAINEN, Z. F. 2008. Neural substrates of sensory-guided locomotor decisions in the rat superior colliculus. *Neuron*, 60, 137-148.
- FENDT, M., ENDRES, T. & APFELBACH, R. 2003. Temporary inactivation of the bed nucleus of the stria terminalis but not of the amygdala blocks freezing induced by trimethylthiazoline, a component of fox feces. *Journal of Neuroscience*, 23, 23-28.
- FERREIRA-PINTO, M. J., RUDER, L., CAPELLI, P. & ARBER, S. 2018. Connecting circuits for supraspinal control of locomotion. *Neuron*, 100, 361-374.
- FILOSA, A., BARKER, A. J., DAL MASCHIO, M. & BAIER, H. 2016. Feeding state modulates behavioral choice and processing of prey stimuli in the zebrafish tectum. *Neuron*, 90, 596-608.
- FOTOWAT, H. & GABBIANI, F. 2007. Relationship between the phases of sensory and motor activity during a looming-evoked multistage escape behavior. *Journal of Neuroscience*, 27, 10047-10059.
- FRANK, L. M., BROWN, E. N. & WILSON, M. 2000. Trajectory encoding in the hippocampus and entorhinal cortex. *Neuron*, 27, 169-178.
- FREEDMAN, E. G. 2008. Coordination of the eyes and head during visual orienting. *Experimental brain research*, 190, 369.
- FREEDMAN, E. G. & SPARKS, D. L. 1997. Eye-head coordination during head-unrestrained gaze shifts in rhesus monkeys. *Journal of neurophysiology*, 77, 2328-2348.
- FREEDMAN, E. G., STANFORD, T. R. & SPARKS, D. L. 1996. Combined eye-head gaze shifts produced by electrical stimulation of the superior colliculus in rhesus monkeys. *Journal of neurophysiology*, 76, 927-952.
- FRIES, W. 1984. Cortical projections to the superior colliculus in the macaque monkey: a retrograde study using horseradish peroxidase. *Journal of Comparative Neurology*, 230, 55-76.
- FROHARDT, R. J., BASSETT, J. P. & TAUBE, J. S. 2006. Path integration and lesions within the head direction cell circuit: comparison between the roles of the anterodorsal thalamus and dorsal tegmental nucleus. *Behavioral neuroscience*, 120, 135.
- FROST, B. J. & MOURITSEN, H. 2006. The neural mechanisms of long distance animal navigation. *Current opinion in neurobiology*, 16, 481-488.
- FUHS, M. C. & TOURETZKY, D. S. 2006. A spin glass model of path integration in rat medial entorhinal cortex. *Journal of Neuroscience*, 26, 4266-4276.

- FYHN, M., HAFTING, T., TREVES, A., MOSER, M.-B. & MOSER, E. I. 2007. Hippocampal remapping and grid realignment in entorhinal cortex. *Nature*, 446, 190.
- FYHN, M., MOLDEN, S., WITTER, M. P., MOSER, E. I. & MOSER, M.-B. 2004. Spatial representation in the entorhinal cortex. *Science*, 305, 1258-1264.
- GABBIANI, F., KRAPP, H. G. & LAURENT, G. 1999. Computation of object approach by a wide-field, motion-sensitive neuron. *Journal of Neuroscience*, 19, 1122-1141.
- GANDHI, N. J., BARTON, E. J. & SPARKS, D. L. 2008. Coordination of eye and head components of movements evoked by stimulation of the paramedian pontine reticular formation. *Experimental brain research*, 189, 35.
- GARCÍA DEL CAÑO, G., GERRIKAGOITIA, I. & MARTÍNEZ-MILLÁN, L. 2000. Morphology and topographical organization of the retrosplenio-collicular connection: a pathway to relay contextual information from the environment to the superior colliculus. *Journal of Comparative Neurology*, 425, 393-408.
- GAYMARD, B., PLONER, C. J., RIVAUD, S., VERMERSCH, A. & PIERROT-DESEILLIGNY, C. 1998a. Cortical control of saccades. *Experimental Brain Research*, 123, 159-163.
- GAYMARD, B., RIVAUD, S., CASSARINI, J., DUBARD, T., RANCUREL, G., AGID, Y. & PIERROT-DESEILLIGNY, C. 1998b. Effects of anterior cingulate cortex lesions on ocular saccades in humans. *Experimental brain research*, 120, 173-183.
- GHOJOGH, B. & CROWLEY, M. 2019. Linear and Quadratic Discriminant Analysis: Tutorial. *arXiv preprint arXiv:1906.02590*.
- GIRE, D. H., KAPOOR, V., ARRIGHI-ALLISAN, A., SEMINARA, A. & MURTHY, V. N. 2016. Mice develop efficient strategies for foraging and navigation using complex natural stimuli. *Current Biology*, 26, 1261-1273.
- GOLOB, E. J. & TAUBE, J. S. 1999. Head direction cells in rats with hippocampal or overlying neocortical lesions: evidence for impaired angular path integration. *Journal of Neuroscience*, 19, 7198-7211.
- GOODRIDGE, J. P., DUDCHENKO, P. A., WORBOYS, K. A., GOLOB, E. J. & TAUBE, J. S. 1998. Cue control and head direction cells. *Behavioral neuroscience*, 112, 749.
- GOODRIDGE, J. P. & TAUBE, J. S. 1995. Preferential use of the landmark navigational system by head direction cells in rats. *Behavioral neuroscience*, 109, 49.
- GOODROE, S. C., STARNES, J. & BROWN, T. I. 2018. The complex nature of hippocampal-striatal interactions in spatial navigation. *Frontiers in human neuroscience*, 12, 250.
- GOTHARD, K. M., SKAGGS, W. E. & MCNAUGHTON, B. L. 1996. Dynamics of mismatch correction in the hippocampal ensemble code for space: interaction between path integration and environmental cues. *Journal of Neuroscience*, 16, 8027-8040.

- GRANTYN, A. & GRANTYN, R. 1982. Axonal patterns and sites of termination of cat superior colliculus neurons projecting in the tecto-bulbo-spinal tract. *Experimental Brain Research*, 46, 243-256.
- GRANTYN, A., OLIVIER, E. & KITAMA, T. 1993. Tracing premotor brain stem networks of orienting movements. *Current opinion in neurobiology*, 3, 973-981.
- GROSS, C. T. & CANTERAS, N. S. 2012. The many paths to fear. *Nature Reviews Neuroscience*, 13, 651.
- GU, Y., FETSCH, C. R., ADEYEMO, B., DEANGELIS, G. C. & ANGELAKI, D. E. 2010. Decoding of MSTd population activity accounts for variations in the precision of heading perception. *Neuron*, 66, 596-609.
- GUEDRY, F. E. 1974. Psychophysics of vestibular sensation. *Vestibular System Part 2: Psychophysics, Applied Aspects and General Interpretations*. Springer.
- GUITTON, D., DOUGLAS, R. & VOLLE, M. 1984. Eye-head coordination in cats. *Journal of Neurophysiology*, 52, 1030-1050.
- HAFTING, T., FYHN, M., MOLDEN, S., MOSER, M.-B. & MOSER, E. I. 2005. Microstructure of a spatial map in the entorhinal cortex. *Nature*, 436, 801.
- HALES, J. B., SCHLESIGER, M. I., LEUTGEB, J. K., SQUIRE, L. R., LEUTGEB, S. & CLARK, R. E. 2014. Medial entorhinal cortex lesions only partially disrupt hippocampal place cells and hippocampus-dependent place memory. *Cell reports*, 9, 893-901.
- HALLETT, P. & LIGHTSTONE, A. 1976. Saccadic eye movements towards stimuli triggered by prior saccades. *Vision research*, 16, 99-106.
- HARKER, K. T. & WHISHAW, I. Q. 2002. Impaired spatial performance in rats with retrosplenial lesions: importance of the spatial problem and the rat strain in identifying lesion effects in a swimming pool. *Journal of Neuroscience*, 22, 1155-1164.
- HARRISON, F., HOSSEINI, A. & MCDONALD, M. 2009. Endogenous anxiety and stress responses in water maze and Barnes maze spatial memory tasks. *Behavioural brain research*, 198, 247-251.
- HARVEY, C. D., COEN, P. & TANK, D. W. 2012. Choice-specific sequences in parietal cortex during a virtual-navigation decision task. *Nature*, 484, 62.
- HAYDEN, B. Y. & PLATT, M. L. 2010. Neurons in anterior cingulate cortex multiplex information about reward and action. *Journal of Neuroscience*, 30, 3339-3346.
- HEIDE, W., BLANKENBURG, M., ZIMMERMANN, E. & KÖMPF, D. 1995. Cortical control of double-step saccades: implications for spatial orientation. *Annals of Neurology: Official Journal of the American Neurological Association and the Child Neurology Society*, 38, 739-748.
- HEMMI, J. M. 2005. Predator avoidance in fiddler crabs: 1. Escape decisions in relation to the risk of predation. *Animal Behaviour*, 69, 603-614.

- HENNIG, C. W., DUNLAP, W. P. & GALLUP, G. G. 1976. The effect of distance between predator and prey and the opportunity to escape on tonic immobility in *Anolis carolinensis*. *The Psychological Record*, 26, 312-320.
- HERBERHOLZ, J. & MARQUART, G. D. 2012. Decision making and behavioral choice during predator avoidance. *Frontiers in neuroscience*, 6, 125.
- HIGHAM, T. E., DAVENPORT, M. S. & JAYNE, B. C. 2001. Maneuvering in an arboreal habitat: the effects of turning angle on the locomotion of three sympatric ecomorphs of *Anolis* lizards. *Journal of Experimental Biology*, 204, 4141-4155.
- HIKOSAKA, O., TAKIKAWA, Y. & KAWAGOE, R. 2000. Role of the basal ganglia in the control of purposive saccadic eye movements. *Physiological reviews*, 80, 953-978.
- HINMAN, J. R., CHAPMAN, G. W. & HASSELMO, M. E. 2019. Neuronal representation of environmental boundaries in egocentric coordinates. *Nature Communications*, 10, 2772.
- HOFFMANN, G. 1983. The random elements in the systematic search behavior of the desert isopod *Hemilepistus reaumuri*. *Behavioral Ecology and Sociobiology*, 13, 81-92.
- HOK, V., LENCK-SANTINI, P.-P., ROUX, S., SAVE, E., MULLER, R. U. & POU CET, B. 2007. Goal-related activity in hippocampal place cells. *Journal of Neuroscience*, 27, 472-482.
- HOLLAND, R. A., THORUP, K., VONHOF, M. J., COCHRAN, W. W. & WIKELSKI, M. 2006. Navigation: Bat orientation using Earth's magnetic field. *Nature*, 444, 702.
- HOLLUP, S. A., MOLDEN, S., DONNETT, J. G., MOSER, M.-B. & MOSER, E. I. 2001. Accumulation of hippocampal place fields at the goal location in an annular watermaze task. *Journal of Neuroscience*, 21, 1635-1644.
- HONZIK, C. H. 1936. The sensory basis of maze learning in rats. *Comparative Psychology Monographs*.
- HORTON, T. W., HOLDAWAY, R. N., ZERBINI, A. N., HAUSER, N., GARRIGUE, C., ANDRIOLO, A. & CLAPHAM, P. J. 2011. Straight as an arrow: humpback whales swim constant course tracks during long-distance migration. *Biology letters*, rsbl20110279.
- HØYDAL, Ø. A., SKYTØEN, E. R., ANDERSSON, S. O., MOSER, M.-B. & MOSER, E. I. 2019. Object-vector coding in the medial entorhinal cortex. *Nature*, 568, 400.
- HUBER, R. & KNADEN, M. 2015. Egocentric and geocentric navigation during extremely long foraging paths of desert ants. *Journal of Comparative Physiology A*, 201, 609-616.
- HUERTA, M. F., KRUBITZER, L. A. & KAAS, J. H. 1986. Frontal eye field as defined by intracortical microstimulation in squirrel monkeys, owl monkeys, and macaque monkeys: I. Subcortical connections. *Journal of Comparative Neurology*, 253, 415-439.
- HUNSPERGER, R. W. 1963. Comportements affectifs provoqués par la stimulation électrique du tronc cérébral et du cerveau antérieur. *Journal de Physiologie*, 55, 45-+.

- HUSAK, J. F. 2006. Does survival depend on how fast you can run or how fast you do run? *Functional Ecology*, 20, 1080-1086.
- HWANG, E. J., HAUSCHILD, M., WILKE, M. & ANDERSEN, R. A. 2012. Inactivation of the parietal reach region causes optic ataxia, impairing reaches but not saccades. *Neuron*, 76, 1021-1029.
- IARIA, G., CHEN, J. K., GUARIGLIA, C., PTITO, A. & PETRIDES, M. 2007. Retrosplenial and hippocampal brain regions in human navigation: complementary functional contributions to the formation and use of cognitive maps. *European Journal of Neuroscience*, 25, 890-899.
- INGLE, D. J. 1990. Visually elicited evasive behavior in frogs. *BioScience*, 40, 284-291.
- INO, T., DOI, T., HIROSE, S., KIMURA, T., ITO, J. & FUKUYAMA, H. 2007. Directional disorientation following left retrosplenial hemorrhage: a case report with fMRI studies. *Cortex*, 43, 248-254.
- ISOSAKA, T., MATSUO, T., YAMAGUCHI, T., FUNABIKI, K., NAKANISHI, S., KOBAYAKAWA, R. & KOBAYAKAWA, K. 2015. Htr2a-expressing cells in the central amygdala control the hierarchy between innate and learned fear. *Cell*, 163, 1153-1164.
- ITO, H. T., ZHANG, S.-J., WITTER, M. P., MOSER, E. I. & MOSER, M.-B. 2015. A prefrontal-thalamo-hippocampal circuit for goal-directed spatial navigation. *Nature*, 522, 50.
- JACOB, P.-Y., CASALI, G., SPIESER, L., PAGE, H., OVERINGTON, D. & JEFFERY, K. 2017. An independent, landmark-dominated head-direction signal in dysgranular retrosplenial cortex. *Nature neuroscience*, 20, 173.
- JACOBS, J., KAHANA, M. J., EKSTROM, A. D., MOLLISON, M. V. & FRIED, I. 2010. A sense of direction in human entorhinal cortex. *Proceedings of the National Academy of Sciences*, 107, 6487-6492.
- JACOBS, J., WEIDEMANN, C. T., MILLER, J. F., SOLWAY, A., BURKE, J. F., WEI, X.-X., SUTHANA, N., SPERLING, M. R., SHARAN, A. D. & FRIED, I. 2013. Direct recordings of grid-like neuronal activity in human spatial navigation. *Nature neuroscience*, 16, 1188.
- JAY, M. F. & SPARKS, D. L. 1987. Sensorimotor integration in the primate superior colliculus. II. Coordinates of auditory signals. *Journal of Neurophysiology*, 57, 35-55.
- JENSEN, D. D. 1961. Operationism and the question "Is this behavior learned or innate?". *Behaviour*, 1-8.
- JERCOG, P. E., AHMADIAN, Y., WOODRUFF, C., DEB-SEN, R., ABBOTT, L. F. & KANDEL, E. R. 2019. Heading direction with respect to a reference point modulates place-cell activity. *Nature communications*, 10, 2333.
- JOG, M. S., KUBOTA, Y., CONNOLLY, C. I., HILLEGART, V. & GRAYBIEL, A. M. 1999. Building neural representations of habits. *Science*, 286, 1745-1749.

- JOHANSEN, J. P., TARPLEY, J. W., LEDOUX, J. E. & BLAIR, H. T. 2010. Neural substrates for expectation-modulated fear learning in the amygdala and periaqueductal gray. *Nature neuroscience*, 13, 979.
- JOHNSON, A. & REDISH, A. D. 2007. Neural ensembles in CA3 transiently encode paths forward of the animal at a decision point. *Journal of Neuroscience*, 27, 12176-12189.
- JORDAN, J. T. 2019. The rodent hippocampus as a bilateral structure: A review of hemispheric lateralization. *bioRxiv*, 150193.
- JULIAN, J. B., KEINATH, A. T., MARCHETTE, S. A. & EPSTEIN, R. A. 2018. The neurocognitive basis of spatial reorientation. *Current Biology*, 28, R1059-R1073.
- JUN, J. J., MITELUT, C., LAI, C., GRATIY, S., ANASTASSIOU, C. & HARRIS, T. D. 2017a. Real-time spike sorting platform for high-density extracellular probes with ground-truth validation and drift correction. *bioRxiv*, 101030.
- JUN, J. J., STEINMETZ, N. A., SIEGLE, J. H., DENMAN, D. J., BAUZA, M., BARBARITS, B., LEE, A. K., ANASTASSIOU, C. A., ANDREI, A. & AYDIN, Ç. 2017b. Fully integrated silicon probes for high-density recording of neural activity. *Nature*, 551, 232.
- KALIA, A. A., SCHRATER, P. R. & LEGGE, G. E. 2013. Combining path integration and remembered landmarks when navigating without vision. *PloS one*, 8, e72170.
- KEAY, K. A., REDGRAVE, P. & DEAN, P. 1988. Cardiovascular and respiratory changes elicited by stimulation of rat superior colliculus. *Brain research bulletin*, 20, 13-26.
- KELLER, E. 1974. Participation of medial pontine reticular formation in eye movement generation in monkey. *Journal of Neurophysiology*, 37, 316-332.
- KELLER, E. 1979. Colliculoreticular organization in the oculomotor system. *Progress in brain research*. Elsevier.
- KELLY, J. B., JUDGE, P. W. & FRASER, I. H. 1987. Development of the auditory orientation response in the albino rat (*Rattus norvegicus*). *Journal of Comparative Psychology*, 101, 60.
- KESNER, R. P., FARNSWORTH, G. & DIMATTIA, B. V. 1989. Double dissociation of egocentric and allocentric space following medial prefrontal and parietal cortex lesions in the rat. *Behavioral neuroscience*, 103, 956.
- KIM, S., SAPIURKA, M., CLARK, R. E. & SQUIRE, L. R. 2013. Contrasting effects on path integration after hippocampal damage in humans and rats. *Proceedings of the National Academy of Sciences*, 110, 4732-4737.
- KIMMEL, C. B., PATTERSON, J. & KIMMEL, R. O. 1974. The development and behavioral characteristics of the startle response in the zebra fish. *Developmental Psychobiology: The Journal of the International Society for Developmental Psychobiology*, 7, 47-60.

- KING, A. J., HUTCHINGS, M. E., MOORE, D. R. & BLAKEMORE, C. 1988. Developmental plasticity in the visual and auditory representations in the mammalian superior colliculus. *Nature*, 332, 73.
- KING, S. M., DEAN, P. & REDGRAVE, P. 1991. Bypassing the saccadic pulse generator: possible control of head movement trajectory by rat superior colliculus. *European Journal of Neuroscience*, 3, 790-801.
- KIRSCH, D. L. & NICHOLS, F. 2013. Cranial electrotherapy stimulation for treatment of anxiety, depression, and insomnia. *Psychiatric Clinics*, 36, 169-176.
- KNIERIM, J. J., KUDRIMOTI, H. S. & MCNAUGHTON, B. L. 1998. Interactions between idiothetic cues and external landmarks in the control of place cells and head direction cells. *Journal of neurophysiology*, 80, 425-446.
- KOLB, B., SUTHERLAND, R. J. & WHISHAW, I. Q. 1983. A comparison of the contributions of the frontal and parietal association cortex to spatial localization in rats. *Behavioral neuroscience*, 97, 13.
- KORN, H. & FABER, D. S. 2005. The Mauthner cell half a century later: a neurobiological model for decision-making? *Neuron*, 47, 13-28.
- KOTLER, B. P., BROWN, J. S. & MITCHELL, W. A. 1994. The role of predation in shaping the behavior, morphology and community organization of desert rodents. *Australian Journal of Zoology*, 42, 449-466.
- KRAUSE, J. & GODIN, J.-G. J. 1996. Influence of prey foraging posture on flight behavior and predation risk: predators take advantage of unwary prey. *Behavioral Ecology*, 7, 264-271.
- KROPFF, E., CARMICHAEL, J. E., MOSER, M.-B. & MOSER, E. I. 2015. Speed cells in the medial entorhinal cortex. *Nature*, 523, 419.
- KUNWAR, P. S., ZELIKOWSKY, M., REMEDIOS, R., CAI, H., YILMAZ, M., MEISTER, M. & ANDERSON, D. J. 2015. Ventromedial hypothalamic neurons control a defensive emotion state. *Elife*, 4, e06633.
- KÜNZLE, H. 1995. Regional and laminar distribution of cortical neurons projecting to either superior or inferior colliculus in the hedgehog tenrec. *Cerebral Cortex*, 5, 338-352.
- KURYLO, D. D. & SKAVENSKI, A. A. 1991. Eye movements elicited by electrical stimulation of area PG in the monkey. *Journal of Neurophysiology*, 65, 1243-1253.
- KUYPERS, H. G. & LAWRENCE, D. G. 1967. Cortical projections to the red nucleus and the brain stem in the rhesus monkey. *Brain research*, 4, 151-188.
- LACHANCE, P. A., TODD, T. P. & TAUBE, J. S. 2019. A sense of space in postrhinal cortex. *Science*, 365, eaax4192.
- LAURENS, J., ABREGO, A., CHAM, H., POPENEY, B., YU, Y., ROTEM, N., AARSE, J., DICKMAN, D. & ANGELAKI, D. 2019. Multiplexed code of navigation variables in the anterior limbic system. *bioRxiv*, 684464.

- LAYNE, J. E., BARNES, W. J. P. & DUNCAN, L. M. 2003a. Mechanisms of homing in the fiddler crab *Uca rapax* 1. Spatial and temporal characteristics of a system of small-scale navigation. *Journal of experimental biology*, 206, 4413-4423.
- LAYNE, J. E., BARNES, W. J. P. & DUNCAN, L. M. 2003b. Mechanisms of homing in the fiddler crab *Uca rapax* 2. Information sources and frame of reference for a path integration system. *Journal of Experimental Biology*, 206, 4425-4442.
- LEDOUX, J. & DAW, N. D. 2018. Surviving threats: neural circuit and computational implications of a new taxonomy of defensive behaviour. *Nature Reviews Neuroscience*, 19, 269.
- LEDOUX, J. E. 2014. Coming to terms with fear. *Proceedings of the National Academy of Sciences*, 111, 2871-2878.
- LEDOUX, J. E. & PINE, D. S. 2016. Using neuroscience to help understand fear and anxiety: a two-system framework. *American journal of psychiatry*.
- LEE, C., ROHRER, W. H. & SPARKS, D. L. 1988. Population coding of saccadic eye movements by neurons in the superior colliculus. *Nature*, 332, 357.
- LEHRMAN, D. S. 1953. A critique of Konrad Lorenz's theory of instinctive behavior. *The Quarterly review of biology*, 28, 337-363.
- LI, A., GONG, H., ZHANG, B., WANG, Q., YAN, C., WU, J., LIU, Q., ZENG, S. & LUO, Q. 2010. Micro-optical sectioning tomography to obtain a high-resolution atlas of the mouse brain. *Science*, 330, 1404-1408.
- LI, C.-I., MAGLINAO, T. L. & TAKAHASHI, L. K. 2004. Medial amygdala modulation of predator odor-induced unconditioned fear in the rat. *Behavioral neuroscience*, 118, 324.
- LI, C.-S. R., MAZZONI, P. & ANDERSEN, R. A. 1999. Effect of reversible inactivation of macaque lateral intraparietal area on visual and memory saccades. *Journal of Neurophysiology*, 81, 1827-1838.
- LI, Y., ZENG, J., ZHANG, J., YUE, C., ZHONG, W., LIU, Z., FENG, Q. & LUO, M. 2018. Hypothalamic circuits for predation and evasion. *Neuron*, 97, 911-924. e5.
- LIDEN, W. H., PHILLIPS, M. L. & HERBERHOLZ, J. 2010. Neural control of behavioural choice in juvenile crayfish. *Proceedings of the Royal Society B: Biological Sciences*, 277, 3493-3500.
- LIMA, S. L. 1993. Ecological and evolutionary perspectives on escape from predatory attack: a survey of North American birds. *The Wilson Bulletin*, 1-47.
- LIN, C.-T., CHIU, T.-C. & GRAMANN, K. 2015. EEG correlates of spatial orientation in the human retrosplenial complex. *NeuroImage*, 120, 123-132.
- LINES, C. R. & MILNER, A. D. 1985. A deficit in ambient visual guidance following superior colliculus lesions in rats. *Behavioral Neuroscience*, 99, 707.

- LINGLE, S. & PELLIS, S. 2002. Fight or flight? Antipredator behavior and the escalation of coyote encounters with deer. *Oecologia*, 131, 154-164.
- LOMBER, S. G. & PAYNE, B. R. 1996. Removal of two halves restores the whole: reversal of visual hemineglect during bilateral cortical or collicular inactivation in the cat. *Visual neuroscience*, 13, 1143-1156.
- LOMBER, S. G., PAYNE, B. R. & CORNWELL, P. 2001. Role of the superior colliculus in analyses of space: superficial and intermediate layer contributions to visual orienting, auditory orienting, and visuospatial discriminations during unilateral and bilateral deactivations. *Journal of Comparative Neurology*, 441, 44-57.
- LOWRY, H., LILL, A. & WONG, B. B. 2013. Behavioural responses of wildlife to urban environments. *Biological reviews*, 88, 537-549.
- LOZANO, Y. R., PAGE, H., JACOB, P.-Y., LOMI, E., STREET, J. & JEFFERY, K. 2017. Retrosplenial and postsubicular head direction cells compared during visual landmark discrimination. *Brain and neuroscience advances*, 1, 2398212817721859.
- LUSCHEI, E. S. & FUCHS, A. F. 1972. Activity of brain stem neurons during eye movements of alert monkeys. *Journal of Neurophysiology*, 35, 445-461.
- MAASWINKEL, H., JARRARD, L. E. & WHISHAW, I. Q. 1999. Hippocampectomized rats are impaired in homing by path integration. *Hippocampus*, 9, 553-561.
- MAASWINKEL, H. & WHISHAW, I. Q. 1999. Homing with locale, taxon, and dead reckoning strategies by foraging rats: sensory hierarchy in spatial navigation. *Behavioural brain research*, 99, 143-152.
- MAHLER, S. V. & ASTON-JONES, G. 2018. CNO Evil? Considerations for the use of DREADDs in behavioral neuroscience. *Neuropsychopharmacology*, 43, 934.
- MAJCHRZAK, M. & DI SCALA, G. 2000. GABA and muscimol as reversible inactivation tools in learning and memory. *Neural plasticity*, 7, 19-29.
- MANSER, M. B., BELL, M. B. & FLETCHER, L. B. 2001. The information that receivers extract from alarm calls in suricates. *Proceedings of the Royal Society of London. Series B: Biological Sciences*, 268, 2485-2491.
- MANVICH, D. F., WEBSTER, K. A., FOSTER, S. L., FARRELL, M. S., RITCHIE, J. C., PORTER, J. H. & WEINSHENKER, D. 2018. The DREADD agonist clozapine N-oxide (CNO) is reverse-metabolized to clozapine and produces clozapine-like interoceptive stimulus effects in rats and mice. *Scientific reports*, 8, 3840.
- MARCHETTE, S. A., VASS, L. K., RYAN, J. & EPSTEIN, R. A. 2014. Anchoring the neural compass: coding of local spatial reference frames in human medial parietal lobe. *Nature neuroscience*, 17, 1598.
- MARTINEZ, R., CARVALHO-NETTO, E., RIBEIRO-BARBOSA, E., BALDO, M. & CANTERAS, N. 2011. Amygdalar roles during exposure to a live predator and to a predator-associated context. *Neuroscience*, 172, 314-328.

- MASFERRER, M. E., SILVA, B. A., NOMOTO, K., LIMA, S. Q. & GROSS, C. T. 2018. Differential encoding of predator fear in the ventromedial hypothalamus and periaqueductal grey. *bioRxiv*, 283820.
- MASULLO, L., MARIOTTI, L., ALEXANDRE, N., FREIRE-PRITCHETT, P., BOULANGER, J. & TRIPODI, M. 2019. Genetically defined functional modules for spatial orienting in the mouse superior colliculus. *Current Biology*, 29, 2892-2904. e8.
- MATHIS, A., MAMIDANNA, P., CURY, K. M., ABE, T., MURTHY, V. N., MATHIS, M. W. & BETHGE, M. 2018. DeepLabCut: markerless pose estimation of user-defined body parts with deep learning. Nature Publishing Group.
- MAYS, L. E. & SPARKS, D. L. 1980. Dissociation of visual and saccade-related responses in superior colliculus neurons. *Journal of Neurophysiology*, 43, 207-232.
- MCCOY, A. N., CROWLEY, J. C., HAGHIGHIAN, G., DEAN, H. L. & PLATT, M. L. 2003. Saccade reward signals in posterior cingulate cortex. *Neuron*, 40, 1031-1040.
- MCDONALD, R. J. & WHITE, N. M. 1994. Parallel information processing in the water maze: evidence for independent memory systems involving dorsal striatum and hippocampus. *Behavioral and neural biology*, 61, 260-270.
- MCHUGH, T. J., BLUM, K. I., TSIEN, J. Z., TONEGAWA, S. & WILSON, M. A. 1996. Impaired hippocampal representation of space in CA1-specific NMDAR1 knockout mice. *Cell*, 87, 1339-1349.
- MCNAUGHTON, B., BARNES, C. A. & O'KEEFE, J. 1983. The contributions of position, direction, and velocity to single unit activity in the hippocampus of freely-moving rats. *Experimental brain research*, 52, 41-49.
- MCNAUGHTON, B., CHEN, L. & MARKUS, E. 1991. "Dead reckoning," landmark learning, and the sense of direction: a neurophysiological and computational hypothesis. *Journal of Cognitive Neuroscience*, 3, 190-202.
- MCNAUGHTON, B. L., BATTAGLIA, F. P., JENSEN, O., MOSER, E. I. & MOSER, M.-B. 2006. Path integration and the neural basis of the 'cognitive map'. *Nature Reviews Neuroscience*, 7, 663.
- MCNAUGHTON, N. & CORR, P. J. 2004. A two-dimensional neuropsychology of defense: fear/anxiety and defensive distance. *Neuroscience & Biobehavioral Reviews*, 28, 285-305.
- MCPEEK, R. M. & KELLER, E. L. 2004. Deficits in saccade target selection after inactivation of superior colliculus. *Nature neuroscience*, 7, 757.
- MENZEL, R., GREGGERS, U., SMITH, A., BERGER, S., BRANDT, R., BRUNKE, S., BUNDROCK, G., HÜLSE, S., PLÜMPE, T. & SCHAUPP, F. 2005. Honey bees navigate according to a map-like spatial memory. *Proceedings of the National Academy of Sciences*, 102, 3040-3045.

- MERY, F. & BURNS, J. G. 2010. Behavioural plasticity: an interaction between evolution and experience. *Evolutionary Ecology*, 24, 571-583.
- MITCHELL, A. S., CZAJKOWSKI, R., ZHANG, N., JEFFERY, K. & NELSON, A. J. 2018. Retrosplenial cortex and its role in spatial cognition. *Brain and Neuroscience Advances*, 2, 2398212818757098.
- MITTELSTAEDT, H. & MITTELSTAEDT, M.-L. 1982. Homing by path integration. *Avian navigation*. Springer.
- MITTELSTAEDT, M.-L. & GLASAUER, S. 1991. Idiothetic navigation in gerbils and humans. *Zool. Jb. Physiol*, 95.
- MITTELSTAEDT, M.-L. & MITTELSTAEDT, H. 1980. Homing by path integration in a mammal. *Naturwissenschaften*, 67, 566-567.
- MIYASHITA, T. & ROCKLAND, K. S. 2007. GABAergic projections from the hippocampus to the retrosplenial cortex in the rat. *European Journal of Neuroscience*, 26, 1193-1204.
- MIZUMORI, S. & WILLIAMS, J. 1993. Directionally selective mnemonic properties of neurons in the lateral dorsal nucleus of the thalamus of rats. *Journal of Neuroscience*, 13, 4015-4028.
- MOBBS, D., MARCHANT, J. L., HASSABIS, D., SEYMOUR, B., TAN, G., GRAY, M., PETROVIC, P., DOLAN, R. J. & FRITH, C. D. 2009. From threat to fear: the neural organization of defensive fear systems in humans. *Journal of Neuroscience*, 29, 12236-12243.
- MOBBS, D., PETROVIC, P., MARCHANT, J. L., HASSABIS, D., WEISKOPF, N., SEYMOUR, B., DOLAN, R. J. & FRITH, C. D. 2007. When fear is near: threat imminence elicits prefrontal-periaqueductal gray shifts in humans. *Science*, 317, 1079-1083.
- MOHLER, C. W. & WURTZ, R. H. 1976. Organization of monkey superior colliculus: intermediate layer cells discharging before eye movements. *Journal of neurophysiology*, 39, 722-744.
- MONGEAU, R., MILLER, G. A., CHIANG, E. & ANDERSON, D. J. 2003. Neural correlates of competing fear behaviors evoked by an innately aversive stimulus. *Journal of Neuroscience*, 23, 3855-3868.
- MOORE, T. Y., COOPER, K. L., BIEWENER, A. A. & VASUDEVAN, R. 2017. Unpredictability of escape trajectory explains predator evasion ability and microhabitat preference of desert rodents. *Nature communications*, 8, 440.
- MORRIS, R. 1984. Developments of a water-maze procedure for studying spatial learning in the rat. *Journal of neuroscience methods*, 11, 47-60.
- MORRIS, R. G. 1981. Spatial localization does not require the presence of local cues. *Learning and motivation*, 12, 239-260.

- MORRIS, R. G., GARRUD, P., RAWLINS, J. A. & O'KEEFE, J. 1982. Place navigation impaired in rats with hippocampal lesions. *Nature*, 297, 681.
- MOSER, E. I., KROPFF, E. & MOSER, M.-B. 2008. Place cells, grid cells, and the brain's spatial representation system. *Annual review of neuroscience*, 31.
- MOSER, E. I., ROUDI, Y., WITTER, M. P., KENTROS, C., BONHOEFFER, T. & MOSER, M.-B. 2014. Grid cells and cortical representation. *Nature Reviews Neuroscience*, 15, 466.
- MOSER, M.-B., ROWLAND, D. C. & MOSER, E. I. 2015. Place cells, grid cells, and memory. *Cold Spring Harbor perspectives in biology*, 7, a021808.
- MOTTA, S. C., GOTO, M., GOUVEIA, F. V., BALDO, M. V., CANTERAS, N. S. & SWANSON, L. W. 2009. Dissecting the brain's fear system reveals the hypothalamus is critical for responding in subordinate conspecific intruders. *Proceedings of the National Academy of Sciences*, 106, 4870-4875.
- MÜLLER, M. & WEHNER, R. 1988. Path integration in desert ants, *Cataglyphis fortis*. *Proceedings of the National Academy of Sciences*, 85, 5287-5290.
- MULLER, R. U. & KUBIE, J. L. 1987. The effects of changes in the environment on the spatial firing of hippocampal complex-spike cells. *Journal of Neuroscience*, 7, 1951-1968.
- MURAKAMI, M., VICENTE, M. I., COSTA, G. M. & MAINEN, Z. F. 2014. Neural antecedents of self-initiated actions in secondary motor cortex. *Nature neuroscience*, 17, 1574.
- NICOLELIS, M. A., GHAZANFAR, A. A., STAMBAUGH, C. R., OLIVEIRA, L. M., LAUBACH, M., CHAPIN, J. K., NELSON, R. J. & KAAS, J. H. 1998. Simultaneous encoding of tactile information by three primate cortical areas. *Nature neuroscience*, 1, 621.
- NIKBAKHT, N., TAFRESHIHA, A., ZOCCOLAN, D. & DIAMOND, M. E. 2018. Supralinear and supramodal integration of visual and tactile signals in rats: psychophysics and neuronal mechanisms. *Neuron*, 97, 626-639. e8.
- O'BRIEN, T. J. & DUNLAP, W. P. 1975. Tonic immobility in the blue crab (*Callinectes sapidus*, Rathbun): Its relation to threat of predation. *Journal of comparative and physiological psychology*, 89, 86.
- O'KEEFE, J. 1976. Place units in the hippocampus of the freely moving rat. *Experimental neurology*, 51, 78-109.
- O'KEEFE, J. & CONWAY, D. 1978. Hippocampal place units in the freely moving rat: why they fire where they fire. *Experimental brain research*, 31, 573-590.
- O'KEEFE, J. & DOSTROVSKY, J. 1971. The hippocampus as a spatial map: preliminary evidence from unit activity in the freely-moving rat. *Brain research*.
- O'KEEFE, J. & NADEL, L. 1978. *The hippocampus as a cognitive map*, Oxford: Clarendon Press.

- O'KEEFE, J. & SPEAKMAN, A. 1987. Single unit activity in the rat hippocampus during a spatial memory task. *Experimental brain research*, 68, 1-27.
- O'LEARY, T. P. & BROWN, R. E. 2009. Visuo-spatial learning and memory deficits on the Barnes maze in the 16-month-old APP<sup>swe</sup>/PS1<sup>dE9</sup> mouse model of Alzheimer's disease. *Behavioural brain research*, 201, 120-127.
- O'LEARY, T. P., SAVOIE, V. & BROWN, R. E. 2011. Learning, memory and search strategies of inbred mouse strains with different visual abilities in the Barnes maze. *Behavioural brain research*, 216, 531-542.
- OH, S. W., HARRIS, J. A., NG, L., WINSLOW, B., CAIN, N., MIHALAS, S., WANG, Q., LAU, C., KUAN, L. & HENRY, A. M. 2014. A mesoscale connectome of the mouse brain. *Nature*, 508, 207.
- OLIVA, D., MEDAN, V. & TOMSIC, D. 2007. Escape behavior and neuronal responses to looming stimuli in the crab *Chasmagnathus granulatus* (Decapoda: Grapsidae). *Journal of Experimental Biology*, 210, 865-880.
- OLSON, J. M., LI, J., MONTGOMERY, S. E. & NITZ, D. A. 2019. Secondary Motor Cortex Transforms Spatial Information into Planned Action During Navigation. *bioRxiv*, 776765.
- OLTON, D. S. & SAMUELSON, R. J. 1976. Remembrance of places passed: spatial memory in rats. *Journal of Experimental Psychology: Animal Behavior Processes*, 2, 97.
- OSAWA, A., MAESHIMA, S. & KUNISHIO, K. 2008. Topographic disorientation and amnesia due to cerebral hemorrhage in the left retrosplenial region. *European neurology*, 59, 79-82.
- PACHITARIU, M., STEINMETZ, N., KADIR, S., CARANDINI, M. & HARRIS, K. D. 2016. Kilosort: realtime spike-sorting for extracellular electrophysiology with hundreds of channels. *BioRxiv*, 061481.
- PACKARD, M. G. & MCGAUGH, J. L. 1992. Double dissociation of fornix and caudate nucleus lesions on acquisition of two water maze tasks: further evidence for multiple memory systems. *Behavioral neuroscience*, 106, 439.
- PACKARD, M. G. & MCGAUGH, J. L. 1996. Inactivation of hippocampus or caudate nucleus with lidocaine differentially affects expression of place and response learning. *Neurobiology of learning and memory*, 65, 65-72.
- PAPI, F., FIORE, L., FIASCHI, V. & BENVENUTI, S. 1971. The influence of olfactory nerve section on the homing capacity of carrier pigeons. *Monitore Zoologico Italiano-Italian Journal of Zoology*, 5, 265-267.
- PARÉ, M. & WURTZ, R. H. 1997. Monkey posterior parietal cortex neurons antidromically activated from superior colliculus. *Journal of Neurophysiology*, 78, 3493-3497.
- PARÉ, M. & WURTZ, R. H. 2001. Progression in neuronal processing for saccadic eye movements from parietal cortex area lip to superior colliculus. *Journal of Neurophysiology*, 85, 2545-2562.

- PARRON, C. & SAVE, E. 2004. Evidence for entorhinal and parietal cortices involvement in path integration in the rat. *Experimental Brain Research*, 159, 349-359.
- PATAI, E. Z., JAVADI, A.-H., OZUBKO, J. D., O'CALLAGHAN, A., JI, S., ROBIN, J., GRADY, C., WINOCUR, G., ROSENBAUM, R. S. & MOSCOVITCH, M. 2019. Hippocampal and retrosplenial goal distance coding after long-term consolidation of a real-world environment. *Cerebral Cortex*, 29, 2748-2758.
- PATIL, S. S., SUNYER, B., HÖGER, H. & LUBEC, G. 2009. Evaluation of spatial memory of C57BL/6J and CD1 mice in the Barnes maze, the Multiple T-maze and in the Morris water maze. *Behavioural brain research*, 198, 58-68.
- PAUS, T., PETRIDES, M., EVANS, A. C. & MEYER, E. 1993. Role of the human anterior cingulate cortex in the control of oculomotor, manual, and speech responses: a positron emission tomography study. *Journal of neurophysiology*, 70, 453-469.
- PELLOW, S., CHOPIN, P., FILE, S. E. & BRILEY, M. 1985. Validation of open: closed arm entries in an elevated plus-maze as a measure of anxiety in the rat. *Journal of neuroscience methods*, 14, 149-167.
- PEREYRA, P., PORTINO, E. G. & MALDONADO, H. 2000. Long-lasting and context-specific freezing preference is acquired after spaced repeated presentations of a danger stimulus in the crab *Chasmagnathus*. *Neurobiology of learning and memory*, 74, 119-134.
- PÉREZ-GÓMEZ, A., BLEYMEHL, K., STEIN, B., PYRSKI, M., BIRNBAUMER, L., MUNGER, S. D., LEINDERS-ZUFALL, T., ZUFALL, F. & CHAMERO, P. 2015. Innate predator odor aversion driven by parallel olfactory subsystems that converge in the ventromedial hypothalamus. *Current Biology*, 25, 1340-1346.
- PETREANU, L., HUBER, D., SOBCZYK, A. & SVOBODA, K. 2007. Channelrhodopsin-2-assisted circuit mapping of long-range callosal projections. *Nature neuroscience*, 10, 663.
- PFEIFFER, B. E. & FOSTER, D. J. 2013. Hippocampal place-cell sequences depict future paths to remembered goals. *Nature*, 497, 74.
- PIERROT-DESEILLIGNY, C., RIVAUD, S., GAYMARD, B., MÜRI, R. & VERMERSCH, A. I. 1995. Cortical control of saccades. *Annals of Neurology: Official Journal of the American Neurological Association and the Child Neurology Society*, 37, 557-567.
- PITCHER, T. J. & WYCHE, C. J. 1983. Predator-avoidance behaviours of sand-eel schools: why schools seldom split. *Predators and prey in fishes*. Springer.
- PITTS, M. W. 2018. Barnes Maze Procedure for Spatial Learning and Memory in Mice. *Bio-protocol*, 8.
- POMPL, P. N., MULLAN, M. J., BJUGSTAD, K. & ARENDASH, G. W. 1999. Adaptation of the circular platform spatial memory task for mice: use in detecting cognitive impairment in the APP<sup>sw</sup> transgenic mouse model for Alzheimer's disease. *Journal of neuroscience methods*, 87, 87-95.

- POULTER, S., HARTLEY, T. & LEVER, C. 2018. The Neurobiology of Mammalian Navigation. *Current Biology*, 28, R1023-R1042.
- PRENDERGAST, B. J., ONISHI, K. G. & ZUCKER, I. 2014. Female mice liberated for inclusion in neuroscience and biomedical research. *Neuroscience & Biobehavioral Reviews*, 40, 1-5.
- PUTMAN, N. F., SCANLAN, M. M., BILLMAN, E. J., O'NEIL, J. P., COUTURE, R. B., QUINN, T. P., LOHMANN, K. J. & NOAKES, D. L. 2014. An inherited magnetic map guides ocean navigation in juvenile Pacific salmon. *Current Biology*, 24, 446-450.
- QI, S., HASSABIS, D., SUN, J., GUO, F., DAW, N. & MOBBS, D. 2018. How cognitive and reactive fear circuits optimize escape decisions in humans. *Proceedings of the National Academy of Sciences*, 115, 3186-3191.
- QUINN, T. P., VOLK, E. C. & HENDRY, A. P. 1999. Natural otolith microstructure patterns reveal precise homing to natal incubation sites by sockeye salmon (*Oncorhynchus nerka*). *Canadian Journal of Zoology*, 77, 766-775.
- QUIRK, G. J., MULLER, R. U. & KUBIE, J. L. 1990. The firing of hippocampal place cells in the dark depends on the rat's recent experience. *Journal of Neuroscience*, 10, 2008-2017.
- QUIRK, G. J., MULLER, R. U., KUBIE, J. L. & RANCK, J. 1992. The positional firing properties of medial entorhinal neurons: description and comparison with hippocampal place cells. *Journal of Neuroscience*, 12, 1945-1963.
- RAGAN, T., KADIRI, L. R., VENKATARAJU, K. U., BAHLMANN, K., SUTIN, J., TARANDA, J., ARGANDA-CARRERAS, I., KIM, Y., SEUNG, H. S. & OSTEN, P. 2012. Serial two-photon tomography for automated ex vivo mouse brain imaging. *Nature methods*, 9, 255.
- RAO, C. R. 1948. The utilization of multiple measurements in problems of biological classification. *Journal of the Royal Statistical Society. Series B (Methodological)*, 10, 159-203.
- REDISH, A. D. 1999. *Beyond the cognitive map: from place cells to episodic memory*, MIT press.
- REYES-PUERTA, V., KIM, S., SUN, J.-J., IMBROSCI, B., KILB, W. & LUHMANN, H. J. 2015. High stimulus-related information in barrel cortex inhibitory interneurons. *PLoS computational biology*, 11, e1004121.
- ROBERTSON, R., KAITZ, S. S. & ROBARDS, M. J. 1980. A subcortical pathway links sensory and limbic systems of the forebrain. *Neuroscience letters*, 17, 161-165.
- ROBINSON, D. & FUCHS, A. 1969. Eye movements evoked by stimulation of frontal eye fields. *Journal of Neurophysiology*, 32, 637-648.
- ROBINSON, D. A. 1972. Eye movements evoked by collicular stimulation in the alert monkey. *Vision research*, 12, 1795-1808.

- ROOT, C. M., DENNY, C. A., HEN, R. & AXEL, R. 2014. The participation of cortical amygdala in innate, odour-driven behaviour. *Nature*, 515, 269.
- ROTH, B. L. 2016. DREADDs for neuroscientists. *Neuron*, 89, 683-694.
- ROWLAND, D. C., ROUDI, Y., MOSER, M.-B. & MOSER, E. I. 2016. Ten years of grid cells. *Annual review of neuroscience*, 39, 19-40.
- ROZESKE, R. R., JERCOG, D., KARALIS, N., CHAUDUN, F., KHODER, S., GIRARD, D., WINKE, N. & HERRY, C. 2018. Prefrontal-periaqueductal gray-projecting neurons mediate context fear discrimination. *Neuron*, 97, 898-910. e6.
- SAHIBZADA, N., DEAN, P. & REDGRAVE, P. 1986. Movements resembling orientation or avoidance elicited by electrical stimulation of the superior colliculus in rats. *Journal of Neuroscience*, 6, 723-733.
- SAREL, A., FINKELSTEIN, A., LAS, L. & ULANOVSKY, N. 2017. Vectorial representation of spatial goals in the hippocampus of bats. *Science*, 355, 176-180.
- SARGOLINI, F., FYHN, M., HAFTING, T., MCNAUGHTON, B. L., WITTER, M. P., MOSER, M.-B. & MOSER, E. I. 2006. Conjunctive representation of position, direction, and velocity in entorhinal cortex. *Science*, 312, 758-762.
- SAVAGE, M. A., MCQUADE, R. & THIELE, A. 2017. Segregated fronto-cortical and midbrain connections in the mouse and their relation to approach and avoidance orienting behaviors. *Journal of Comparative Neurology*, 525, 1980-1999.
- SAVE, E. & MOGHADDAM, M. 1996. Effects of lesions of the associative parietal cortex on the acquisition and use of spatial memory in egocentric and allocentric navigation tasks in the rat. *Behavioral neuroscience*, 110, 74.
- SAVE, E. & POU CET, B. 2000. Involvement of the hippocampus and associative parietal cortex in the use of proximal and distal landmarks for navigation. *Behavioural brain research*, 109, 195-206.
- SCHADEGG, A. C. & HERBERHOLZ, J. 2017. Satiation level affects anti-predatory decisions in foraging juvenile crayfish. *Journal of Comparative Physiology A*, 203, 223-232.
- SCHEIBEL, M. E. & SCHEIBEL, A. B. 1958. Structural substrates for integrative patterns in the brain stem reticular core.
- SCHIFF, W. 1965. Perception of impending collision: A study of visually directed avoidant behavior. *Psychological Monographs: General and Applied*, 79, 1.
- SCHILLER, P. H. 1998. The neural control of visually guided eye movements. *Cognitive neuroscience of attention*. Psychology Press.
- SCHILLER, P. H. & CHOU, I.-H. 1998. The effects of frontal eye field and dorsomedial frontal cortex lesions on visually guided eye movements. *Nature neuroscience*, 1, 248.

- SCHILLER, P. H. & STRYKER, M. 1972. Single-unit recording and stimulation in superior colliculus of the alert rhesus monkey. *Journal of neurophysiology*, 35, 915-924.
- SCHILLER, P. H., TRUE, S. D. & CONWAY, J. L. 1980. Deficits in eye movements following frontal eye-field and superior colliculus ablations. *Journal of Neurophysiology*, 44, 1175-1189.
- SCHLAG-REY, M., SCHLAG, J. & DASSONVILLE, P. 1992. How the frontal eye field can impose a saccade goal on superior colliculus neurons. *Journal of Neurophysiology*, 67, 1003-1005.
- SCUDDER, C. A., KANEKO, C. R. & FUCHS, A. F. 2002. The brainstem burst generator for saccadic eye movements. *Experimental brain research*, 142, 439-462.
- SEEGER, T., FEDOROVA, I., ZHENG, F., MIYAKAWA, T., KOUSTOVA, E., GOMEZA, J., BASILE, A. S., ALZHEIMER, C. & WESS, J. 2004. M2 muscarinic acetylcholine receptor knock-out mice show deficits in behavioral flexibility, working memory, and hippocampal plasticity. *Journal of Neuroscience*, 24, 10117-10127.
- SEGRAVES, M. A. 1992. Activity of monkey frontal eye field neurons projecting to oculomotor regions of the pons. *Journal of Neurophysiology*, 68, 1967-1985.
- SEYFARTH, R. & CHENEY, D. 1990. The assessment by vervet monkeys of their own and another species' alarm calls. *Animal Behaviour*, 40, 754-764.
- SEYFARTH, R. M. & CHENEY, D. L. 1980. The ontogeny of vervet monkey alarm calling behavior: a preliminary report. *Zeitschrift für Tierpsychologie*, 54, 37-56.
- SHANG, C., LIU, Z., CHEN, Z., SHI, Y., WANG, Q., LIU, S., LI, D. & CAO, P. 2015. A parvalbumin-positive excitatory visual pathway to trigger fear responses in mice. *Science*, 348, 1472-1477.
- SHARP, P. E. & GREEN, C. 1994. Spatial correlates of firing patterns of single cells in the subiculum of the freely moving rat. *Journal of Neuroscience*, 14, 2339-2356.
- SHARP, P. E., TINKELMAN, A. & CHO, J. 2001. Angular velocity and head direction signals recorded from the dorsal tegmental nucleus of gudden in the rat: implications for path integration in the head direction cell circuit. *Behavioral neuroscience*, 115, 571.
- SHEN, K. & PARÉ, M. 2014. Predictive saccade target selection in superior colliculus during visual search. *Journal of Neuroscience*, 34, 5640-5648.
- SHERRILL, K. R., ERDEM, U. M., ROSS, R. S., BROWN, T. I., HASSELMO, M. E. & STERN, C. E. 2013. Hippocampus and retrosplenial cortex combine path integration signals for successful navigation. *Journal of Neuroscience*, 33, 19304-19313.
- SHINE, J. P., VALDÉS-HERRERA, J. P., HEGARTY, M. & WOLBERS, T. 2016. The human retrosplenial cortex and thalamus code head direction in a global reference frame. *Journal of Neuroscience*, 36, 6371-6381.

- SHRAGER, Y., KIRWAN, C. B. & SQUIRE, L. R. 2008. Neural basis of the cognitive map: path integration does not require hippocampus or entorhinal cortex. *Proceedings of the National Academy of Sciences*, 105, 12034-12038.
- SILVA, B. A., GROSS, C. T. & GRÄFF, J. 2016a. The neural circuits of innate fear: detection, integration, action, and memorization. *Learning & memory*, 23, 544-555.
- SILVA, B. A., MATTUCCI, C., KRZYWKOWSKI, P., CUOZZO, R., CARBONARI, L. & GROSS, C. T. 2016b. The ventromedial hypothalamus mediates predator fear memory. *European Journal of Neuroscience*, 43, 1431-1439.
- SILVA, B. A., MATTUCCI, C., KRZYWKOWSKI, P., MURANA, E., ILLARIONOVA, A., GRINEVICH, V., CANTERAS, N. S., RAGOZZINO, D. & GROSS, C. T. 2013. Independent hypothalamic circuits for social and predator fear. *Nature neuroscience*, 16, 1731.
- SLEE, S. J. & YOUNG, E. D. 2013. Linear processing of interaural level difference underlies spatial tuning in the nucleus of the brachium of the inferior colliculus. *Journal of Neuroscience*, 33, 3891-3904.
- SMITH, K. S., BUCCI, D. J., LUIKART, B. W. & MAHLER, S. V. 2016. DREADDS: Use and application in behavioral neuroscience. *Behavioral neuroscience*, 130, 137.
- SOLSTAD, T., BOCCARA, C. N., KROPFF, E., MOSER, M.-B. & MOSER, E. I. 2008. Representation of geometric borders in the entorhinal cortex. *Science*, 322, 1865-1868.
- SOMMER, M. A. & WURTZ, R. H. 2000. Composition and topographic organization of signals sent from the frontal eye field to the superior colliculus. *Journal of Neurophysiology*, 83, 1979-2001.
- SPARKS, D. L. 1986. Translation of sensory signals into commands for control of saccadic eye movements: role of primate superior colliculus. *Physiological reviews*, 66, 118-171.
- SPARKS, D. L. 1988. Neural cartography: Sensory and motor maps in the superior colliculus. *Brain, behavior and evolution*, 31, 49-56.
- SPARKS, D. L. 1989. The neural encoding of the location of targets for saccadic eye movements. *Journal of Experimental Biology*, 146, 195-207.
- SPARKS, D. L. & MAYS, L. E. 1980. Movement fields of saccade-related burst neurons in the monkey superior colliculus. *Brain Res*, 190, 39-50.
- SPRAGUE, J. M. & MEIKLE JR, T. H. 1965. The role of the superior colliculus in visually guided behavior. *Experimental neurology*, 11, 115-146.
- STACHNIAK, T. J., GHOSH, A. & STERNSON, S. M. 2014. Chemogenetic synaptic silencing of neural circuits localizes a hypothalamus→ midbrain pathway for feeding behavior. *Neuron*, 82, 797-808.

- STACKMAN, R. W., GOLOB, E. J., BASSETT, J. P. & TAUBE, J. S. 2003. Passive transport disrupts directional path integration by rat head direction cells. *Journal of neurophysiology*, 90, 2862-2874.
- STACKMAN, R. W. & HERBERT, A. M. 2002. Rats with lesions of the vestibular system require a visual landmark for spatial navigation. *Behavioural brain research*, 128, 27-40.
- STACKMAN, R. W. & TAUBE, J. S. 1998. Firing properties of rat lateral mammillary single units: head direction, head pitch, and angular head velocity. *Journal of Neuroscience*, 18, 9020-9037.
- STANKOWICH, T. & COSS, R. G. 2006. Effects of risk assessment, predator behavior, and habitat on escape behavior in Columbian black-tailed deer. *Behavioral Ecology*, 18, 358-367.
- STANTON, G., GOLDBERG, M. & BRUCE, C. 1988. Frontal eye field efferents in the macaque monkey: II. Topography of terminal fields in midbrain and pons. *Journal of Comparative Neurology*, 271, 493-506.
- STERBING, S. J., HARTUNG, K. & HOFFMANN, K.-P. 2002. Representation of sound source direction in the superior colliculus of the guinea pig in a virtual auditory environment. *Experimental brain research*, 142, 570-577.
- SUGAR, J., WITTER, M. P., VAN STRIEN, N. & CAPPAERT, N. 2011. The retrosplenial cortex: intrinsic connectivity and connections with the (para) hippocampal region in the rat. An interactive connectome. *Frontiers in neuroinformatics*, 5, 7.
- SUKIKARA, M. H., MOTA-ORTIZ, S. R., BALDO, M. V., FELICIO, L. F. & CANTERAS, N. S. 2010. The periaqueductal gray and its potential role in maternal behavior inhibition in response to predatory threats. *Behavioural brain research*, 209, 226-233.
- SUTHERLAND, R., WHISHAW, I. & KOLB, B. 1988. Contributions of cingulate cortex to two forms of spatial learning and memory. *Journal of Neuroscience*, 8, 1863-1872.
- SUTHERLAND, R. J. & DYCK, R. H. 1984. Place navigation by rats in a swimming pool. *Canadian Journal of Psychology/Revue canadienne de psychologie*, 38, 322.
- SWANSON, L. & COWAN, W. 1977. An autoradiographic study of the organization of the efferent connections of the hippocampal formation in the rat. *Journal of Comparative Neurology*, 172, 49-84.
- TAKAHASHI, N., KAWAMURA, M., SHIOTA, J., KASAHATA, N. & HIRAYAMA, K. 1997. Pure topographic disorientation due to right retrosplenial lesion. *Neurology*, 49, 464-469.
- TAUBE, J. S. 1995. Head direction cells recorded in the anterior thalamic nuclei of freely moving rats. *Journal of Neuroscience*, 15, 70-86.
- TAUBE, J. S. 2007. The head direction signal: origins and sensory-motor integration. *Annu. Rev. Neurosci.*, 30, 181-207.

- TAUBE, J. S., MULLER, R. U. & RANCK, J. B. 1990a. Head-direction cells recorded from the postsubiculum in freely moving rats. I. Description and quantitative analysis. *Journal of Neuroscience*, 10, 420-435.
- TAUBE, J. S., MULLER, R. U. & RANCK, J. B. 1990b. Head-direction cells recorded from the postsubiculum in freely moving rats. II. Effects of environmental manipulations. *Journal of Neuroscience*, 10, 436-447.
- TERBURG, D., SCHEGGIA, D., DEL RIO, R. T., KLUMPERS, F., CIOBANU, A. C., MORGAN, B., MONTOYA, E. R., BOS, P. A., GIOBELLINA, G. & VAN DEN BURG, E. H. 2018. The basolateral amygdala is essential for rapid escape: A human and rodent study. *Cell*, 175, 723-735. e16.
- TERVO, D. G. R., HWANG, B.-Y., VISWANATHAN, S., GAJ, T., LAVZIN, M., RITOLA, K. D., LINDO, S., MICHAEL, S., KULESHOVA, E. & OJALA, D. 2016. A designer AAV variant permits efficient retrograde access to projection neurons. *Neuron*, 92, 372-382.
- THOMPSON, G. C. & MASTERTON, R. B. 1978. Brain stem auditory pathways involved in reflexive head orientation to sound. *Journal of neurophysiology*, 41, 1183-1202.
- THORUP, K., BISSON, I.-A., BOWLIN, M. S., HOLLAND, R. A., WINGFIELD, J. C., RAMENOFSKY, M. & WIKELSKI, M. 2007. Evidence for a navigational map stretching across the continental US in a migratory songbird. *Proceedings of the National Academy of Sciences*, 104, 18115-18119.
- TINBERGEN, N. 1951. The study of instinct.
- TOLIMIERI, N., JEFFS, A. & MONTGOMERY, J. C. 2000. Ambient sound as a cue for navigation by the pelagic larvae of reef fishes. *Marine Ecology Progress Series*, 207, 219-224.
- TOLMAN, E. C. 1948. Cognitive maps in rats and men. *Psychological review*, 55, 189.
- TOVOTE, P., ESPOSITO, M. S., BOTTA, P., CHAUDUN, F., FADOK, J. P., MARKOVIC, M., WOLFF, S. B., RAMAKRISHNAN, C., FENNO, L. & DEISSEROTH, K. 2016. Midbrain circuits for defensive behaviour. *Nature*, 534, 206.
- TOVOTE, P., FADOK, J. P. & LÜTHI, A. 2015. Neuronal circuits for fear and anxiety. *Nature Reviews Neuroscience*, 16, 317.
- TREIT, D. & FUNDYTUS, M. 1988. Thigmotaxis as a test for anxiolytic activity in rats. *Pharmacology Biochemistry and Behavior*, 31, 959-962.
- TSOAR, A., NATHAN, R., BARTAN, Y., VYSSOTSKI, A., DELL'OMO, G. & ULANOVSKY, N. 2011. Large-scale navigational map in a mammal. *Proceedings of the National Academy of Sciences*, 108, E718-E724.
- ULANOVSKY, N. & MOSS, C. F. 2007. Hippocampal cellular and network activity in freely moving echolocating bats. *Nature neuroscience*, 10, 224.

- VALE, R., EVANS, D. & BRANCO, T. 2018. A Behavioral Assay for Investigating the Role of Spatial Memory During Instinctive Defense in Mice. *JoVE (Journal of Visualized Experiments)*, e56988.
- VAN CAUTER, T., CAMON, J., ALVERNHE, A., ELDUAYEN, C., SARGOLINI, F. & SAVE, E. 2012. Distinct roles of medial and lateral entorhinal cortex in spatial cognition. *Cerebral Cortex*, 23, 451-459.
- VAN GROEN, T. & WYSS, J. M. 1990. The postsubicular cortex in the rat: characterization of the fourth region of the subicular cortex and its connections. *Brain research*, 529, 165-177.
- VAN GROEN, T. & WYSS, J. M. 1992. Connections of the retrosplenial dysgranular cortex in the rat. *Journal of Comparative Neurology*, 315, 200-216.
- VAN SCHAIK, C. P. & VAN NOORDWIJK, M. A. 1989. The special role of male Cebus monkeys in predation avoidance and its effect on group composition. *Behavioral Ecology and Sociobiology*, 24, 265-276.
- VANN, S. D. & AGGLETON, J. P. 2002. Extensive cytotoxic lesions of the rat retrosplenial cortex reveal consistent deficits on tasks that tax allocentric spatial memory. *Behavioral neuroscience*, 116, 85.
- VANN, S. D. & AGGLETON, J. P. 2003. Evidence of a spatial encoding deficit in rats with lesions of the mammillary bodies or mammillothalamic tract. *Journal of Neuroscience*, 23, 3506-3514.
- VANN, S. D. & AGGLETON, J. P. 2005. Selective dysgranular retrosplenial cortex lesions in rats disrupt allocentric performance of the radial-arm maze task. *Behavioral neuroscience*, 119, 1682.
- VANN, S. D., AGGLETON, J. P. & MAGUIRE, E. A. 2009. What does the retrosplenial cortex do? *Nature Reviews Neuroscience*, 10, 792.
- VEDDER, L. C., MILLER, A. M., HARRISON, M. B. & SMITH, D. M. 2016. Retrosplenial cortical neurons encode navigational cues, trajectories and reward locations during goal directed navigation. *Cerebral Cortex*, 27, 3713-3723.
- VERMEIJ, G. J. 1982. Unsuccessful predation and evolution. *The American Naturalist*, 120, 701-720.
- VOGT, B. A. 1985. Cingulate cortex. *Association and auditory cortices*. Springer.
- VON REYN, C. R., BREADS, P., PEEK, M. Y., ZHENG, G. Z., WILLIAMSON, W. R., YEE, A. L., LEONARDO, A. & CARD, G. M. 2014. A spike-timing mechanism for action selection. *Nature neuroscience*, 17, 962.
- VORHEES, C. V. & WILLIAMS, M. T. 2006. Morris water maze: procedures for assessing spatial and related forms of learning and memory. *Nature protocols*, 1, 848.

- WALKER, J., GHALAMBOR, C., GRISET, O., MCKENNEY, D. & REZNICK, D. 2005. Do faster starts increase the probability of evading predators? *Functional Ecology*, 19, 808-815.
- WALLACE, D. G., HINES, D. J., PELLIS, S. M. & WHISHAW, I. Q. 2002. Vestibular information is required for dead reckoning in the rat. *Journal of Neuroscience*, 22, 10009-10017.
- WALLRAFF, H. G. & WALLRAFF, H. G. 2005. *Avian navigation: pigeon homing as a paradigm*, Springer Science & Business Media.
- WALTON, M. M., BECHARA, B. & GANDHI, N. J. 2007. Role of the primate superior colliculus in the control of head movements. *Journal of neurophysiology*, 98, 2022-2037.
- WANG, C., CHEN, X., LEE, H., DESHMUKH, S. S., YOGANARASIMHA, D., SAVELLI, F. & KNIERIM, J. J. 2018. Egocentric coding of external items in the lateral entorhinal cortex. *Science*, 362, 945-949.
- WANG, L., CHEN, I. Z. & LIN, D. 2015. Collateral pathways from the ventromedial hypothalamus mediate defensive behaviors. *Neuron*, 85, 1344-1358.
- WANG, S. & REDGRAVE, P. 1997. Microinjections of muscimol into lateral superior colliculus disrupt orienting and oral movements in the formalin model of pain. *Neuroscience*, 81, 967-988.
- WATSON, J. B. 1907. Kinæsthetic and organic sensations: Their role in the reactions of the white rat to the maze. *The Psychological Review: Monograph Supplements*, 8, i.
- WEHNER, R. & MÜLLER, M. 2006. The significance of direct sunlight and polarized skylight in the ant's celestial system of navigation. *Proceedings of the National Academy of Sciences*, 103, 12575-12579.
- WEI, P., LIU, N., ZHANG, Z., LIU, X., TANG, Y., HE, X., WU, B., ZHOU, Z., LIU, Y. & LI, J. 2015. Processing of visually evoked innate fear by a non-canonical thalamic pathway. *Nature Communications*, 6, 6756.
- WHISHAW, I. Q. & MAASWINKEL, H. 1998. Rats with fimbria–fornix lesions are impaired in path integration: a role for the hippocampus in “sense of direction”. *Journal of Neuroscience*, 18, 3050-3058.
- WHISHAW, I. Q., MAASWINKEL, H., GONZALEZ, C. L. & KOLB, B. 2001. Deficits in allothetic and idiothetic spatial behavior in rats with posterior cingulate cortex lesions. *Behavioural brain research*, 118, 67-76.
- WHITLOCK, J. R., SUTHERLAND, R. J., WITTER, M. P., MOSER, M.-B. & MOSER, E. I. 2008. Navigating from hippocampus to parietal cortex. *Proceedings of the National Academy of Sciences*, 105, 14755-14762.
- WICKERSHAM, I. R., LYON, D. C., BARNARD, R. J., MORI, T., FINKE, S., CONZELMANN, K.-K., YOUNG, J. A. & CALLAWAY, E. M. 2007. Monosynaptic restriction of transsynaptic tracing from single, genetically targeted neurons. *Neuron*, 53, 639-647.

- WIENER, S. I. 1993. Spatial and behavioral correlates of striatal neurons in rats performing a self-initiated navigation task. *Journal of Neuroscience*, 13, 3802-3817.
- WILBER, A. A., CLARK, B. J., FORSTER, T. C., TATSUNO, M. & MCNAUGHTON, B. L. 2014. Interaction of egocentric and world-centered reference frames in the rat posterior parietal cortex. *Journal of Neuroscience*, 34, 5431-5446.
- WILENT, W. B., OH, M. Y., BUETEFISCH, C. M., BAILES, J. E., CANTELLA, D., ANGLE, C. & WHITING, D. M. 2010. Induction of panic attack by stimulation of the ventromedial hypothalamus: Case report. *Journal of neurosurgery*, 112, 1295-1298.
- WILLS, T. J., CACUCCI, F., BURGESS, N. & O'KEEFE, J. 2010. Development of the hippocampal cognitive map in preweanling rats. *Science*, 328, 1573-1576.
- WILSON, J. J., ALEXANDRE, N., TRENTIN, C. & TRIPODI, M. 2018. Three-dimensional representation of motor space in the mouse superior colliculus. *Current Biology*, 28, 1744-1755. e12.
- WILSON, M. A. & MCNAUGHTON, B. L. 1993. Dynamics of the hippocampal ensemble code for space. *Science*, 261, 1055-1058.
- WITTER, M. P., OSTENDORF, R. H. & GROENEWEGEN, H. J. 1990. Heterogeneity in the dorsal subiculum of the rat. Distinct neuronal zones project to different cortical and subcortical targets. *European Journal of Neuroscience*, 2, 718-725.
- WOLFF, S. B. & ÖLVECZKY, B. P. 2018. The promise and perils of causal circuit manipulations. *Current opinion in neurobiology*, 49, 84-94.
- WRIGHT, P. C. 1998. Impact of predation risk on the behaviour of *Propithecus diadema edwardsi* in the rain forest of Madagascar. *Behaviour*, 483-512.
- WURTZ, R. H. & GOLDBERG, M. E. 1971. Superior colliculus cell responses related to eye movements in awake monkeys. *Science*, 171, 82-84.
- WYNN, M. L., CLEMENTE, C., NASIR, A. F. A. A. & WILSON, R. S. 2015. Running faster causes disaster: trade-offs between speed, manoeuvrability and motor control when running around corners in northern quolls (*Dasyurus hallucatus*). *Journal of Experimental Biology*, 218, 433-439.
- XIONG, X. R., LIANG, F., ZINGG, B., JI, X.-Y., IBRAHIM, L. A., TAO, H. W. & ZHANG, L. I. 2015. Auditory cortex controls sound-driven innate defense behaviour through corticofugal projections to inferior colliculus. *Nature communications*, 6, 7224.
- YAMAMOTO, K., NAKATA, M. & NAKAGAWA, H. 2003. Input and output characteristics of collision avoidance behavior in the frog *Rana catesbeiana*. *Brain, behavior and evolution*, 62, 201-211.
- YAMAWAKI, N., RADULOVIC, J. & SHEPHERD, G. M. 2016. A corticocortical circuit directly links retrosplenial cortex to M2 in the mouse. *Journal of Neuroscience*, 36, 9365-9374.

- YDENBERG, R. C. & DILL, L. M. 1986. The economics of fleeing from predators. *Advances in the Study of Behavior*. Elsevier.
- YILMAZ, M. & MEISTER, M. 2013. Rapid innate defensive responses of mice to looming visual stimuli. *Current Biology*, 23, 2011-2015.
- YODER, R. M., CLARK, B. J., BROWN, J. E., LAMIA, M. V., VALERIO, S., SHINDER, M. E. & TAUBE, J. S. 2011. Both visual and idiothetic cues contribute to head direction cell stability during navigation along complex routes. *Journal of neurophysiology*, 105, 2989-3001.
- YOGANARASIMHA, D., YU, X. & KNIERIM, J. J. 2006. Head direction cell representations maintain internal coherence during conflicting proximal and distal cue rotations: comparison with hippocampal place cells. *Journal of Neuroscience*, 26, 622-631.
- ZACARIAS, R., NAMIKI, S., CARD, G. M., VASCONCELOS, M. L. & MOITA, M. A. 2018. Speed dependent descending control of freezing behavior in *Drosophila melanogaster*. *Nature communications*, 9, 3697.
- ZANI, P., JONES, T., NEUHAUS, R. & MILGROM, J. 2009. Effect of refuge distance on escape behavior of side-blotched lizards (*Uta stansburiana*). *Canadian Journal of Zoology*, 87, 407-414.
- ZEIL, J. 1998. Homing in fiddler crabs (*Uca lactea annulipes* and *Uca vomeris*: Ocypodidae). *Journal of comparative physiology A*, 183, 367-377.
- ZEIL, J. & LAYNE, J. 2002. Path integration in fiddler crabs and its relation to habitat and social life. *Crustacean experimental systems in neurobiology*. Springer.
- ZHAO, X., LIU, M. & CANG, J. 2014. Visual cortex modulates the magnitude but not the selectivity of looming-evoked responses in the superior colliculus of awake mice. *Neuron*, 84, 202-213.
- ZHENG, T., YANG, Z., LI, A., LV, X., ZHOU, Z., WANG, X., QI, X., LI, S., LUO, Q. & GONG, H. 2013. Visualization of brain circuits using two-photon fluorescence micro-optical sectioning tomography. *Optics express*, 21, 9839-9850.
- ZHU, H. & ROTH, B. L. 2014. Silencing synapses with DREADDs. *Neuron*, 82, 723-725.
- ZIRKELBACH, J., STEMMLER, M. & HERZ, A. V. 2019. Anticipatory neural activity improves the decoding accuracy for dynamic head-direction signals. *Journal of Neuroscience*, 39, 2847-2859.
- ZUGARO, M. B., ARLEO, A., BERTHOZ, A. & WIENER, S. I. 2003. Rapid spatial reorientation and head direction cells. *Journal of Neuroscience*, 23, 3478-3482.
- ZUGARO, M. B., TABUCHI, E. & WIENER, S. I. 2000. Influence of conflicting visual, inertial and substratal cues on head direction cell activity. *Experimental brain research*, 133, 198-208.